ENDOCANNABINOID SYSTEM MODULATION OF THE OCULAR IMMUNE RESPONSE

by

J. Thomas Toguri

Submitted in partial fulfilment of the requirements
for the degree of Doctor of Philosophy

at

Dalhousie University
Halifax, Nova Scotia
July 2015

DEDICATION PAGE

This thesis is dedicate this to my colleagues, friends and family, those who have been there for me through these years.

Table of Contents

List of Tables

List of Figures

Abstract

The endocannabinoid system (ECS) is an endogenous lipid signaling system, comprised of receptors, ligands, and their degradative enzymes. The cannabinoid 2 receptor (CB_2R) is localized on immune cells and modulates immune function in health and disease. Activation of the CB_2R has anti-inflammatory actions in several organ systems, however, the effects of ECS modulation during ocular inflammation has not been thoroughly investigated. Novel therapeutics for ocular inflammation are needed as current treatments can exhibit lack of efficacy, become refractory, and produce side effects. To address these problems, the work presented in this thesis examined the manipulation of the ECS during ocular inflammation and the effects of CB_2R activation on the inflammatory response. To examine the effects of CB_2R activation, *in vivo* and *in vitro* models of inflammation were generated using bacterial endotoxin (lipopolysaccharide, LPS). LPS interacts with the cell surface Toll-like receptor 4 (TLR4) to induce inflammation. Following systemic or intraocular injection of LPS, leukocyte-endothelial interactions and local blood flow were investigated in the iridial microcirculation as a marker of inflammation. Cannabinoid treatments were administered i.v. or topically to the eye. Pharmacological treatments and genetic knock out animals were used to confirm the receptor and cellular targets of cannabinoid agonists. Endocannabinoid levels, release of inflammatory mediators, generation of intracellular signaling molecules, and receptor expression were investigated during the inflammatory response and following treatment to elucidate mechanisms of action. This was further probed by *in vitro* assays investigating the mitogen activated protein kinase (MAPK) pathway. Taken together, the findings presented in this thesis demonstrated that activation of CB_2R has anti-inflammatory properties during acute ocular inflammation with efficacy comparable to current clinical therapies. CB_2R treatment decreases leukocyte-endothelial adhesion, improves local blood flow and diminishes release of inflammatory mediators. Additionally, I have proposed a mechanism of action for these anti-inflammatory effects based on my findings. My results suggest that CB_2R agonists inhibit activation of the MAPK pathway by the LPS-TLR4 interactions in activated macrophages. This prevents activation of pro-inflammatory transcription factors and the subsequent release of the associated pro-inflammatory mediators. Overall, activation of the CB_2R provides a potential therapeutic target for the treatment of ocular inflammation.

List of Abbreviations Used

Δ^9-THC	Δ^9-tetrahydrocannabinol
2-AG	2-arachidonoyl glycerol
5-HT	5-hydroxytryptamine
AA	arachidonic acid
AC	adenylate/adenylyl cyclase
ACKR1	atypical chemokine receptor
Abs	antibodies
AD	*Anno Domini*
ADP	adenosine biphosphate
ACEA	arachidonyl-2-chloroethylamide
AEA	arachidonoyl ethanolamide or anandamide
AH	aqueous humor
AM281	1-(2,4-Dichlorophenyl)-5-(4-iodophenyl)-4-methyl-N-4-morpholinyl-1H- pyrazole-3-carboxamide
AM630	1-[2-(morpholin-4-yl)ethyl]-2-methyl-3-(4-methoxybenzoyl)-6-iodoindole
AML	acute monocytic leukemia
AMP	adenosine monophosphate
AMPK	AMP-activated protein kinase

ANOVA	analysis of variance
AP-1	activating protein-1
APC	antigen presenting cell
AppCCL$_2$p	adenosine-5'-[β-γ-dichloromethylene]triphosphate
ATF	Activating transcription factor
ATP	adenosine triphosphate
BSA	bovine serum albumin
bp	base pairs
C3	complement component 3
CACF	Carelton Animal Care Facility
cAMP	cyclic adenosine monophosphate
CASP	colon ascendens stent peritonitis
CB$_1$R	cannabinoid 1 receptor
CB$_2$R	cannabinoid 2 receptor
CB$_2$KO	cannabinoid 2 receptor knock-out
CBR	cannabinoid receptor
CCL	CC chemokine ligand
CCR	CC chemokine receptor
CD	cluster of differentiation
CGRP	calcitonin gene-related peptide

CHO	Chinese hamster ovary
Clodronate	dichloromethylene-1,1-bisphosphonate
CNS	central nervous system
COX	cyoclooxygenase
CP	CP-55,940
CREB	cAMP responsive element-binding protein
cyPG	cyclopentenone prostaglandin
CXCL	CXC chemokine ligand
CXCR	CXC chemokine receptor
DAG	diacylglycerol
DAGL	diacylglycerol lipase
DARC	Duffy antigen receptor for chemokines
DC	dendritic cell
DMEM	*Dulbecco's Modified Eagle's medium*
DMSO	Dimethyl Sulfoxide
DNA	deoxyribonucleic acid
EAE	experimental autoimmune encephalitis
EAU	experimental autoimmune uveoretinitis/uveitis
ECS	endocannabinoid system
EIU	endotoxin-induced uveitis

ERK	extracellular signaling regulated kinases
FAAH	fatty acid amide hydrolase
FBS	fetal bovine serum
FITC	fluorescein isothiocyanate
GPCR	G-protein coupled receptor
HPLC	High-performance liquid chromatography
HPRT	hypoxanthine-guanine phosphoribosyltransferase
HU308	[(1R,2R,5R)-2-[2,6-dimethoxy-4-(2-methyloctan-2-yl)phenyl]-7,7- dimethyl-4-bicyclo[3.1.1]hept-3-enyl] methanol
Ig	immunoglobulin
IKK	inhibitor of NF-κB
IL	interleukin
IMBF	iridial microcirculation blood flow
i.p.	intraperitoneal
i.v.	intravenous
ivt	intravitreal
ICAM	intracellular adhesion molecule;
IFN-γ	interferon- γ
iNOS	inducible nitric oxide synthase

IVM	intravital microscopy
JAM	junctional adhesion molecule
JNK	c-Jun NH_2-terminal kinase
JWH 133	3-(1′1′-dimethylbutyl)-1-deoxy-Δ^8-THC
LDF	laser Doppler flowmetry
LFA-1	lymphocyte functional associated antigen-1
LOX	lipoxygenase
LPI	lysophosphatidic acid
LPS	lipopolysaccharide
MAC-1	macrophage-1 antigen
MAGL	monoacylglycerol lipase
MAP	mean arterial pressure
MAPK	mitogen activated protein kinase
MCP	monocyte chemotactic protein
MHC	major histocompatibility complex
MIP	macrophage inflammatory protein
MKP	mitogen-activated protein kinase-phosphatase
NAPE	N-arachidonoyl phosphatidylethanolamide
NF-κB	nuclear factor κB
NFAT	nuclear factor of activated T-cells
NLR	Nod-like receptor

NO	nitric oxide
OEA	oleoylethanolamide
p38	p38 mitogen activated protein kinase
PAMP	pathogen associated molecular patter
PCR	polymerase chain reaction
PECAM	platelet endothelial cell adhesion molecule
pERK	phosphorylated extracellular signal-regulated kinase
PFA	paraformaldehyde
PGD_2	prostaglandin D2
PGE_2	prostaglandin E2
PGF_2	prostaglandin F2
pJNK	phosphorylated c-Jun-N-terminal kinase
PKA	protein kinase A
PLA_2	phospholipase A 2
PLC	phospholipase C
PMN	polymorphonuclear leukocytes
PNS	peripheral nervous system
pp38	phosphorylated p38 mitogen activated protein kinase
PPARγ	peroxisome proliferator-activated receptor

PRR	pathogen-associated molecular patterns
PSGL-1	P-selectin glycoprotein ligand
qRT-PCR	quantitative reverse transcriptase polymerase chain reaction
RAGE	receptor for advanced glycation end products
RANTES	regulated on activation, normal T cell expressed and secreted
RBC	red blood cell
RLS	RIG-I-like receptor
RT	reverse transcription
SAPK	stress-activated protein kinase
Sal	saline
SDF	sidestream darkfield imaging
SEM	standard error of the mean
sICAM	soluble intracellular adhesion molecule
sVCAM	soluble vascular cell adhesion molecule
TEM	transendothelial migration
TGF- β	transforming growth factor β
TIR	Toll-interleukin 1 receptor
TLR	toll-like receptor
TNF-α	tumor necrosis factor-α
TRAM	TRIF related adapter protein,

TRIF	TIR-domain-containing adapter-inducing interferon-β
TRPV1	transient receptor potential vanilloid type 1 receptor
VCAM	vascular cell adhesion molecule
VLA-4	very late antigen-4
WHO	World Health Organization
WIN	WIN-55,212-2
WT	wild type

Acknowledgments

I would like to thank my supervisors, Dr. Melanie Kelly and Dr. Christian Lehmann for mentoring me throughout this degree. Without them this work would not have not been possible. I was fortunate enough to gain from both of their expertise and I cannot express my gratitude enough. I also must thank Dr. Anna-Maria Szczesniak, you have been amazing to work with. So many people have helped me to reach this point especially my fellow lab members in both the Kelly Lab and Lehmann Lab, both past and present. I appreciated everyone who took the time to teach and help me throughout this journey. The Department of Pharmacology has been amazing to me. Thank you all.

Chapter I: Introduction

The endocannabinoid system (ECS) is an endogenous lipid signaling system that consists of two G protein coupled receptors, cannabinoid 1 receptor (CB_1R) and cannabinoid 2 receptor (CB_2R), endogenous endocannabinoid ligands as well as biosynthetic and degradative enzymes **[**Figure 1; (Devane *et al*., 1992; Matsuda *et al*., 1990; Mechoulam *et al*., 1995; Munro *et al*., 1993; Pacher *et al*., 2006; Petrosino *et al*., 2009)]. Increasing evidence supports the ECS as a key regulatory system in the control of a number of vital homeostatic functions including: feeding, metabolism, cardiovascular and CNS function (Burston & Woodhams, 2014; Chiou *et al*., 2013; Pacher *et al*., 2005; Vemuri *et al*., 2008). Additionally, the emerging role of the ECS in modulating pain and inflammation supports an important auto-protective role for the ECS in regulating sensory neural activity and immune system modulation (Ashton & Glass, 2007; Burston & Woodhams, 2014; Chiou *et al*., 2013; Rom & Persidsky, 2013; Tanasescu & Constantinescu, 2010; Ullrich *et al*., 2007; Vanegas *et al*., 2010). For example, it has been documented that changes occur in the levels of cannabinoid receptors and endocannabinoid ligands during inflammation and endogenous regulation of the ECS modulates the immune response

Figure 1. Endocannabinoid system. CB_1R in a neuron (left) and CB_2R in a leukocyte (right). Endocannabinoids [arachidonoyl ethanolamide (AEA) and 2-arachidonoyl glycerol (2-AG)] act at cannabinoid receptors and are transported into the cytoplasm of the cells to be degraded by enzymes [fatty acid amide hydrolase (FAAH) and monoacylglycerol lipase (MAGL), respectively].

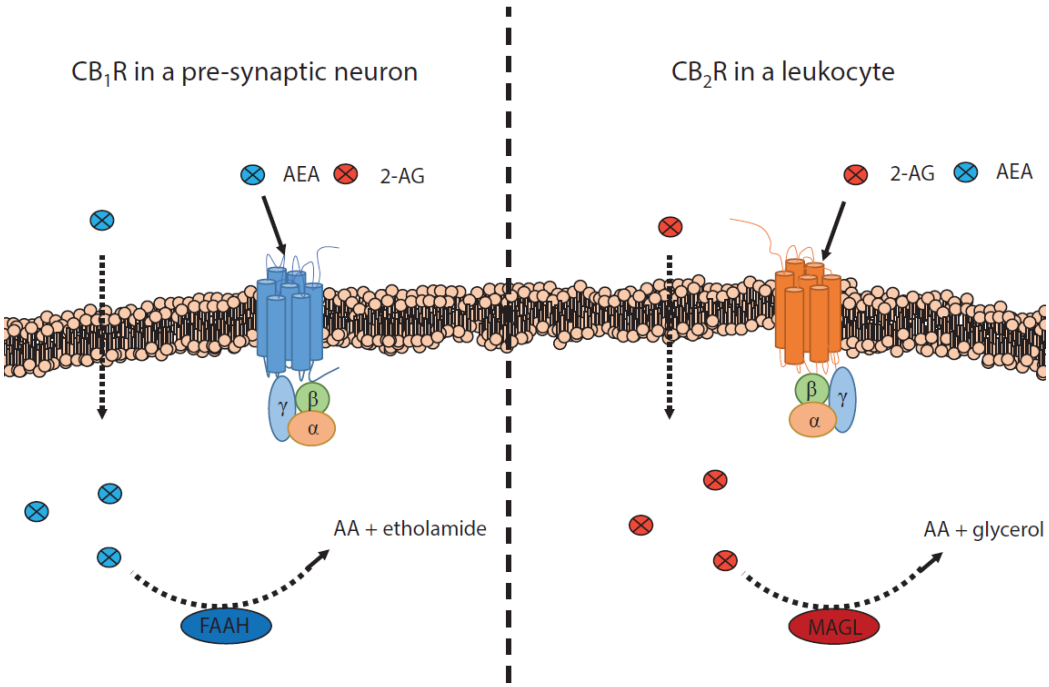
CB1R in a pre-synaptic neuron
CB2R in a leukocyte
AEA
2-AG
2-AG
AEA
γ
β
α
β
γ
α
AA + etholamide
AA + glycerol
FAAH
MAGL

(Maccarrone *et al*., 2002; Marini *et al*., 2013; McHugh & Ross, 2009; Ramirez *et al*., 2012; Tanasescu & Constantinescu, 2010). However, the use of ECS targeted drugs as therapeutics for inflammatory diseases, including those of the eye, still remains in its infancy. This reflects the need for further research identifying tissue-specific components of the ECS and the functional role of this important biological system in the physiology and pathophysiology of individual organs in the body.

Individual elements of the ECS including receptors, endocannabinoids and their cognate enzymes have been localized within the eye and evidence indicates that a local ocular ECS contributes to several essential ocular functions including: regulation of intraocular pressure, blood flow, retinal neuron activity and ocular immune response (Straiker *et al*., 1999). Ocular inflammation can result in decreased vision or blindness (Barisani-Asenbauer *et al*., 2012; Caspi, 2010; Chang & Wakefield, 2002; Read, 2006; Resnikoff *et al*., 2004). While therapeutics are currently available for ocular inflammation, many are ineffective, have deleterious side effects, or these drugs become refractory (Larson *et al*., 2011; Lehoang, 2012). The ECS, therefore, presents the opportunity to identify novel targets for the treatment of ocular inflammation. This thesis examines the role of the ECS in regulating the ocular immune response and, more specifically, focuses on the immunopharmacology of drugs that target cannabinoid receptors in the inflamed eye.

The following sections provide an introduction to inflammation and the immune system, with a specific emphasis on the ocular immune system and the role of the ECS. This is followed by the hypothesis and objectives for my research work examining ECS modulation in an *in vivo* model of endotoxin-induced uveitis and relevant *in vitro* cell systems.

1.1 Inflammation and the Immune System

Inflammation is the body's response to infection or tissue damage. Its purpose is to restore the structure and function of tissue with minimal negative consequences. Inflammation has classically been characterised by five major signs, which were described as early as 30 AD by Celsus and expanded by Virchow in 1858* (Ryan & Majno, 1977). The cardinal documented signs of inflammation as documented by Galen are *calor* (heat), *rubor* (redness), *tumor* (swelling), *dolor* (pain) and *function laesa* (loss of function) (Lawrence *et al*., 2002; Ryan & Majno, 1977). These processes occur due to alterations in vascular hemodynamics, infiltration of immune cells and the release of pro-inflammatory mediators. Inflammatory mediators are chemical messengers that interact with cells to potentiate or decrease inflammation (Larsen & Henson, 1983). The inflammatory response can occur over an acute or chronic time scale. Depending on the time scale, different types of immune responses occur, some of these

actions occur during both acute and chronic inflammation while other aspects are restricted to only one type of inflammation. Innate immunity is active during acute inflammation while adaptive immunity contributes more prominently during chronic inflammation. Each type of inflammation can associate with a particular set of processes to initiate the immune response. These immune system components are described below (sections 1.2.1-1.2.5) in the context of the inflammatory response.

1.1.1 Innate Immunity during Acute Inflammation

The innate immune system is the first line of defence, acting rapidly and non-specifically to limit possible infection and inflammation caused by a pathogen or trauma to tissue. Following an infection the innate immune system actively targets pathogens for destruction. The initial obstacle is the physical barrier created by the tissue epithelium, which inhibits pathogens from the environment from entering. In addition to a physical barrier, epithelial cells express and produce anti-microbial peptides including defensins (Tosi, 2005). Anti-microbial peptides can act primarily by creating pores in the cellular membrane or disrupting the electrostatic interactions of the lipid membrane of microbes (Tosi, 2005). Once inside the body, the complement system, a group of approximately 50 proteins localized within the plasma and on cell surfaces, acts to increase microbial and bacterial cell lysis, as well as recruit phagocytic cells

(Speth *et al*., 2015; Tosi, 2005). These reactions can occur in a number of ways including the interaction of antibodies known as immunoglobulins (Igs) binding to antigens on microbial pathogens. However, the end result of these pathways is the creation of a membrane-attack complex, a pore in the membrane leading to cell lysis (Fujita, 2002). If the pathogen is not directly lysed by the complement protein the complement protein can mark the pathogen to be phagocytized by white blood cells though a process called opsonisation (Speth *et al*., 2015). The most well defined components of the innate immune system are the actions of the immune cells including, polymorphonuclear leukocytes (PMNs) that comprise neutrophils, basophils and eosinophils and mononuclear cells including, monocytes, macrophages, and dendritic cells (DCs) (Takeda *et al*., 2003). These cells play important roles in the elimination of pathogens by actions such as phagocytosis, while some act as cellular sentinels to alert and activate other immune cells (Kumar & Sharma, 2010; McMenamin, 1997).

1.1.2 Immune Cells of the Innate Immune System

The cellular component of the innate immune system constitutes not only the immune cells, but additional cell populations including epithelial and endothelial cells (Takeda *et al*., 2003). The immune cells that are active in the innate immune system are derived from a myeloid linage of cells, hematopoietic stem cells, located in the bone marrow and spinal cord (Figure 2). Differentiation

Figure 2. Leukocyte differentiation. Leukocytes differentiate from hematopoietic stem cells to common myeloid progenitors or common lymphoid progenitors. Common myeloid progenitors change to myeloblast cells that can differentiate to PMN cells and monocytes. Myeloblasts can also differentiate to alternative cells such as erythrocytes. Common lymphoid progenitors are associated with the adaptive immune system.

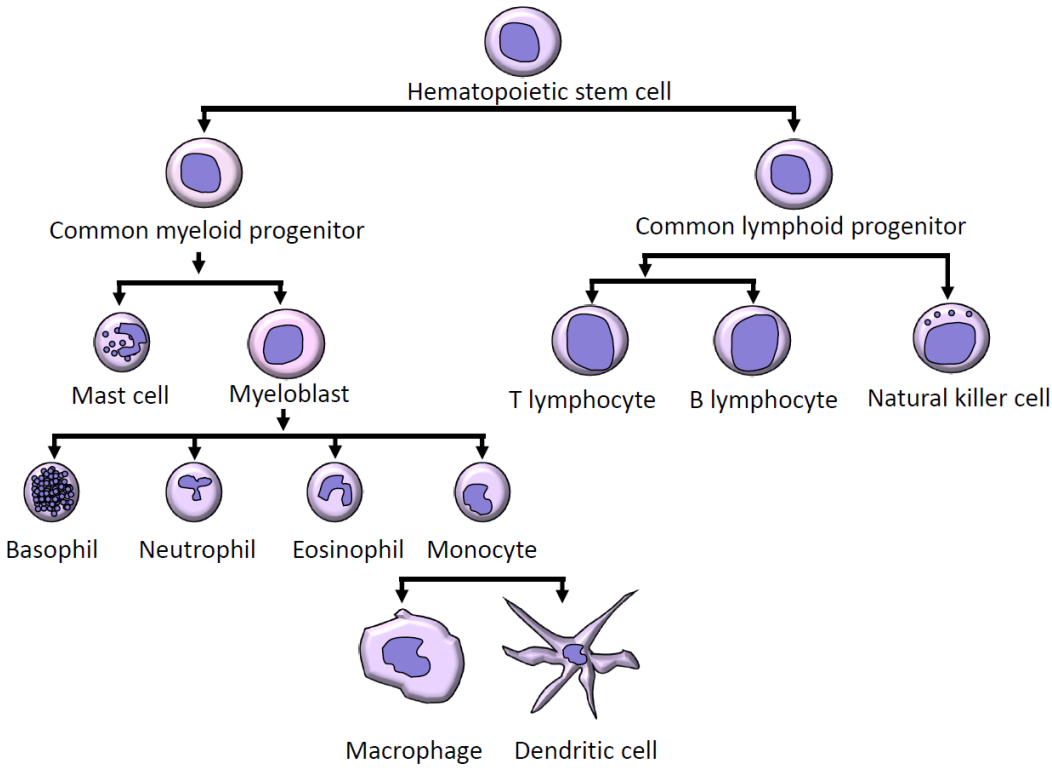
Hematopoietic stem cell
Common myeloid progenitor
Common lymphoid progenitor
Mast cell
Myeloblast
T lymphocyte
B lymphocyte
Natural killer cell
Basophil
Neutrophil
Eosinophil
Monocyte
Macrophage
Dendritic cell

into specific leukocytes occurs following exposure to growth factors and cytokines (Zhao *et al*., 2015). This myeloid linage of cells can be subdivided into cell types primarily based on nuclear composition; those that have multi-lobed nuclei, also known as PMNs, and those that have a unilobular nucleus/mononuclear cells including, monocytes, macrophages and DCs (Figure 2). Of the PMNs the most important cell type during the innate immune response is neutrophils, although this class also contains basophils and eosinophils (Takeda *et al*., 2003).

Neutrophils are the first line of immune cell defence in the innate immune system. They contribute to antimicrobial activity with cytotoxic granules that contain molecules such as myeloperoxidase, proteases, and lactoferrin, which undergo exocytosis to damage pathogens (Kumar & Sharma, 2010). Additionally, neutrophils can release neutrophil extracellular traps made from chromatin and proteases to effectively snare and kill bacteria (Kumar & Sharma, 2010). Neutrophils can also phagocytosis pathogens and release factors to attract more neutrophils and mononuclear cells. Once in proximity, neutrophils interact with these other immune cells to generate more inflammatory mediators, thereby amplifying the immune response (Kumar & Sharma, 2010).

Monocytes are important during inflammation for the destruction of pathogens. Monocytes survey the endothelial lining for integrity, recruit neutrophils when necessary and are precursors to mononuclear phagocytes

(macrophages and DCs). Although traditionally it was thought monocytes always gave rise to tissue resident macrophages, this is not always the case. More recently tissue resident macrophages have been shown to be derived from embryonic precursor cells early in development. These macrophages retain the ability to differentiate and repopulate tissue. These tissue resident macrophages function as phagocytic and antigen presenting cells (APCs) (Ginhoux & Jung, 2014). Another APC cell type is DCs, which primarily interact with T lymphocytes or T cells in the lymph tissue. These T cells are immune cells derived from an alternative lineage, the lymphoid lineage, and play a role in the adaptive immune response which will be briefly discussed below (Schenten & Medzhitov, 2011). This interaction initiates primary and secondary T cell activation and proliferation important in the adaptive immune response. An alternative type of DC, are located in the B-lymphoid follicle and these cells hold antigens for longer periods re-stimulating B lymphocytes (Hart, 1997). Two of the main roles of the immune cells of the innate immune system are phagocytosis and antigen presentation and these are described further below.

One of the primary functions of immune cells during the inflammatory response is to phagocytize foreign entities and damaged host cells. These phagocytic cells undergo leukocyte recruitment migrating to the site of inflammation, recognize microbes and ingest their cellular targets. These pathogens can also be destroyed by hydrolytic and proteolytic enzymes that are

release from immune cells. An additional mechanism to digest this material is generation of reactive oxygen species (Lawrence *et al*., 2002). The process of phagocytosis can work in synergy with the complement system by opsonisation, where an antigen of the compliment system (e.g complement component 3, C3) marks a pathogen cell for phagocytosis (Lawrence *et al*., 2002).

The other principal function of the innate immune system cells is the ability to present antigens to other immune cells, heighten the inflammatory response by activating leukocytes, enable proliferation, differentiation and prime the adaptive immune system (Holling *et al*., 2004; Hou *et al*., 2008; Xu *et al*., 2007). This group of cells, known as APCs constitutes macrophages and DCs in the periphery and microglia in the CNS (London *et al*., 2013). APCs play a vital role as the fundamental link between the innate and adaptive immune systems. The role of APCs during the innate response involves their recognition of pathogens and damaged cells, phagocytosis of these, and release of inflammatory mediators to recruit PMN cells (González-navajas *et al*., 2010; McMenamin & Crewe, 1995; Yanaba *et al*., 2009). The function of APCs in adaptive immunity involves all of the aforementioned, as well as additional roles outlined briefly in the following section (section 1.1.3).

1.1.3 Adaptive Immunity during Chronic Inflammation

The adaptive immune system is responsible for the expansion of antigen-specific T and B cell clones to target antigens and provide immunological memory (Figure 2). APCs stimulate T cells allowing for activation of other T and B cells (Schenten & Medzhitov, 2011). This occurs through the major histocompatibility complex (MHC) class I and II. These cell surface molecules bind pathogen fragments to APCs so they can be recognized by T cells (Holling *et al*., 2004). APCs also play a similar role in the adaptive immune response to innate immunity, releasing pro-inflammatory mediators. It is the continual activation and the inability to resolve this inflammation which underlies chronic inflammation. In cases of autoimmune diseases, T cells do not distinguish antigens made by the host from those of pathogens (Caspi, 2010).

1.1.4 Cellular Recognition of Pathogens: Pathogen Recognition Receptors

Immune, endothelial and epithelial cells use a specialized group of pattern recognition receptors (PRRs) to identify highly conserved molecular motifs called pathogen-associated molecular patterns (PAMPs) (Chang *et al*., 2006). Ligands for PAMPs are derived from bacteria, viruses and fungi including: lipopolysaccharide (LPS), lipoteichoic acid, peptidoglycans, specific motifs of bacterial DNA and viral RNA (Tosi, 2005). As the innate immune system can also be activated by tissue and cellular damage, PRRs also recognize endogenous

molecules released by damaged cells, called alarmins (Bianchi, 2007). There are several different classes of PRRs, including RIG-I-like receptors (RLRs), Nod-like receptors (NLRs) and Toll-like receptors (TLRs), each distinct family having several members, which respond to various PAMPs and alarmins (Kawai & Akira, 2010). One important PRRs are the TLR family. Since their initial discovery in the 90s, there have been over 10/12 different members revealed (humans/mice). The TLR family has two subgroups respective to where the receptors are localized, cellular surface receptors or intracellular receptors (Kawai & Akira, 2010). Upon activation by their respective ligands, PRRs signal to induce the inflammatory response (see section 1.3.7 for further explanation of the PRR, TLR4).

1.1.5 Vascular Dysregulation during Inflammation

The microcirculation is the narrowest vasculature branch of the circulatory system, consisting of blood vessels that are less than 100 μm in diameter and comprised of arterioles, capillaries and venules. The microcirculation serves several functions including, oxygen and nutrient transport, removal of waste such as CO_2 from tissues. The microcirculation plays a central role in the inflammatory response. The microcirculation is made of endothelial cells, pericytes, smooth muscle cells, and blood components: erythrocytes, leukocytes, platelets and plasma. (Ince, 2005). Blood flow though

the microcirculation is controlled by the vascular tone which is regulated by myogenic, metabolic and neurohumoral mechanisms that function though autocrine and paracrine actions (Klijn *et al*., 2008). Some of these regulating factors of vascular tone are altered during inflammation influencing hemodynamics within this system. Dysregulation of the microvasculature plays an important role in inflammation.

Upon an inflammatory assault the immune system releases inflammatory mediators that cause vasodilation. This phenomenon occurs because mediators such as nitric oxide (NO) interact with smooth muscle in the microvasculature leading to vasodilation and increased blood flow. In conjunction with vasodilation, NO and other mediators increase vascular permeability (Guzik & Korbut, 2003). During this process, inflammatory mediators up-regulate adhesion molecules on leukocytes and the endothelium, which induce leukocyte-endothelial interactions. Parallel to the increase in adhesion molecules, cytokines and chemokines are released, increasing leukocyte recruitment to the area of inflammation. Once at the site of inflammation, leukocytes undergo tethering, rolling, and adherence to the endothelium. This is followed by transendothelial migration (TEM) into the tissue to phagocytize pathogens and damaged host cells. During inflammation the body undergoes changes in physiology increasing the ability for leukocytes to be recruited and interact with the endothelium prior to TEM (Lawrence *et al*., 2002).

Vascular alterations are amongst the first changes that occur during inflammation altering the calibre (vessel diameter), flow and vascular permeability. These deviations are of utmost importance as they influence tissue and thus organ perfusion. Calibre and flow are regulated during inflammation by the release of NO and prostaglandins (prostaglandin D2, PGD_2, prostaglandin E2, PGE_2), causing vasodilation. Increases in vascular permeability can arise by two mechanisms 1) trauma and 2) PAMPs mediated inflammatory molecule release. During direct trauma, vascular leakage is not limited to one particular region and can occur at arterioles, capillaries and venules. In comparison, indirect changes to permeability by local mediators such as histamine and bradykinin mediate endothelial cell contraction and can increase leakage at post-capillary venules of the microcirculation (Guzik & Korbut, 2003; Ryan & Majno, 1977). Vascular leakage can be amplified by endothelial damage and dysfunction which can occur during the immune response. Leukocyte extravasation and neutrophil degranulation, normally beneficial, when exacerbated can breakdown gap junctions contributing to vascular damage (Gill *et al*., 1998; Xu *et al*., 2005). This over-amplification of the immune response results in a dysregulated microcirculation altering tissue perfusion, leading to alterations in red blood cell (RBC) rigidity, coagulation factors and immune function, ultimately ending in organ failure (Ince, 2005).

1.2 Mechanisms of Leukocyte Recruitment during Inflammation

Leukocyte recruitment is a fundamental process of the inflammatory progression, allowing leukocytes to eliminate pathogens and damaged tissue that give rise to inflammation. Recruitment of leukocytes to a site of injury is regulated by the release of pro-inflammatory cytokines and chemokines subsequent to the stimulation of a PRR, such as TLR4.

Cytokines are proteins or glycoproteins that act through paracrine or autocrine actions to coordinate the immune response that results from activation of PRRs located on immune cells and endothelial cells. Cytokines are produced by a multitude of cells including, leukocytes, keratinocytes, synovial cells, and osteoblasts (Borish & Steinke, 2003). Each cytokine plays a specific role in the immune system, interacting with particular receptors on leukocytes and endothelial cells to elicit their response; however there is redundancy and some cytokines bind to more than one receptor. This ligand promiscuity also allows individual cytokines to activate different signal transduction pathways via distinct receptors.

Cytokine receptors signal though intracellular domains, which consist of enzymes (kinases, phosphatases or proteases) and/or docking modules. Prior to activation of downstream signal cascades, receptor dimerization must occur (Grötzinger, 2002). Cytokine receptor activation is involved in cellular

development, growth, homeostasis, activation, differentiation, regulation, and functions of innate and adaptive immunity (Borish & Steinke, 2003).

Chemokines are a subset of cytokines that induce the chemotactic (migratory) response of leukocytes to inflamed endothelium as well as contribute to development and differentiation of leukocytes (Barreiro *et al*., 2010; Borish & Steinke, 2003; Griffith *et al*., 2014). There are four families of chemokines, these are named C-X-C, C-C, C and CX3C, based on their N-terminal cysteine groups where the cysteine(s) residue, (c) and an additional amino acid, (X), lie. The largest of these families are C-X-C which primarily targets neutrophils and C-C which interact with monocytes, dendritic cells and T-cells (Borish & Steinke, 2003). Interestingly, all chemokine receptors are G-protein coupled receptors (GPCRs), with exception of Duffy antigen receptor for chemokines (DARC), also known as atypical chemokine receptor (ACKR1). GPCR chemokine receptors signal through G_i subtype of G-proteins, while DARC is not coupled to a G-protein (Griffith *et al*., 2014).

LPS is a component of Gram negative bacteria's cellular wall, as such it is a PAMP which is used by PRRs to identify a pathogen in the body (Schenten & Medzhitov, 2011). LPS stimulation of the PRR, TLR4, induces synthesis and release of cytokines and chemokines is up-regulated. This occurs on endothelial cells, epithelial cell and immune cells, with each cell type releasing a specific set

of inflammatory mediators. For example, upon stimulation of TLR4, APCs induce, but are not limited to, increases in the expression of CXC chemokine ligand (CXCL)1, CXCL2, CXCL8, monocyte chemotactic protein 1 (MCP-1)/ CC chemokine ligand (CCL) 2, macrophage inflammatory protein (MIP) 1-α/ CCL3, MIP1-β/CCL4, regulated on activation, normal T cell expressed and secreted (RANTES)/ CCL5 and CXCL16 (Griffith *et al*., 2014). Additionally, TLR4 activation increases levels of cytokine tumor necrosis factor-α (TNF-α), interleukin (IL)-1β, interferon (IFN)-γ, IL-6 and chemokines IL-8 to name a few (Griffith *et al*., 2014; Krakauer, 2002; Toguri *et al*., 2014). In addition to direct up-regulation by LPS, chemokine and cytokine production can be modulated in an autocrine manner to increase the recruitment of leukocytes (Barreiro *et al*., 2010; Griffith *et al*., 2014). This increase recruits leukocytes which then interact with the endothelium.

In addition to the chemotactic stimuli, leukocytes respond to chemokines to upregulate levels of adhesion molecules (Barreiro et al., 2010; Hajishengallis & Chavakis, 2013). These adhesion molecules form bonds between inflammatory cells and the inflamed endothelium (Sarantos *et al*., 2005). Two categories of adhesion molecules exist, selectins and integrins. Selectins are primarily associated with the first steps of leukocyte-endothelial interaction, tethering and rolling (Figure 3). There are several different selectins involved in this process.

Figure 3. Leukocyte recruitment, endothelial interactions and TEM during inflammation. Leukocytes are recruited to a site of inflammation by cytokines and chemokines. Once in the microcirculation of the inflamed tissue, leukocytes interact with adhesion molecules called selectins resulting in tethering and then slow rolling. Leukocytes then bind to integrins which causes firm adhesion to the endothelium. Once firmly adhered to the endothelium, leukocytes exit the lumen through TEM and can then phagocytise pathogens or damaged cells.

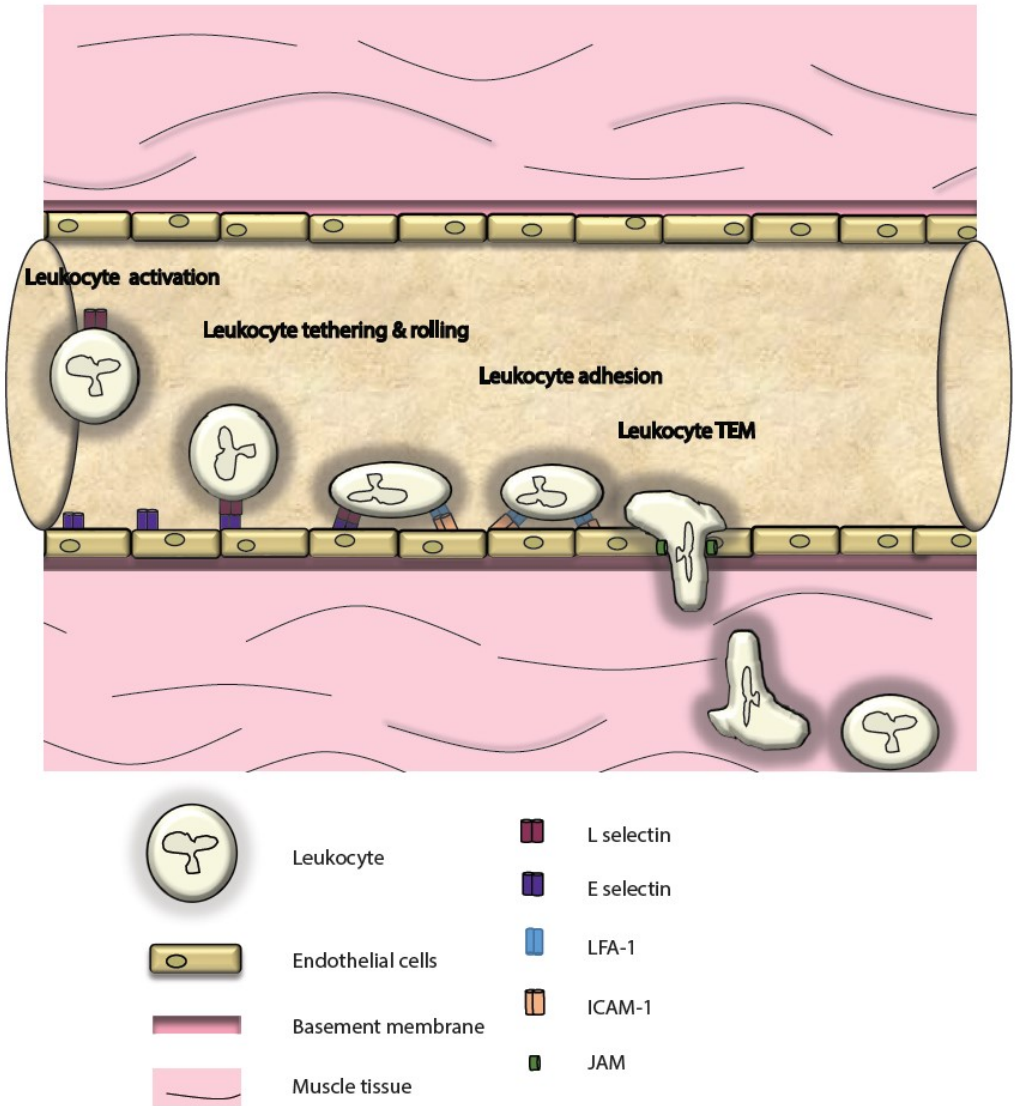
Leukocyte activation
Leukocyte tethering & rolling
Leukocyte adhesion
Leukocyte TEM
Leukocyte
Endothelial cells
Basement membrane
Muscle tissue
L selectin
E selectin
LFA-1
ICAM-1
JAM

P- and E- selectin on the endothelial surface interact with their ligands located on leukocytes. P-selectin is also found on platelets. P and E-selectin interact with L-selectin and P-selectin glycoprotein ligand (PSGL-1) expressed on leukocytes (Barreiro *et al*., 2010).Tethering of leukocytes to the endothelium occurs by interactions of selectins and their ligand thereby decreasing their velocity in the blood stream. Once leukocyte velocity is decreased both selectins and integrins can bind to their ligands on leukocytes. The final process of leukocyte-endothelial interactions is adhesion, where leukocytes firmly adhere to the endothelial wall prior to transendothelial migration. This process involves the alternative group of adhesion molecules, integrins. Similarly, to selectins, activated integrin expression is up-regulated by cytokine stimulation. Binding of chemokine receptors localised on leukocytes and endothelium during tethering and rolling alters the conformational shape of integrins into an active form. Once in this active form, integrins are able to bind to their ligands (Barreiro *et al*., 2010). Endothelial bound chemokines CXCL1, CXCL2 and CXCL8 interact with neutrophils to change leukocyte-endothelial interactions from rolling to adhesion (Griffith *et al*., 2014). The alteration of leukocytes rolling on the endothelium to firmly adhering to the vasculature also involves adhesion molecules called integrins. The integrins involved in this stage include intracellular adhesion molecule (ICAM)-1, ICAM -2, vascular cell adhesion molecule (VCAM)-1, and receptor for advanced glycation end products (RAGE); these integrins on the

endothelium interact with their ligands located on leukocytes; respectively, lymphocyte function-associated antigen (LFA)-1 (αLβ2; cluster of differentiation (CD)11a/CD18), macrophage-1 antigen (Mac-1) (CD11b/CD18), very late antigen (VLA)-4 (α4β1) (Fritz, 2011; Hajishengallis & Chavakis, 2013; Xie et al., 1995).

Differing populations of leukocytes have specific subsets of integrins. For example, LFA-1 is primarily associated with neutrophils and lymphocytes as opposed to VLA-4 which is preferentially found on monocytes (Barreiro *et al*., 2010). During inflammation, E-selectin, ICAM-1, VCAM-1 can undergo proteolytic cleavage and remain in the blood as soluble E-selectin (sE-selectin), soluble ICAM-1 (sICAM-1), and soluble VCAM-1 (sVCAM-1). Measurement of these inflammatory markers have often been used to quantify endothelial activation during an inflammatory response (Page & Liles, 2013; Witkowska & Borawska, 2004).

The final step in leukocyte recruitment is diapedesis or TEM. This is when leukocytes leave the lumen of the vasculature and undergo extravasation to the tissue primarily by passing though gap junctions; however, they have also been noted to go through transcellular routes (Barreiro *et al*., 2010). The process of TEM through gap-junctions is mediated by a specific subset of adhesion molecules, junctional adhesion molecules (JAMs) and platelet endothelial cell

adhesion moeleucle-2 (PECAM-2), in addition to LFA-1, Mac-1 and endothelial ICAM-1 and ICAM-2 (Barreiro et al., 2010; Hajishengallis & Chavakis, 2013). This process also can involve chemokines and their receptors, as is the case for CCL2 during neutrophil and monocyte TEM.

The last stage of the inflammatory response is clearance and resolution of inflammation. This is a highly controlled process involving the regulation of pro-inflammatory genes and transcription factors, the senescence of leukocyte activation and migration and the clearance of inflammatory cells (Lawrence *et al*., 2002). To counterbalance the elevated pro-inflammatory mediator levels that occur during inflammation, endogenous immunomodulatory mediators are released to facilitate resolution of inflammation and restoration of normal tissue function. Vascular tone, including permeability is decreased by release of several factors including adrenaline, noradrenaline and serotonin/ 5-hydroxytryptamine (5-HT) (Lawrence *et al*., 2002). Elevated levels of intracellular cyclic adenosine monophosphate (cAMP) suppress release of inflammatory mediators and modulate chemotaxis in a plethora of different immune cells (McHugh & Ross, 2009; Moore & Willoughby, 1995). Glucocorticoids are amongst the best-known endogenous anti-inflammatory agents. They resolve inflammation through inhibition of pro-inflammatory transcription factors in the nucleus, with resultant decreases in cytokine and chemokine production. Additionally, lipoxins and

cyclopentenone prostaglandins (cyPGs) also participate in resolving inflammation. Lipoxins are derived from arachidonic acid (AA) by lipoxygenase (LOX) or a combination of LOX and cyclooxygenase (COX) enzymes (Lawrence *et al*., 2002; Romano *et al*., 2015). Lipoxins inhibit chemotaxis of neutrophils and eosinophils, but also have chemoattractant properties for monocytes. This recruitment of monocytes has been proposed to function in clearance of necrotic and apoptotic cells. Although many COX metabolites are pro-inflammatory cyPGs have bene shown to have anti-inflammatory properties (Díez-Dacal & Pérez-Sala, 2010). These cyPGs are created from prostaglandins by spontaneously nonenzymatic reactions such as dehydration of PGE and PGD_2 (reviewed by Diex-Dacal and Perez-Sala, 2010). One cyPG with anti-inflammatory effects is $15dPGJ_2$which has been shown to decreasing leukocyte-endothelial interactions by inhibiting ICAM-1 and VCAM-1 (Lawrence *et al*., 2002).

The inflammatory response and its resolution are critical to preserve tissue and organ function from pathogens and damaged tissue. Despite the beneficial effects of inflammation, during a prolonged or dysregulated immune response the dynamic events triggered can stop being beneficial and become detrimental. In such cases, the amplified immune response contributes to the pathogenesis of some disease states (Lawrence *et al*., 2002). In an organ such as

the eye, the immune response must be tightly regulated to prevent vision loss and blindness that can result from ocular inflammation, as such the eye has developed a unique immunological property called immune privilege (sections1.3.3)

1.3 The Eye and Inflammation

In 2010 the World Health Organization (WHO) estimated that over 285 million people were living with visual impairment; 39 million of which were categorized as blind (Chestnov, 2013). Ocular inflammation contributes to the vast numbers of individuals with decreased or lost sight, accounting for up to 10% of blindness (Chang & Wakefield, 2002; Read, 2006). Ocular inflammation can occur due to many different factors, each causing specific cellular responses. There are three main categories by which ocular inflammation, known as uveitis occur, these are infectious, non-infectious and idiopathic inflammation (Fiorelli *et al*., 2010). Infectious forms of uveitis occur over acute and chronic time scales while ocular inflammation driven by autoimmune disorders are often persistent and recurrent (Chang *et al*., 2005; Fiorelli *et al*., 2010).The infectious agents range from bacteria, viruses, and fungi (Drancourt *et al*., 2008) while non-infectious causes occur by ocular trauma and autoimmune dysfunction (Parver *et al*., 2012; Wakefield *et al*., 2011). It is difficult to determine the exact incidence of individuals affected by each category of uveitis and the role of ocular

inflammation in the loss of sight as it is often a sequelae to cataracts, glaucoma and retinal damage, which account for the highest incidence of blindness (Suttorp-Schulten & Rothova, 1996).

1.3.1 Ocular Form and Function

The eye is divided into three anatomical layers: the sclera and cornea (outer layer), the uvea (middle layer), and the retina (inner layer). Figure 4 illustrates a schematic of ocular anatomy. The most anterior section of the eye is the cornea. The cornea is avascular and functions to protect the eye, however its structure is of utmost importance for sight. The transparency of the cornea, primarily made of collagen, allows for the refraction of light further into the eye. The posterior of the cornea connects with the sclera. The sclera is a protective layer of the eye, beginning just posterior to the cornea at the limbus and continuing to the optic nerve head. The sclera constitutes 85% of the external eye surface and is comprised of muscle and connective tissue (Oyster, 1999). The sclera attaches the eye to the rest of the body and maintains the curvature and axial length needed for many optical properties (Malhotra *et al*., 2011; Oyster, 1999). The uvea, or uveal tract, lies inner to the sclera and consists of the iris, ciliary body and choroid. The iris is a thin layer of tissue, which separates the anterior portion of the eye from the posterior, it is suspended between the

Figure 4. Anatomical structure of the eye. A sagittal section of the human eye. The anterior portion includes the cornea, iris, ciliary body, pupil, zonular fibers and aqueous humor. The posterior portion includes the retina and the optic nerve with the vitreous humor lying between the lens and the retina. The scleral tissue surrounds the eye.

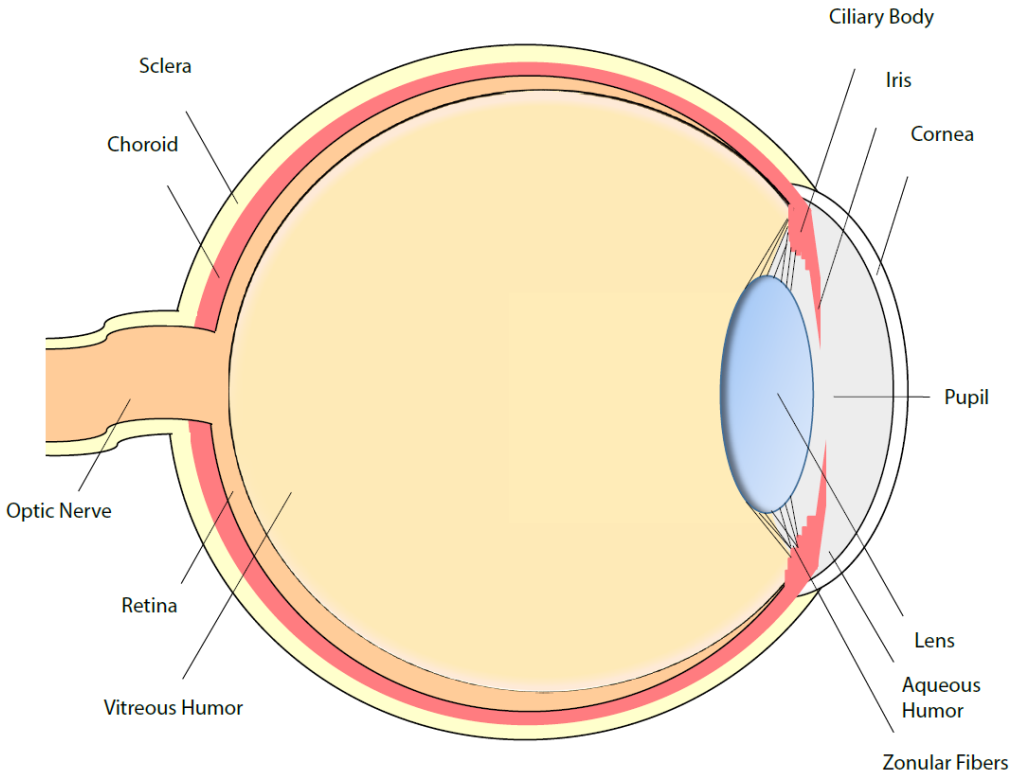
Ciliary Body
Sclera
Iris
Choroid
Cornea
Pupil
Optic Nerve
Retina
Lens
Aqueous
Humor
Vitreous Humor
Zonular Fibers

cornea and the lens in the aqueous humor (AH). This layer of tissue is made up of epithelium, stroma mix of fibroblasts, melanocytes collagen, blood vessels and muscle, and is responsible for the regulation of light into the eye through the pupil. This function is important to visual acuity as it affects image intensity, image spread, field of view and depth of focus (Oyster, 1999). Anchoring the iris to the globe of the eye is its attachment to the ciliary body, which then connects to the choroid. The ciliary body is the site of AH production, providing nutrition the cornea needs in addition to playing a role in the immunological functions of the eye (Taylor, 2003). In the AH, there are factors, such as calcitonin gene-related peptide (CGRP) which can interact with immune cells. These factors within the AH modulate immune cells in several ways, by suppression of macrophage activity, thus decreasing innate and adaptive immunity and direct immunosuppression by interaction with receptors on T cells of the adaptive immune system (Taylor, 2003). The ciliary body also anchors the lens in the globe by suspensory ligaments called zonular fibers. The position of the lens is imperative for vision as it functions to focus light onto the fovea of the retina (Purves *et al*., 2001). The retina is covered by the choroid, a vascularized tissue containing the arteries and veins that lead to the ciliary body and iris. The choroid provides the retina with sustenance through choroidal capillaries and the central retinal artery. The most inner layer of the eye is the retina, the sensory layer that transduces incoming light to an electrical signal and consists of: photoreceptors,

bipolar, horizontal and amacrine neurons and ganglion cells, the axons of which form the optic nerve. The retinal pigment epithelium (RPE) is a highly pigmented tissue that interfaces with the sensory retina and the choroidal vascular layer. The RPE plays a role in light absorption, secretion and ion transport, recycling of retinol during the visual cycle and phagocytosis of shed photoreceptor outer segments (Malhotra *et al*., 2011). The RPE is an integral part of the retinal (or blood ocular) barrier, which plays a role during inflammation. The RPE has been shown to respond to cytokines as well create a barrier of tight junctions inhibiting leukocytes from the periphery from easily entering into the retinal vasculature (Bharadwaj *et al*., 2013; Malhotra *et al*., 2011).

1.3.2 Ocular Inflammation

During ocular inflammation, a deregulated immune response is detrimental to ocular tissue function and can have sight-threatening consequences. The eye is a unique organ as it contains both the peripheral and CNS components of the immune system, although the two immune systems function by analogous mechanisms including the detection of pathogens. Similar to most other organ systems in the body, the eye has tissue resident macrophages and DCs that induce innate immune responses. These cell populations have been shown to be localized to the cornea, iris, ciliary body, and choroid, while no immune cells are present

in the AH and lens during normal conditions (Li *et al*., 2013; McMenamin *et al*., 1994; Pouvreau *et al*., 1998). Each immune cell population and its location is depicted in Figure 5. In the corneal epithelium specialised DCs called Langerhans cells are located in the stroma (Akpek & Gottsch, 2003; Hamrah *et al*., 2003), while in the iris both macrophages (700 - 800 cells/mm^2) and MHC II class DCs (400 - 500 cells/mm^2) are found in close proximity to the pupil and near the ciliary body (McMenamin, 1997). The choroid is highly populated with APCs (over 700 DCs/mm^2 and 400 macrophages/mm^2) found throughout the stromal connective tissue (McMenamin, 1997). Mast cells have been localized in the choroid, and may play a role in susceptibility to development of inflammation in some experimental models (McMenamin, 1997).

The immune cell population in the anterior eye is mirrored in the retina by microglia, macrophages and DCs within the connective tissue of the sclera (Eter *et al*., 2008; Kezic & McMenamin, 2008; London *et al*., 2013). The tissue resident populations of immune cells are shown in Figure 5. These cellular populations in the periphery are primarily divided between tissue resident macrophages and DCs. These cells have the ability to phagocytize foreign bodies, release inflammatory mediators, recruit and present antigens to immune cells, and induce differentiation and proliferation of other cells. Although the eye has a

Figure 5. The ocular immune system: resident immune cells. The sagittal section shows the anterior portion of the eye connecting to the posterior section with the type and location of resident immune cells. The most prominent concentrations of tissue resident immune cells in the eye are macrophages and DCs are localized to the uvea (iris, ciliary body and choroid). Microglia are only present in the retina.

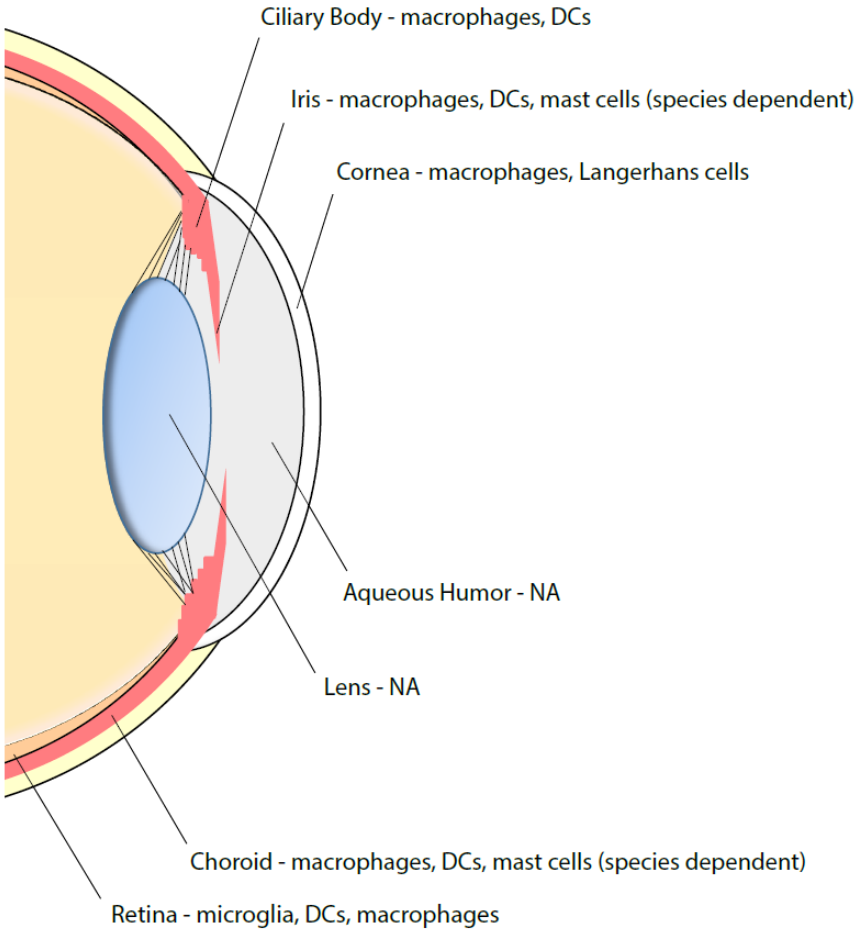
Ciliary Body - macrophages, DCs
Iris - macrophages, DCs, mast cells (species dependent)
Cornea - macrophages, Langerhans cells
Aqueous Humor - NA
Lens - NA
Choroid - macrophages, DCs, mast cells (species dependent)
Retina - microglia, DCs, macrophages

collection of resident immune cells acting as sentinels and activators of the immune system it also has a special condition known as immune privilege.

1.3.3 The Immune Privilege of the Eye: a Complicating Factor

The complexity of the ocular immune response is furthered complicated by the immune privilege status of the eye, and was first described by Medawar in 1948. The development of immune privilege in the eye is thought to have occurred as an evolutionary mechanism limiting the negative aspects of the immune response, such as tissue damage, which could pose a threat to sight. Immune privilege is a term that describes the series of processes that work cooperatively to accomplish this task. This includes the suppression of pro-inflammatory mediators, and inhibition of the induction of sensitization used in the adaptive immune response. Immune privilege is made up of two factors, those that are passive and are intrinsic to ocular anatomy, such as the physical barriers and active factors such as immunomodulatory proteins. Passive factors are barriers to decrease infiltration of immune cells to the ocular environment including the blood-ocular barrier formed by endothelial cells within the iridial and retinal vasculature, the epithelium bound by tight-junctions of the ciliary body and retina and the lack of lymphatic vessels within the eye (Streilein *et al*.,

2002). Active factors which contribute to the immune privilege, include the endogenous release of immunomodulatory factors into the aqueous humor such as transforming growth factor-β (TGF- β), immunoregulation via cell-to cell contact mechanisms with corneal endothelium and iris pigmented epithelium, and APC development of antigen tolerance (Caspi, 2010; London *et al*., 2013; Mochizuki *et al*., 2013; Streilein, 2003; Taylor & Kaplan, 2010). Together these adaptations help to maintain the ocular microenvironment and proper ocular function.

1.3.4 Uveitis: Intraocular Inflammation

Uveitis is an overarching term which describes inflammation of the uvea and the uveal tissue includes the iris, ciliary body and choroid. Additionally, uveitis can also refer to inflammation of the sclera, retina, vitreous and optic nerve (Larson *et al*., 2011; Read, 2006). As such, uveitis is not a single disease but instead a multitude of inflammatory conditions (Nussenblatt, 1990). Uveitis has a prevalence of 38 to 370 per 100,000 individuals, depending on population, and, as such, can be considered a rare disease (Barisani-Asenbauer *et al*., 2012; Chang & Wakefield, 2002; Read, 2006; Resnikoff *et al*., 2004). Despite the classification as a rare disease, uveitis is the fourth most common cause of blindness amongst the working-age population and is responsible for 2.8 to 10%

of blindness (Barisani-Asenbauer *et al*., 2012; Caspi, 2010; Chang & Wakefield, 2002; Read, 2006). In addition to visual loss, uveitis is responsible a significant economic burden associated with treatment, healthcare costs and resource utilization (Barisani-Asenbauer *et al*., 2012; Chu *et al*., 2013).

1.3.5 Etiology, Pathology and Treatment of Uveitis

The anatomical location of inflammation allows for several designations of uveitis: anterior, intermediate, posterior or pan-uveitis, with additionally classification of acute or chronic depending on the duration of the inflammation. The type of uveitis can also be sub-categorized by how the inflammatory response is generated. This ranges from infectious and non-infectious etiology and can occur as local effect within the eye or due to systemic complications (Larson *et al*., 2011). Infections can be caused by bacterial, fungal and viral pathogens while non-infectious etiology range from autoimmune dysfunction to trauma. Non-infectious uveitis can also occur due to systemic syndromes that are associated with autoimmune dysfunction such as juvenile arthritis and ankylosing spondylitits (Caspi, 2010). In addition to systemic influences, uveitis can be associated with other ocular diseases and can lead to their pathology. Cataracts, glaucoma and cystoid macular edema all are known co-morbidities of patients

with recurrent acute anterior uveitis (Markomichelakis *et al*., 2004; Smith *et al*., 1998).

As uveitis is associated with several different forms of ocular inflammation the recommended treatments coincide with disease progression. However, the current gold standard for the treatment of uveitis is corticosteroids (*i.e*. pregnisolone, dexamethasone) (Lehoang, 2012). Corticosteroid treatment is used in both infectious and non-infectious uveitis, often in conjunction with other treatments (Bodaghi *et al*., 2001; Chopra & Roberts, 2001; Ghannoum & Rice, 1999; Lehoang, 2012). Corticosteroids work by binding to glucocorticoid response elements, which control gene transcription, most notably nuclear factor kappa-light-chain-enhancer of activated B cells (NF-κB) and activator protein-1 (AP-1) (Lehoang, 2012). Although corticosteroids remain the primary treatment of uveitis, there are many associated adverse effects with these drugs, which are dependent on both dose and duration of therapy (Lehoang, 2012; Uchiyama *et al*., 2014). Topical therapies decrease inflammation in the short term, though patients are often subject to recurring bouts of uveitis with an unknown outcome for a final prognosis (Lehoang, 2012). Side effects ranging from the development of cataracts in upwards of 15% of patients, increases of intraocular pressure (often resulting in glaucoma), increased susceptibility to infection, impaired wound healing, cornea and scleral thinning are among a long list of adverse effects

associated with steroid use (reviewed by LeHoang, 2012 and Uchiyama *et al*., 2014) . NSAIDs were the primary treatment for uveitis prior to corticosteroid availability. NSAIDs exhibit their anti-inflammatory properties by inhibition of the cyclooxygenase pathway, decreasing the synthesis of prostaglandins, which play a role in vascular permeability and cytokine expression (Ricciotti & Fitzgerald, 2011). Due to limited efficacy in uveitis, NSAIDs are often used in high dose and in conjunction with other treatments. Chronic use of NSAIDs can lead to severe side effects such gastrointestinal (GI) ulcers and increased risk of cardiovascular problems including myocardial infarction and stroke (Fiorelli *et al*., 2010).

When uveitis is induced by pathogens, treatment regiments also include antimicrobials (antibiotics, antivirals and/or antifungals) in addition to immunosuppression. These antimicrobials are generally well tolerated by patients eliminating the pathogen, however they do not resolve the inflammation (Bodaghi *et al*., 2001; Chopra & Roberts, 2001). In aggressive, chronic uveitis treatment regiments can include antimetabolites and alkylating agents (often used for treating cancer), however due to the serious side effects such as bone marrow suppression, increased liver enzymes and leukopenia these treatments are final resorts (Heo *et al*., 2012; Larson *et al*., 2011).

In recent years, there has been a number of biological therapeutics that have been undergoing clinical trials with some that have been introduced to the clinic. These biologics use antibodies to selectively target cellular receptors (e.g CD20), cytokines (e.g. TNF-α) and growth factors (e.g. vascular endothelial growth factor, VEGF) that modulate the immune response (Heo *et al*., 2012; Larson *et al*., 2011). Some of these treatments target specific types of ocular inflammation such as Rituximad, a CD20 antibody, causing lysis of B cells for improvement of autoimmune dysfunction (Heo *et al*., 2012). Although some alternative treatments have become available they are associated with serious risk factors such as increased chances of developing cancers, aggravation of demyelinating disease and congestive heart failure (Heo *et al*., 2012).

In summary, current pharmacological treatments for uveitis are not sufficient and are subject to a medley of side effects. This is true for both classical treatments and newer biological agents, the latter of which also are associated with considerable expense and the need to be administered by a healthcare professional (Dick, 2000; Larson *et al*., 2011). The lack of appropriate treatments for uveitis underscores a need for identification of new therapeutic agents to be investigated for the treatment of ocular inflammatory disease and points to the need for continued development of relevant experimental models to provide an

increased understanding of the roles that the innate and adaptive immune system play during disease progress.

1.3.6 Animal Models of Uveitis

To properly identify new therapeutics for inflammation, appropriate animals models are often used, and this is no exception in uveitis. In general, uveitis is described by the anatomical location and duration of the inflammatory pathology. In a clinical setting, acute uveitis is considered uveal inflammation that lasts for no longer than 3 months, anything longer than this is considered to be chronic inflammation, as defined by the International Uveitis Study Group. Unfortunately, in experimental modeling of uveitis a time course of over 3 months is a considerable period (Hill *et al*., 2005). Many investigators consider models of uveitis to be chronic when inflammation does not naturally resolved by one week. Existing animal models of uveitis include endotoxin-induced uveitis, using systemic or intraocular injection of endotoxin, or the use of combinations of melanin protein/retinal antigens for induction of experimental autoimmune uveitis/uveoretinitis (EAU) and experimental melanin-induced uveitis (Al-Banna *et al*., 2013).

My research utilized an experimental model of endotoxin-induced uveitis generated by either systemic or intravitreal injection of LPS to generate inflammation within the eye (Rosenbaum *et al*., 1980). The endotoxin, LPS, a component of Gram-negative bacterial cell wall, is able to induce an exaggerated inflammatory response by increasing inflammatory mediators such as cytokines, chemokines and adhesion molecules and activating the innate immune system. Systemic injection of LPS produces a robust acute response in the anterior section of the eye and is widely used as an animal model of acute anterior uveitis seen in humans called endotoxin-induced uveitis (EIU) (Wakefield *et al*., 2011). In 1995, Quian *et al*., conducted a study in which they determined that not all animal strains were equally susceptible to EIU. Here they determined that compared to other commonly used in-bred and out-bred strains, the BALB/c strain of mice, an in-bred strain, develops more severe uveitis (Li *et al*., 1995). It has also been noted in the literature that the inflammatory response to systemic LPS is species specific and is not as robust in mice as it is in rats (Rosenbaum *et al*., 2011). My research work (Toguri *et al*., 2014), as well as that of others (Kezic *et al*., 2011; Rosenbaum *et al*., 2011), has reported that direct injection of LPS by intravitreal injection, another type of EIU, induces a robust inflammatory response in both rats and mice and that this response is more pronounced depending on mouse strain *i.e* BALB/c > C57 BL/6. The molecular mechanisms and signaling pathways associated with LPS-induced inflammation in other organs have

previously been reported (Dyson & Singer, 2009; Lehmann *et al*., 2014; Płóciennikowska *et al*., 2014; Yuan *et al*., 2011). In the eye, as elsewhere, inflammation occurs via activation of TLR4 signaling (Chen *et al*., 2009; Kezic *et al*., 2011; Li, Lu, *et al*., 2010) (see section 1.3.7).

1.3.7 LPS and TLR4 Signaling

LPS is a PAMP which acts as a ligand for the PRR, TLR4 (Poltorak, 1998). TLR4 activation has been attributed to be the cause of severe septic shock in patients with infections of Gram-negative bacteria that contain LPS (Dyson & Singer, 2009; Lehmann *et al*., 2014; Płóciennikowska *et al*., 2014). TLR4s are located on a variety of cells including antigen presenting cells (macrophages and dendritic cells), granulocytes (neutrophils, eosinophils and basophils), T cells, B cells, endothelial and epithelial cells (González-navajas *et al*., 2010; Parker *et al*., 2005; Takeda *et al*., 2003; Yanaba *et al*., 2009). TLR4 is a transmembrane bound receptor, with PAMP recognition located on the extracellular domain, transmembrane domains, and an intracellular Toll-interleukin 1 (IL-1) receptor (TIR) domains which permits downstream signal transduction (Kawai & Akira, 2010). The signaling cascade of TLR4 can be seen in Figure 6. LPS requires LPS-binding protein (LBP) to form a complex which is recognized by CD14; subsequently LPS then can interact with TLR4 (Takeda *et al*., 2003). Upon

Figure 6. The Toll-like receptor 4 (TLR4) pathway. The TLR4 is a PPR which can be stimulated by LPS. Activation of TLR4 causes signal transduction via two pathways, the myeloid differentiation primary-response protein 88 (MyD88) and MyD88-independent or TRIF pathway. Both pathways lead to increased transcription of pro-inflammatory genes, resulting in synthesis of cytokines, chemokines and adhesion molecules.

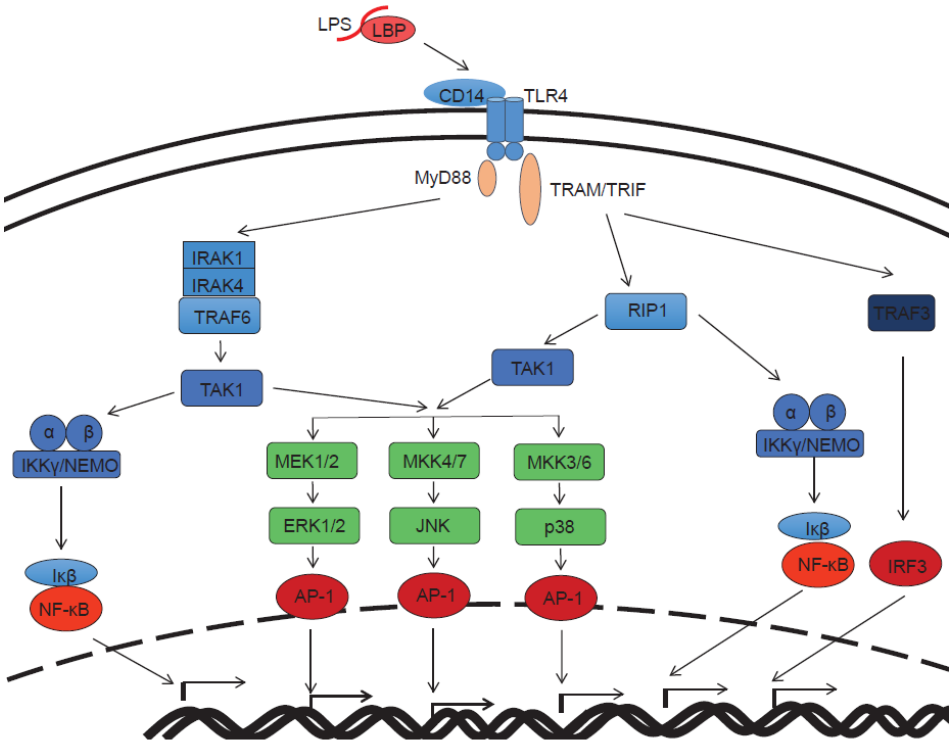

Gene transcription of cytokines, chemokines and adhesion molecules

interaction of CD14 and TLR4, myeloid differentiation primary-response protein 88 (MyD88) is recruited to activate one of downstream signaling pathways; alternatively, signaling can also occur in a MyD88 independent manner. In 2011, Kezic *et al*., used MyD88 genetic knockout mice to demonstrate the involvement of the MyD88 pathway in EIU (Kezic *et al*., 2011). Downstream signaling of the MyD88 pathway includes activation of IL-1 receptor-associated kinases-1 and -4 (IRAK1 and IRAK4) and TNF-receptor associated factor 6 (TRAF6). TRAF6 diverges into two pathways; one to cause dissociation of the inhibitor of nuclear factor kappa-light-chain-enhancer of activated B cells kinase (IKK) complex (Akira & Takeda, 2004a; Karin, 1999). Activation of the IKK complex results in phosphorylation of inhibitor of NF-κB. Once phosphorylated, NF-κB translocates from the cytoplasm into the nucleus where it acts as an early phase transcription factor leading to the production of tumor necrosis factor (TNF-α), interleukin (IL) -1β and IL-6. The second pathway activated by TRAF6 recruits transforming-growth- factor-β-activated kinase (TAK1) (Akira & Takeda, 2004a; Karin, 1999). Activation of TAK1 allows for a mitogen-activated protein kinases (MAPKs) signaling to occur. This leads to the phosphorylation of c-Jun N-terminal kinases (JNKs), extracellular-signaling-regulated kinases (ERKs), p38 and cAMP response-binding protein (CREB), leading to the activation of transcription factor AP-1. Transcription of AP-1 increases pro-inflammatory cytokines such as TNF and IL-12 (Blasius & Beutler, 2010).

The MyD88-independent path or TRIF pathway acts through a different cellular signaling pathway to activate a later phase NF-κB and interferon-regulatory factor 3 (IRF3), a transcription factor for the products interferon (IFN) (Akira & Takeda, 2004a). The MyD88-independent pathway occurs by the TIR of TLR4, activating the TIR-domain-containing adaptor protein inducing INF-β (TRIF) as well as TRIF-related adaptor molecule (TRAM). These molecules independently continue signaling. First, TRIF activates inhibitor of NF-κB kinase ε (IKK-ε), then phosphorylates TRAF-family-member-associated NF-κB activator binding kinase 1 (TBK1) activating the transcription factor, interferon-regulatory factor 3. TRAM activates NF-κB, causing translocating into the nucleus (Akira & Takeda, 2004a).

Taken together, evidence supports EIU as a robust, well established model for studying mechanisms of ocular inflammation (Kezic *et al*., 2011; Rosenbaum *et al*., 2011) and a useful research tool to identify putative novel experimental treatments that can target PAMP signaling, including ECS modulatory drugs (Toguri *et al*., 2014).

1.4 The Endocannabinoid System

1.4.1 Cannabinoid ligands for Treatment of Ocular Inflammation

The most important discovery to the field of cannabinoids was the extraction and isolation of Δ^9 -tetrahydrocannabinol (THC) in 1964 from the *Cannabis sativa* plant by Gaoni and Mechoulam (Gaoni & Mechoulam, 1964). To-date, there have been over 60 unique compounds extracted from the cannabis plant. These constitute one category of cannabinoid ligands called phytocannabinoids, all of which are derived from the cannabis plant (Sagar *et al*., 2009). The discovery of phytocannabinoids subsequently led to the synthesis of cannabinoid analogs which can be divided into four classes: classical cannabinoids, structurally similar to Δ^9-THC; non-classical cannabinoids with structures related to CP-55,940 (CP), the first synthetic cannabinoid to confirm the presence of CB_1R in the brain (Lambert & Fowler, 2005; Pacher *et al*., 2006); aminoalkylindoles, structurally similar to WIN55,212-2 (WIN) a synthetic cannabinoid agonist, and eicosanoid-related compounds (Lambert & Fowler, 2005; Pacher *et al*., 2006). Eicosanoids are lipid signaling molecules that are derived from omega-3 or omega-6 fatty acids like AA (Kasuga *et al*., 2015). Non-selective cannabinoid receptor agonists, such as CP and WIN, act at both CB_1R and CB_2R, while ligands such as arachidonyl-2-chloroethylamide (ACEA), and [(1R,2R,5R)-2-[2,6-dimethoxy-4-(2-methyloctan-2-yl)phenyl]-7,7- dimethyl-4-

bicyclo[3.1.1]hept-3-enyl] methanol (HU308), are selective for CB_1R and CB_2R, respectively. Antagonists/inverse agonists of CB_1R include 1-(2,4-Dichlorophenyl)-5-(4-iodophenyl)-4-methyl-N-4-morpholinyl-1H- pyrazole-3-carboxamide (AM281) and 1-[2-(morpholin-4-yl)ethyl]-2-methyl-3-(4-methoxybenzoyl)-6-iodoindole (AM630) is an antagonist for CB_2R (Lambert & Fowler, 2005).

Endocannabinoids are endogenous cannabinoid ligands that are lipid derivatives from AA. The first endocannabinoid to be identified by Devane *et al*. (1992) was arachidonoyl ethanolamide (AEA). AEA was aptly named, anandamide, a word derived from *ananda*, the Sanskrit word for bliss (Devane *et al*., 1992). AEA has a high affinity for CB_1R and elicits a similar response in animals to Δ^9-THC. Following the discovery of AEA, a second endocannabinoid, 2-arachidonoylglycerol (2-AG) was discovered by Mechoulam *et al.,* (1995) and Sugiura *et al*., (1995). AEA acts as a full and/or a partial agonist of CB_1R depending on the cell type/tissue and biological response measured (Gonsiorek *et al*., 2000). AEA also binds to CB_2R but with lower affinity than 2-AG (Gonsiorek *et al*., 2000; Tanasescu & Constantinescu, 2010). Both AEA and 2-AG are synthesised *de novo* instead of stored within cells (Pacher *et al*., 2006). Synthesis of AEA primarily occurs by enzymatic hydrolysis via a phospholipase D from the membrane lipid N-arachidonoyl phosphatidylethanolamide (NAPE) as depicted in Figure 7A. Other synthesis pathways have been proposed such as

Figure 7. Endocannabinoid synthesis and degradation. Synthesis and metabolism of (A) AEA (B) 2-AG.

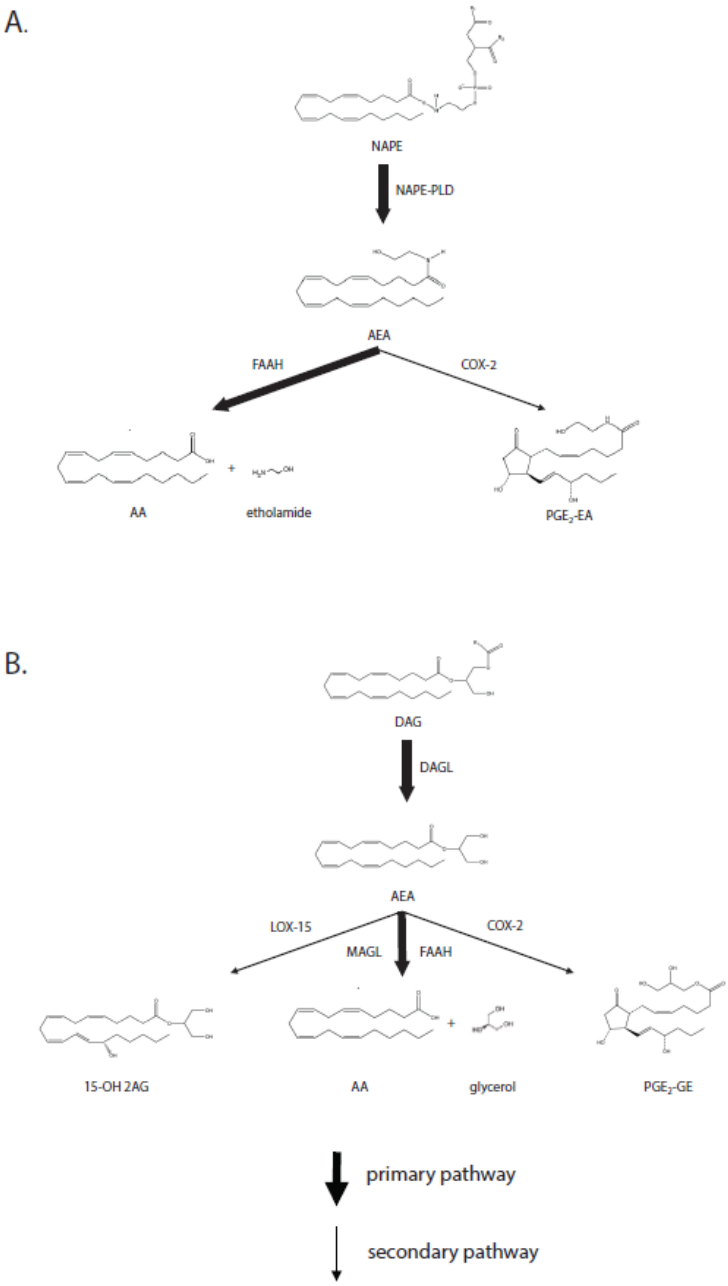
A.
NAPE
NAPE-PLD
AEA
FAAH
COX-2
AA
etholamide
PGE2-EA
B.
DAG
DAGL
AEA
LOX-15
MAGL
FAAH
COX-2
15-OH 2AG
AA
glycerol
PGE2-GE
primary pathway
secondary pathway

phospholipase A2 (PLA_2) that catalyzes hydrolysis of N-acyl-PE to N-acyl-lysoPE. This N-acyl-lysoPE can be changed to anandamide by lysoPLD. 2-AG synthesis occurs from the second messenger diacylglycerol (DAG) by DAG lipase (Figure 7B) (Pacher *et al*., 2006).

Once synthesised and released, endocannabinoids must be internalised intracellularly and degraded. Evidence has been generated supporting the existence of an anandamide (endocannabinoid) membrane transporter at the plasma membrane, however at this time no credible candidate has yet been cloned (Fowler, 2013; Hillard, 2000; Nicolussi & Gertsch, 2015). Other postulates are that endocannabinoids can passively diffuse across the plasma membrane by facilitated diffusion. This theory relies on a concentration gradient of endocannabinoids driving transport (Fowler, 2013; Nicolussi & Gertsch, 2015). To create a concentration gradient that drives endocannabinoids into the cell, the endocannabinoids within the cell must be degraded. AEA is metabolised by a fatty acid amide hydrolase (FAAH) to AA and ethanolamine (Figure 7A) while 2-AG is degraded by both FAAH and monoacylglycerol lipase (MAGL) to AA and glycerol (Figure 7B), although 2-AG is primarily metabolised by MAGL (Pertwee, 2006) (Figure 7A&B). Alternative, other minor pathways for endocannabinoid metabolism include the cyclooxygenase-2 (COX-2),

lipoxygenase (LOX), cytochrome P450, and serine hydrolases (Savinainen *et al*., 2012; Zelasko *et al*., 2014).

1.4.2 Cannabinoid Receptors

Cannabinoid receptors CB_1R and CB_2R, both belong to the Rodopsin-like G-protein coupled receptor (GPCR) family containing seven transmembrane domains. Interestingly, CB_1R and CB_2R lack high levels of homologous, with similarities in only 44% of their proteins and 68% of transmembrane domain (Pacher *et al*., 2006). CB_1R was first cloned by Matsuda *et al*. in 1990 and is highly localized in the central nervous system (CNS) and peripheral nervous system (PNS) on nerve terminals where receptor activation inhibits neurotransmitter release. Activation of CNS CB_1R generates the psychotropic effects and hypokinesia and catalepsy that is associated with smoking marijuana (Pertwee, 2006). In the periphery, CB_1R is also localized to adipocytes, leukocytes, spleen, thymus, heart, smooth muscle, vascular epithelium, retina and the urinary and reproductive system (Begg *et al*., 2001; Galiègue *et al*., 1995a; Liu *et al*., 2000; Munro *et al*., 1993; Murumalla *et al*., 2011; Straiker *et al*., 1999).

CB_1R preferentially signals via coupling to $G\alpha_{i/o}$ G proteins, as seen in Figure 8 (Bosier *et al*., 2010). Most notably CBR activation leads to the inhibition of

Figure 8. Cannabinoid receptor signaling: CB_1R and CB_2R. The left side of the diagram signaling pathways activated or inhibited by the stimulation of neuronal CB_1R, while the right side depicts signal transduction pathways coupled to CB_2R activation on leukocytes.

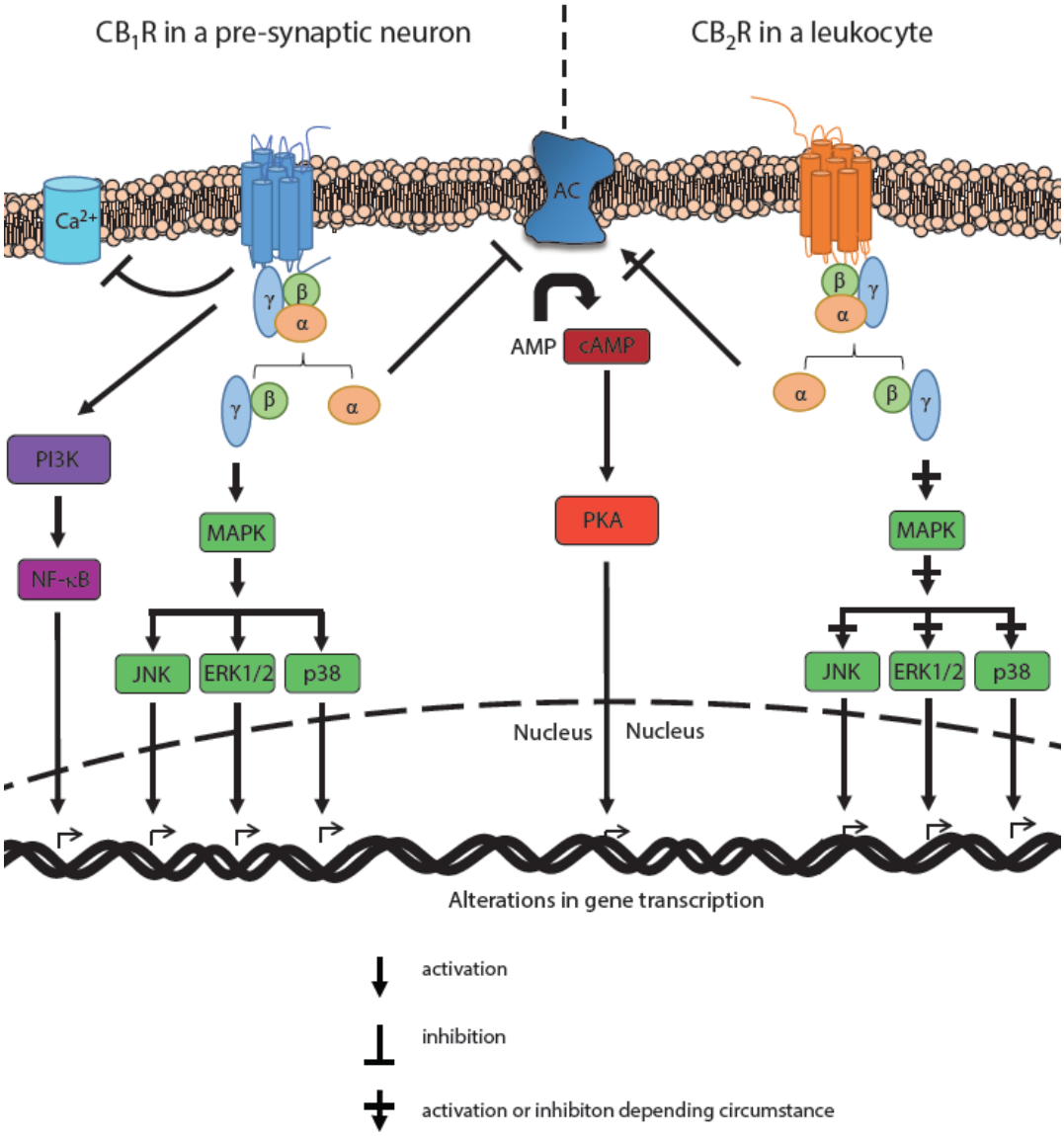
CB1R in a pre-synaptic neuron
CB2R in a leukocyte
Ca2+
AC
γ
β
α
AMP
cAMP
PI3K
NF-κB
MAPK
PKA
JNK
ERK1/2
p38
Nucleus
Nucleus
Alterations in gene transcription
activation
inhibition
activation or inhibiton depending circumstance

adenylate/adenylyl cyclase (AC), decreasing levels of adenosine monophosphate conversion to cyclic adenosine monophosphate (cAMP) in cells. Diminished cAMP reduces activation of protein kinase A (PKA) which is responsible for phosphorylating cyclic AMP response-element binding-protein (CREB), a transcription factor (Bosier *et al*., 2010). CREB has a multitude of functions including inducing proliferation, survival and differentiation in a variety of cells, some of these include monocytes macrophages and T and B cells (Kyriakis & Avruch, 2001; Mangmool & Kurose, 2011). It has been reported that the Gβγ subunit of the $G_{i/o}$-protein can activate mitogen activated protein kinases (MAPKs), which include extracellular signaling kinase -1 and -2 (ERK1/2), c-Jun N-terminal kinase (JNK) and p38 MAPK (Bosier *et al*., 2010; Howlett & Mukhopadhyay, 2000; Krishnan & Chatterjee, 2012; Tanasescu & Constantinescu, 2010). Activation of CB_1R activates the MAPK signaling and modulates transcription factors regulating cell survival, apoptosis and glucose metabolism (Bosier *et al*., 2010). Other signal transduction pathways include CB_1R inhibition of N- and P/Q-type voltage-gated Ca^{2+} channels and activation of inwardly rectifying K^+ channels (Bosier *et al*., 2010). CB_2R was initially identified from cDNA from human promyelocytic leukaemia cell line, HL60 and also from rat macrophages in the marginal zone of the spleen (Munro *et al*., 1993). Subsequently, it has been demonstrated that CB_2R are primarily localized on a variety of immune cells (Galiègue *et al*., 1995b). Activation of the CB_2R has

immunomodulatory properties influencing release of inflammatory mediators including cytokines, chemokines and adhesion molecules, inhibition of chemotaxis of immune cells, and modulate proliferation and antigen presentation (De Filippo et al., 2013; Matias et al., 2002; McHugh et al., 2008; Pertwee, 2006; Rajesh et al., 2007; Rom et al., 2013). Immune cell subsets have been shown to have varying levels of CB_2R mRNA, with B-cells > natural killer cells > monocytes > polymorphonuclear cells > CD 8 T cells > CD 4 T cells (Galiègue *et al*., 1995b). Interestingly, the expression of CB_2R has been shown to be a function of the cells activation state and can be mediated by inflammatory mediators (Mukhopadhyay *et al*., 2006). CB_2Rs are also localized on APCs, macrophages and dendritic cells which play a large role in the immune response (Adhikary *et al*., 2012; Matias *et al*., 2002). Besides the expression of CB_2R on immune cell they are found on osteoclasts, osteoblasts and osteocytes, influencing bone mass, endothelial cells, the testes, the gastrointestinal system, and peripheral nerve terminals (Atwood & MacKie, 2010; Sophocleous *et al*., 2011; Tanasescu & Constantinescu, 2010). In addition to the periphery, CB_2Rs are reported in the brain where they have been proposed to be on endothelial cells, immune cells and neurons (Pacher *et al*., 2006; Ramirez *et al*., 2012; Tanasescu & Constantinescu, 2010; Van Sickle *et al*., 2005).

Similarly to CB_1R, CB_2R is well defined to couple to $G\alpha_{i/o}$ signaling pathways modulating AC and cAMP levels and MAPKs modulation [Figure 8, (Choi *et al*., 2013; El-Remessy *et al*., 2003; Hanus *et al*., 1999; Howlett & Mukhopadhyay, 2000; Rom & Persidsky, 2013; Romero-Sandoval *et al*., 2009; Tanasescu & Constantinescu, 2010)]. This in-turn influences cAMP levels and the PKA pathway with both stimulation and inhibition of cAMP levels reported dependant on the duration of agonist activation of CB_2R receptor (Basu & Dittel, 2011). Additionally within the immune system, CB_2R agonists modulate AMP-activated protein kinase (AMPK) (Choi *et al*., 2013), MAPKs (El-Remessy *et al*., 2003; Howlett & Mukhopadhyay, 2000; Rom & Persidsky, 2013; Romero-Sandoval *et al*., 2009), MKPs (Casals-Casas *et al*., 2009; Eljaschewitsch *et al*., 2006; Romero-Sandoval *et al*., 2009). These signaling cascades directly modulate transcription factors responsive element binding protein (CREB) (Choi *et al*., 2013; Wen *et al*., 2010), NF-κB (Do *et al*., 2004; Toguri *et al*., 2014), AP-1 (Jeong *et al*., 2013; Toguri *et al*., 2014) and nuclear factor of activated T-cells (NFAT) (Ngaotepprutaram *et al*., 2013) which regulate cellular growth, differentiation, proliferation and release of the inflammatory mediators (Casals-Casas *et al*., 2009; Kaminski, 1998). In addition to CB_1R and CB_2R, several recently de-orphaned receptors have been suggested to be novel candidate cannabinoid receptors, including GPR55, GPR18 and GPR119. However, while these receptors can bind some cannabinoids, the endogenous ligands for these

receptors are lysophosphatidic acid (LPI), N-arachidonoyl glycine and oleoylethanolamide (OEA), respectively (Brown, 2007; Henstridge *et al*., 2009; McHugh *et al*., 2010a). In addition to these receptors, there is evidence for some cannabinoids activating nuclear peroxisome proliferator- activated receptors (PPARs), transient receptor potential vanilloid type 1 receptor (TRPV1), as well as non-receptor targets including, Ca^{2+},Na^{+} or K^{+} channels (Bosier *et al*., 2010). Several of these targets have recently been shown to have anti-inflammatory including GPR18, GPR119, PPAR-α and TRPV1 (Brown, 2007; Hu *et al*., 2014; McHugh *et al*., 2010b; O'Sullivan *et al*., 2010; Verme *et al*., 2005).

1.4.3 Cannabinoid Receptor Modulation and Ocular Inflammation

Both CB_1R and CB_2R agonists have been investigated for use as anti-inflammatory agents. With respect to the role of CB_1R during inflammation, peripheral administration of the endocannabinoid, AEA, decreased capsaicin-induced edema, an effect attributed to CB_1R mediated decreases in neuropeptide secretion and a reduction in neurogenic inflammation (Richardson *et al*., 1998). Rossi *et al*., (2011) also reported that CB_1R regulates inflammation-induced neurodegeneration during experimental autoimmune encephalomyelitis (EAE) in a mouse model of multiple sclerosis (MS); CB_1R genetic knock-out (KO) mice exhibited a worse clinical EAE outcome than wild type (WT) animals, while

deletion of FAAH, with resultant increases in AEA levels, decreased severity of EAE (Rossi et al., 2011a). In contrast to the anti-inflammatory properties of CB_1R, several reports have described pro-inflammatory actions of CB_1R stimulation. Use of CB_1R antagonist SR141716 inhibited retinal cellular death during a mouse model of diabetic retinopathy attenuating oxidative stress, decreasing NF-κB, ICAM-1 and VCAM-1 in the retina (El-Remessy *et al*., 2011). CB_1R antagonism was demonstrated to decrease leukocyte-endothelial adhesion in the intestinal microcirculation during systemic LPS induced inflammation (Kianian *et al*., 2013). In addition to this, CB_1R activation in human endothelial cells induced reactive oxygen species, which can lead to vascular dysfunction (Rajesh *et al*., 2010). In other studies, Smith *et al*., (2000) reported that the non-selective cannabinoids WIN and HU210 decreased serum levels of TNF-α and IL-12 in mice primed with bacteria and challenged with LPS and this effect was partially antagonised by CB_1R block with SR141716. Additionally, CB_1R has also been reported to have vasomodulatory actions, which could influence inflammation. CB_1R antagonism inhibited the hypotension caused by LPS during endotoxic shock in rats (Varga *et al*., 1998) and increased aortic, carotid, mesenteric and renal blood flow in animals during endotoxemia (Kadoi *et al*., 2005). These findings are important as vasodilation of the microcirculation improves tissue perfusion during inflammation (Bagher & Segal, 2011).

In contrast to the somewhat contradictory role of CB_1R modulation during inflammation, there is a vast amount of literature describing the anti-inflammatory properties of CB_2R activation reviewed by (Basu & Dittel, 2011; Berdyshev, 2000; Rom & Persidsky, 2013). CB_2R activation possess several anti-inflammatory properties, which differentially effect the inflammatory response. These effects has been demonstrated in many different models of inflammation, using CB_2R agonists and CB_2KO animals (Sardinha *et al*., 2014; Tschöp *et al*., 2009),in both the periphery and CNS. Reports have documented that activation of CB_2R play an integral role in the progression of leukocyte recruitment, inhibiting neutrophil activation and recruitment when the CB_2R gene is knocked out (Tschöp *et al*., 2009). Results from animal models using CB_2R stimulation show decrease gene and protein expression of important inflammatory mediators (cytokines, chemokines and adhesion molecules), recruitment of leukocytes to areas of inflammation and decreases in tissue damage and death associated with an over-amplified immune response (Facchinetti *et al*., 2003; Gómez-Gálvez *et al*., 2015; Sardinha *et al*., 2014; Tomar *et al*., 2015; Xu *et al*., 2007; Zarruk *et al*., 2012). There are several hypotheses about how CB_2R activation modulated inflammatory mediators; however, it is more than likely that different ligands can signal though alternative pathways dependant on the cell type and the inflammatory stimuli (Bosier *et al*., 2010; Howlett & Mukhopadhyay, 2000; Tanasescu & Constantinescu, 2010).

1.5 Hypothesis and Objectives

Current treatments administered for ocular inflammation are often inadequate, with limited efficacy or unacceptable side effects. Existing literature indicates that cannabinoid receptor modulation is anti-inflammatory and could be a suitable therapeutic target.

My hypothesis is that the ECS plays an integral role during the ocular immune response and that activation of the CB_2R can decrease inflammation. The goal of this research is to examine the effects of cannabinoid receptor modulation on measurable outcomes of inflammation.

The specific objectives are: 1) To evaluate the effects of cannabinoid receptor modulation in animal models of ocular inflammation 2) Elucidate the anti-inflammatory effects of CB_2R modulation and efficacy against current clinical treatments for ocular inflammation 3) Investigate the role of the ECS, and signaling transduction pathways involved during ocular inflammation and the effect of CB_2R activation.

Chapter II: Methods

2.1 Animals

All animal care and experimental procedures complied with the Canadian Council for Animal Care guidelines (http:// www.ccac.ca/) and were approved by the Dalhousie University Committee on Laboratory Animals. All studies involving animals are reported in accordance with the ARRIVE guide-lines for reporting experiments involving animals (http://www.nc3rs.org.uk/). Animals were housed in ventilated racks and allowed to acclimatize for a minimum of one week in the Carleton Animal Care Facility (CACF) at Dalhousie University, Halifax, Canada. All animals were kept on a light/dark cycle (07:00–19:00), with standard room temperature 22°C, humidity between 55% -60% and fed ad libitum.

Male Lewis rats were purchased from Charles River Laboratories International Inc., (Wilmington, MA, USA) and used in experiments when they were a size of 250 – 400 g. Male BALB/c mice (Charles River) used for experiments were from 20 – 30 g. CB_2R knockout animals on a BALB/c background were bred in-house by crossing male CB_2KO mice on a C57BL/6J congenic background (strain B6.129P2-Cnr2tm1Dgen/J; Jackson Laboratory, Bar Harbour, ME, USA) with inbred BALB/c female mice (Charles River) for 6

generations. Heterozygote mice from separate parents were then bred for a homozygote knock-out of the CB_2R. Conformation of animals lacking the CB_2R was conducted by genotyping.

2.1.1 Genotyping of CB_2KO mice

Polymerase chain reaction **(**PCR) genotyping of the knock-out mice was performed from DNA extracted from ear punches using Accustart II Mouse Genotyping Kit (Quanta Biosciences, MD, USA) according to manufacturer's instructions. The following specific PCR primers were used: moIMR0086 (GGG GAT CGA TCC GTC CTG TAA GTC T; mutant forward), oIMR7552 (GAC TAG AGC TTT GTA GGT AGG CGG G; common backward), and oIMR7565 (GGA GTT CAA CCC CAT GAA GGA GTA C; wild-type forward). The PCR program was 94°C for 1 min, 30 cycles of 94°C 30 s, an annealing temperature of 62.5 °C for 30 s, and 72°C for 1 min. Samples were loaded in a on 1.5% gel at 125 V for 35 min. The expected results were a single band at ~ 550 base pairs (bp) for a CB_2R knock-out (CB_2KO), a single band at ~ 385 bp for a wild-type (WT) and a band at ~ 550 and 385 bp for heterozygote animals (Figure 9) .

Figure 9. DNA banding patterns distinguising WT, CB_2KO, and heterozygote animals during genotyping protocol and gel electrophoresis. This was conducted while generating a CB_2KO mouse colony on a BALB/c background.

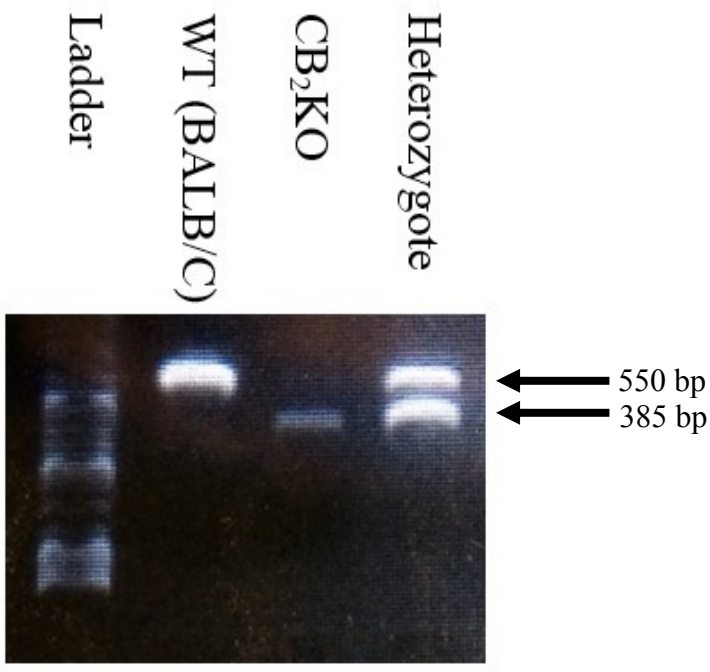
Heterozygote
CB2KO
WT (BALB/C)
Ladder
550 bp
385 bp

2.2 Anesthesia

All animals were weighed prior to experiments using a commercially available scale. Rats were anesthetized given an intraperitoneal (i.p.) injection of sodium pentobarbital (65 mg/kg; Ceva Sante Animale, Montreal, QC, Canada). Anesthesia for mice was given by an i.p. injection of sodium pentobarbital (65 mg/kg; Ceva Sante Animale) or induced by isoflurane and depth of anesthesia was monitored by toe pinch. Depth of anesthesia was assessed by toe pinch every 15 min for the duration of the experiment. Anesthesia was maintained by additional injections of pentobarbital either intravenously (i.v.) or i.p. as needed.

2.3 Femoral Vein and Artery Catheterization of Rats

Rats were placed on a heating pad to maintain their temperature at 37 °C and monitored and recorded via a rectal thermometer every 15 min for the duration of the experiment. The groin region of the rat was shaved and cleaned with isopropyl alcohol swabs (Health Care, Toronto, Canada). An incision was made in the inner thigh that was approximately 2-3 cm and the femoral artery and vein are cannulated with the PE 50 catheters. Catheters were made by enveloping a 23 gauge needle with Intramedic Non-radiopaque polyethelene tubing (PE 50; Clay Adams, Sparks, MD, USA) and secured by an epoxy adhesive. This

occurred by dissection of the femoral artery and vein by blunt forceps. Once the vein and artery were dissected the distal ends are ligated by silk string. Pressure was applied to the proximal end of the vessel by a loose surgical knot and cut with micro-scissors at the distal end. The curved fine tipped forceps are inserted into the vessel and used to open the interior so that the PE 50 catheter is applied to the proximal end of the vessel by a loose surgical knot and cut with micro-scissors at the distal end. The curved fine tipped forceps are inserted into the vessel and used to open the interior so that the PE 50 catheter can be inserted into the vessel using forceps. Catheters were secured by firmly tying the silk string on the proximal end of the vessel. This was further secured by attachment of both proximal and distal string to a piece of surgical tape placed on the catheter. Both catheters were attached to intravenous (i.v.) infusion pumps (Lifecare 5000 Plum Infusion Pump; Abbott, IL, USA) in conjunction with the Marquette Eagle 4000 Patient Monitor (General Electric, North Bergen, NJ, USA). The venous system at a continuous infusion rate of 1ml/hour of saline (0.9% Sodium Chloride) and the arterial system at a continuous rate of 2ml/hour for administration of fluid (0.9% Sodium Chloride). Haemodynamic variables, including mean arterial pressure (MAP and heart rate (HR) were measured from the arterial catheter every 15 min. Animals with a MAP below 70 mm Hg were excluded from the study (Dellinger *et al*., 2013). The venous catheter was used for the

administration of drugs, anesthetic agents and fluorochromes. Rats were euthanized, under anaesthesia, by i.v. injection of KCl (0.142 mL·kg−1).

2.4 Endotoxemia Induced by Systemic LPS Challenge in Rats

Rats were anesthetized and cannulation of the femoral vein and artery occurred as described previously. A baseline level of inflammation was measured by intravital microscopy (IVM) prior to any injection of LPS or saline. Details of IVM will be outlined in section 2.6. After baseline measurements were conducted rats were administered 2 mg/kg lipopolysacharide i.v. (LPS, *Escherichia coli,* 026:B6, Sigma-Aldrich, Oakville, ON, Canada) dissolved in normal saline (0.9% sodium chloride, Hospira, Montreal, QC, Canada) over 15 min to generate endotoxemia. Control animals received an i.v. bolus of normal saline at an equal volume. As described blood pressure, heart rate and temperature were measured every 15 min. IVM measurements were conducted hourly after LPS administration for 2 hr. Laser Doppler flowmetry (LDF), described in section 2.7 was also conducted at baseline, 1 and 2 hr. Cannabinoid treatments were given 15 min following induction of endotoxemia. When antagonists were administered, they were given prior to agonists. An experimental timeline is given in Figure 10.

Figure 10. Experimental timeline for endotoxemia studies in rats.

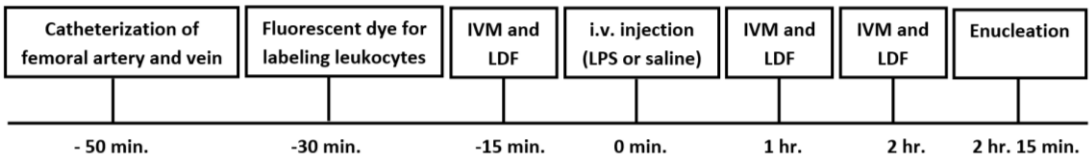
Catheterization of femoral artery and vein
Fluorescent dye for labeling leukocytes
IVM and LDF
i.v. injection (LPS or saline)
IVM and LDF
IVM and LDF
Enucleation
- 50 min.
-30 min.
-15 min.
0 min.
1 hr.
2 hr.
2 hr. 15 min.

2.5 Endotoxin-Induced Uveitis (EIU) by Intraocular Injection in Rats and Mice

Intravitreal injection of either LPS or saline was given into the left eye, through the pars plana, under a WILD M37 dissecting microscope (Leitz Canada, Kitchener, ON, Canada) using a Hamilton syringe (Hamilton Company, Reno, NV, USA) fitted to a 30G needle. Control animals received 5 µL of sterile saline, while experimental animals were injected with 100 ng LPS (Escherichia coli, 026:B6, Sigma-Aldrich, Oakville, ON, Canada) in 5 µL of saline. Once the injection was completed, pressure was applied to the puncture wound with autoclaved q-tips and 3M Vetbond Tissue Adhesive (3M Animal Products, St. Paul, MN, USA) was used to glud shut the wound.

A similar procedure was conducted for mice, however mice were anesthetized by isoflurane. Mice received similar intravitreal injections, however control animals received 2 µL of sterile saline, while experimental animals were injected with 250 ng LPS (125 ng/µl; *E. coli* 026:B6 L8274 lot 100M4102V; Sigma-Aldrich, Oakville, ON, Canada) in 2 µL of saline. If blood entered the orbit of the eye animals were immediately sacrificed. This technique was modified from Becker *et al*., 2000.

Rats were studied each hour for the first 6 hr, when leukocyte-endothelial adhesion was maximum, in addition to no overt changes in gross tissue

morphology/histology. Following this, preliminary trials were conducted in mice and IVM was only conducted at 6 hr. Drug treatments were given either i.v. or topically 15 min after intraocular injection of LPS. An experimental timeline is given in Figure 11 and Figure 12 for experiments conducted with rats and mice, respectively.

2.6 Intravital Microscopy

The iridial microcirculation was observed with the Olympus OV 100 Small Animal Imaging System (ON, Canada). The OV100 contains an MT-20 light source and a DP70 CCD camera (Suetsugu *et al*., 2011). Fluorescence excitation was generated by a xenon lamp (150W), and eight position excitation filters to block for rhodamine-6G (excitation 515– 560 nm, emission 590 nm) and FITC (450–490 nm, emission 520 nm). Images were captured by a black and white DP70 CCD C-mount camera in real time and recorded in a digital format by the software Wassabi (Hamatsu, Herrsching, Germany) on a computer connected to the OV100. Rats and mice were placed in a stereotactic frame (Kopf, CA, USA), and Tear-Gel® (Novartis Pharmaceuticals Canada Inc., Dorval, QC, Canada) was placed on the cornea to prevent dehydration of the tissue throughout the experiment. Rhodamine-6G (1.5 mL·kg−1; Sigma-Aldrich) and FITC-

Figure 11. Experimental timeline for EIU in rats by intravitreal injection of LPS. IVM was conducted hourly.

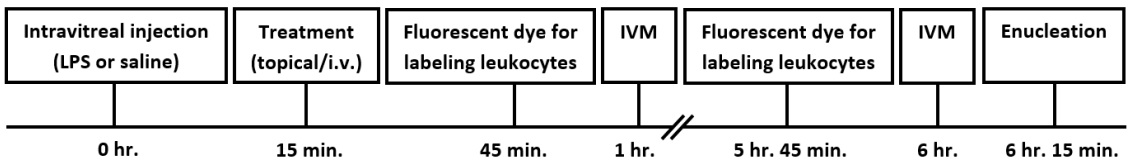
Intravitreal injection (LPS or saline)
Treatment (topical/i.v.)
Fluorescent dye for labeling leukocytes
IVM
Fluorescent dye for labeling leukocytes
IVM
Enucleation
0 hr.
15 min.
45 min.
1 hr.
5 hr. 45 min.
6 hr.
6 hr. 15 min.

Figure 12. Experimental timeline for EIU in mice by intravitreal injection of LPS.

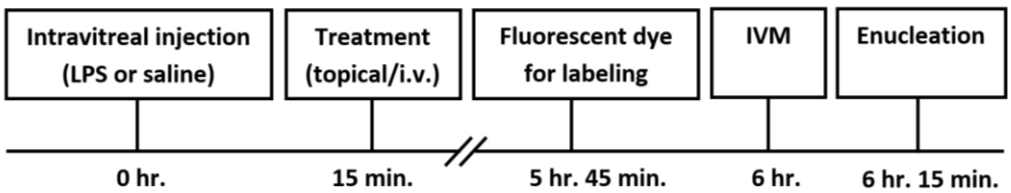
Intravitreal injection
(LPS or saline)
Treatment
(topical/i.v.)
Fluorescent dye
for labeling
IVM
Enucleation
0 hr.
15 min.
5 hr. 45 min.
6 hr.
6 hr. 15 min.

albumin (1 mL·kg−1; Sigma-Aldrich) were injected i.v. 15 min before initiating intravital microscopy (IVM). The fluorescent dye rhodamine-6G labelled mitochondria in leukocytes within the vessel and FITC-albumin allowed for the visualization of blood flow through the vasculature. Animals were placed on a heating pad to maintain body temperature at 37°C. IVM was carried out in four regions of interest. In each region of interest, four randomly selected vessels were observed, and 30 s recordings were made per hour of each vessel for the duration of the experiment. For IVM studies, data were analysed off-line without knowledge of the treatment groups. Recordings of the iridial microcirculation were analysed using the imaging software ImageJ (National Institute of Health, USA). The length, measured between points of branching and diameter of the vessels were used to calculate the endothelial surface. Adhering leukocytes were defined as white blood cells that were attached to the vessel wall and were immobile for a 30 s observation period; adhering cells were reported as the number of cells per square millimetre of endothelial surface. Leukocytes which interacted with the endothelium at a slower velocity than midstream blood cell velocity past an arbitrary line perpendicular to the endothelial wall during the 30 s were quantified as rolling leukocytes.

Initially, examination of vessels was divided into those that were greater or less than 25 μm in diameter; vessels of greater than 25 μm are confluent vessels in the rat microvasculature. No measurements were conducted in vessels larger

than 100 μm. Following our initial study, we examined all vessels of the microvasculature, with no distinction of their diameter.

2.7 Laser Doppler Flowmetry

Laser Doppler flowmetry (LDF) was used to measure the iridial microcirculation blood flow (IMBF). This method quantifies IMBF by the detection of erythrocyte movement by the Doppler effect. A glass fibre laser Doppler probe (diameter 120 μm, wave length 810 nm, resulting penetration depth about 1–2 mm) is used to monitor infrared light from a fibre optic cable to measure the light scatter by stationary tissue and moving blood cells within a region of interest approximately 1 mm^3 in area. Scattered light from moving cells results in a Doppler frequency shift of the infrared light while stationary tissue does not. This Doppler frequency shift is then quantified by analysis of the backscatter of light proportional to the flow of blood cells within the region of interest.

LDF readings were taken from rat eyes following placement of a glass fiber laser Doppler probe 1-2 mm away from the cornea at a 90° angle so as to not come in contact with any tissue. The laser Doppler probe was focused on the iridial vasculature and IMBF measurements were taken for 180 sec at 5 min before systemic injection of either saline or LPS, and at 60 and 120 min after injection. The LDF signal was recorded using a PeriFlux System 5000 (Perimed

Inc., Ardmore, PA, USA) and DIAdem 8.0.1 software (National Instruments, Vaudreuil-Dorion, Quebec, Canada). All LDF values were calculated after normalization to baseline blood flow readings as 100% for each animal.

2.8 Tissue Collection

Following IVM and or LDF rat eyes were enucleated, bi-dissected with the use of micro-scissors and a dissection plate at the corneal-scleral junction to obtain anterior uveal tissue. The eye was held in place by 30 g needle and the dissection plate was covered in ice cold water on a bed of ice to decrease protein degradation. Once complete, tissue was flash frozen in liquid nitrogen in a cryogenic tube and stored at –80°C for subsequent use. Alternatively, eyes were enucleated and fixed in 4% paraformaldehyde (PFA) for histology.

2.9 Heamotoxylin and Eosin Staining

Following fixation, eyes were immersed in 30% sucrose for 24–72 h at 4°C. The lens was removed by creating an opening with micro-scissors in the posterior region of the eye. Whole eyes were then frozen in OCT compound and sectioned (10 μm) using a Leica CM1950 cryostat (Leica Microsystems Inc., Concord, ON, Canada). Tissue sections were cut at 10 μm, mounted onto Superfrost glass slides (Fisher Scientific, Nepean, ON, Canada) and allowed to air dry overnight. Slides were then placed into Wheaton jars and covered with

Harris's haematoxylin (Sima-Aldrich, Oakville, ON, Canada) for 5 min and rinsed with tap water. Slides were then immersed in a solution of 1% acid alcohol (70% ethanol solution with 1 M HCl) under running tap water for 10-15 sec. Sections were then placed in Scott's tap water for 2 min and then dipped in the 1% acid alcohol solution until the background was clear. Sections were then stained in 1% acidified eosin for 5-10 sec, with loner staining for more contrast between tissues. Sections were then dehydrated by undergoing dipping into increasing graded alcohol solutions (50%, 70%, 95%, 100%) and cleared with xylene. Cover slips were then added using Cytoseal (Stephens Scientific Riverdale, NJ, USA). Sections were then visualized using light microscopy.

2.10 Multiplex Assay of Inflammatory Mediators

Anterior (iris, ciliary body and cornea) tissue was homogenized in 100 µL of PBS and 1% BSA, supplemented with a protease inhibitor cocktail (Sigma, St. Louis, MO, USA) for 2 min on a bed of ice. Homogenates were centrifuged at 13 000× g for 15 min at 4°C twice and supernatant was collected. The Bio- Rad Protein Assay (Mississauga, ON) was used to determine protein concentration according to the manufacturer's instructions to make protein loading consistent for each sample. Homogenates were aliquoted into autoclaved 1.5 ml tubes and frozen at -80 °C.

Multiplex ELISAs were conducted after protein was diluted to a concentration of 3620 μg/mL in PBS then diluted 1:1 in rat diluent provided within the Procarta Multiplex Cytokine Assay Kit (Freemont, CA, USA). The Bio-Rad 200 instrument was calibrated and validated prior to each experiment. Samples were analysed for TNF-α, IL-1β, IL-6, IL-10, INF-γ, CCL5, CXCL2, sVCAM and ICAM using a Procarta Multiplex Cytokine Assay kit from Affymetrix and the Bio-Rad 200 instrument with Bio-Plex software according to the manufacturer's instructions. All samples were run in duplicate. A standard curve for each inflammatory mediator was generated using the reference cytokine concentrations supplied with the kit.

Briefly, 50 μl of polystyrene beads conjugated to antibodies were added to a flat-bottom 96 well plate and washed with buffer. Following this 50 μl of sample with diluent, standards and negative controls were added to the wells. After incubation at 300 rpm and 30 min in darkness plates were washed thrice. Streptavidin-PE was then incubated in absence of light for 10 min. Plates were washed three more times and the Bio-Rad 200 luminometer was used to read plates.

2.11 Quantitative Reverse Transcription Polymerase Chain Reaction

RNA was harvested from supernatant from homogenized ocular tissue in 500 µL of PBS and protease inhibitor cocktail (Sigma) using the Trizol® (Invitrogen; Life Technologies Inc., Burlington, ON, Canada) extraction method according to the manufacturer's instructions. Reverse transcription reactions were carried out with SuperScript III® reverse transcriptase (+RT; Invitrogen), or without (−RT) as a negative control for use in subsequent PCR experiments according to the manufacturer's instructions. Two micrograms of RNA were used per RT reaction. Quantitative reverse transcription polymerase chain reaction **(**qRT-PCR) was conducted using the LightCycler® system and software (version 3.0; Roche, Laval, QC, Canada). Reactions were comprised of a primer-specific concentration of MgCl2 (Table 1), 0.5 µM each of forward and reverse primers (Table 1), 2 µL of LightCycler FastStart Reaction Mix SYBR Green I, and 1 µL cDNA to a final volume of 20 µL with distilled water (Roche). The PCR program was 95°C for 10 min, 50 cycles of 95°C 10 s, a primer-specific annealing temperature for 5 s, and 72°C for 10 s (Table 1). Experiments included sample-matched RT controls, a no-sample distilled water control and a standard control containing product- specific cDNA of a known concentration. cDNA abundance was calculated by comparing the cycle number at which a sample entered the logarithmic phase of amplification to a standard curve generated by amplification

of cDNA samples of known concentration (LightCycler Software version 4.1; Roche). Here qRT-PCR data were normalized to the expression of hypoxanthine-guanine phosphoribosyltransferase (HPRT) or β actin.

2.12 Macrophage Depletion During EIU in Mice

Dichloromethylene-1,1-bisphosphonate (clodronate) causes selective depletion of macrophages, monocytes and microglia (König *et al*., 2014). Clodronate is cytotoxic to cells because of its intracellular metabolite which is a non-hydrolyzabe analog of adenosine triphosphate (ATP) called adenosine-5'-[β-γ-dichloromethylene]triphosphate ($AppCCL_2p$). $AppCCL_2p$ competes with ATP at the adenosine diphosphate (ADP)/ATP translocase of the mitochondrial membrane; during prolonged inhibition of functioning ADP/ATP translocase the mitochondrial membrane potential collapses and the cell initiates apoptosis (Lehenkari *et al*., 2002).

To ablate macrophages and monocytes, mice were injected i.p. daily, for six days with 200 μl of a suspension of liposome-encapsulated clodronate (5 mg clodronate/ml) or control, PBS encapsulated in liposomes (clodronateliposomes.com, Haarlem, The Netherlands). These liposomes are phospholipid bilayers which encapsulate clodronate, a highly hydrophobic molecule which rarely crosses the phospholipid membrane. Liposome-

Table 1. Target, sequence, annealing temperatures, $MgCl_2$ content and reference for primer sequences used in qRT-PCR

Target	Oligonucleotide Sequence (5' - 3')	Anneal. Temp. (°C)	$MgCl_2$ (mM)	Reference
Rat NF-κB, p65	5'- GCG TAC ACA TTC TGG GGA GT -3′ 5'- CCG AAG CAG GAG CTA TCA AC -3′	59	2	(Cao *et al*., 2006)
Rat AP-1, c-Fos	5'- CTC CGG GCT GTT CAT CTG TT -3′ 5'- CCG GGA CTT GTG AGC TTC TT -3′	59	2	(Toguri *et al*., 2014)
Rat HPRT	5'- GCT GGT GAA AAG GAC CTC T -3′ 5'- CAC AGG ACT AGA ACA CCT GC -3′	59	3	(McCaw *et al*., 2004)
Rat TLR4	5′-GGC ATC ATC TTC ATT GTC CTT G -3′ 5′- AGC ATT GTC CTC CCA CTC G -3′	57	4	(Liu *et al*., 2010)
Rat CB_2R	5'-CTG AGT GAG GAG AGG CGT AG -3' 5'-CTG CTT CTA CCG GAG CTG TT -3'	57	3	(Toguri *et al*., 2014)
Rat IRF3	5′-TAA GGG AGA TCG GCT GGC TG-3′ 5′- TGA TGG AGA GGT CCC CAA GG-3′	57	5	(Liu *et al*., 2010)
Rat RIP-1	5'- GCA CCA GCT GTC AGG GCC AG -3' 5'- GCC CAG CTT TC GGG CAC AGT -3'	57	3	(Takaoka *et al*., 2005)
Mouse CB_2R	5'- GGA TGC CGG GAG ACA GAA GTG A -3′ 5'- CCC ATG AGC GGC AGG TAA GAA AT -3′	57	2	(Laprairie *et al*., 2014)
Mouse β-actin	5'- AAG GCC AAC CGT GAA AAG AT -3′ 5'- GTG GTA CGA CCA GAG GCA TAC -3′	59	2	(Blázquez *et al*., 2011)

encapsulated clodronate becomes phagocytosed by macrophages and other APCs disrupting the lipid bilayer of the liposome allowing clodronate to be realised into the cellular cytosol causing death (Kumamaru *et al*., 2012). On the seventh day after receiving liposome-encapsulated clodronate, or the control received an intraocular injection of saline or LPS in saline.

2.13 Inhibition of Jun N-terminal Kinase (JNK) during EIU in Mice

BALB/c mice (25 – 30 g) were administered 15 mg kg^{-1} SP600125 (150 µL) *i.v.* (Sigma-Aldrich, St. Louis, MO, USA), or vehicle (150 µL) in vehicle (10% DMSO/ 10% Cremophor/ 80% saline) 15 min before intraocular injection of LPS or saline. SP600125 selectively inhibits JNK-1, -2 and -3 isoforms with similar potency, and has a 10 – 300-fold selectivity for JNK relative to other MAP kinases involved in inflammation (Bennett *et al*., 2001).

2.14 Cell Culture

RAW 264.7 were kindly were provided by Dr. Christopher J. Sinal (Dalhousie University). Cells were maintained at 37 °C under 5% CO_2 in DMEM (Gibco BRL, New York, USA) supplemented with heat-inactivated 10% fetal bovine serum (Gibco BRL, USA), 20 mM HEPES (Gibco BRL, USA), 2 mM L-

Gluatamine (Gibco BRL, USA) and 10^4 units/mL penicillin/streptomycin. Mycoplasma-free RAW 264.7 cells were cultured at a seeding density of 5 X 10^4 cells per 100 mm culture plate in supplemented DMEM and grown to 70-80 % confluence. Cell viability was assessed by trypan blue staining. Prior to stimulation with LPS, cells were serum-deprived for 4 hr. Cells were treated with HU308 at 10^{-6}, 10^{-7}, 10^{-8} M based on preliminary results from a larger dose range (10^{-3} – 10^{-9} M) and results from a cAMP luciferase reporter assay with CB_2R transfected into HEK293 cells and stimulated with HU308. Following HU308 treatment cells were washed for 2 min PBS then incubated with LPS in serum-deprived media (1 μg/ml) or serum-deprived media for the fifteen min, washed with PBS for 2 min and fixed. This time period was chosen based on previous reports (Chen *et al*., 2002; Hambleton, Weinstein, *et al*., 1996). Hambelton *et al*., (1996) described maximum activation of JNK in response to LPS starting 5 min after stimulation, reaching a maximum JNK phosphorylation 20 min after LPS exposure, while Chen *et al*., (2002) confirm an increase in MAPK phosphorylation at 15 min. Hambelton *et al*., as well as others (Xagorari *et al*., 2002) noted a decrease after 30 min stimulation with LPS. Due to the speed which MAPKs become dephosphorylated after LPS treatment in cell culture, and preliminary experiments pre-treatment of HU308 was deemed optimal for elucidating possible cellular mechanisms of HU308 through the MAPK pathway.

2.15 In-cell™ Western Analysis

Cells were fixed for 10 min at room temperature with 4% PFA and washed three times with 0.1 M PBS for 5 min each. Cells were incubated with blocking solution (20% Odyssey Blocking Buffer containing 0.3% TritonX-100 in dH_2O) for 1 h at room temperature. Cells were incubated with primary antibody solutions directed against ERK1/2 (1:200), pERK1/2(Tyr205/185) (1:200), (Santa Cruz Biotechnology), JNK (1:200) (Cell Signaling Technology), pJNK(Thr 183/Tyr 185) (1:200) (Santa Cruz Biotechnology), p38 (1:200), pp38 (1:400) (Cell Signaling Technology) diluted in blocking solution overnight at 4°C. Cells were washed three times with 0.1 M PBS for 5 min each. Cells were incubated in $IR^{CW700dye}$ or $IR^{CW800dye}$ (1:500; Rockland Immunochemicals) and again washed three times with 0.1 M PBS for 5 min each. In-cell™ Western analyses were then conducted using the Odyssey Imaging system and software (version 3.0; Li-Cor).

2.16 Statistical Analysis

2.16.1 Statistics Analysis of Animal Experiments

Animals were coded and were analysed in a non-biased fashion. Normality was confirmed by the D'Agostino and Pearson omnibus normality test. All data were analysed with the statistical software Prism v.6 (GraphPad Software Inc., San Diego, CA, USA). Unless otherwise stated, all data was analysed using an unpaired two-tailed t-test, a one-way or two-way analysis of variance (ANOVA). Data which compared two groups were compared by a two-tailed t-test. Data sets with three or more groups testing one measurable variable were tested by a one-way ANOVA, while those with two variables were tested by a two-way ANOVA. Data was subject to various *post-hoc* measures including Dunnett's (IVM), Tukey's (qPCR) or Fisher's LSD (endocannabinoids) test or a Bonferroni (two way for hemodynamics and leukocyte adhesion). All data are presented as means ± standard error of the mean (SEM). $P < 0.05$ was considered statistically significant.

2.16.2 Statistical Analysis of Cell Culture Experiments

Goodness of fit to the Variable Slope (4 parameter) non-linear regression model was tested in GraphPad (v. 6.0, Prism). Statistical analyses were conducted by one- or two-way analysis of variance (ANOVA), as indicated, using GraphPad

(version 6.0, Prism). *Post-hoc* analyses were performed using Bonferroni's or Tukey's tests, as indicated. Homogeneity of variance was confirmed using Bartlett's test. All results are reported as the mean ± SEM from at least 3 independent experiments.

Chapter III: C_2R activation reduces leukocyte activation and improves capillary perfusion in the iridial microcirculation during systemic inflammation

3.1 Manuscript status and student contribution

The figures and text presented in this chapter are from a manuscript accepted to Clinical Hemoheology and Microcirculation. Toguri, J. T., Moxsom, R., Szczesniak, A.M., Zhou, J., Kelly, M.E.M., Lehmann, C. (2015) Cannabinoid 2 receptor activation reduces leukocyte activation and improves capillary perfusion in the iridial microvasculature during systemic inflammation. *Clin Hemor Microcirc.*

As first author on this article, I performed all of the experiments, analysis, data interpretation, statistics and wrote the manuscript. Ryan Moxsom assisted with experiments. Dr. J. Zhou established the animal model of iris IVM and edited the manuscript. Dr. A. M. Szczesniak, Dr. M. E. M. Kelly. and Dr. C. Lehmann edited the manuscript.

3.2 Abstract

Background: Leukocyte adhesion to the endothelium and decreased microvascular blood flow causing microcirculatory dysfunction are hallmarks of systemic inflammation. We studied the impact of cannabinoid receptor activation on the iridial microcirculation, which is accessible non-invasively *in vivo*, in systemic inflammation induced by endotoxin challenge.

Methods: 40 Lewis rats were used in the experiments. Endotoxemia was induced by 2 mg/kg i.v. lipopolysaccharide (LPS). Cannabinoid receptors (CBRs) were stimulated by i.v. administration of WIN 55212-2 (WIN; 1 mg/kg). CB_1R antagonist (AM281; 2.5 mg/kg i.v.) or CB_2R antagonist (AM630; 2.5 mg/kg i.v.) treatment prior to WIN was injected to identify the anti-inflammatory effects underlying each CBR subtype. Leukocyte-endothelial interactions were examined in rat iridial microvasculature by intravital microscopy at baseline and 1 and 2 h post-LPS. Additionally, systemic (mean arterial pressure, heart rate) and local (laser Doppler flow) hemodynamic variables were measured prior to and during cannabinoid treatments.

Results: Endotoxemia resulted in severe inflammation as shown by significantly increased numbers of adherent leukocytes at 1 and 2 h observation time post-LPS challenge and decreased microcirculatory blood flow at 2 h within the iridial microcirculation. WIN treatment significantly reduced leukocyte adhesion in

iridial microvessels with a diameter greater and less than 25 μm during endotoxemia ($p < 0.05$). Pre-treatment of animals by CB_1R antagonist, AM281, did not affect WIN effects on LPS-induced leukocyte adhesion. When pre-treated with the CB_2R antagonist, AM630, a reversal of the WIN-induced reduction in leukocyte adhesion was noticed in vessels with a diameter of less than 25 μm ($p < 0.05$). Cannabinoid treatment significantly increased the local iridial microcirculatory blood flow 2 hours after systemic LPS administration ($p < 0.05$).

Conclusions: Systemic administration of the CBR agonist, WIN, decreased leukocyte-adhesion and improved iridial microvascular blood flow. This effect is most likely mediated by CB_2R activation. Our findings indicate that the iris microvasculature can serve as a model to study the microcirculation during systemic inflammation and help to identify potential therapies to treat microcirculatory dysfunction in diseases such as sepsis.

3.3 Introduction

Systemic inflammation occurs in several acute and chronic medical conditions. Typically, immune cells are activated globally causing a cytokine storm and release of other inflammatory mediators such as nitric oxide and prostaglandins. Finally, alterations of the microcirculatory blood flow and therefore, the oxygen and nutrient supply to the tissues can be observed (Berdyshev, 2000; Ince, 2005; Levy *et al*., 2003; Pranskunas *et al*., 2012).

Studies investigating microcirculatory dysfunction in systemic inflammation have experimental constraints due to limited access to microcirculatory beds. Often, access to these areas involves surgical procedures that can induce additional local inflammation or diminish the integrity of the microvasculature. The eye, due to its anatomical location and the translucent cornea provides a unique opportunity for direct, non-invasive observation of the microcirculation *in vivo* (Toguri *et al*., 2014). Methods such as intravital microscopy (IVM) and laser Doppler flowmetry (LDF) can be employed to study the microvasculature of the iris during systemic inflammation (Chamot *et al*., 1999; Toguri *et al*., 2014). The iridial microcirculation can be used to model other microvascular beds experiencing dysfunction in systemic inflammatory conditions such as sepsis. Furthermore, these techniques provide the ability to evaluate the efficacy of potential therapeutic candidates *in vivo* including cannabinoid ligands.

The endocannabinoid system (ECS) is a bioactive lipid signaling system that is comprised of two G-protein coupled receptors, the cannabinoid 1 receptor (CB_1R) and the cannabinoid 2 receptor (CB_2R), together with endogenous ligands (endocannabinoids) and enzymes responsible for their synthesis and degradation (Berdyshev, 2000). CB_1R is expressed throughout the central nervous system (CNS) and activation of presynaptic neuronal CB_1R inhibits neurotransmitters release (Diana *et al*., 2002; Laaris *et al*., 2010). Additionally, modulation of non-neuronal CB_1R is associated with an anti-inflammatory response in the CNS (Rossi et al., 2011b). The anti-inflammatory effects of CB_1R have been linked to a decrease in inflammatory mediators and reduced leukocyte migration (Rajesh *et al*., 2010). It has also been reported that CB_1R influences hemodynamics, which may also affect the immune response (Dannert *et al*., 2007; Kadoi *et al*., 2005; Varga *et al*., 1998).CB_2R is primarily expressed on immune cells and activation of this receptor has been documented to be immunosuppressive (Berdyshev, 2000; Munro *et al*., 1993). CB_2R activation decreases levels of pro-inflammatory mediators including cytokines (TNF-α, IL-1β, IL-6), chemokines (CCL2, CCL5, CXCL2) and adhesion molecules (ICAM-1, VCAM-1 and integrin β1) (Rajesh *et al*., 2007; Rom *et al*., 2013; Toguri *et al*., 2014; Xu *et al*., 2007). CB_2R-mediated reductions in pro-inflammatory mediators have been attributed to decreased levels of mRNA for transcription factors NF-κB and AP-1 (Rajesh *et al*., 2007; Toguri *et al*., 2014). In support of an immunosuppressive

role for CB_2R, selective CB_2R agonists decrease migration of specific leukocyte populations both *in vitro* and *in vivo* during an inflammatory response (Murikinati *et al*., 2010; Rom *et al*., 2013). Additionally, it has been found that CB_2R agonists have vasodilatory effects resulting in a local increase in the blood flow (McDougall *et al*., 2008). Taken together, this evidence suggests that activation of the endocannabinoid system may decrease inflammation and microcirculatory dysfunction. WIN-55,212-2 (WIN) is an aminoalkylindole synthetic cannabinoid that activates both CB_1R and CB_2R (McIntosh *et al*., 2007). Selective inhibition of CB_1R and CB_2R allow for the investigation the therapeutic benefits of each receptor independently.

The purpose of the present study was 1) to determine if the iridial microcirculation shows the typical signs of immune cell activation in systemic inflammation and therefore, could be used as an accessible model for dysfunctional microvascular beds in diseases such as sepsis, and 2) to examine the impact of both CB_1R and CB_2R activation by WIN on microcirculatory dysfunction due to endotoxin challenge. Specifically, we investigated leukocyte-endothelial interactions in vessels of varying diameters within the iridial microvasculature as well as macro- and micro-hemodynamic parameters including mean arterial pressure, heart rate, and iridial microcirculatory blood flow.

3.4 Methods

3.4.1 Animals

All animal procedures were approved by the Dalhousie University Committee on Laboratory Animals and complied with the Canadian Council for Animal Care guidelines (http://www.ccac.ca/). All studies involving animals are in accordance with the ARRIVE (Animal Research: Reporting *In Vivo* Experiments) guidelines (http://www.nc3rs.org.uk/).

Male Lewis rats (250 – 400 g, n = 8/group; Charles River Laboratories International Inc., Wilmington, MA, USA) were maintained on a light/dark cycle (07:00-19:00), and fed *ad libitum*. Animals were anesthetised by intraperitoneal (i.p.) injection of sodium pentobarbital (65 mg/kg; Ceva Sante Animale, Montreal, QC, Canada). Depth of anesthesia was assessed by toe-pinch every 15 min. The femoral vein and artery were catheterized using non-radiopaque polyethylene tubing (PE 50; Clay Adams, Sparks, MD, USA). Both catheters were attached to infusion pumps (Lifecare 5000 Plum Infusion Pump; Abbott, IL, USA). The venous catheter was used for the administration of drugs, anaesthetic agents and fluorochromes. The arterial catheter was used to monitor the vital signs with the Marquette Eagle 4000 Patient Monitor (General Electric, North Bergen, NJ, USA). Animals were sacrificed at the end of the experiment, under anaesthesia, by intravenous (i.v.) injection of KCl (0.142 mL/kg).

3.4.2 Endotoxemia

Rats were administered 2 mg/kg lipopolysacharide i.v. (LPS, *Escherichia coli,* 026:B6, Sigma-Aldrich, Oakville, ON, Canada) dissolved in normal saline (0.9% sodium chloride, Hospira, Montreal, QC, Canada) to generate endotoxemia. Control animals received an i.v. bolus of normal saline at an equal volume. Animals were studied for 2 h following LPS challenge as described previously (Caspi, 2006; Sardinha *et al*., 2014).

3.4.3 Drugs

The non-selective cannabinoid agonist, WIN (WIN, 55,212-2, (*R*)-(+)-[2,3-Dihydro-5-methyl-3-(4-morpholinylmethyl)pyrrolo[1,2,3-*de*]-1,4-benzoxazin-6-yl]-1-naphthalenylmethanone mesylate), was administered i.v. at 1 mg/kg. The CB_1R antagonist, AM281 (1-(2,4-Dichlorophenyl)-5-(4-iodophe nyl)-4-methyl-*N*-4-morpholinyl-1*H*-pyrazole-3-carboxamide) was administered i.v. at 2.5 mg/kg, and the CB_2R antagonist, AM630 (6-iodo-2-methyl-1-[2-(4-morpholinyl)ethyl]-1H-indol-3-yl](4-methoxyphenyl)methanone) was administered i.v. at 2.5 mg/kg. Drug treatments were given 15 min after LPS. When antagonists were administered, they were given prior to WIN. All cannabinoids were obtained from Tocris Bioscience (Ellisville, MO, USA). All drugs were prepared in Dimethyl Sulfoxide (DMSO; Sigma-Aldrich Canada Ltd., Oakville, ON, Canada) and diluted 1:1 with saline, and given i.v over a 15 min

period. The dose of WIN was determined by previous studies described in the literature which demonstrated anti-inflammatory effects (Fernández-López *et al*., 2012; Smith, Denhardt, *et al*., 2001). WIN has a K_i value of 5.05 nM for the CB_1R and 3.13 for the CB_2R (Iwamura *et al*., 2001). The doses of the CB_1R antagonist, AM281 (2.5 mg/kg), and the CB_2R antagonist, AM630 (2.5 mg/kg), were based on previous published studies (Lehmann *et al*., 2012; Szczesniak *et al*., 2011; Toguri *et al*., 2014).

3.4.4 Intravital Microscopy

The iridial microcirculation was observed with the Olympus OV100 Small Animal Imaging System (ON, Canada). The OV100 contained a MT-20 light source and a DP70 CCD camera. Fluorescence excitation was generated by xenon lamp (150W), and 8 position excitation filters to block for rhodamine-6G (excitation 515-560 nm, emission 590 nm) and FITC (450-490 nm, emission 520 nm). Images were captured in real-time and recorded in a digital format by the software, Wassabi (Hamatsu, Herrsching, Germany). Each rat was placed in a stereotactic frame (Kopf, CA, USA), and Tear-Gel (Novartis Pharmaceuticals Canada Inc., Dorval, QC, Canada) was applied on the cornea to prevent dehydration of the tissue throughout the experiment. Rhodamine-6G (1.5 ml/kg; Sigma-Aldrich, ON, Canada) and FITC-albumin (1 ml/kg; Sigma-Aldrich, ON, Canada) were injected i.v. 15 min before initiating IVM. The fluorescent dye

Rhodamine-6G tags leukocytes within the vessels, and FITC-albumin allowed for the visualization of blood flow through the vasculature.

Animals were placed on a heating pad to maintain body temperature at 37 °C and IVM was carried out in four regions of interest, each in a different quarter of the iridial microcirculation. Each region of interest was recorded for 30 s and four randomly selected vessels (diameter <100 μm) were observed hourly. For IVM studies, data were analysed off-line in a blinded manner using the imaging software ImageJ (National Institute of Health, USA). The length measured between points of branching and diameter of the vessel was used to calculate the endothelial area. Adhering leukocytes were defined as white blood cells that attached to the vessel wall and were immobile for a 30 s observation period; adhering cells were reported as the number of cells per mm^2 of endothelial surface. Leukocytes which interacted with the endothelium at a slower velocity than midstream blood cell velocity past an arbitrary line perpendicular to the endothelial wall during the 30 s were quantified as rolling leukocytes. Examination of vessels was divided into those that were greater or less than 25 μm in diameter; vessels of greater than 25 μm are confluent vessels in the rat microvasculature. No measurements were conducted in vessels larger than 100 μm.

3.4.5 Hemodynamics

Haemodynamic variables, including mean arterial pressure (MAP) and heart rate (HR) were measured from the femoral artery catheter every 15 min. Animals with a MAP below 70 mm Hg were excluded from the study (Dellinger *et al*., 2013).

3.4.6 Laser Doppler Flowmetry

Laser Doppler flowmetry (LDF) was used to measure the iridial microcirculation blood flow (IMBF). This method quantifies IMBF by the detection of erythrocyte movement by the Doppler effect. A glass fibre laser Doppler probe (diameter 120 μm, wave length 810 nm, resulting penetration depth about 1–2 mm) is used to monitor infrared light from a fibre optic cable to measure the light scatter by stationary tissue and moving blood cells within a region of interest approximately 1 mm^3 in area. Scattered light from moving cells results in a Doppler frequency shift of the infrared light while stationary tissue does not. This Doppler frequency shift is then quantified by analysis of the backscatter of light proportional to the flow of blood cells within the region of interest.

LDF readings were taken from rat eyes following placement of a glass fiber laser Doppler probe 1-2 mm away from the cornea at a 90° angle so as to not come in contact with any tissue. The laser Doppler probe was focused on the

iridial vasculature and IMBF measurements were taken for 180 sec at 5 min before systemic injection of either saline or LPS, and at 60 and 120 min after injection. The LDF signal was recorded using a PeriFlux System 5000 (Perimed Inc., Ardmore, PA, USA) DIAdem 8.0.1 software (National Instruments, Vaudreuil-Dorion, Quebec, Canada). All LDF values were calculated after normalization to baseline blood flow readings as 100% for each animal.

3.4.7 Statistical Analysis

Individual animals in each of the treatment groups (n = 8/group) were coded and data was derived in a non-biased fashion. The D'Agostino and Pearson omnibus normality test was used to confirm normality of the data. All data are presented as means ± SEM and were analysed with the statistical software Prism v.6 (GraphPad Software Inc., San Diego, CA, USA). IVM data was analysed by two-way ANOVA with Dunnett's *post-hoc* test, comparing all experimental groups to the LPS treated group in vessels of all sizes. Additional analysis by a one-way ANOVA with Dunnett's *post-hoc* test was conducted to decipher if cannabinoid treatments affected leukocyte adhesion in different regions of the microvasculature. As with IVM, hemodynamic variables were analysed at -15 min, 1 h and 2 h by two-way ANOVA with Dunnett's *post-hoc* test with respect to LPS administration. LDF data was analyzed after baseline blood flow of each animal was set to 100% to eliminate variation in iridial blood flow in the

microcirculation due to systemic hemodynamic variables. Changes of blood flow during the experiments are shown in percentage of baseline and observations from each treatment group were averaged per time point. Prior to LDF measurements being normalised to 100% at baseline, a one-way ANOVA was conducted to ensure that there were no significant differences in ocular blood flow prior to injection of saline controls or LPS. Differences were considered significant at $p < 0.05$.

3.5 RESULTS

3.5.1 Leukocyte adherence

Systemic administration of LPS significantly increased the number of leukocytes adhering to iridial microvascular endothelium at 1 and 2 h after induction compared to saline treated control animals ($p < 0.05$, Figure 13 A & B). Administration of the vehicle, DMSO + saline, did not significantly alter the number of adherent leukocytes throughout the experiment compared to LPS (data not shown). WIN treatment - in absence or presence of the CBR antagonists, respectively - did not significantly attenuate leukocyte adhesion to the iridial microvasculature at 1 h after LPS challenge. However, at 2 h after LPS administration, WIN significantly reduced the number of leukocytes adhering to vessels of all diameter in the iridial microvasculature compared to untreated LPS animals. Pre-administration of the CB_1R or CB_2R antagonists (AM281 and

Figure 13. Leukocyte-adhesion in the iridial microvasculature after systemic administration of LPS and selective activation of CB_1R and CB_2R agonists. Bar graph representing adherent leukocytes in vessels of a diameter greater (A) or less (B) than 25 μm at -15, 60 and 120 min. Treatment with LPS + WIN and LPS + AM281 + WIN significantly decreased the number of leukocytes adhering to the endothelium in all the vessels (A, B) compared to untreated LPS animals while treatment with LPS + AM630 + WIN also significantly decreased the number of leukocytes adhering to the endothelium compared to LPS animals in the vessels of a diameter < 25 μm. Values represent mean ± SEM. * $P < 0.05$ compared to the LPS group.

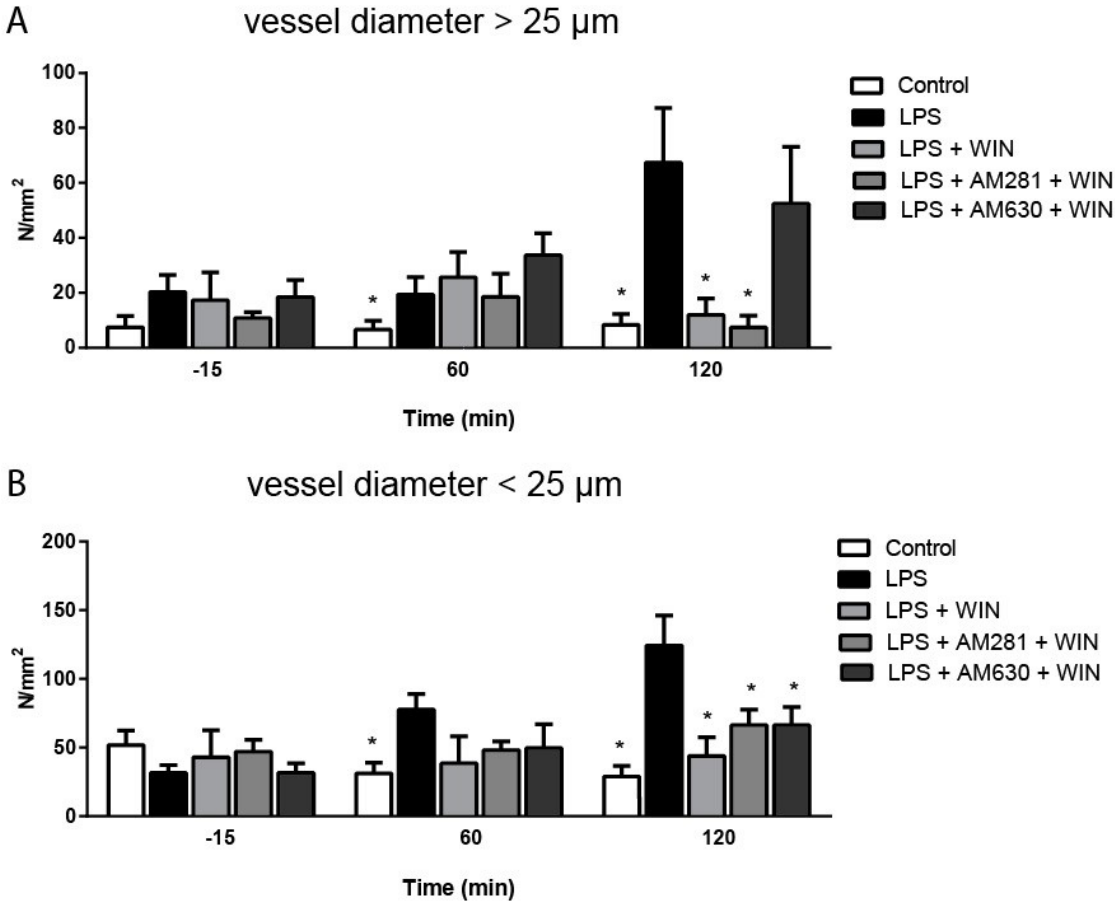
A
vessel diameter > 25 µm
100
80
60
40
20
0
N/mm2
-15
60
120
Time (min)
Control
LPS
LPS + WIN
LPS + AM281 + WIN
LPS + AM630 + WIN
B
vessel diameter < 25 µm
200
150
100
50
0
N/mm2
-15
60
120
Time (min)
Control
LPS
LPS + WIN
LPS + AM281 + WIN
LPS + AM630 + WIN

AM630, respectively) did not prevent the WIN-induced reduction in leukocytes adhering to the endothelium in vessels with a diameter < 25 μm, although block of either CBR reduced the effectiveness of WIN. However, treatment with the selective CB_2R antagonist, AM630, but not the CB_1R antagonist AM281 prior to WIN, abolished the decrease in leukocytes adherence in the vessels larger than 25 μm produced by WIN.

3.5.2 Leukocyte rolling

There were no significant changes in leukocyte rolling 1 or 2 h after LPS administration, as compared to saline control. Treatment of animals with cannabinoid ligands, WIN, AM281 + WIN and AM630 + WIN, did not result in any significant changes in leukocytes rolling, as compared to LPS treated group, in all categories of vessels analyzed (Table 2).

3.5.3 Hemodynamics

No significant differences in MAP were observed between any group at 15 min before saline or LPS injections (Figure 14 A). At 1 h post LPS all animal with endotoxemia had a significantly decreased MAP in comparison to the

Table 2. Leukocyte-endothelial rolling in the iridial microvasculature 2 hr after systemic administration of LPS and selective activation of CB_1R and CB_2R agonists. Data shown (mean ± SEM) are from control, LPS, and LPS with WIN, combination of AM281 + WIN and combination of AM630 + WIN, n = 10. No significant differences between groups were found.

	Control	LPS	LPS + WIN	LPS + AM281 + WIN	LPS + AM630 + WIN
All vessels	0.723 ± 0.483	0.772 ± 0.219	1.913 ± 1.218	0.437 ± 0.101	0.574 ± 0.114
>25 µm	0.268 ± 0.011	0.634 ± 0.177	0.233 ± 0.145	0.089 ± 0.089	0.309 ± 0.172
< 25 µm	0.617 ± 0.021	0.889 ± 0.072	0.726 ± 0.087	0.659 ± 0.120	0.524 ± 0.075

Figure 14. Effects of LPS and cannabinoid treatments on systemic hemodynamics including blood pressure and heart rate. (A) Mean arterial pressure (mmHg). (B) Heart rate (beats per minute). Groups: control, LPS, LPS + WIN, LPS + AM281 + WIN, LPS + AM630 + WIN. All groups treated with LPS had a significant but transient decrease in blood pressure at 1 h. At 2 h no significant changes were observed. No significant changes in heart rate were observed. Values represent mean ± SEM. + $P < 0.05$ compared to control group.

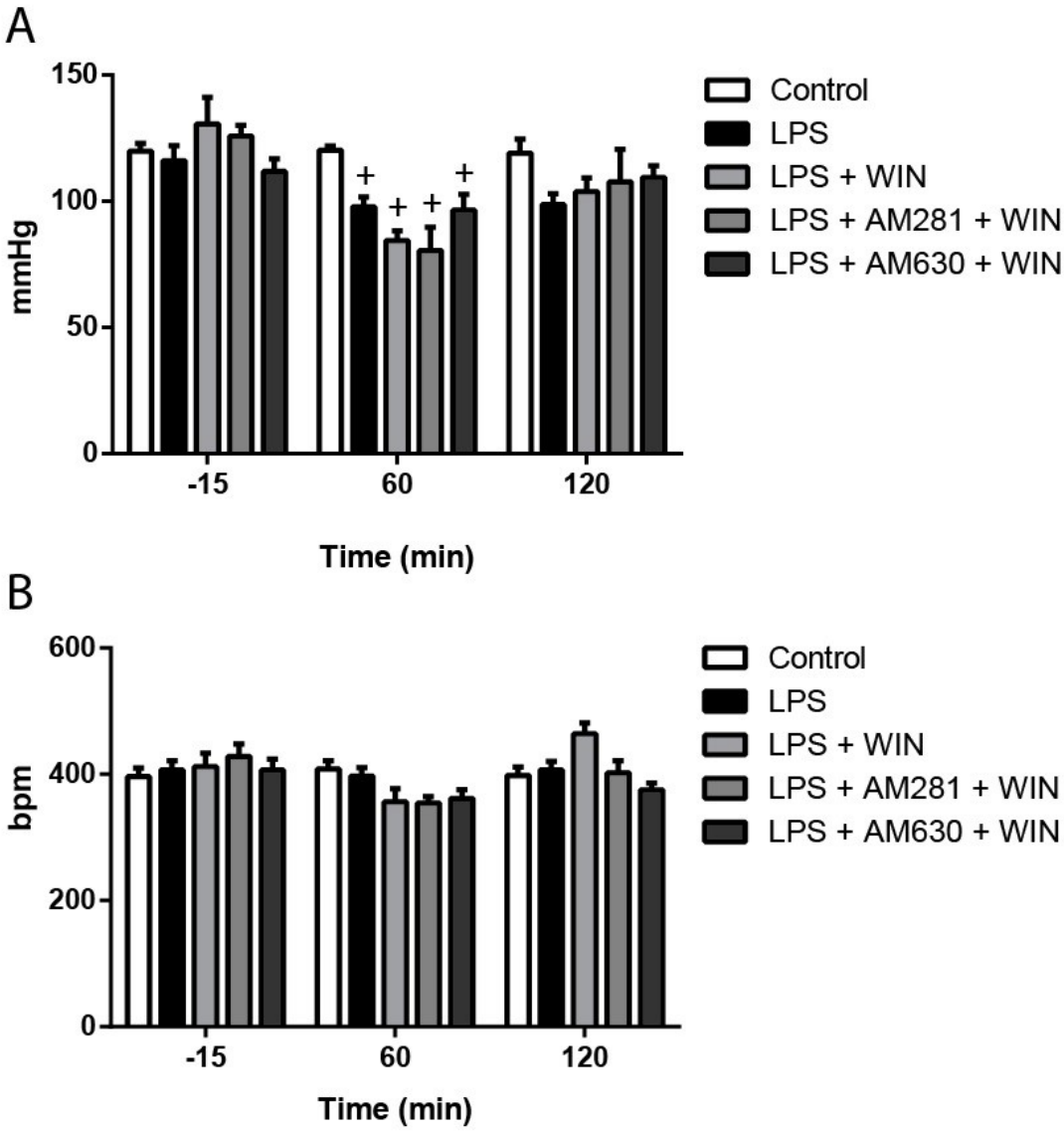
A
150
100
50
0
mmHg
+
+
+
+
-15
60
120
Time (min)
Control
LPS
LPS + WIN
LPS + AM281 + WIN
LPS + AM630 + WIN
B
600
400
200
0
bpm
-15
60
120
Time (min)
Control
LPS
LPS + WIN
LPS + AM281 + WIN
LPS + AM630 + WIN

control group ($p<0.05$), while at 2 h this difference was abolished. There was no significant difference in MAP between animals which received LPS and animals treated with cannabinoids (WIN, WIN+AM281, WIN+AM630) at 1 or 2 h.

No significant difference in heart rate (HR) was observed between any groups at -15 min before induction of endotoxemia or 1 and 2 h post-LPS challenge.

3.5.4 Iridial Microcirculation Blood Flow

Local blood flow in the iris was not significantly altered at 1 h following LPS compared to saline treated animals ($p<0.05$). Treatment with WIN, AM281 + WIN or AM630 + WIN did not significantly alter the blood flow in comparison to untreated LPS animals. By 2 h IMBF significantly decreased by 46% in LPS treated animals compared to control animals ($p<0.05$). All cannabinoid treatments: WIN (145%, $p>0.05$), and WIN in combination with AM281 (137%, $p>0.05$), or AM630 (116%, $p>0.05$), significantly increased IMBF flow at 2 h post-LPS injection in comparison to untreated LPS animals (Figure 15).

Figure 15. Modulation of iridial microvascular blood flow after LPS administration and subsequent treatment with selective cannabinoid receptor activation. Iridial microvascular blood flow (% of baseline) in the following treatment groups: control, LPS, LPS + WIN, LPS + AM281 + WIN, LPS + AM630 + WIN. A significant decrease in IMBF was observed in animals with endotoxemia by 2 h. Treatment with CBR agonists during LPS challenge reversed decreased IMBF. Values represent mean ± SEM. * $P < 0.05$ compared to the LPS group.

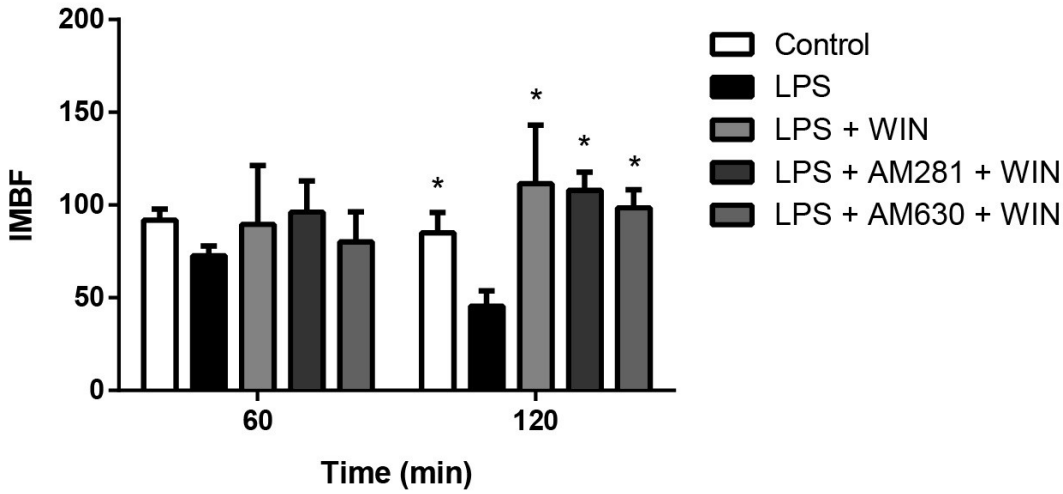
200
150
100
50
0
IMBF
60
120
Time (min)
*
*
*
Control
LPS
LPS + WIN
LPS + AM281 + WIN
LPS + AM630 + WIN

3.6 DISCUSSION

3.6.1 Iridial Microcirculation as a Model for the Microcirculatory Dysfunction during Systemic Inflammation

This study demonstrates the possibility of using the eye to non-invasively study microcirculatory dysfunction in systemic inflammation. Herein, we have provided evidence that both leukocyte activation and microcirculatory blood flow changes can be observed in the iris 2 h after systemic LPS challenge. Our results of increases in leukocyte-endothelial interactions and alterations in iridial microvascular blood flow are consistent with other investigations of systemic inflammation (De Backer *et al*., 2013; Enigk *et al*., 2014; Hiltebrand *et al*., 2000; Iba *et al*., 2014; Lehmann *et al*., 2012; Villela *et al*., 2014).

We report that reduction in IMBF by 46% occurs within 2 h after systemic LPS administration. Previous reports have speculated upon the heterogeneity of the microcirculatory blood flow during critical illness (De Backer *et al*., 2013; Hiltebrand *et al*., 2000; Pranskunas *et al*., 2012). Hiltebran *et al*., (2000) showed that jejunal mucosal blood flow was not significantly decreased during peritonitis and septic shock, however there was approximately a 50% reduction in regional blood flow in the stomach mucosa, colon, liver, pancreas and kidney (Hiltebrand *et al*., 2000). These results indicate that the iridial microcirculation represents the microcirculation of organs undergoing shunting of blood and potential failure more dominantly than those organs not as affected during sepsis and septic shock.

Once we established that the iridial microcirculation responded similarly to other regions of microvasculature in systemic inflammation, we investigated the ability of cannabinoid ligands to decrease inflammation and microcirculatory blood flow.

3.6.2 Cannabinoid Effects on Leukocyte-Endothelial Interactions

The present study describes that, in particular, activation of CB_2R decreases leukocyte-endothelial interactions within the iridial microcirculation after systemic LPS administration. It has been documented that both CB_1R and CB_2R agonists play a role in the immune response and regulation of the immune system. Activation of both cannabinoid receptors by the non-selective cannabinoid WIN has been demonstrated to attenuate leukocyte-endothelial interactions in a model of autoimmune encephalomyelitis (Ni *et al*., 2004). Another study with WIN reported a dose-dependent decreased release of TNF-α after LPS stimulation in murine immune cells (Facchinetti *et al*., 2003). The effects of WIN could be compound specific, however these responses may be elicited by selective activation of the CB_1R and CB_2R.

Here, we report that selective activation of the CB_2R by administration of WIN and CB_1R inhibition by AM281 decreased leukocyte adhesion in all vessels of the iridial microcirculation during endotoxemia. This observation corroborates earlier reports of the anti-inflammatory effects of CB_2R activation in systemic

inflammation (Caldwell *et al*., 2010; Gui *et al*., 2013; Lehmann *et al*., 2012; Tschöp *et al*., 2009). Similarities between the anti-inflammatory effects of CB_2R agonists in the eye and other microcirculatory beds provides further reason to accept the use of the iris as a model to study microcirculatory inflammation during sepsis.

We have documented that selective CB_1R activation, by administration of WIN and CB_2R inhibition by AM630, decreases leukocyte adhesion to the iridial microvasculature with a diameter less than 25 μm. Several reports attribute CB_1R anti-inflammatory effects to central as well as peripheral CB_1R modulation of cytokine-related pathways. WIN delayed the release of cheomoattractants (KC and MIP-2) in mice with peritonitis, consequently inhibiting neutrophil migration. When these animals were pretreated with selective CB_1R antagonist, SR141716A, neutrophil migration returned to normal (Smith, Denhardt, *et al*., 2001). Similar results were found by Sacerdote *et al*., (2000) in which the non-selective cannabinoid receptor agonist, CP55, 940 and a CB_2R antagonist reduced macrophage recruitment. Krustev *et al*., (2014) found that inhibiting endocannabinoid degradation reduced leukocyte-endothelial interactions in experimental joint inflammation, and this effect was mediated by both CB_1R and CB_2R activation (Krustev *et al*., 2014).

In systemic inflammation, actions of the CB_1R have been focused on CB_1R inhibition to improve GI motility (Li, *et al*., 2010) and implications of

CB_1R mediated hypotension (Varga *et al*., 1998). In our investigation in endotoxemia, activation of the CB_1R attenuated leukocyte-endothelial adhesion within the sub-population of the microvasculature which had a diameter of less than 25 μm. These results may be explained by CB_1R vasodilatory effects. Wagner *et al*., (2001) demonstrated that several selective CB_1R agonists differently altered cardiac output and total peripheral resistance. Many of the measurable outcomes due to vasodilation are focused on macro-hemodynamics. One focus includes decreases in systemic blood pressure (Wagner *et al*., 2001). This alteration in systemic blood pressure does not necessarily equate to changes in localised blood flow (Michelson *et al*., 1994). Vasodilation within the microvasculature contributes to increasing local blood flow; reviewed by Bagher and Segal (2011). Increased blood flow strengthens shear forces, inhibiting adhesion of leukocytes to the endothelium (Cunningham & Gotlieb, 2005). These effects of shear forces and reduced leukocyte adhesion may deteriorate as microvasculature becomes larger (>25 μm).

3.6.3 Iridial Microvascular Blood Flow

In the present study administration of LPS resulted in a significant decrease in the blood flow within the iridial microcirculation. This observation is consistent with reports of decreased blood flow during sepsis or septic shock in several microcirculatory beds such as the stomach mucosa, pancreas, liver, colon,

and kidney (Assadi et al., 2012; Hiltebrand et al., 2000). Cannabinoid treatment was able to significantly increase the IMBF. Since this increase was not reversible by CB_1R or CB_2R antagonists, respectively, CBR independent effects may also be involved. These actions could have occurred by non-CB_1R/CB_2R activation at GPR18, GPR55 or TRPV1 receptors which can be activated by cannabinoid ligands with the potential to have vasomodulatory actions (Akerman *et al*., 2004; Johns *et al*., 2007; Macintyre *et al*., 2014; Pacher *et al*., 2004).

As discussed previously, activation of the CB_2R is documented to be immunomodulatory, having effects on cytokine, chemokine and adhesion molecule regulation decreasing the number of leukocytes recruited to the area of inflammation (Hajishengallis & Chavakis, 2013). Relationships between leukocytes and platelets play key roles in blood coagulation (Popel & Johnson, 2005). If leukocytes, platelets and coagulation factors are activated within the microvasculature they decrease and consequently inhibit microcirculatory blood flow (Li *et al*., 2000). A decrease in leukocytes recruitment by CB_2R activation attenuating the release of inflammatory mediators would inhibit platelet-leukocyte interactions and resultant coagulation factors that would intrinsically decrease vascular blood flow (Li *et al*., 2000; Rajesh *et al*., 2007; Rom *et al*., 2013; Toguri *et al*., 2014; Xu *et al*., 2007). Therefore, the increases that are seen in microcirculatory blood flow could be consequences of CB_2R activation.

It was previously eluded to that CB_1R activation can increase the blood flow of the iridial microcirculation by its vasoactive effects. WIN, amongst other CB_1R agonists, has been shown to be a vasodilator (Wagner *et al*., 2001). Within the ocular microcirculation vasodilators have been observed to increase the microcirculatory flow by LDF. Hétu *et al*. showed in rats administered with potent vasodilator, CO_2, a transient increase in blood perfusion in the ocular microcirculation. The opposite was also true, when animals were exposed to O_2, vasoconstriction occurred and blood flow in the microcirculation of the choroid and retina transiently decreased (Hétu *et al*., 2013). These observations in conjunction with decreasing leukocyte adhesion could be working together as a positive feedback loop reinforcing the beneficial effects of each other.

3.6.4 Conclusions

In conclusion, the present study has demonstrated microcirculatory dysfunction in the iris during systemic inflammation. The alterations in leukocyte adhesion and blood flow were attenuated by the non-selective CBR agonist WIN. As the effects of WIN were attenuated by both CB_1R and CB_2R in small vessels and CB_2R in large vessels this provides evidence that both CB_1R and CB_2R activation could potentially improve microcirculatory dysfunction. The iris microcirculation could be used as a model for changes in those microvascular

beds that cannot be investigated by non-invasive techniques in systemic inflammation.

Chapter IV: Anti-inflammatory effects of C_2R activation in endotoxin-induced uveitis

4.1 Manuscript status and student contribution

The figures and text presented in this chapter have been reproduced with copyright permission (Appendix I) from the article: Toguri, J. T., Lehmann, C., Laprairie, R.B., Szczesniak, A.M., Zhou, J., Denovan-Wright, E.D. Kelly, M.E.M (2014) Anti-inflammatory effects of Cannabinoid 2 Receptor activation in endotoxin-induced uveitis. *British Journal of Pharmacology* **171**: 1448 – 1461

As first author on this article, I performed most of the experiments, analysis, data interpretation and statistics. Dr. A. M. Szczesniak helped to conduct intraocular injections. Robert B. Laprairie conducted qPRC for NF-κB, AP-1 and HPRT and taught me how to conduct qPCR. Dr. J. Zhou taught me surgical techniques and intravital microscopy. Several experiments were conducted in the laboratory of Dr. E. M. Denovan-Wright. I wrote the manuscript which was edited by Dr. C. Lehmann and Dr. M. E. M. Kelly.

4.2 Abstract

Background and purpose: CB_2R stimulation has immunomodulatory effects. This study investigated the effects of CB_2R modulation on leukocyte-endothelial adhesion and inflammatory mediator release in experimental endotoxin-induced uveitis (EIU).

Experimental approach: EIU was induced by intraocular injection of lipopolysaccharide (LPS, 20 ng/μL). Effects of the CB_2R agonist, HU308 (1.5% topical), the CB_2R antagonist, AM630 (2.5 mg kg^{-1} i.v.), or a combination of agonist and antagonist on leukocyte-endothelial interactions were examined hourly for 6 hrs in rat iridial vasculature using intravital microscopy. The anti-inflammatory actions of HU308 were compared to clinical treatments for uveitis: dexamethasone, prednisolone and nepafenac. Transcription factors (NF-κβ, AP-1) and inflammatory mediators (cytokines, chemokines and adhesion molecules) were measured in iris and ciliary body tissue.

Key results: Increased leukocyte-endothelium adherence was seen in iridial microvasculature between 4-6 hrs after LPS. HU308, reduced adherent leukocytes at 4, 5, and 6 hrs after LPS injection ($p<0.05$) and decreased pro-inflammatory mediators: TNF-α, IL-1β, IL-6, CCL5 and CXCL2 ($p<0.05$). AM630, blocked the actions of HU-308, and significantly increased leukocyte-endothelium adhesion ($p<0.05$). HU-308 decreased transcription factors NF-κB

and AP-1 ($p<0.001$ and $p<0.001$), while AM630 increased levels of NF- κβ ($p<0.05$).Topical treatments with dexamethasone, prednisolone, or nepafenac, failed to alter leukocyte adhesion or mitigate LPS-induced increases in inflammatory mediators during the 6 hr EIU time-course ($p>0.05$).

Conclusion and implications: Stimulation of CB_2R is anti-inflammatory in a model of acute EIU by a mechanism involving a reduction in NF-κβ, AP-1 and inflammatory mediators. CB_2R may be a promising drug target for the development of novel ocular anti-inflammatory agents.

4.3 Introduction

The endocannabinoid system is an endogenous lipid ligand signalling system consisting of two G-protein-coupled receptors, the cannabinoid 1 receptor (CB_1R) and the cannabinoid 2 receptor (CB_2R), endogenous ligands including N-arachidonoylethanolamine (AEA) and 2-arachidonoyl glycerol (2-AG), and their respective cognate biosynthetic and degradative enzymes (Pertwee, 2005; Pacher *et al*., 2006; Di Marzo, 2009). CB_1R are found throughout the nervous system and in the periphery and activation of CB_1R modulates presynaptic release of neurotransmitters (Scotter *et al*., 2010). CB_2R are highly localized on immune cells; their stimulation with either endogenous or exogenous cannabinoids is associated with immunomodulatory effects (reviewed by Tanasescu and Constantinescu, 2010; De Petrocellis and Di Marzo, 2009).

Recently, several studies have reported that modulating CB_2R in experimental models of sepsis decreased inflammation (Lehmann *et al*., 2011; Lehmann *et al*., 2012), and reduced survival in CB_2R-null animals (Tschop *et al*., 2009). Attenuation of the inflammatory response by CB_2R activation has also been reported in the brain; a study examined pial vessels that form the blood brain barrier in a model of LPS-induced encephalitis (Ramirez *et al*., 2012). This study demonstrated that activation of CB_2R decreased adhesion molecules in the brain tissue and leukocyte-endothelial adhesion in the pial vessels (Ramirez *et al*., 2012).

To-date the involvement of CB_2R in immune responses in the eye has not been extensively examined. However, it has been shown that CB_2R activation has anti-inflammatory effects in the retina in a chronic experimental model of autoimmune uveoretinitis (EAU), and is associated with inhibition of leukocyte trafficking *in vivo* and reduction of inflammatory mediators *in vitro* (Xu *et al*., 2007). The immunomodulatory actions of CB_2R have not been investigated in the anterior chamber of the eye and, while CB_2R have been reported in porcine trabecular meshwork tissue (Zhong *et al*., 2005), other studies have not detected CB_2R expression in anterior ocular tissues (Straiker *et al*., 1999). Furthermore, in contrast to CB_1R, conflicting reports have been published on the role of drugs activating CB_2R in the eye, including their effects on intraocular pressure and aqueous humor outflow (Zhong *et al*., 2005; Szczesniak *et al*., 2011; for review see, Tomida *et al*., 2004).

This study examined the effects of CB_2R modulation in the anterior iridial microvasculature in an experimental model of endotoxin-induced uveitis. This model is a widely used animal model of human bacterially-derived uveitis, involving inflammation of the uveal tract. The uveal tract comprises the middle layer of the eye, including the iris, ciliary body and the choroid. Uveitis causes upwards of 10% of vision loss globally accounting for a prevalence of 38 to 370 per 100,000 individuals depending on genetic, geographic and environmental variables (Nussenblatt, 1990; Chang and Wakefield, 2002). Current treatments

for uveitis include topical, periocular or systemic administration of corticosteroids, or non-steroidal anti-inflammatory drugs (NSAIDS). Despite these available treatments, some patients become refractory to chronic use of these drugs, and several of the drugs can cause significant complications, including decreases in wound healing, corneal epithelium toxicity, increased intraocular pressure, cataracts and glaucoma (Rosenbaum *et al*., 1980; Cheng *et al*., 1995; Giuliano, 2004; Raizman, 1996; Comstock and Decory, 2012). Therefore, identification of novel anti-inflammatory therapeutics with fewer side-effects for the treatment of uveitis is warranted.

Experimental endotoxin-induced uveitis (EIU) can be induced via systemic or intraocular injection of LPS (Rosenbaum *et al*., 1980; Caspi, 2006; Xie *et al*., 2010). The inflammatory response induced by LPS occurs through its interaction with Toll-like receptor 4 (TLR4) on leukocytes and endothelium. Stimulation of TLR4 activates cellular inflammatory pathways, including those including the transcription factors NF-κB and AP-1, with resultant release of cytokines, chemokines and increased expression of adhesion molecules (Akira and Takeda, 2004; Johnson and Lapadat, 2002; Cho and Kim, 2009; Aomatsu *et al*., 2008; Andonegui *et al*., 2009). The key inflammatory mediators released during uveitis include the cytokines, TNF-α, IL-1β, IL-6, IFN-γ, and IL-10, chemokines, CCL5 and CXCL2, and adhesion molecules including soluble vascular cell adhesion molecule (sVCAM), and intracellular adhesion molecule

(ICAM) (Smith *et al*., 1998; Koizumi, 2003, Murray *et al*., 1990; Becker *et al*., 2001, Becker *et al*., 2000; Lehmann *et al*., 2012). The inflammatory cytokines and chemokines released during inflammation are critical in the activation and recruitment of leukocytes. Adhesion molecules are an essential component for leukocyte-endothelial interactions at the inflamed site for leukocyte tethering, rolling and adhesion to the endothelium (Becker *et al*., 2001). Pro-inflammatory cytokines, TNF-α, IL-1β and IL-6, are released from macrophages, monocytes, fibroblasts and endothelial cells, and have been shown to be increased during uveitis (Murray *et al*., 1990; De Vos *et al*., 1994, Olszewski *et al*., 2007). The anti-inflammatory cytokine, IL-10, is produced by monocytes during acute inflammation and has been suggested to contribute to the resolution of ocular inflammation (Caspi, 1999). The chemokines, CCL5 and CXCL2, are secreted by endothelial cells (Läubli *et al*., 2009) and macrophages (Kawamura *et al*., 2012), respectively. Once released, these chemokines promote immune cells to infiltrate the area of inflammation. CCL5 attracts mononuclear cells (Läubli *et al*., 2009), while CXCL2 influences neutrophil and macrophage chemoattraction (Kawamura *et al*., 2012). Additionally, the adhesion molecules, ICAM-1 and VCAM-1, are upregulated on endothelial cells during ocular inflammation playing a vital role for the adhesion of leukocytes and the endothelium (Silverman *et al*., 2001). Although leukocyte activation and recruitment are important components of the immune response, allowing for wound healing and pathogen

clearance, an escalation of the initial inflammatory response in the vasculature of the eye leads to pathology and vision loss (Bellingan, 2000).

Our study utilized *in vivo* real-time non-invasive imaging and *ex-vivo* analysis of inflammatory mediators in an acute model of EIU generated by intraocular LPS injection. We examined the immunomodulatory effects of both CB_2R agonists and antagonists and compared these to clinically effective immunosuppressive agents (Becker *et al*.2000; LeHoang, 2012; Siddique and Shah, 2011; Gaynes and Onyekwuluje, 2008). Our results provide novel data demonstrating that CB_2R activation is anti-inflammatory in the eye. The immunosuppressive actions of topical CB_2R modulation in this acute EIU model had a rapid onset, were more efficacious than clinically relevant topical steroid and NSAID agents, and were mediated by a decrease in the transcription factors NF-κB and AP-1 with resultant reduction in multiple key pro-inflammatory mediators.

4.4 Methods

*4.4.1 Animal*s

Lewis rats (250 – 400 g; Charles River Laboratories International Inc., Wilmington, MA, USA) were kept on a light/dark cycle (07:00-19:00), and fed *ad libitum*. All experimental procedures were approved by the Dalhousie University Committee on Laboratory Animals and handled according to the

Canadian Council for Animal Care guidelines (http://www.ccac.ca/). Studies were conducted in compliance with the ARRIVE (Animal Research: Reporting *In Vivo* Experiments) guidelines (http://www.nc3rs.org.uk/).

Animals were anesthetised by intraperitoneal (i.p.) injection of sodium pentobarbital (65 mg kg^{-1}; Ceva Sante Animale, Montreal, QC, Canada). Depth of anesthesia was assessed by toe-pinch every 15 min. The femoral vein and artery were catheterized using Intramedic non-radiopaque polyethylene tubing (PE 50; Clay Adams, Sparks, MD, USA). Both catheters were attached to intravenous (i.v.) infusion pumps (Abbott Lifecare 5000 Plum Infusion Pump, IL, USA) in conjunction with the Marquette Eagle 4000 Patient Monitor (General Electric, New Jersey, USA). Hemodynamic variables, including heart rate and mean arterial pressure were measured from the arterial catheter every 15 min. The venous catheter was used for the administration of drug, anesthetic agents and fluorochromes. Animals were sacrificed by i.v. injection of KCl (0.142 ml kg^{-1}).

4.4.2 Endotoxin-Induced Uveitis

Intravitreal injection of either LPS or saline was given into the left eye, through the pars plana, under a WILD M37 dissecting microscope (Leitz Canada, Kitchener, ON, Canada) using a Hamilton syringe (Hamilton Company, Reno, Nevada, USA) fitted to a 30G needle. Control animals received 5 µl of sterile

saline, while experimental animals were injected with 100 ng lipopolysacharide (LPS, *Escherichia coli,* 026:B6, Sigma-Aldrich, Oakville, ON, Canada) in 5µL of saline. Once the injection was completed the puncture wound was glued shut with 3M Vetbond Tissue Adhesive (3M Animal Products, St. Paul MN, USA). This technique was modified from Becker *et al*., 2000. Animals were analyzed for the first 6 hrs post-injection, a time where leukocyte adhesion and extravasation was occurring with no overt changes in gross tissue morphology (Figure 16).

4.4.3 Drugs

Briefly, rats were divided into eleven groups (n = 7-15). Saline solution (0.9% sodium chloride) was obtained from Hospira (Montreal, QC, Canada). The CB_2R agonist, HU308 (4-[4-(1,1-Dimethylheptyl)-2,6-dimethoxyphenyl]-6,6-dimethylbicyclo[3.1.1]hept-2-ene-2-methanol), was obtained from Cayman Chemical (Ann Arbor, MI,USA) and dissolved in Tocrisolve™ 100 (Tocris Bioscience, Ellisville, MO, USA) for topical application at 1.5% (w v^{-1}). The CB_2R antagonist, AM630 (6-iodo-2-methyl-1-[2-(4-morpholinyl)ethyl]-1H-indol-3-yl](4-methoxyphenyl)methanone) was obtained from Tocris Bioscience (Ellisville, MO) and prepared in Dimethyl Sulfoxide (DMSO; Sigma-Aldrich Canada Ltd., Oakville, ON, Canada) and administered i.v. at 2.5 mg kg^{-1} in a 1:1 dilution with saline. In addition, immunosuppressive and anti-inflammatory

pharmacological agents at doses currently used in the treatment of ocular inflammation, including Maxidex™ (0.1% dexamethasone, Alcon, Fort Worth, Texas), Nevanac™ (0.1% nepafenac, Alcon, Fort Worth, Texas) and Pred Forte™ (1% prednisolone, Allergan, Irvine, CA), were also tested, and their effects were compared to cannabinoid compounds. All drugs were given as 5 µl of topical ophthalmic drops, except AM630, which was given i.v over a 15 min after the intravitreal injection. Blood pressure and heart rate were monitored throughout the experimental time-course using a Marquette Eagle 4000 Patient Monitor (General Electric, New Jersey, USA) and did not significantly differ in any of the treatment groups (Table 3A and 3B).

4.4.4 Intravital Microscopy

The iridal microcirculation was observed with the Olympus OV 100 Small Animal Imaging System (ON, Canada). The OV100 contains an MT-20 light source and a DP70 CCD camera (Suetsugu *et al*., 2011). Fluorescence excitation was generated by xenon lamp (150W), and 8 position excitation filters to block for rhodamine-6G (excitation 515-560 nm, emission 590 nm) and FITC (450-490 nm, emission 520 nm). Images were captured by a black and white DP70 CCD C-mount camera in real-time and recorded in a digital format by the software, Wassabi (Hamatsu, Herrsching, Germany) on the computer connected

Figure 16. Representative histological cross section of the eye stained with H&E. (A) Control animal cornea, (B) LPS treated animal cornea, (C) Control animal iris, (D) LPS treated animal iris. (E) Histogram of inflammatory cells infiltrating the anterior chamber of the eye. ESS = anterior corneal epithelial stratified squamous; CS = corneal stroma; K = keratocyte; PE = posterior endothelium; AC = anterior chamber; IIC = infiltrating inflammatory cell; PC = posterior chamber. Magnification 10X. Scale bar = 100 μm.

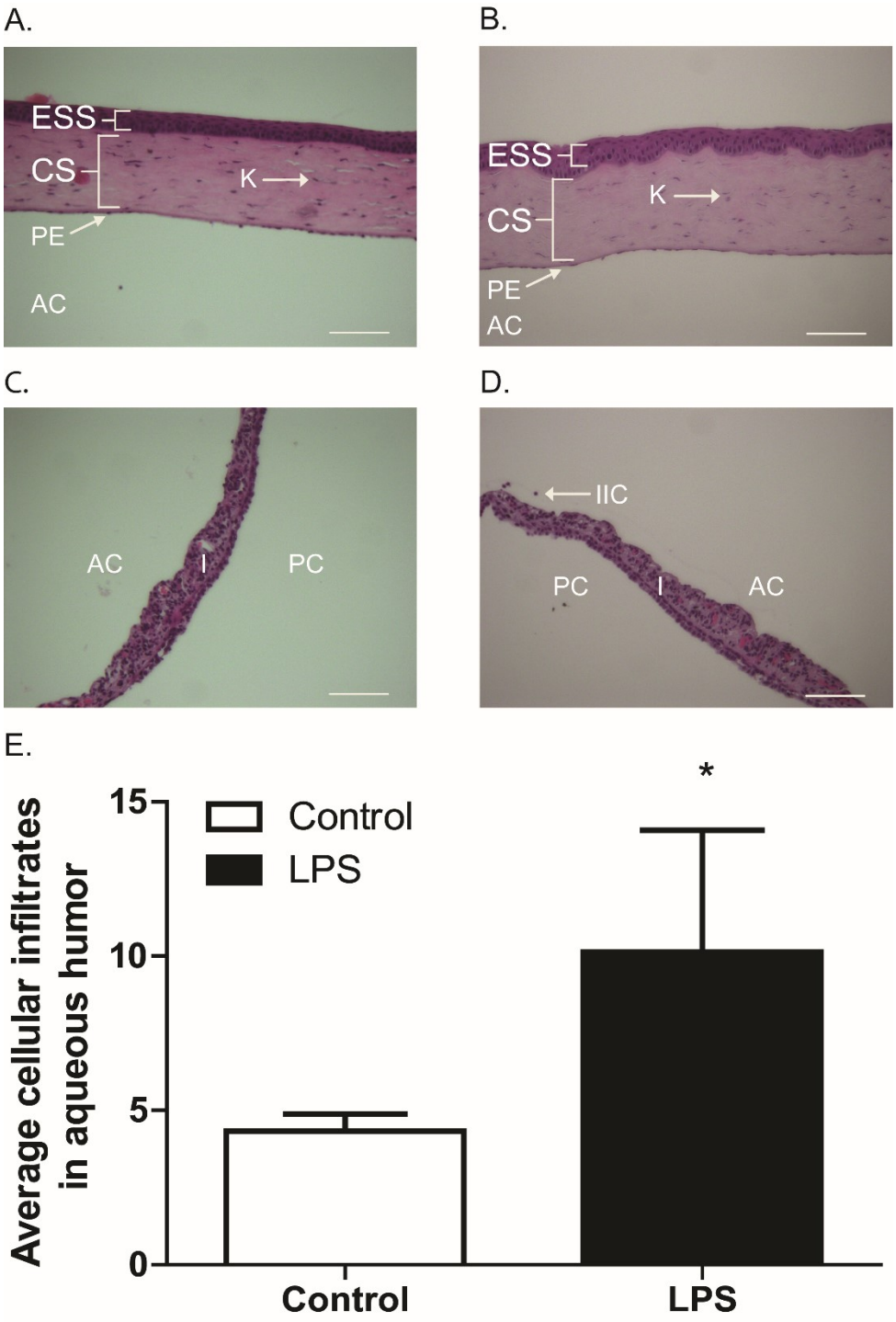
A.
ESS
CS
K
PE
AC
B.
ESS
K
CS
PE
AC
C.
AC
I
PC
D.
IIC
PC
I
AC
E.
Average cellular infiltrates in aqueous humor
15
10
5
0
Control
LPS
*
Control
LPS

to the OV100. Rats were placed in a stereotactic frame (Kopf, CA, USA), and Tear-Gel (Novartis Pharmaceuticals Canada Inc., Dorval, QC, Canada) was placed on the cornea to prevent dehydration of the tissue throughout the experiment. Rhodamine-6G (1.5 ml/kg; Sigma-Aldrich, ON, Canada) and FITC-albumin (1 ml/kg; Sigma-Aldrich, ON, Canada) were injected i.v. 15 min before initiating IVM. The fluorescent dye Rhodamine-6G labelled mitochondria in leukocytes within the vessel and FITC-albumin allowed for the visualization of blood flow through the vasculature. Animals were placed on a heating pad to maintain body temperature at 37 °C. IVM was carried out in four regions of interest. In each region of interest, four randomly selected vessels were observed, and 30 s recordings were made per hr of each vessel for the duration of the experiment. For IVM studies, data was analysed off-line in a blinded manner. Recordings of the iridial microcirculation were analysed using the imaging software ImageJ (National Institute of Health, USA). The length, measured between points of branching and diameter of the vessels were used to calculate the volume within the vessel. Adhering leukocytes were defined as white blood cells that were attached to the vessel wall and were immobile for a 30 s observation period; adhering cells were reported as the number of cells per square millimetre of endothelial surface.

Table 3: Haemodynamic measurements including mean arterial pressure (MAP) and heart rate during EIU and respective drug treatments. (A) Mean arterial pressure (mmHg) (B) Heart rate (beats per minute) in the following treatment groups: Control, LPS, LPS + 1.5% HU308, LPS + 2.5 mg kg^{-1} AM630, LPS+ HU308 + AM630, LPS + 0.1% dexamethasone, LPS + 0.1% nepafenac, n = 4 – 8, $P<0.05$; compared to LPS. Values represent mean ± SEM.

A)

	Control	LPS	LPS + HU308	LPS + AM630	LPS + AM630 + HU308	LPS + 0.1% dexamethasone	LPS + 1% prednisolone	LPS + 0.1% nepafenac
1 hr	116 ± 6	118 ± 1	127 ± 10	124 ± 17	120 ± 9	117 ± 5	116 ± 6	125 ± 4
2 hr	111 ± 5	131 ± 2	121 ± 27	117 ± 10	120 ± 5	119 ± 4	112 ± 4	126 ± 10
3 hr	117 ± 4	128 ± 6	123 ± 9	115 ± 11	122 ± 5	122 ± 3	118 ± 4	119 ± 8
4 hr	124 ± 8	127 ± 6	121 ± 16	107 ± 10	115 ± 4	123 ± 4	123 ± 4	119 ± 9
5 hr	122 ± 7	120 ± 12	127 ± 30	108 ± 13	109 ± 12	126 ± 6	122 ± 4	115 ± 7
6 hr	110 ± 10	132 ± 6	109 ± 17	104 ± 14	10 ± 9	128 ± 5	112 ± 3	119 ± 7

B)

	Control	LPS	LPS + HU308	LPS + AM630	LPS + AM630 + HU308	LPS + 0.1% dexamethasone	LPS + 1% prednisolone	LPS + 0.1% nepafenac
1 hr	380 ± 11	378 ± 30	402 ± 42	392 ± 11	336 ± 15	423 ± 6	116 ± 8	125 ± 21
2 hr	364 ± 8	378 ± 30	342 ± 30	380 ± 17	342 ± 14	423 ± 13	112 ± 32	126 ± 21
3 hr	400 ± 35	414 ± 6	390 ± 6	390 ± 12	366 ± 19	417 ± 3	118 ± 16	119 ± 22
4 hr	288 ± 17	408 ± 12	384 ± 12	388 ± 17	393 ± 22	415 ± 12	123 ± 19	119 ± 16
5 hr	424 ± 17	384 ± 12	390 ± 54	402 ± 13	387 ± 24	418 ± 12	122 ± 19	115 ± 13
6 hr	388 ± 11	354 ± 6	366 ± 30	402 ± 13	360 ± 11	399 ± 13	112 ± 13	119 ± 15

Eyes were enucleated bi-dissected at the corneal scleral junction to obtain anterior uveal tissue and flash frozen in liquid nitrogen and stored at – 80 °C for subsequent analyzes of inflammatory mediators (cytokines, chemokines, and adhesion molecules) or fixed in 4% paraformaldehyde for hematoxylin and eosin (H&E) staining and light microscopy.

4.4.5 Measurement of Inflammatory Markers

Frozen tissue was homogenized in 100 µl of phosphate-buffered saline (PBS) and 1% bovine serum albumin (BSA), supplemented with a protease inhibitor cocktail (Sigma, St. Louis, MO). Homogenates were centrifuged at 13,000 G for 15 min at 4 °C, and supernatant was collected. The Bio-Rad Protein Assay (Mississauga, ON) was used to determine protein concentration according to the manufacturer's instructions. Protein was diluted to a concentration of 3620 µg/ml in PBS then diluted 1:1 in rat diluent provided within the Procarta Multiplex Cytokine Assay Kit (Freemont, CA). Samples were analyzed using a Procarta Multiplex Cytokine Assay kit from Affymetrix and the Bio-Rad 200 instrument with Bio-Plex software (Mississauga, ON) according to the manufacturer's instructions. Samples were run in duplicates and tested for levels of TNF-α, IL-1β, IL-6, IL-10, INF-γ, CCL5, CXCL2, sVCAM, and ICAM. Standard curves for each cytokine were generated using the reference cytokine concentrations supplied with the kit.

4.4.6 Histology

Following fixation, eyes were immersed in 30% sucrose for 24-72 hours at 4°C and the lens removed. Whole eyes were then frozen in OCT compound and sectioned (10 μm) using a Leica CM1950 cryostat. Tissue sections were cut at 10 μm, mounted onto slides and stained with H&E. Stained sections were visualized using light microscopy (Figure 16).

4.4.7 qRT-PCR

RNA was harvested from supernatant from homogenized tissue in PBS and protease inhibitor cocktail (Sigma, St. Louis, MO) using the Trizol® (Invitrogen) extraction method according to the manufacturer's instruction. Reverse transcription reactions were carried out with SuperScript III® reverse transcriptase (+RT; invitrogen), or without (-RT) as a negative control for use in subsequent PCR experiments according to the manufacturer's instructions. Two micrograms of RNA were used per RT reaction. qRT-PCR was conducted using the LightCycler® system and software (version 3.0; Roche, Laval, QC). Reactions were composed of a primer-specific concentration of $MgCL_2$ (Table 1 in methods), 0.5 μM each of forward and reverse primers (Table 1), 2 μL of LightCycler® FastStart Reaction Mix SYBR Green I, and 1 μL cDNA to a final volume of 20 μL with dH_2O (Roche). The PCR program was: 95 ° C for 10 min,

50 cycles of 95 ° C 10 s, a primer-specific annealing temperature for 5 s, and 72 ° C for 10 s (Table 1). Experiments included sample-matched RT controls, a no-sample dH_2O control, and a standard control containing product-specific cDNA of a known concentration. cDNA abundance was calculated by comparing the cycle number at which a sample entered the logarithmic phase of amplification to a standard curve generated by amplification of cDNA samples of known concentration (LightCycler Software version 4.1; Roche). Here qRT-PCR data were normalized to the expression of hypoxanthine-guanine phosphoribosyltransferase (HPRT).

4.4.8 Statistical Analyses

Individual animals in each of the treatment groups were coded and data and statistical analysis was conducted in a blinded manner. Hemodynamic variables were analysed by two-way ANOVA and Bonferroni *post-hoc* testing after confirmation of normal distribution according to Kolmogoroff-Smirnov. IVM data and inflammatory mediators were analysed by one-way ANOVA with Dunnett's *post-hoc* test, comparing all experimental groups to the LPS-treated group. qRT-PCR data were analyzed by one-way ANOVA with Tukey's test. All data are presented as mean ± SEM, where $p < 0.05$ was considered statistically significant. Data was analyzed with the statistical software GraphPad Prism v.5. (GraphPad Software Inc., San Diego, CA, USA).

4.5 Results

4.5.1 Leukocyte-Endothelial Interactions in the Iridial Microcirculation

Figure 17A-B shows representative IVM images of the iridial microvasculature at 6 hrs from control eyes (Figure 17A), and eyes from animals with EIU following an intravitreal injection of 100 ng of LPS in 5 μl of saline (Figure 17B). The histogram in Figure 17C shows that the number of firmly adhering leukocytes in the microvasculature was significantly increased at 4, 5, and 6 hrs (146 ± 68, 182 ± 101, 232 ± 176, respectively, n = 15, $p<0.05$), in comparison to the control group at the same time-points (37 ± 23, 65 ± 51, 69 ± 33, n = 11, respectively). There was no significant difference between leukocyte adhesion in animals challenged with LPS alone or LPS plus the topical vehicle, Tocrisolve®, or LPS plus i.v. DMSO, or LPS plus both i.v. DMSO and topical Tocrisolve® at 6 hrs (113 ± 66, 104 ± 76, 133 ± 86, $p < 0.05$, n=6, respectively, for all vehicle treatment groups).

Figure 18A-D shows representative images of the iridial microcirculation obtained in LPS-treated (100 ng) eyes and eyes treated with LPS plus the following cannabinoids: the CB_2R agonist, HU308 (1.5%) , the CB_2R antagonist, AM630 (2.5 mg kg^{-1}) , and AM630 in conjunction with HU308. The doses of cannabinoid drugs were based on route of delivery, and the dose-response for inhibition of leukocytes adhering to the endothelium (Figure 19). For topical

HU308, a dose of 1.5% was chosen based on the IC_{50} (0.8 %) and E_{Max} (1.5 %) for inhibition of leukocytes adhering to the endothelium in EIU. The CB_2R agonist, HU308 is highly selective for CB_2R with a K_i of > 10 μM for CB_1R and a Ki of 22.7 ± 3.9 nM (Breauer *et al*., 1999; Rajesh *et al*., 2007). Antagonist dose was based on previous published studies (Szczesniak *et al*., 2011; Lehmann *et al*., 2012). Topical application of the CB_2R agonist HU308 (1.5%) significantly attenuated the number of leukocytes adhering to the endothelium at 4, 5, and 6 hr (39 ± 12, 58 ± 7, 89 ± 72, respectively, n = 12, $p<0.05$), compared to LPS alone (Figure 18E). Treatment with the CB_2R antagonist AM630 (2.5 mg kg^{-1}, i.v.) significantly exacerbated leukocyte adhesion to the endothelium at 4, 5, and 6 hr (418 ± 330, 576 ± 309, 539 ± 338, respectively, n = 8, $p<0.05$ compared to LPS alone). Figure 18E also shows that no significant difference was found in leukocyte-endothelial adhesion at 6 hr between LPS- injected eyes and in LPS-injected eyes of animals treated with AM630 + HU308 (225 ± 102, n = 7, $p>0.05$).

4.5.2 Effects of Cannabinoids on Ocular Inflammatory Mediators

In order to determine the potential mechanisms contributing to the anti-inflammatory actions of CB_2R activation, measurements of pro-inflammatory and anti-inflammatory cytokines released following immune cell recruitment and activation were obtained from anterior ocular tissue (iris and ciliary body), in the absence and presence of cannabinoid treatments (Table 1). The most applicable

inflammatory molecules were chosen for measurement based on animal and clinical studies of uveitis and LPS-induced inflammation.

Induction of EIU by intravitreal LPS injection significantly increased inflammatory mediators, TNF-α, IL-1β, IL-6, CCL5, and CXCL2 in the anterior uveal tissues of the rat eye. Topical application of the CB_2R agonist, HU308, resulted in a significant decrease in cytokines, TNF-α, IL-1β, IL-6, IL-10, INF-γ ($p<0.05$), as well as chemokines, CCL5 and CXCL2, but had no effect on adhesion molecule levels ($p>0.05$). TNF-α decreased by 64 fold, IL-1β by 9 fold, IL-6 by 4 fold, IL-10 by 2 fold, INF-γ by 3 fold, CCL5 by 4 fold, and CXCL2 by 9 fold. Treatment with the CB_2R antagonist AM630 alone, reduced LPS-induced inflammatory mediators; decreasing levels of TNF-α, IL-10 and CXCL2 compared to un-treated EIU animals ($p<0.05$). A combination of both the CB_2R antagonist, AM630, and agonist, HU308, decreased the release of pro-inflammatory cytokines, TNF-α, IL-1β, IL-6, and chemokines CXCL2 and CXC5 but failed to attenuate the levels of adhesion molecules measured.

4.5.3 Effects of Cannabinoids on NF-κB and AP-1 mRNA during Ocular Inflammation

The LPS pro-inflammatory response has been shown to be mediated by TLR4 (Akira and Takeda, 2004). Activation of TLR4 causes downstream signaling by a number of different pathways, which can either directly or

Figure 17. Leukocyte-adhesion in the iridial microvasculature in Lewis rat 6 hr following endotoxin-induced uveitis (EIU) generated by intravitreal endotoxin injection A. & B: Representative intravital microscopy images of iridial microcirculation in rat eye showing adherent leukocytes at 6 hrs after intravitreal injection of: (A) saline, and (B) LPS. (C) Bar graph represents the time-course for the mean number of adherent leukocytes in the following groups: control (n = 11); LPS (n = 15); LPS + the following vehicles (n=6 for each vehicle group) including Tocrisolve100 ® (topical); DMSO (i.v.); Tocrisolve100 ® + DMSO. Arrows indicate adherent leukocytes. Scale Bar =100 μm. + $P<0.05$ compared to the LPS group. Values represent mean ± SEM.

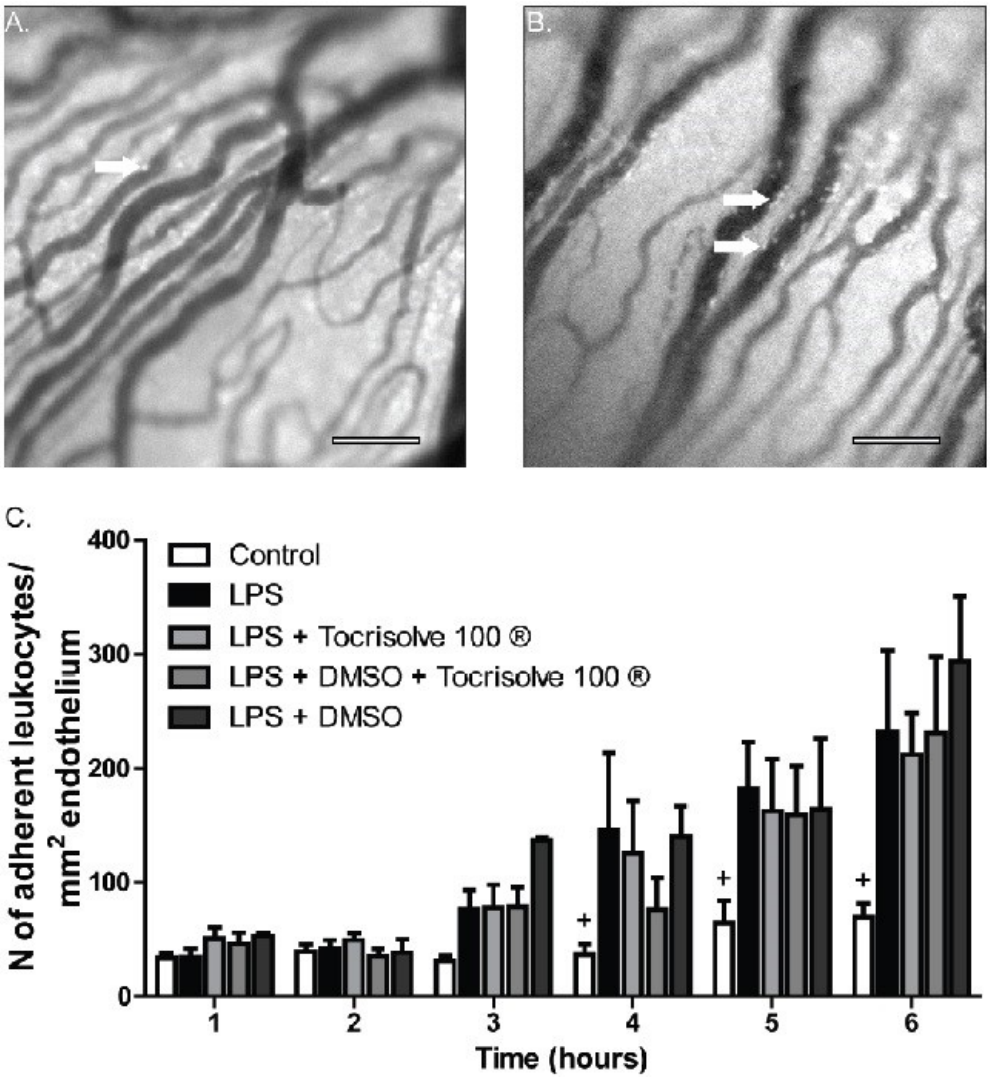
A.
B.
C.
N of adherent leukocytes/ mm2 endothelium
400
300
200
100
0
Control
LPS
LPS + Tocrisolve 100 ®
LPS + DMSO + Tocrisolve 100 ®
LPS + DMSO
+
+
+
1
2
3
4
5
6
Time (hours)

Figure 18. CB_2R modulation of leukocyte-adhesion during EIU. Representative intravital microscopy images of iridial microcirculation in rat eyes at 6 hrs after intravitreal LPS injection in the following groups: (A) LPS injection only, (B) LPS + CB_2R agonist, HU308 (1.5%, topical), (C) LPS + CB2R antagonist, AM630 (2.5 mg kg^{-1}, i.v.), and (D) LPS + AM630+ HU308. (E) Bar graph represents the time course for the mean number of adherent leukocytes in the iridial microcirculation for groups including: LPS (n = 15), LPS + HU308 (n = 12), AM630 (n = 8), and AM630 + HU308 (n = 7). Arrows indicate adherent leukocytes. Scale Bar =100 μm. * $P<0.05$ compared to the LPS group. Values represent mean ± SEM.

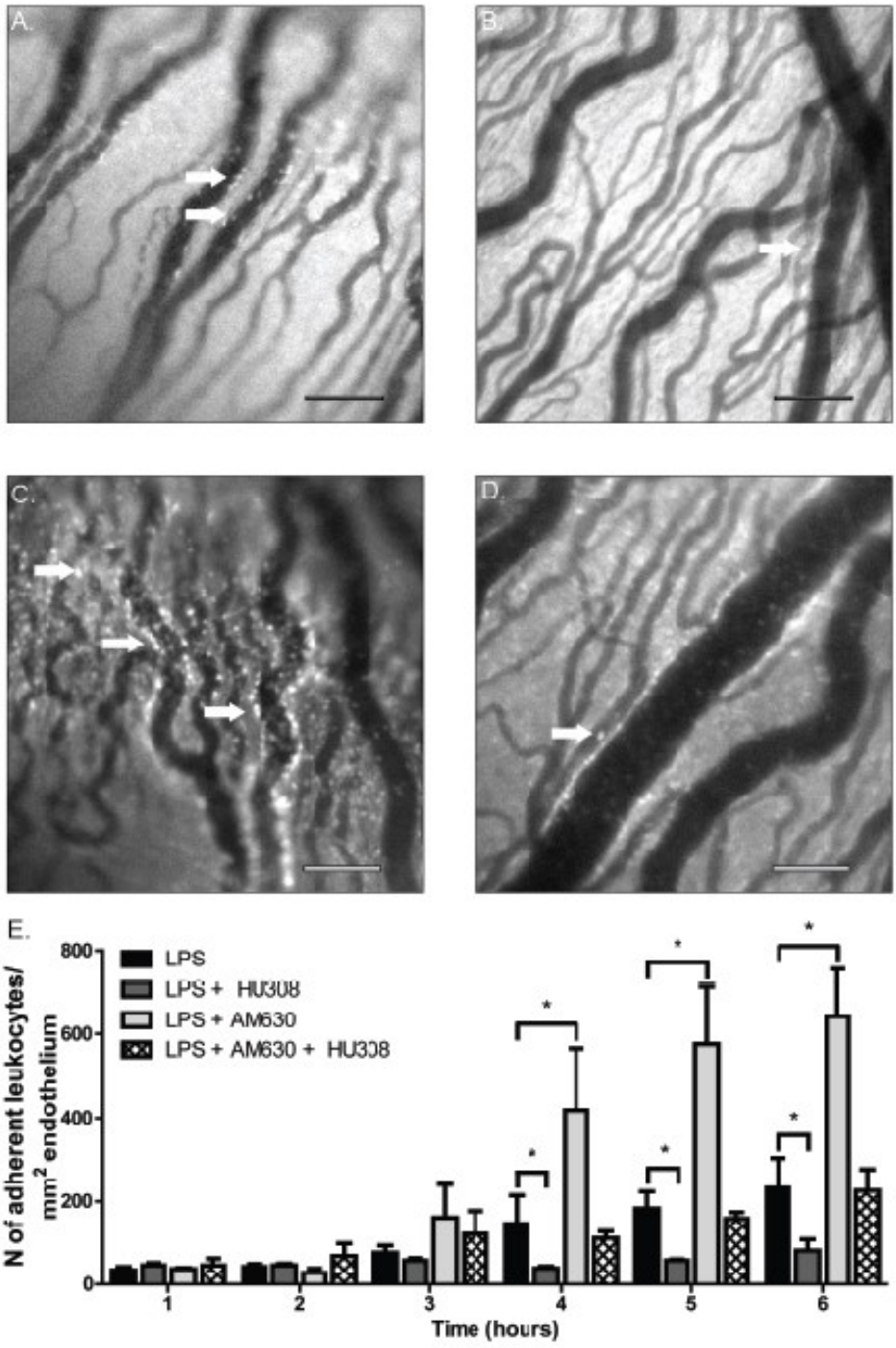
A.
B.
C.
D.
E.
LPS
LPS + HU308
LPS + AM630
LPS + AM630 + HU308
N of adherent leukocytes/ mm² endothelium
800
600
400
200
0
1
2
3
4
5
6
Time (hours)
*

Figure 19. The doses of cannabinoid drugs were based on route of delivery, and the dose-response for inhibition of leukocytes adhering to the endothelium. Dose-response curve for the topical administration (0.1-1.5 %) of, cannabinoid agonist, HU308, on leukocyte adhesion in iridial venules. Values are represented as percentage change in leukocyte adhesion to endothelium and normalised to the minimal response of control animals and maximum of those receiving only LPS. IC_{50} for HU308-mediated decrease in leukocyte adhesion is 0.7867 % (w/v).

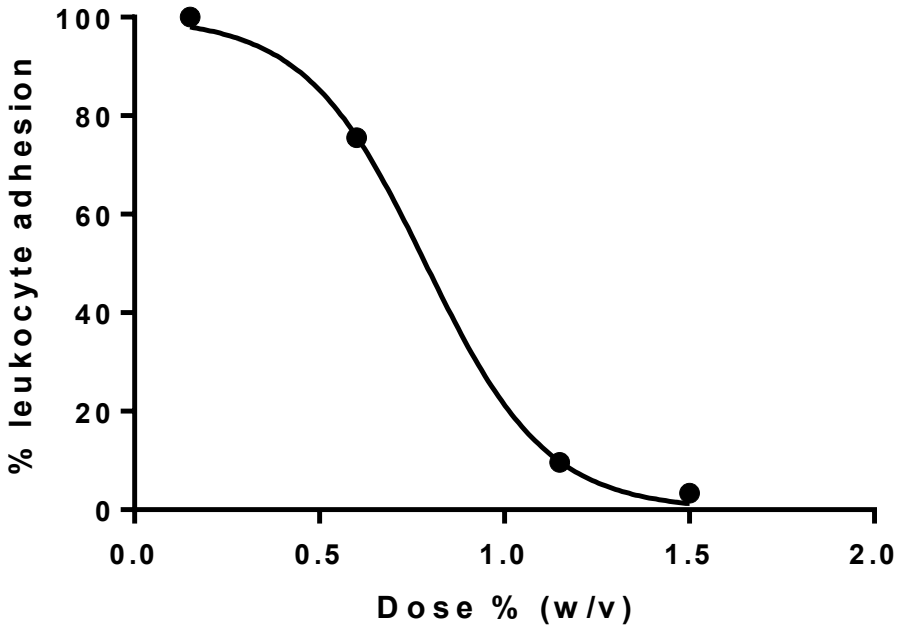
100
80
60
40
20
0
% leukocyte adhesion
0.0
0.5
1.0
1.5
2.0
Dose % (w/v)

indirectly activate transcription factors which modulate the levels of inflammatory mediators. The transcription factor NF-κB is activated directly by the TLR4 pathway, increasing inflammatory cytokines (Akira and Takeda, 2004). Alternatively, phosphorylation cascades can indirectly activate other transcription factors that influence inflammatory mediators such as activator protein-1 (AP-1) (Johnson and Lapadat, 2002). Together, transcription factors activated directly and indirectly by LPS through TLR4 can increase inflammatory mediators, cytokines, chemokines and adhesion molecules (Cho and Kim, 2009). Figure 20A shows that an intravitreal injection of LPS significantly increases mRNA levels of the p65 component of NF-κB compared to the saline-injected control group (control, 0.02 ± 0.01 (NF-κβ/ HPRT), n = 9; LPS, 7.92 ± 1.83 (NF-κβ/ HPRT), n = 6, $p<0.001$). Topical application of HU308, the CB_2R agonist deceased mRNA levels of NF-κB compared to the group treated with LPS (LPS + HU308, 0.01 ± 0.008 (NF-κβ/ HPRT), n = 13, $p<0.001$ compared to LPS-only). In contrast, treatment with AM630, the CB_2R antagonist, significantly increased mRNA levels of NF-κB compared to LPS-treated animals (LPS + AM630, 14.03 ± 2.14 (NF-κB/ HPRT), n = 10, $p<0.05$ compared to LPS-only). Combination treatment with AM630 and HU308, however, significantly decreased mRNA levels of NF-κB compared to LPS treated animals (LPS + AM630 + HU308, 0.02 ± 0.01 (NF-κβ/ HPRT), n = 10, $p<0.001$ compared to LPS-only).

Figure 20B shows that ocular inflammation induced by LPS increased mRNA levels of the transcription factor AP-1 in comparison to the control group (control, $3X10^{-4} \pm 1X10^{-4}$ (AP-1/ HPRT), n = 9; LPS, $1.6X10^{-3} \pm 1X10^{-4}$ (AP-1/ HPRT), n = 6, $p<0.001$). The levels of AP-1mRNA were significantly decreased in HU-308-treated animals in comparison to LPS-only (LPS + HU308, $3X10^{-3} \pm 1X10^{-3}$ (AP-1/ HPRT), n = 13, $p<0.001$). No significant difference was found in RNA levels of AP-1 in the LPS-only group and the group treated with the CB_2R antagonist, AM630 (LPS + AM630, $1.1X10^{-3} \pm 3X10^{-3}$ (AP-1/ HPRT), n = 10, $p>0.05$). Combination treatment with both the CB_2R antagonist, AM630 and the CB_2R agonist, HU308 significantly decreased AP-1 mRNA levels in LPS-treated animals by 8 times compared to the LPS-only treated group (LPS + HU308, $2X10^{-4} \pm 1X10^{-4}$ (AP-1/ HPRT), n = 10, $p< 0.001$). Figure 20C shows there was no significant changes of IRF3 mRNA levels of the control group ($5.11\ X10^{-4} \pm 3.2088\ X10^{-4}$ IRF3/ HRPT) compared to the LPS group ($2.63X10^{-4} \pm 8.9X10^{-5}$ IRF3/ HRPT). Treatment with saline, LPS and cannabinoid treatments failed to cause any significant changes in IRF3 mRNA levels (LPS + HU308, $1.520X10^{-3} \pm 7.25X10^{-4}$, IRF3/ HRPT; LPS + AM603, $1.10X10^{-4} \pm 7.0X10^{-5}$, IRF3/ HRPT; LPS + AM630 + HU308, $0.55X10^{-7} \pm 3X10^{-6}$ IRF3/ HRPT). To determine if increased NF-κB and AP-1 occurred by the MyD88 or MyD88 independent pathway after TLR4 activation we investigated mRNA expression of RIP-1. RIP-1 is an enzyme located upstream of NF-κB and AP-1 in the MyD88 independent

Table 4: Levels of inflammatory mediators (pg/ml) in extracts of the iris and ciliary body at 6 hrs. Data shown (mean ± SEM) are from control, LPS and LPS with treatments of CB receptor ligands: CB_2 receptor agonist, HU308, CB2 receptor antagonist, AM630, and combination of AM630 + HU308, n = 8 – 11, +P<0.05; compared to the control group. *P<0.05; compared to the EIU group.

	Control	LPS	LPS + HU308	LPS + AM630	LPS + AM630 + HU308
TNF-α	5.9 ± 4.1 *	52.6 ± 18.12 +	0.82 ± 0.6 *	16.8 ± 7.1 *	5.9 ± 4.2 *
IL-1β	264.2 ± 71.4 *	5572 ± 1076 +	602.7 ± 214.4 *	3564 ± 1453 +	549.7 ± 136.9 *
IL-6	8.9 ± 2.2 *	32.9 ± 5.1 +	7.5 ± 2.3 *	16.5 ± 3.7 *	7.2 ± 2.3 *
IL-10	11.1 ± 1.8	18 ± 1.5	6.9 ± 1.3 *	14.2 ± 3.0	12.9 ± 2.7
INF-γ	1.3 ± 0.4	2.5 ± 3.8	0.8 ± 0.4 *	1.4 ± 0.4	1.2 ± 0.6
CCL5	53.16 ± 17.9 *	288.8 ± 49.0 +	66.2 ± 17.1 *	191.7 ± 57.29 +	51.09 ± 13.2 *
CXCL2	101.0 ± 34.64 *	2023 ± 417.7 +	213.3 ± 58.7 *	852.0 ± 361.7 *	288.0 ± 101.7 *
sVCAM	213.8 ± 34.3	362.5 ± 50.5	190.8 ± 27.1	359.6 ± 81.97	244.1 ± 43.4
ICAM	1304 ± 234.3	2118 ± 368.4	1208 ± 115.7	2333 ± 557.2	1589 ± 271.0

Figure 20. mRNA expression of inflammatory transcription factors NF-κB and AP-1 during EIU and CB_2R modulation. (A) NF κβ (B) AP-1 (C) IRF3 in the uveal tissues, including the iris and ciliary body, at 6 hrs in the following treatment groups: control (n = 9), LPS (n = 6), LPS + HU308 (n = 13), LPS + AM630 (n = 10), and LPS + AM630 + HU308 (n = 10). Values are reported compared to the house keeping gene HPRT. *P<0.05, **P<0.01, **P<0.001; compared to the EIU group. Values represent mean ± SEM.

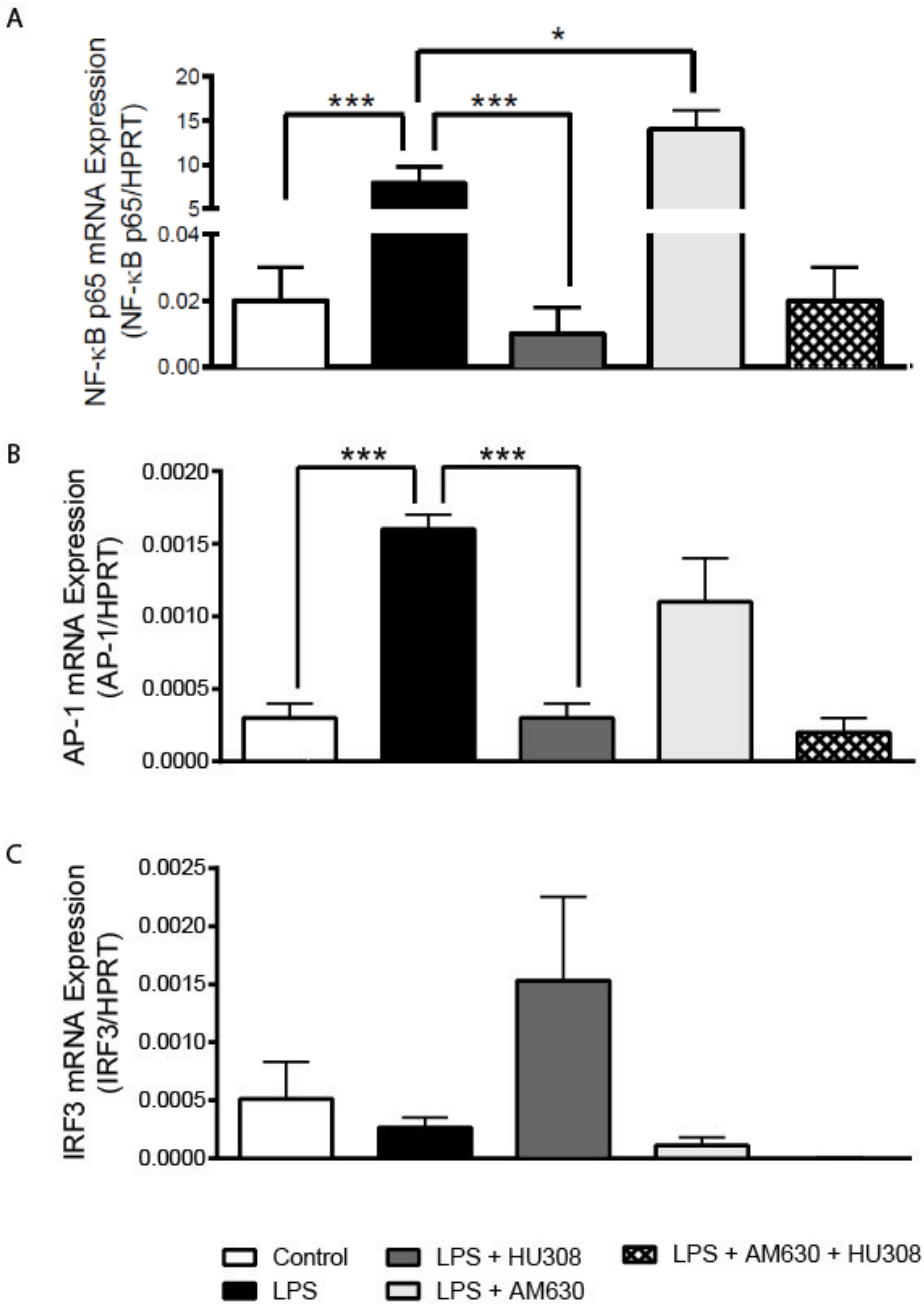
A
NF-κB p65 mRNA Expression
(NF-κB p65/HPRT)
20
15
10
5
0.04
0.02
0.00
***
***
*
B
AP-1 mRNA Expression
(AP-1/HPRT)
0.0020
0.0015
0.0010
0.0005
0.0000
***
***
C
IRF3 mRNA Expression
(IRF3/HPRT)
0.0025
0.0020
0.0015
0.0010
0.0005
0.0000
Control
LPS
LPS + HU308
LPS + AM630
LPS + AM630 + HU308

pathway but not the MyD88 dependent pathway. No significant changes were seen in RIP-1 mRNA expression in any group (control, $2.65X10^{-4} \pm 5X10^{-6}$, RIP-1/HRPT; LPS $1.98X10^{-4} \pm 5.7X10^{-5}$, RIP-1/HPRT; LPS + AM630, $1.80X10^{-4} \pm 7.5X10^{-5}$, RIP-1/HPRT; LPS + HU308 + AM630, $1.26X10^{-4} \pm 7.0X10^{-6}$, RIP-1/HPRT; Figure 21).

Finally, mRNA levels of CB_2R and TLR4 were investigated. Figure 22 A shows that even after limited exposure to LPS, CB_2R mRNA levels are increased in comparison to control animals by 7.35 times (Control, 0.524 ± 0.149256 CB_2R/HRPT, LPS 3.85 ± 1.05 CB_2R/HRPT). Treatment with any cannabinoid drugs failed to attenuate the increase of CB_2R mRNA caused by LPS (LPS + HU308, 2.63 ± 0.84, CB_2R/HRPT; LPS + AM630, 2.57 ± 0.41, CB_2R/HRPT, LPS + AM630 + HU308, 2.95 ± 0.67 CB_2R/HRPT). In contrast to CB_2R mRNA, levels of TLR4 mRNA in the uveal tissue were not significantly altered 6 hr after LPS compared to control animals (control, $9.73X10^{-4}$, ± $3.26X10^{-4}$, TLR4/HRPT, LPS $5.59X10^{-4} \pm 1.64X10^{-4}$, TLR4/HRPT). Treatment with LPS, HU308 and AM630 + HU308 failed to alter mRNA levels of TLR4 (LPS + HU308, $5.99X10^{-4} \pm 1.90X10^{-4}$, TLR4/HRPT; LPS + HU308 + AM630, 3.39X10-4 ± $1.57X10^{-4}$, TLR4/HRPT),surprisingly TLR4 mRNA was significantly decreased in the LPS + AM630 + HU308 group compared to the control group (LPS + AM630, $1.94X10^{-4} \pm 8.28X10^{-5}$, TLR4/HRPT).

Figure 21: mRNA expression of RIP-1 during EIU and CB_2R modulation. mRNA expression levels of the RIP-1 enzyme upstream of NF-κB and AP-1 of the TLR4 MyD88 independent pathway in the uveal tissues, including the iris and ciliary body, at 6 hrs in the following treatment groups: control (n = 9), LPS (n = 6), LPS + HU308 (n = 13), LPS + AM630 (n = 10), and LPS + AM630 + HU308 (n = 10). Values are reported compared to the house keeping gene HPRT. *P<0.05, **P<0.01, **P<0.001; compared to the EIU group. Values represent mean ± SEM.

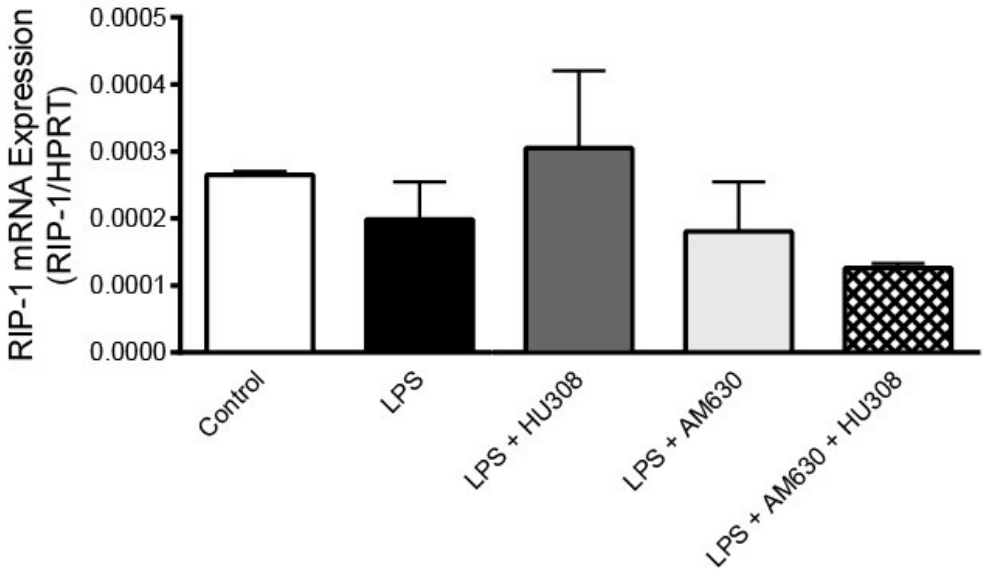
RIP-1 mRNA Expression
(RIP-1/HPRT)
0.0005
0.0004
0.0003
0.0002
0.0001
0.0000
Control
LPS
LPS + HU308
LPS + AM630
LPS + AM630 + HU308

Figure 22. mRNA expression of CB2R and TLR4 during EIU and CB_2R modulation. (A) CB_2R (B) TLR4 in the uveal tissues, including the iris and ciliary body, at 6 hrs in the following treatment groups: control (n = 9), LPS (n = 6), LPS + HU308 (n = 13), LPS + AM630 (n = 10), and LPS + AM630 + HU308 (n = 10). Values are reported compared to the house keeping gene HPRT. *P<0.05; compared to the EIU group, # P<0.05 compared to control group. Values represent mean ± SEM.

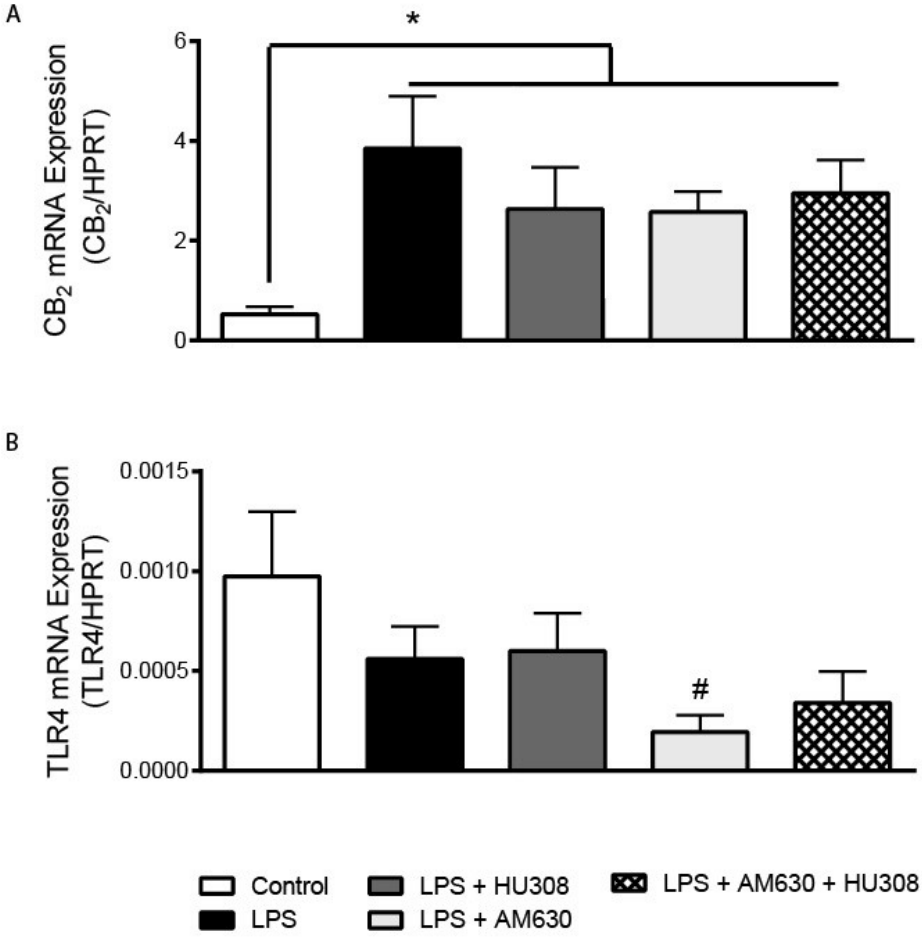
A
*
6
4
2
0
CB2 mRNA Expression
(CB2/HPRT)
B
0.0015
0.0010
0.0005
0.0000
TLR4 mRNA Expression
(TLR4/HPRT)
#
Control
LPS
LPS + HU308
LPS + AM630
LPS + AM630 + HU308

4.5.4 Effects of Clinical Immunosuppressive Drugs in EIU

Leukocyte-endothelial interactions in the iridial microcirculation were also examined in EIU following treatment with topical dexamethasone, prednisolone and nepafenac. These drugs are used clinically at 0.1-1% respectively to treat uveitis (Gaynes *et al*., 2008; Cheng *et al*., 1995). Figure 23 A-D shows representative images of the iridial microcirculation and leukocytes within the vasculature following LPS injection in untreated eyes (Figure 23A), following treatment with 0.1% dexamethasone (Figure 23B), 1% prednisolone (Figure 23C), or 0.1% nepafenac (Figure 23D). Figure 23E depicts the average quantified number of adherent leukocytes per mm^2 of endothelium over the 6 hr time-course in EIU in untreated eyes, and following either corticosteroid or NSAID treatments. In this acute model of EIU, all three of these drugs at doses used clinically, or previously reported to reduce inflammation in experimental models (Kanai *et al*., 2012; Medeiros *et al*., 2008; Hariprasad *et al*., 2009), failed to significantly reduce leukocyte adhesion in the iridial vasculature within the observed 6 hr post-LPS observation period (0.1% dexamethasone, 247 ± 105, n = 9, 1% prednisolone, 214 ± 99, n = 8, 0.1% nepafenac, 134 ± 30, n = 6, $p>0.05$ compared to LPS-only).

Examination of levels of inflammatory mediators after topical application of 0.1% dexamethasone, 1% prednisolone, and 0.1% nepafenac in

Figure 23. Leukocyte-endothelial adhesion in the iridial microvasculature during EIU after treatment of clinically available drugs for uveitis compared to CB2R agonist, HU308. Representative intravital microscopy images of iridial microcirculation in rat eyes at 6 hrs after intravitreal LPS injection in the following groups: (A) LPS injection only (n = 15), (B) LPS + dexamethasone (0.1% topical), (C) prednisolone (1% topical), and (D) nepafenac (0.1% topical). (E) Bar graph represents the time course for the mean number of adherent leukocytes in the above treatment groups (n=9 for all groups). Arrows indicate adherent leukocytes. Scale Bar =100 μm. * $P<0.05$; compared to the LPS group. Values represent mean ± SEM.

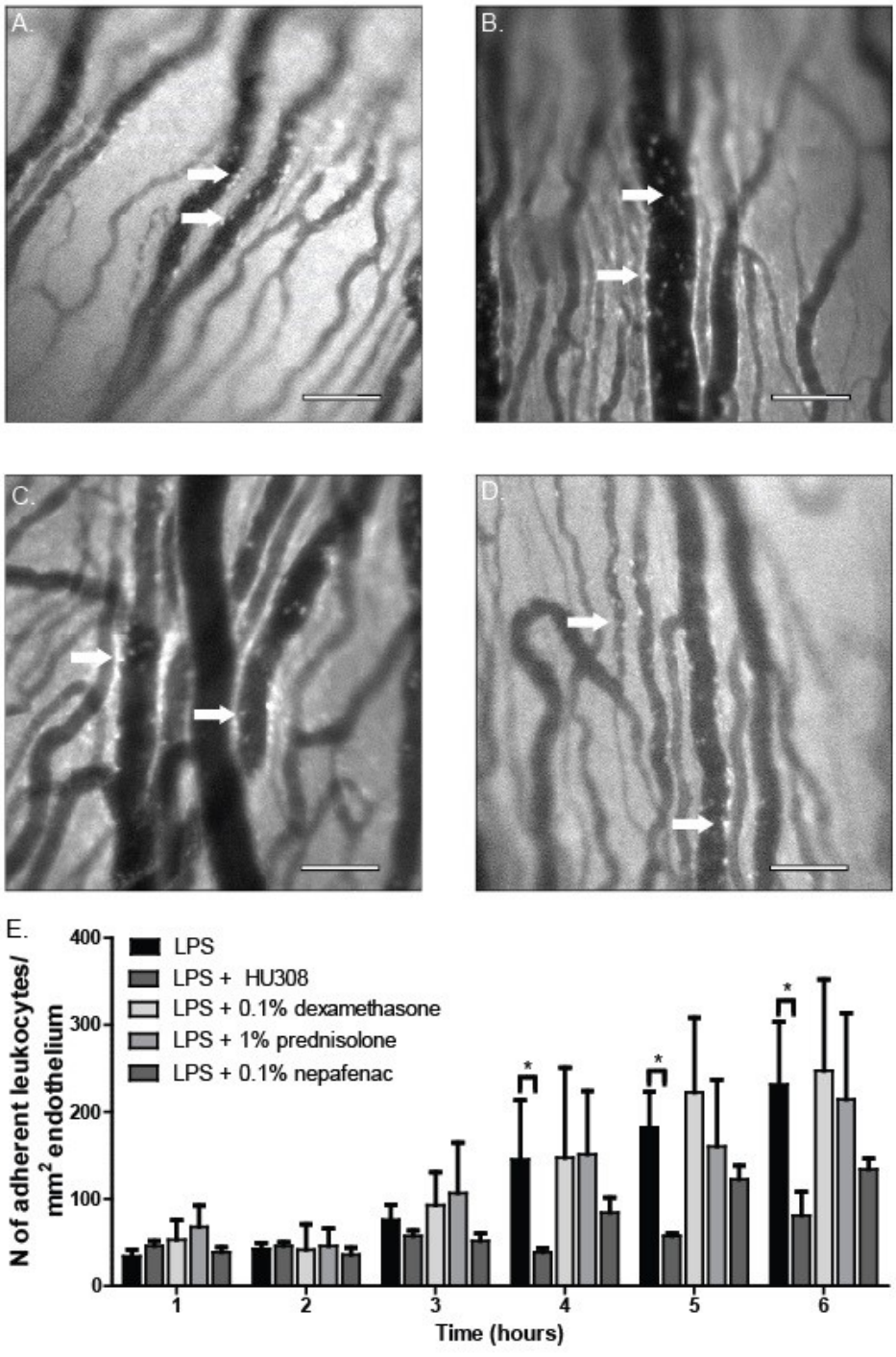
A.
B.
C.
D.
E.
N of adherent leukocytes/ mm² endothelium
400
300
200
100
0
LPS
LPS + HU308
LPS + 0.1% dexamethasone
LPS + 1% prednisolone
LPS + 0.1% nepafenac
*
*
*
1
2
3
4
5
6
Time (hours)

the EIU model was consistent with intravital measurements of leukocyte-endothelial adhesion, where there was no significant change in the number leukocyte adhesion to the endothelium as compared to LPS. With the exception of prednisolone which significantly decreased the levels of IL-1β at 6 hrs ($p>0.05$), the steroids, dexamethasone or prednisolone, and the NSAID, nepafenac, did not significantly reduced the concentrations of inflammatory mediators measured in the iris and ciliary body tissue compared to untreated LPS-only animals (Table 5).

4.6 Discussion

Our results provide novel findings demonstrating that activation of ocular CB_2R in EIU by the synthetic cannabinoid agonist, HU-308, significantly attenuates leukocyte-endothelial adhesion in the iridial microvasculature and reduces the release of pro-inflammatory mediators (TNF-α, IL-1β, IL-6, INF-γ, CCL5 and CXCL2) and the transcription factors (NF-κB and AP-1) which mediate the transcription of pro-inflammatory genes (Akira and Takeda, 2004 ;Johnson and Lapadat, 2002). Furthermore, to the best of these authors' knowledge, this is the first time that a topical cannabinoid treatment has been shown to be anti-inflammatory in an experimental model of acute ocular inflammation.

Table 5. Alterations of inflammatory mediators in the iris and ciliary body of Lewis rats with EIU with or without immunomodulatory clinical treatments. Levels of inflammatory mediators (pg/m) in extracts of the iris and ciliary body at 6 hrs. Data shown (mean ± SEM) are from control, LPS, and LPS with dexamethasone, prednisolone or nepafenac treatments for uveitis, n = 7 – 11, +$P<0.05$; compared to control, *$P<0.05$; compared to LPS.

	LPS	LPS + dexamethasone	LPS + prednisolone	LPS + nepafenac
TNF-α	52.6 ± 18.12 $^{+}$	31.59 ± 21.3	24.7 ± 13.1	15.4 ± 6.7
IL-1β	5572 ± 1076 $^{+}$	2639 ± 798.1	2381 ± 1203 *	2888 ± 946.5
IL-6	32.9 ± 5.1 $^{+}$	29.7 ± 9.9 $^{+}$	24.8 ± 5.6	14.5 ± 5
IL-10	18 ± 1.5	16.53 ± 2.7	16.5 ± 6.2	13.5 ± 2.0
INF-γ	2.5 ± 3.8	1.3 ± 0.5	2.1 ± 0.9	2.2 ± 0.8
CCL5	288.8 ± 49.0 $^{+}$	195.8 ± 57.1	142.7 ± 48.7	277.3 ± 69.0 $^{+}$
CXCL2	2023 ± 417.7 $^{+}$	1994 ± 852.4 $^{+}$	1199 ± 365.2	1340 ± 531.4
sVCAM	362.5 ± 50.5	410.3 ± 81.6	389.9 ± 141.7	380.6 ± 41.24
ICAM	2118 ± 368.4	2174 ± 352	2676 ± 925.8	2616 ± 393.3

4.6.1 Immunomodulatory Effects of CB_2R Activation

CB_2R are upregulated following inflammation in several different tissues (including ileum, pancreas, and throughout the CNS), and this increase in CB_2R signaling has been suggested to play a role in the physiological and homeostatic mechanisms evoked to resolve injury (Michler *et al*., 2013; Cabral *et al*., 2008; D'Argenio *et al*., 2006). To date, several studies have suggested that CB_2R activation is anti-inflammatory in the vasculature of different tissues, such as the intestine, pial vessels, and retinal vessels (Lehmann *et al*., 2012; Ramirez *et al*., 2012; Xu *et al*., 2007). Our results are supportive of these findings, and further show that the decrease in leukocyte-endothelial adhesion seen in the iridial microvasculature following topical application of the CB_2R agonist, HU308, is mediated via the CB_2R. Inhibition of this receptor by the CB_2R antagonist, AM630, prevented the anti-inflammatory effects of HU308. In agreement with our findings, systemic treatment with the CB_2R antagonist, SR144528, in combination with CB_2R agonist, JWH133 prevented the anti-inflammatory actions of CB_2R activation in pial vessels during LPS induced inflammation in an encephalitis model (Ramirez *et al*., 2012). However, in EIU, application of AM630 actually increased the number of adherent leukocytes compared to the LPS-only group. The increase in the number of adhering leukocytes observed when AM630 is administered during EIU suggests endogenous activation of CB_2R. This increase in adherent leukocytes may result from several factors,

including upregulation of CB_2R and increased production of endogenous endocannabinoids and metabolites during inflammation (Michler *et al*., 2013; Cabral *et al*., 2008; D'Argenio *et al*., 2006). It has been speculated that the increased production of AEA during inflammation is anti-inflammatory, given that AEA can attenuate inflammatory mediators released by macrophages, including IL-6, NOS, and COX-2 (Chang *et al*., 2001). Therefore, exacerbated leukocyte-endothelium adhesion by AM630 in EIU could arise due to the competitive inhibition of the anti-inflammatory effects of AEA stimulation of CB_2R. Additionally, increased production of AEA metabolites during inflammation, including N-arachidonoyl glycine can activate the promigratory lipid receptor, GPR18 (McHugh *et al*., 2010b). N-arachidonoyl glycine can also induce the expression of COX-2 which then metabolizes N-arachidonoyl glycine to pro-inflammatory prostaglandins (Lowin *et al*., 2012; Prusakiewicz *et al*., 2002; Mestre *et al*., 2006), which could result in enhanced leukocyte-endothelial interactions in the presence of CB_2R block by AM630.

4.6.2 Cannabinoid Modulation of Inflammatory Mediators

Leukocyte-endothelial interactions depend on inflammatory mediators that are released during inflammation. As previously reported for other studies of ocular inflammation, we measured an increase in multiple inflammatory mediators during the induction of EIU (Murray *et al*., 1990; De Vos *et al*., 1994,

Olszewski *et al*., 2007). These included TNF-α, IL-1β, IL-6, CCL5, and CXCL2. CB_2R activation by HU308 in EIU produced a decrease in several key pro-inflammatory cytokines including, TNF-α, IL-1β, and IL-6. This finding is in line with previous *in vivo* and *in vitro* studies carried out in different tissues and cell types, including the intestine (Lehmann *et al*., 2012), pial vasculature (Ramirez *et al*., 2012), and isolated macrophages and dentritic cells (Selvi *et al*., 2008; Greineisen and Turner 2010). A decrease in pro-inflammatory cytokine TNF-α would limit leukocyte infiltration by halting the upregulation of adhesion molecules and macrophage activation. IL-1β is associated with the infiltration of polymophonuclear cells and consequent breakdown of the blood-retinal barrier; a reduction in concentration of IL-1β would reduce acute inflammatory cell permeation, and decreased release of IL-6 would impede macrophage activation (Ooi *et al*., 2006).

We also found that CB_2R activation reduces levels of the chemokines, CCL5 and CXCL2, in the anterior chamber of the LPS-treated eye. A decline in chemokines, CCL5 and CXCL2 would be responsible for reducing mononuclear and neutrophil chemoattraction into the ocular tissue (Läubli *et al*., 2009; Kawamura *et al*., 2012). Consistent with our results, a recent intravital study of systemic endotoxemia also reported that application of the CB_2R agonist, HU308, was able to suppress elevated levels of the chemokines, CCL5 and CXCL2, in intestinal tissues of LPS-treated animals (Lehmann *et al*., 2012). Other studies

have also indicated that CB_2R activation decreases the levels of these chemokines thereby attenuating macrophage and neutrophil migration, respectively (Raborn *et al*., 2008; De Filippo *et al*., 2013). However, in our study, activation of ocular CB_2R by HU308 failed to significantly decrease the adhesion molecules ICAM and sVCAM, a finding that was seen in other studies using CB_2R agonists in models of inflammation and sepsis (Lehman *et al*., 2012; Ramirez *et al*., 2012; Rajesh *et al*., 2007). This difference in our results may be due to the dose-dependence of HU308 in inhibiting adhesion molecules versus leukocyte-endothelial adhesion in the eye; doses of the agonist chosen were based on the IC_{50} of topical HU308 for inhibition of leukocyte-endothelial adhesion and the modulation of the levels of inflammatory mediators.

With the exception of TNF-α, IL-10, and CXCL2, treatment of animals with the CB_2R antagonist, AM630, did not alter the release of inflammatory mediators during EIU. A similar observation was reported by Roche *et al*. (2008), in which AM630 reduced circulating TNF-α in rats that had received systemic LPS. However, AM630 increased leukocyte-endothelial adhesion despite the observed decreases in TNF-α. Given that leukocyte recruitment and adhesion are dependent on multiple factors, including mediators measured in this study (Kumar *et al*., 2004; Greineisen and Turner 2010), it would seem reasonable that a reduction in TNF-α alone would not be sufficient to prevent leukocyte recruitment and adhesion in this model of LPS-induced EIU.

4.6.3 Effects of CB_2R Ligands on NF-κβ, AP-1and IRF3 mRNA during Ocular Inflammation

LPS-induced increases in NF-κB have been well documented in the literature (Akira and Takeda, 2007; Tak and Firestein, 2001). Our results demonstrated that the CB_2R agonist, HU308, decreased LPS-induced NF-κB in EIU. These findings are supported by a previous report by Rajexh *et al*. (2007) indicating that treatment with the CB_2R agonist, HU308, attenuates NF-κB in a human coronary artery endothelial cell line stimulated with TNF-α. The decrease in NF-κB observed in our study following CB2R activation could account for the attenuated levels of cytokines, such as TNF-α, IL-1β, IL-6, as well as chemokines and adhesion molecules as NF-κB binds to the κβ enhancer elements in pro-inflammatory genes allowing for their transcription (Tak and Firestein, 2001). In keeping with our IVM findings, treatment with AM630 increased levels of NF-κβ in EIU when compared to LPS-alone. Although this increase in NF-κB did not correlate with an increase in any of the pro-inflammatory mediators measured in this study, elevated levels of other mediators, such as COX-2, which are also associated with activation of NF-κB may have occurred (Tak and Firestein, 2001). An increase in COX-2 metabolites, such as leukotrienes and prostaglandins, could account for the increase in inflammation (Lowin *et al*.,

2012; Prusakiewicz *et al*., 2002; Mestre *et al*., 2006). The combination of AM630 and HU308 significantly decreased the levels of NF-κB in comparison to LPS-only animals which could account for the decreases of all three cytokines TNF-α, IL-1β and IL-6, as shown in the literature (Tak and Firestein, 2001).

We observed an increase in mRNA for the transcription factor AP-1 in EIU. This increase in AP-1 mRNA levels was reduced by HU308. Consistent with our findings, LPS-induced increases in AP-1 have been previously reported (Johnson and Lapadat, 2002) and a decrease in the proteins which dimerize to form AP-1 was observed following treatment with HU308 during inflammation induced by a trail transaction in Zebrafish (Liu *et al*., 2013). In our study, treatment with the CB_2R antagonist, AM630, had no effect on the levels of AP-1 mRNA in EIU, however, treatment with HU308 attenuated levels of AP-1 mRNA. Surprisingly AM630 treatment in EIU did not block the effects of HU308 on AP-1 mRNA levels. As drug doses were selected based on leukocyte-endothelial adhesion and not ligand binding, it is possible that dose-dependent inhibition of HU308 effects on AP-1would be observed with increased AM630 doses. AM630 may also activate different transcription factors which were not investigated in this study.

Intraocular injection of LPS into the eye did not increase mRNA of IRF3 after 6 hr. Increases in IRF3 is more associated with viral infections, thus it was not shocking that IRF3 mRNA was not significant (Akira & Takeda, 2004b). It

was however important to investigate IRF3 increases as it is a transcription factor for pro-inflammatory cytokines and has been shown to be activated by LPS under different experimental conditions such as preconditioning or in specific cell types such as human macrophages (Reimer *et al*., 2008; Vartanian *et al*., 2011).

Although we did not expect to see drastic alterations in IFR3 is one of the down transcription factors of the MyD88 independent (TRIF) pathway, the absence of its mRNA modulation could indicate that this arm of the TLR4 signaling pathway may not be activated in our model of acute EIU. As NF-κB and AP-1 can be activated by both the MyD88 and independent pathways we examined mRNA of the RIP-1, an enzyme active upstream in only the MyD88 independent pathway (Akira & Takeda, 2004b). Interestingly, no changes were observed in RIP-1 levels suggesting to us that the inflammatory actions of acute EIU occur predominantly due to the MyD88 signaling pathway and that the cannabinoid treatments studied do not alter RIP-1 mRNA production. Our results, corroborate with those conclusions of Kezic *et al*., (2011). This study attributed LPS driven EIU to primarily signal thought the MyD88 pathway by the investigation of cytokine production in MyD88 and TRIF knockout mice and leukocyte recruitment to the iris and aqueous humor (Kezic *et al*., 2011).

The increase in CB_2R mRNA expression we observed is consistent with the literature, although this has not before been documented to occur during ocular inflammation (Maresz et al., 2005; Mukhopadhyay et al., 2006; Storr et

al., 2009). Increases in CB_2R consistently occurs during inflammation, whether the *in vivo* or *in vitro*. *In vivo* up-regulation of CB_2R mRNA occurs both in peripheral and CNS inflammation; in an experimental model of colitis and experimental autoimmune encephalitis CB2R mRNA (Maresz et al., 2005; Storr et al., 2009) while *in vitro* CB_2R mRNA has been demonstrated in activated microglia and macrophages (Maresz *et al*., 2005).

Our results did indicate any significant decreases in TLR4 in LPS treated animals compared to control animals. This result is contradictory to much of the current literature which describe significant decreases of TLR4 mRNA after LPS stimulation; however much of this is based on macrophages which have been isolated and assessed ex vivo or in murine macrophage cell lines such as RAW 264.7 (Fan *et al*., 2002; Nomura *et al*., 2000). This TLR4 mRNA expression is transient and returns to baseline by 20 – 24 hr after stimulation with LPS (Fan *et al*., 2002). Our results could be explained as TLR4 mRNA expression was being derived from the entire anterior portion of the eye and we did not quantify LPS-TLR4 interaction which would allow for significant decrease in TLR4 mRNA expression. It should be noted that despite there was no a significant decrease in TLR4 mRNA expression, there was a trend in all groups which had LPS to be lower than the control group. Interestingly, the only significant decrease in TLR4 mRNA occurred in the LPS + AM630 group in comparison to the control. It has been documented that when concentrations of LPS used to induce inflammation

are decreased, TLR4 expression is not diminished as much as when a higher concentration of LPS is used. These results occurred in parallel with the cytokine profile (Nomura *et al*., 2000). These results allow us to postulate that TLR4 expression is negatively correlated with the severity of the inflammatory response, more inflammation, less TLR4 and vice versa. Thus, during LPS + AM630 administration when leukocyte-endothelial adhesion is exacerbated in comparison to animals treated with LPS alone.

Taken together, our findings suggest that the anti-inflammatory actions of CB_2R activation in EIU involve a decrease in leukocyte-endothelial adhesion in the iridial microvasculature. Activation of CB_2R was associated with suppression of the levels of pro-inflammatory cytokines and chemokines important for chemotaxis of the leukocytes by a mechanism that involves modulation of inflammatory transcription factors NF- κB and AP-1 of the MyD88 dependent pathway. In support of our findings, a number of studies have demonstrated that CB_2R are robustly expressed by leukocytes and have been associated with regulation of a number of leukocyte functions, including splenocyte proliferation, and B and T cell differentiation (Tanasescu and Constantinescu, 2010; Cencioni *et al*., 2010). CB_2R stimulation has also been demonstrated to inhibit the proliferation of macrophages, as well as macrophage release of inflammatory mediators including, cytokines, chemokines, proteases, prostaglandins, and oxygen free radicals (Chang *et al*., 2001; Cabral *et al*., 2008; Pandey *et al*., 2009).

CB_2R activation also suppresses macrophage and microglia phagocytosis (Pandey *et al*., 2009). Therefore, the anti-inflammatory properties of CB_2R activation in uveal tissue in EIU may involve CB_2R mediated actions on tissue resident macrophages and dendritic cells. An increase in levels of CB_2R mRNA could potentially be explained by endocannabinoids endogenously regulating the inflammatory response as levels of 2-AG and AEA which have been documented to occur in humans who had chronic ocular inflammation such as age-related macular degeneration and diabetic retinopathy (Matias *et al*., 2006). Macrophages and dendritic cells have been noted in non-inflamed iris and ciliary body tissue of mouse, rat, and human. These cells have also been reported to contribute to pro-inflammatory mediator release during experimental autoimmune uveoretinitis (McMenamin, 1997).

4.6.4 Immunomodulatory Effects of Clinical Treatments

Dexamethasone, prednisolone and nepafenac are all used as treatments in inflammatory diseases such as uveitis (Larson *et al*., 2011; Hariprasad *et al*., 2009). Dexamethasone and prednisolone are corticosteroids which inhibit the inflammatory response by acting at the glucocorticoid receptor which then binds to co-activators such as CREB binding protein and decrease the activation of transcription factors, such as NF-κB for pro-inflammatory genes (LeHoang, 2012; Barnes, 2006). Nepafenac is a non-steroidal anti-inflammatory COX 1 and

COX 2 inhibitor that decreases prostaglandin synthesis (Harisrasad *et al*., 2009; Gaynes and Onyekwuluje, 2008). Different prostaglandin derivatives are active in the inflammatory process, and act on a variety of cells, including immune cells and endothelial cells, to increase blood flow and microvascular permeability and induce release of inflammatory cytokines (Ricciotti and FitzGerald, 2001).

In the acute model of ocular inflammation used in this study, the steroids, dexamethasone and prednisolone, and the NSAID, nepafanic, were all unable to significantly decrease leukocyte-endothelial adhesion in the iridial microvasculature during the 6 hr observation period after LPS intravitreal injection. In contrast, a study by Kanai *et al*. (2012), using an experimental model of uveitis induced by systemic LPS injection and a similar dose of dexamethasone to our study, reported that dexamethasone was effective in inhibiting ocular inflammation. These authors reported a significant inhibition of the number of cellular infiltrates and protein concentration into the aqueous humor as well as an improvement in histopathological grading score. These results, however, were obtained 24 hr after initial LPS injection and treatments were given every 6 hrs for 24 hrs, including one dosing before EIU was induced (Kanai *et al*., 2012). Similar to dexamethasone, the steroid prednisolone, also failed to inhibit leukocyte-endothelial interactions and inflammatory mediators in our study of acute EIU induced by intravitreal LPS. The dose of prednisolone used in our study (1%) was based on its relative anti-inflammatory potency and half-life in

comparison to dexamethasone (LeHoang, 2012). As with dexamethasone, studies on the acute anti-inflammatory effects of prednisolone are limited. However, predinisolone was reported to decrease cellular infiltrates in the aqueous humor, iris and ciliary body by 24 hrs, similar to dexamethasone (Medeiros *et al*., 2008). As with the steroid agents, nepafenac, a topical NSAID that has been shown to reduce ocular inflammation in humans (Hariprasad *et al*., 2009; Lane *et al*., 2007), was also ineffective in reducing leukocyte-endothelial interactions and inflammation in acute EIU. This finding was unexpected, as a previous study had reported that a single application of 0.1% topical nepafenac inhibited prostaglandin synthesis in the iris and ciliary body after paracentesis-induced ocular inflammation, although this study did not test for reduction of immune cells (Gamache *et al*. 2000).

In conclusion, this study has demonstrated that activation of CB_2R signalling attenuates leukocyte-endothelial adhesion within the iridial microvasculature in an acute model of EIU. Activation of CB_2R signalling was associated with a decrease in inflammatory mediators in uveal tissue including the pro-inflammatory cytokines, TNF-α, IL-1β, IL-6, INF-γ, as well as the chemokines, CCL5 and CXCL2. In contrast, antagonism of CB_2R resulted in an amplified inflammatory response in ocular tissue suggesting that endogenous activation of CB_2R during ocular inflammation is anti-inflammatory. This study also demonstrated that CB_2R stimulation during acute ocular inflammation by the

CB_2R agonist, HU308, exhibited superior anti-inflammatory efficacy compared to other anti-inflammatory agents including, the COX inhibitor nepafenac and corticosteroids, dexamethasone, and prednisolone. While further research is required to elucidate the full spectrum of CB_2R anti-inflammatory effects in the eye, this study indicates that CB_2R should be considered as a potential target for the development of novel drugs for ocular inflammation.

Chapter V: CB_2R activation decreases ocular inflammation via macrophage dependent mechanism

5.1 Manuscript status and student contribution

The figures and text presented in this chapter are from a manuscript I am preparing for submission with the following authors: Toguri, J. T., Szczesniak, A.M., Laprairie, R.B., Straiker, A.J., Bradshaw, H.B., Denovan-Wright, E.M., Lehmann, C., Kelly, M.E.M.

As first author on this article, I performed all animal experiments, analysis, data interpretation and statistics. Dr. A. M. Szczesniak helped to conduct intraocular injections. Robert B. Laprairie conducted qPRC for CB_2R and β-actin. Dr. A.J. Straiker provided immunohistochemistry. Dr. H.B. Bradshaw conducted endocannabinoid measurements. Several experiments were conducted in the laboratory of Dr. E.M. Denovan-Wright. I wrote the manuscript, which was edited by Dr. Ch. Lehmann and Dr. M. E. M. Kelly.

5.2 Abstract

Background: Cannabinoid 2 receptor (CB_2R) agonists can decrease ocular inflammation. In this study, the involvement of CB_2R in endotoxin-induced uveitis (EIU), was investigated. Signalling pathways, involved in CB_2R suppression of inflammation EIU were examined in EIU, as well as in an *in vitro* macrophage cell line.

Methods: EIU was induced by intraocular injection of lipopolysaccharide (LPS 250 ng) in WT and CB_2KO mice. The CB_2R agonist, HU308, was applied topically and the inflammatory response was quantified by leukocyte adhesion to the iridial microvasculature at 6 h by intravital microscopy. Clodronate treatment was used to deplete the macrophage population. The murine macrophage cell line, RAW 264.7 was used to investigate activation of the signalling molecules ERK and JNK that are associated with LPS-mediated TLR4 activation of pro-inflammatory transcription factors.

Results: HU308 decreased leukocyte adherence in the iridial microvasculature 6 h post-LPS administration. CB_2KO animals showed exacerbated leukocyte-endothelium adherence compared to WT animals in the EIU group. This generation of EIU was inhibited by macrophage depletion. RAW cells stimulated with LPS had increased phosphorylated ERK and JNK, which was inhibited

following treatment with the CB_2R agonist, HU308. Use of a JNK inhibitor *in vivo*, confirmed the involvement of JNK during EIU.

Conclusion: EIU is mediated by the activation of TLR4 on macrophages. CB_2R activation can limit the inflammatory response in EIU via inhibition of macrophage ERK and JNK signalling, and a reduction in the activity of pro-inflammatory transcription factors.

5.3 Introduction

The endocannabinoid system (ECS) consists of two cloned cannabinoid receptors, CB_1R (Devane *et al*., 1988) and CB_2R (Munro *et al*., 1993), endogenous ligands including ethanolamides [N-arachidonoylethanolamine (AEA) (Devane *et al*., 1992)], fatty acids [2-arachidonoyl glycerol (2-AG) (Sugiura *et al*., 1995)], and biosynthetic and degradative enzymes (Cravatt *et al*., 1996). CB_1R is highly expressed in the CNS, and activation of this receptor regulates the presynaptic release of neurotransmitters (Laaris *et al*., 2010). CB_2R is mainly localised on immune cells and has immunomodulatory properties reviewed in Tanasescu & Constantinescu, 2010. The ECS is involved in several disease states including Huntington's disease (Laprairie *et al*., 2013), multiple sclerosis (Rossi et al., 2011b), a plethora of cancers and inflammatory diseases (Di Marzo *et al*., 2000). The medicinal benefits of the ocular ECS have been exploited for diseases such as glaucoma (Buys & Rafuse, 2010; Pinar-Sueiro *et al*., 2011). However, less research has focused on the anti-inflammatory effects of the ECS during ocular inflammation. Recently, several groups, including our own, have demonstrated that CB_2R selective agonists decrease ocular inflammation in models of uveitis (Toguri *et al*., 2014) and uveoretinitis (Xu *et al*., 2007); however, the cellular and molecular mechanisms underlying these actions have yet to be fully elucidated.

In humans, uveitis can result from an ocular bacterial infection and other causes leading to impaired vision. Uveitis is responsible for 10% of all cases of blindness (Suttorp-Schulten & Rothova, 1996). Uveitis can be modelled in rodents using local or systemic injection of lipopolysaccharide (LPS) to generate endotoxin-induced uveitis (EIU). LPS is a cell wall component of gram-negative bacteria which activates Toll-like receptor 4 (TLR 4) on specific cells induces immune cells and endothelial cells (Li *et al*., 2003; Lu *et al*., 2008). TLRs are essential pattern recognition receptors (PRRs), which recognize pathogen-associated molecular proteins (PAMPs), and are essential in mounting innate immune responses. Systemic TLR4 activation affects a multitude of cells types, and contributes to the etiology of several diseases including sepsis, atherosclerosis, cardiovascular disease, inflammatory bowel disease, and cancers [Reviewed in O'Neill *et al*., (2009) and Miller *et al*., (2005)]. LPS, when administered directly in the eye by intraocular injection, stimulates a TLR4 response on immune cells (Chen *et al*., 2009), iridial endothelial cells (Brito *et al*., 2004) and epithelial cells (Chang *et al*., 2006). There are several distinct immune cell types localised in the anterior chamber, iris, ciliary body and chorioid, including dendritic cells and tissue resident macrophages (Brito *et al*., 2004; Chen *et al*., 2009). The retina also contains resident immune cells, microglia which also play a role in ocular inflammation (Kumamaru *et al*., 2012).

The intracellular signaling pathways that are activated following TLR4 stimulation have been characterized. LPS activation of TLR4 can induce both MyD88-dependent and the MyD88-independent (TRAM/TRIF) intracellular signaling pathways. However, it was recently shown by Kezic *et al*. (2011) that EIU in mice is primarily MyD88-dependent. MyD88 pathway activation can result in the phosphorylation of the mitogen-activated protein kinase (MAPK) pathways and the IκB kinase (IKK) complex. The components of the MAPK pathways include: extracellular signal-regulated kinase (ERK), c-Jun-N-terminal kinase (JNK)/ stress-activated protein kinase (SAPK) and p38 protein kinases. ERK signaling has been linked to phosphorylation and activation of inhibitor of NF-κB (IKK) complexes which constitutively inhibit NF-κB (Akira & Takeda, 2004b). JNK has been shown to phosphorylate c-Jun and isoforms of activating transcription factor (ATF), promoting their dimerization and the subsequent formation of transcription factor activating protein-1 (AP-1) (Karin, 1995). c-Fos can also be a component of the dimeric complex that forms AP-1 (Karin *et al*., 1997). Similarly, p38 can activate ATF, causing AP-1 formation and translocation into the nucleus (Jeong *et al*., 2013). Activation of MAPK can increase AP-1 or an alternative pathway, activating NF-κB (Lu *et al*., 2008). Activation of the transcription factors AP-1 and NF-κB increases the production of pro-inflammatory mediators including cytokines (e.g., TNF-α and IL-6), and chemokines (e.g., CCL5/RANTES and CXCL2/MIP-2) (Toguri *et al*., 2014).

This increase in pro-inflammatory mediators can lead to leukocyte recruitment, an exacerbated inflammatory response, and eventual tissue damage (Barreiro *et al*., 2010). As TLR4 is located on both immune and endothelial cells, it is possible that one or both of these cell populations are responsible for up-regulation of inflammatory mediators during EIU.

The aim of this study was to confirm the role of CB_2R during ocular inflammation, investigate which cell population(s) are involved in the generation of EIU, and identify the molecular mechanisms whereby CB_2R limits ocular inflammation in EIU.

5.4 Methods

5.4.1 Animals

All animal care, husbandry and experimental procedures complied with the Canadian Council for Animal Care guidelines (http:// www.ccac.ca/) and were approved by the Dalhousie University Committee on Laboratory Animals. All studies involving animals are reported in accordance with the ARRIVE guidelines for reporting experiments involving animals (http://www.nc3rs.org.uk/). Male BALB/c (20 – 30 g) (Charles River Laboratories International Inc., Wilmington, MA, USA) and CB_2 receptor knockout mice (CB_2KO) were used for experiments. CB_2KO mice were obtained by crossing male C57BL/6J CB_2KO mice (strain B6.129P2-Cnr2tm1Dgen/J;

Jackson Laboratory, Bar Harbour, ME, USA) with inbred BALB/c female mice (Charles River) for 6 generations. Heterozygote mice from separate parents were then bred for a homozygote KO of the CB_2R. CB_2KO was confirmed *via* genotyping. A total of 200 animals were used in the experiments. Mice were housed in groups of 3 – 5, kept on a light/dark cycle (07:00–19:00/19:00-07:00), and fed *ad libitum*.

5.4.2 Genotyping of CB_2KO Animals

PCR genotyping was performed using DNA extracted from ear punches with an Accustart II Mouse Genotyping Kit (Quanta Biosciences, MD, USA) according to manufacturer's instructions. The following PCR primers were used: moIMR0086 (5'-GGGGATCGATCCGTCCTGTAAGTCT-3'; mutant forward), oIMR7552 (5'-GACTAGAGCTTTGTAGGTAGGCGGG-3'; common reverse), and oIMR7565 (5'-GGAGTTCAACCCCATGAAGGAGTAC-3'; wild-type forward). The expected results were a single product at ~550 bp for CB_2KO, a single product at ~385 bp for wild-type and two products at ~550 and 385 bp for heterozygous animals.

5.4.3 Drug Treatments

CB_2R agonist HU308 (4-[4-(1,1-dimethylheptyl)-2,6-dimethoxyphenyl]-6,6- dimethylbicyclo[3.1.1]hept-2-ene-2-methanol) was obtained from Tocris

Bioscience (Bristol, UK) and dissolved in Tocrisolve™ 100 (Tocris Bioscience, Ellisville, MO, USA) for topical application at 1.5% (w v^{-1}).

Dichloromethylene-1,1-bisphosphonate (clodronate) causes selective depletion of macrophages and monocytes (van Rooijen *et al*., 1996). Clodronate is cytotoxic to cells because of its intracellular metabolite which is a non-hydrolyzable analog of adenosine triphosphate (ATP) called adenosine-5'-[β-γ-dichloromethylene]triphosphate (AppCCL_2p). AppCCL_2p competes with ATP at the adenosine diphosphate (ADP)/ATP translocase of the mitochondrial membrane; during prolonged inhibition of functioning ADP/ATP translocase the mitochondrial membrane potential collapses and the cell initiates apoptosis (Lehenkari *et al*., 2002). Liposomes are phospholipid bilayers, which encapsulate clodronate, a highly hydrophobic molecule that rarely crosses the phospholipid membrane. Liposome-encapsulated clodronate becomes phagocytosed by macrophages and other APCs disrupting the lipid bilayer of the liposome allowing clodronate to be realised into the cellular cytosol causing death (Kumamaru *et al*., 2012).

JNK inhibitor SP600125 (anthral[1,9-cd]pyrazol-6 (2 H)-one 1,9-pyrazoloanthrone) obtained from Sigma-Aldrich (St. Louis, MO, USA) and dissolved in 10% DMSO/ 10% Cremophor/ 80% for 15 mg/kg i.v. administration. SP600125 selectively inhibits JNK-1, -2 and -3 isoforms with similar potency,

and has a 10 – 300-fold selectivity for JNK relative to other MAP kinases (Bennett *et al*., 2001).

5.4.4. Macrophage Depletion

To deplete macrophages and monocytes, mice were injected *i.p.* daily, for 6 days with 200 μL of a suspension of liposome encapsulated clodronate (5 mg clodronate mL^{-1}) or control PBS-encapsulated in liposomes (clodronateliposomes.com, Haarlem, The Netherlands) (Baatz, Puchta, *et al*., 2001; Frith *et al*., 2001; Sunderkötter *et al*., 2004). On day 7, animals received an 2 μl intraocular injection of saline or LPS in saline.

5.4.5 Inhibition of Jun N-terminal kinase (JNK) during EIU

BALB/c mice (25 – 30 g) were administered 15 mg kg^{-1} SP600125 (150 μL) *i.v.* or vehicle (150 μL) in vehicle 15 min before intraocular injection of LPS or saline (Bennett *et al*., 2001; Minutoli *et al*., 2004).

5.4.6 Induction of Endotoxin-Induced Uveitis (EIU)

General anesthesia was induced by isoflurane and depth of anaesthesia was monitored by toe pinch. Intravitreal injection of either saline, or LPS in saline, was given through the pars plana, under a WILD M37 dissecting microscope (Leitz Canada, Kitchener, ON, Canada) using a Hamilton syringe

(Hamilton Company, Reno, NV, USA) fitted to a 30 G needle. Control animals received 2 μL of sterile saline, while experimental animals were injected with 250 ng LPS (125 ng μL^{-1}; *E. coli* 026:B6 L8274 lot 100M4102V; Sigma-Aldrich, Oakville, ON, Canada) in 2 μL of saline. Once the injection was completed, the puncture wound was glued shut with 3M Vetbond Tissue Adhesive (3M Animal Products, St. Paul, MN, USA).

5.4.7 Intravital Microscopy

The iridial microcirculation was observed with the Olympus OV 100 Small Animal Imaging System (ON, Canada). The OV100 contains an MT-20 light source and a DP70 CCD camera. Fluorescence excitation was generated by a xenon lamp (150W), and eight position excitation filters to block for rhodamine-6G (excitation 515– 560 nm, emission 590 nm) and FITC (450–490 nm, emission 520 nm). Images were captured by a black and white DP70 CCD C-mount camera in real time and recorded in a digital format by the software Wassabi (Hamatsu, Herrsching, Germany) on a computer connected to the OV100.

During intravital microscopy (IVM), animals were anaesthetised by *i.p.* injection of sodium pentobarbital (65 mg kg^{-1}). Mice were placed in a stereotactic frame, and Tear-Gel® (Novartis Pharmaceuticals Canada Inc., Dorval, QC, Canada) was placed on the cornea to prevent dehydration of the tissue throughout

the experiment. Rhodamine-6G (1.5 mL kg^{-1}; Sigma-Aldrich) was injected *i.v.* 15 min before initiating IVM. The fluorescent dye rhodamine-6G labelled mitochondria in leukocytes within the vessel, and FITC- albumin allowed for the visualization of blood flow through the vasculature. Animals were placed on a heating pad to maintain body temperature at 37°C. IVM was carried out in four (or more) regions of interest. In each region of interest, four randomly selected vessels (a total of 16 vessels) were observed, and 30 s recordings of each vessel were taken. For IVM studies, data were analysed off-line without knowledge of treatment groups. Recordings of the iridial microcirculation were analysed using the imaging software ImageJ version 1.47v (National Institute of Health, USA). The length, measured between points of branching, and diameter of the vessels were used to calculate the volume within the vessel. Adhering leukocytes were defined as white blood cells that were attached to the vessel wall and were immobile for a 30 s observation period; adhering cells were reported as the number of cells per square millimetre of endothelial surface.

IVM was conducted 6 h after induction of EIU, to determine how treatments affected leukocyte-endothelial interactions within the iris. This time-point was chosen on the basis of preliminary experiments.

Following IVM, animals were sacrificed by cervical dislocation while under anesthesia. Eyes were enucleated and either flash frozen in liquid nitrogen and stored at –80°C for subsequent liquid chromatography and mass

spectrometry analysis of endocannabinoids, prostaglandins, ethanolamides, glycerols, fatty acids, prostaglandins and glycines, or fixed in 4% paraformaldehyde for immunohistochemistry.

5.4.9 Immunohistochemistry

Following fixation, eyes were immersed in 30% sucrose at 4°C overnight. Eyes were enucleated then frozen in OCT compound and sectioned (25 μm) using a Leica CM1850 cryostat (Leica Microsystems Inc., Concord, ON, Canada). Tissue sections were thaw-mounted onto Superfrost-plus slides (Fisherbrand Superfrost/Plus, Fisher), washed, incubated with Seablock (Thermo Fisher, Waltham MA) for 30 min, and incubated with primary antibody solutions overnight at 4°C in PBS with saponin (0.2%). Secondary antibodies (Alexa 488, 594, 647 1:500, Invitrogen, Inc. Calsbad, CA, USA) were then applied at room temperature for 1.5 h. The primary antibody was Ly6G clone RB6-8C5 (1:300). Images were acquired with a Leica TCS SP5 confocal microscope (Leica Microsystems, Wetzlar, Germany) using Leica LAS AF software and a 63X oil objective. Images were processed using ImageJ and/or Photoshop (Adobe Inc., San Jose, CA, USA). Images were modified only in terms of brightness and contrast.

5.4.10 Lipid Extraction and LC/MS/MS Analysis and Quantification

Eyes were enucleated, flash frozen in liquid nitrogen and frozen at -80°C until used. AEA, 2-AG and arachidonic acid (AA) levels were measured by liquid chromatography/mass spectrometry from whole eyes as previously described (Stuart *et al*., 2013).

5.4.11 qRT-PCR

RNA was harvested from homogenized tissue in PBS and protease inhibitor cocktail using the Trizol® method according to the manufacturer's instructions (Invitrogen, Burlington, ON). RNA was converted to cDNA *via* reverse transcriptase (RT) reactions, as previously described (Toguri *et al*., 2014). Quantitative PCR was carried out using the LightCycler FastStart Reaction Mix SYBR Green I (Toguri *et al*., 2014). Primers-specific concentrations of $MgCl_2$, forward and reverse primers are given in Table 1. CB_2R cDNA levels were normalized to β-actin cDNA levels. All experiments included –RT, dH_2O, and reference concentration controls.

5.4.12 Cell Culture

RAW 264.7 were obtained from ATCC (Rockville, MD, USA) . Cells were maintained at 37°C, 5% CO_2 in DMEM (Gibco BRL, USA) supplemented with heat-inactivated 10% fetal bovine serum (Gibco BRL, USA), 20 mM

HEPES (Gibco BRL, USA), 2 mM L-Glutamine (Gibco BRL, USA) and 10^4 U/mL Pen/Strep. Mycoplasma-free RAW 264.7 cells were cultured at a seeding density of 5 X 10^4 cells per 100 mm culture plate in supplemented DMEM and grown to confluence. Cell viability was assessed by trypan blue staining. RAW 264.7 cells were serum-deprived for 4 h and treated with HU308 at 10^{-6}, 10^{-7}, 10^{-8} M or DMSO (vehicle) for 15 min, then incubated with LPS in media (1 μg mL^{-1}) or media (control). This time period was chosen based on previous reports (Chen *et al*., 2002; Hambleton, Weinstein, *et al*., 1996).

5.4.13 In-cell™ Western

Cells were fixed for 10 min at room temperature with 4% paraformaldehyde and washed three times with 0.1 M PBS for 5 min each followed by incubation with blocking solution (20% odyssey blocking buffer containing 0.3% TritonX-100 in dH_2O) for 1 h at room temperature. Cells were incubated with primary antibody solutions directed against ERK1/2 (1:200), pERK1/2(Tyr205/185) (1:200), JNK (1:200), pJNK (1:200) diluted in blocking solution overnight at 4°C. All antibodies were purchased from Santa Cruz Biotechnology with the exception of pJNK, which was purchased from Cell Signaling Tchnology. Cells were washed three times with 0.1 M PBS for 5 min each. Cells were incubated in $IR^{CW700dye}$ or $IR^{CW800dye}$ (1:500; Rockland Immunochemicals, Gilbertsville, PA) for 1 h at room temperature, protected from

light, and again washed three times with 0.1 M PBS for 5 min each. In-cell™ Western analyses were then conducted using the Odyssey Imaging system and software (version 3.0; Li-Cor, Lincoln, NE).

5.4.14 Statistical Analysis

Individual animals in each of the treatment groups were coded and data analyzed blinded without knowledge of the treatment groups. All data are presented as mean ± SEM and were analyzed in GraphPad Prism v.5 (GraphPad Software Inc., La Jolla, CA, USA). IVM data and inflammatory mediator data were analysed by one-way ANOVA with Dunnett's *post-hoc* test, comparing all experimental groups to the LPS-treated group. qRT-PCR data were analysed by one-way ANOVA with Tukey's *post-hoc* test. Analysis of endocannabinoid levels was conducted by a one-way ANOVA with a *post-hoc* Fisher's LSD test. $P < 0.05$ was considered statistically significant.

For *in vitro* experiments, goodness of fit to the Variable Slope (4 parameter) non-linear regression model was tested in GraphPad (v. 5.0, Prism). Statistical analyses were conducted by one- or two-way analysis of variance (ANOVA), as indicated, using GraphPad Prism software. *Post-hoc* analyses were performed using Bonferroni's or Tukey's tests, as indicated. Homogeneity of

variance was confirmed using Bartlett's test. All results are reported as the mean ± SEM from at least 3 independent experiments.

5.5 Results

5.5.1 CB_2R Activation Decreased Neutrophil Migration during EIU

Intravital microscopy enables *in vivo* imaging of leukocytes adhering to the endothelium. Figures 24A-B are representative images of the iridial microvasculature 6 h after a control, intraocular injection of 2 µL of saline (Figure 24A), and an intraocular injection of 250 ng of LPS in saline (Figure 24B). Leukocyte-endothelial adhesion increased 6 h after intraocular injection of LPS, as compared to control animals (Figure 24C).

The histogram in Figure 24C shows the number of leukocytes firmly adhering to the iridial microvasculature in the following groups: wild type (WT) + intravitreal (ivt) injection of 2 µL of saline (sal), WT + ivt injection of 250 ng of LPS in 2 µL of sal, WT + LPS + 5 µL of topical 1.5% HU308, CB_2KO + sal, CB_2KO + LPS. Topical application of the CB_2R agonist, HU308 at a concentration of 1.5%, was chosen, based on previous studies (Toguri *et al*., 2014). There was an increase in the number of leukocytes adhering to the endothelium 6 h following induction of EIU in the WT+LPS group compared to WT + sal ($p < 0.05$). Figure 24C shows that application of 1.5% HU308 to WT+ LPS animals significantly decreased leukocyte-endothelial adhesion ($p < 0.05$).

Figure 24. EIU in BALB/c mice and the role of CB_2R during ocular inflammation. Representative IVM images of iridial microcirculation in BALB/c mice at 6 h after **(A)** saline **(B)** LPS. **C)** Bar graph represents the mean number of adherent leukocytes at 6 h in the following groups: WT + saline (n = 8); WT + LPS (n = 13); WT + LPS + HU308 (n = 7); CB_2KO + saline (n = 11); CB_2KO + LPS (n = 9). Values represent mean ± SEM. * $p < 0.05$ compared with the LPS group.

A.

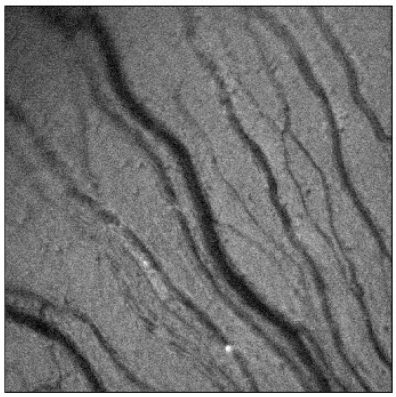

B.

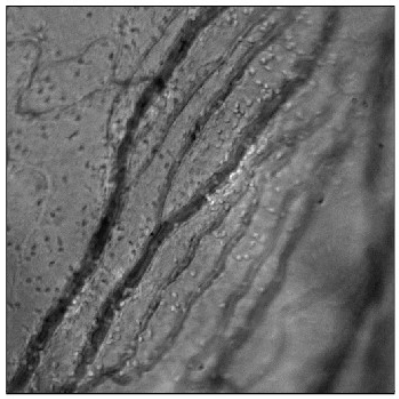

C.

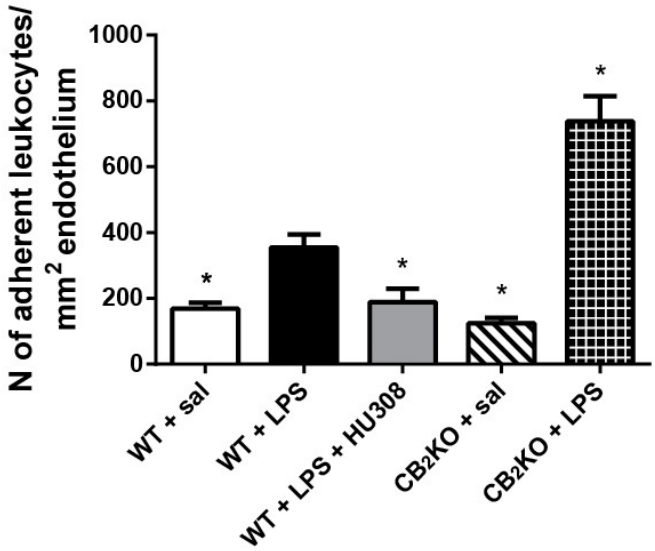
N of adherent leukocytes/ mm2 endothelium
1000
800
600
400
200
0
*
*
*
*
WT + sal
WT + LPS
WT + LPS + HU308
CB2KO + sal
CB2KO + LPS

To confirm the involvement of the CB_2R in the HU-308 mediated decrease in leukocyte adhesion seen in LPS-injected animal, we used CB_2KO animals. CB_2KO mice were given ivt injections of saline or LPS. Injection of saline in CB_2KO mice did not change the number of leukocytes adhering to the iridal microcirculation in comparison to WT mice injected with saline ($p > 0.05$). Similar to WT animals, an increase in adherent leukocytes was observed when CB_2KO mice received an ivt injection of LPS compared to the saline injection ($p < 0.05$, Figure 24C). However, leukocyte adhesion in response to LPS injection in CB_2KO mice was significantly enhanced compared to WT LPS-treated animals ($p < 0.05$).

Immunofluorescence was used to determine the type of immune cells migrating into the anterior chamber of the eye during EIU. Anterior sections were stained with Ly6G antibodies, for neutrophils. Figure 25 shows that there are few immune cells present in the eye when it is injected with saline, however when LPS was administered, neutrophils infiltrated the iris, cornea, ciliary body and were found within the anterior chamber. Topical application of HU308 decreased the number of neutrophils from all anatomical locations within the anterior chamber of the eye.

5.5 2 Endocannabinoid Levels

Endocannabinoid levels were investigated to determine their role in ocular inflammation and if these were altered in CB_2KO animals. The primary focus was on levels of 2-AG and AEA and the metabolite AA. Table 6 contains the levels of all lipid mediators that were measured in each group. The treatment groups were as follows: WT untreated, WT + HU308, WT + sal, WT + LPS, WT + LPS + HU308, CB_2KO untreated, CB_2KO + HU308, CB_2KO + sal, CB_2KO + LPS, CB_2KO + LPS + HU308.

Compared to the saline treatment group no significant changes in AEA levels were found compared to LPS or LPS + HU308 in both WT and CB_2KO animals (Table 6). Additionally, genetic background did not alter AEA concentrations for respective treatments. Similarly, there were no significant differences in 2-AG levels between any treatment groups, regardless of genotype. Levels of AA were significantly increased in WT animals treated with LPS compared to saline-injected control animals. Treatment with topical HU308 during LPS in WT animals attenuated the increase of AA. Interestingly, there were no changes in AA between any treatment groups in CB_2KO animals. There was a less of an increase in AA in CB_2KO treated with LPS compared to WT littermates.

Figure 25. Immunofluorescent staining for identification of immune cells during EIU. Immunofluorescent staining of the anterior portion of the eye for $Ly6G^+$ (neutrophils) after designated treatments in WT or CB_2KO animals. Arrows point to neutrophils.

WT saline

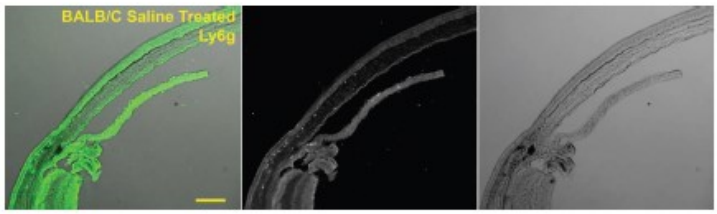

WT LPS

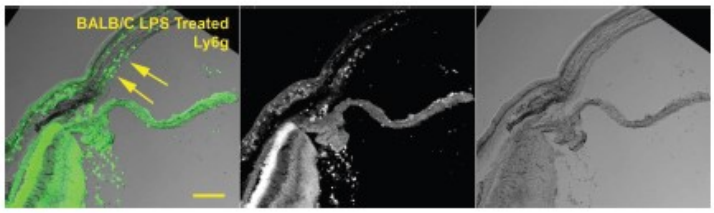

WT LPS
+ HU308

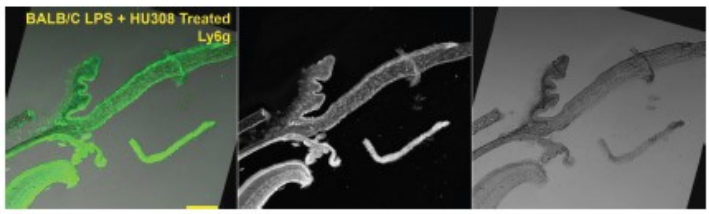

CB2KO saline

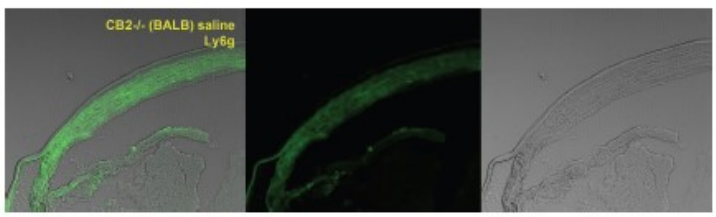

CB2KO LPS

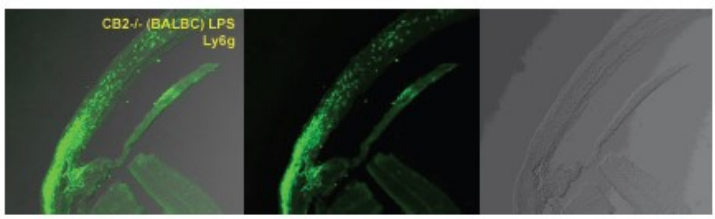

CB2KO LPS
+ HU308

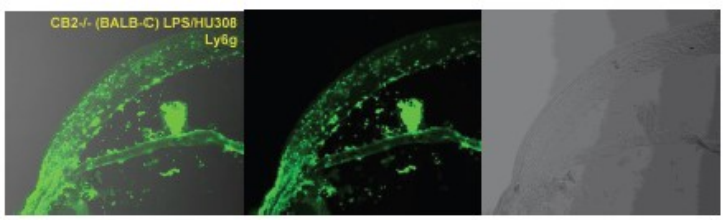

Table 6. Levels of endocannabinoids (AEA and 2-AG) and AA in the eye during EIU and CB_2R modulation. Data shown (mean ± SEM) for WT + sal, WT + LPS, WT + LPS + HU308, CB_2KO + sal, CB_2KO + LPS, CB_2KO + LPS + HU308, n = 8 – 10, † compared to sal on the same genetic background, * < p compared to treatment on WT genetic background.

	WT + saline	WT + LPS	WT + LPS + HU308	CB_2KO + saline	CB_2KO + LPS	CB_2KO + LPS + HU
AEA	2.41E-11 ± 1.49 E - 12	2.88 E - 11 ± 2.57 E - 12	2.60 E - 11 ± 2.81 E - 12	2.90 E - 11 ± 2.75 E - 12	2.51 E - 11 ± 1.56 E - 12	2.46 E - 11 ± 1.67 E - 12
2-AG	2.78 E - 10 ± 3.09 E - 11	3.26 E - 10 ± 4.05 E - 11	5.54 E - 10 ± 5.3 E - 11	5.60 E - 10 ± 5.27 E - 11	4.07 E - 10 ± 5.47 E - 11	4.07 E - 10 ± 3.46 E - 11
AA	3.14 E - 9 ± 1.15 E - 10	4.15 E - 9 ± 6.08 E -10 †	3.40 E- 9 ± 2.93 E -10	3.23 E - 9 ± 2.67 E -10	3.20 E - 9 ± 2.09 E -10 *	2.80 E -9 ± 1.08 E -10

Trauma by needle puncture to the eye altered levels of 2-AG, AEA and AA. Data for WT naïve and CB_2KO naïve can be found in Table 7. AEA levels increased after puncture, while 2-AG levels decreased in both WT and CB_2KO animals. AA levels decreased after trauma in WT mice and increased in CB_2KO mice. However, there was no significant difference between WT and CB_2KO mice to compared naïve mice or those that had trauma by needle puncture. There was a decrease in AA in naïve CB_2KO animals compared to WT animals. These results indicate that trauma by to the eye by needle puncture has a sustained effect on AEA and 2-AG over 6 hr while induction of endocannabinoids does not appear to be highly impacted by induction of EIU in comparison.

5.5.3 CB_2R mRNA Levels Increase in Ocular Tissue during EIU

CB_2R expression has previously been observed to increase during inflammation (Maresz *et al*., 2005; Storr *et al*., 2009). As no changes were observed in endocannabinoid levels in the eye, we determined whether inflammatory stimuli affected CB_2R expression. Treatment with LPS increased CB_2R mRNA levels in WT mice ($p<0.05$) (Figure 26). CB_2R mRNA levels were also higher in mice treated with LPS + HU308, but were not different between LPS- and LPS + HU308-treated mice (Figure 26). Therefore, LPS-induced EIU increased CB_2R mRNA levels, but CB_2R agonist treatment did not affect CB_2R expression.

Table 7. Levels of endocannabinoids (AEA and 2-AG) and AA in the eye from needle puncture. Data shown (mean ± SEM) for naïve WT and naïve CB_2KO, n = 8 – 10

	naïve WT	naïve CB_2KO
AEA	1.59 E - 11 ± 3.39 E – 12	1.32 E - 11 ± 2.65 E - 12
2-AG	1.47 E - 9 ± 9.38 E – 10	1.27 E - 9 ± 3.68 E - 10
AA	4.28 E - 9 ± 8.48 E – 10	2.55 E - 9 ± 4.84 E -10 †

5.5.4 Mononuclear Immune Cell Function during EIU

In order to investigate the role of the mononuclear phagocytic system (monocytes and macrophages) in inflammation during EIU, the bisphosphonate compound, clodronate was injected *i.p.* for 6 days to deplete the macrophage population. For proper absorption, clodronate was encapsulated in liposomes; PBS was also encapsulated in liposomes as a control. No significant difference was found between animals which received liposome-encapsulated PBS for 1 week and an intraocular injection of saline or LPS intraocular injection and those that received only the corresponding intraocular injections (Figure 27A, $p > 0.05$). Upon LPS treatment, the number of leukocytes adhering to the iridial endothelium in clodronate treated group was decreased, as compared to liposome-encapsulated PBS treated mice (Figure 27A, $p < 0.05$). The number of adherent leukocytes in clodronate + LPS treated animals was not different than those found in animals with intraocular injections of saline (saline alone, saline + liposome encapsulated PBS or saline + liposome encapsulated clodronate). There was a marked decrease in the number of recruited neutrophils in animals treated with clondronate compared to the animals injected with PBS (Figure 27A&B). LPS-activated macrophages which can be depleted by clodronate, are fundamental to the induction of EIU.

Figure 26. mRNA expression of CB_2R during EIU and CB_2R modulation. CB_2R mRNA levels at 6 h in the following treatment groups: control (n=10), LPS (n=9), LPS+HU308 (n=10). Values represent mean ± SEM and are reported relative to β-actin. *$p < 0.05$ compared to saline.

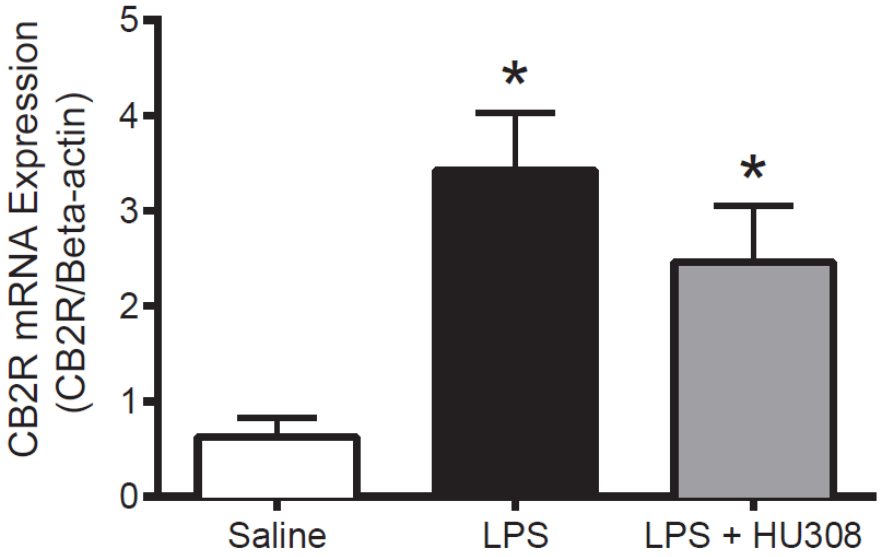
CB2R mRNA Expression
(CB2R/Beta-actin)
5
4
3
2
1
0
*
*
Saline
LPS
LPS + HU308

5.5.5 CB_2R Limited MAPK Phosphorylation during LPS Stimulation in RAW 264.7 Macrophage Cells

RAW cells are regarded as a model cell system that is representative of murine macrophages. The CB_2R is expressed in RAW264.7 cells (Carlisle *et al*., 2002). Additionally, it was shown by Mukhopadhyay *et al*., (2006) that upon stimulation by LPS, CB_2R concentration is increased to a maximum density at 12 h (Carlisle *et al*., 2002; Mukhopadhyay *et al*., 2006). Stimulation of RAW cells with LPS caused an increase in the phosphorylation of ERK and JNK compared to cells treated with media alone (Figure 28A-B). CB_2R agonist, HU308, was tested at three different concentrations (10^{-6} - 10^{-8} M). DMSO or HU308 treatment alone did not effect levels of pERK/Total ERK, or pJNK/Total JNK (Figure 28A-B). In this manuscript we focus our attention to those doses of HU308 that decreased phosphorylation of the MAPKs. HU308 (10^{-6} - 10^{-8} M) ablated the phosphorylation of ERK and JNK (Figure 28A,B). CB_2R activation inhibits the phosphorylation of MAPKs ERK and JNK in macrophages which could alter induction of the pro-inflammatory transcription factor AP-1.

Figure 27. Systemic administration of clodronate depleted resident macrophages in the anterior potion of the eye decreases neutrophil migration. **(A)** Bar graph represents the mean number of adherent leukocytes at 6 h in the following groups: Saline + liposome-encapsulated PBS (n = 6); LPS + liposome encapsulated PBS (n = 9); Saline + liposome encapsulated clodronate (n = 6); LPS + liposome encapsulated clodronate (n = 11). **B,C)** Immunofluorescence staining of the cornea, iris and ciliary body after 7 days of liposome-encapsulated clodronate showed neutrophil depletion in comparison to treatment of liposome-encapsulated PBS. Values represent mean ± SEM. * $p < 0.05$ compared with the LPS group. Arrows point to infiltrating neutrophils.

A.

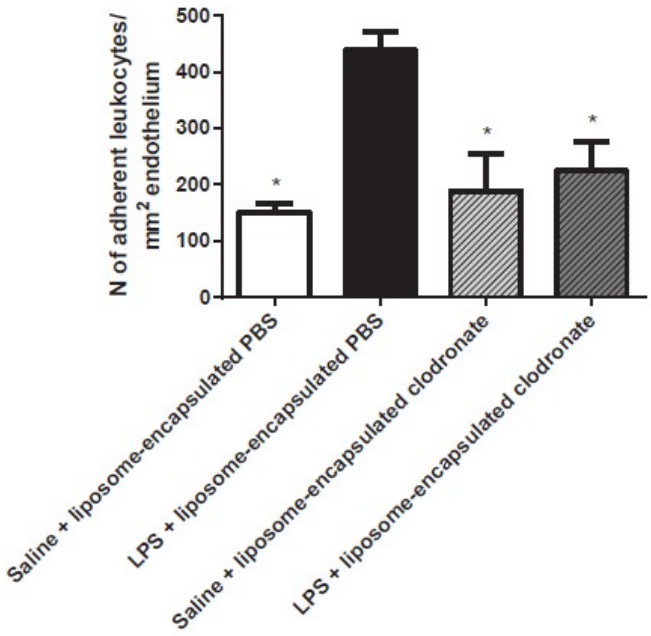
N of adherent leukocytes/ mm2 endothelium
500
400
300
200
100
0
*
*
*
Saline + liposome-encapsulated PBS
LPS + liposome-encapsulated PBS
Saline + liposome-encapsulated clodronate
LPS + liposome-encapsulated clodronate

B.

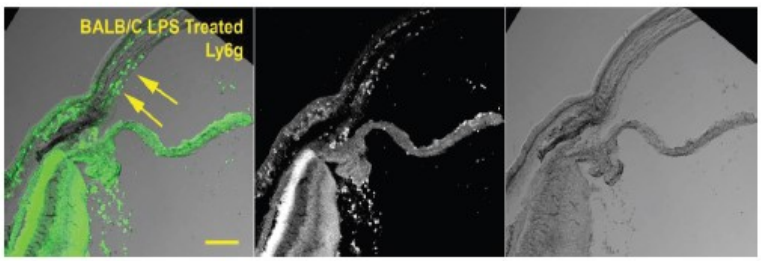
BALB/C LPS Treated
Ly6g

C.

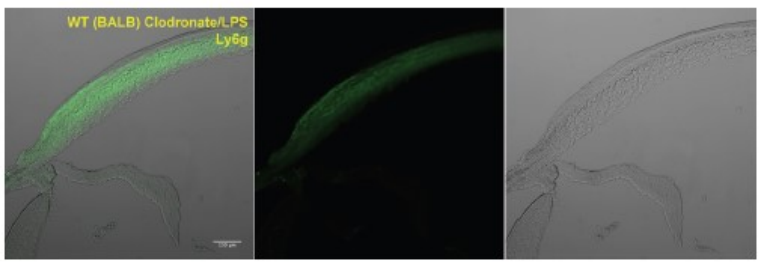
WT (BALB) Clodronate/LPS
Ly6g

5.5.6 Jun N-terminal kinase (JNK) Mediated LPS-induced Leukocyte Adhesion to Endothelium in EIU

In order to investigate the role of the MAP kinase JNK during *in vivo* ocular inflammation, leukocyte endothelium adhesion was quantified in animals treated with LPS, vehicle, or the JNK inhibitor SP600125 (15 mg kg^{-1}). No significant difference was observed in leukocyte endothelium adhesion between LPS-treated animals compared to vehicle-treated animals. The JNK inhibitor, SP600125 (15 mg/kg) reduced the number of adherent leukocytes in comparison to LPS-treated animals, when given 15 min prior to induction of EIU (Figure 29; $p<0.05$). These results demonstrate that inhibition of JNK phosphorylation, one effect of CB_2R stimulation *in vitro*, resulted in anti-inflammatory properties when tested *in vivo*.

5.6 Discussion

Uveitis is a debilitating–disease due to its manifestation of decreased visual acuity and loss of sight (Barisani-Asenbauer *et al*., 2012; Caspi, 2010). Our data provides further evidence that CB_2R agonism, by HU308, may be used to treat ocular inflammation by demonstrating anti-inflammatory activity in a model of EIU. We have demonstrated that the mononuclear phagocytic system plays a

Figure 28. CB_2R agonist modulation of phosphorylation of MAP kinases during LPS stimulation of RAW 264.7 murine macrophage cell line. MAPK phosphorylation (phosphorylated protein/total protein) was quantified via In-cell™ Western assay in RAW 264.7 cells treated with HU308 prior to 1 μg of LPS for 15 min. **A)** Bar graph of ERK phosphorylation with different concentrations of HU308 **B)** Bar graph of JNK phosphorylation with different concentrations of HU308. Values represent mean ± SEM * $p < 0.05$ compared to vehicle treatment group. # $p < 0.05$ compared to LPS + HU308.

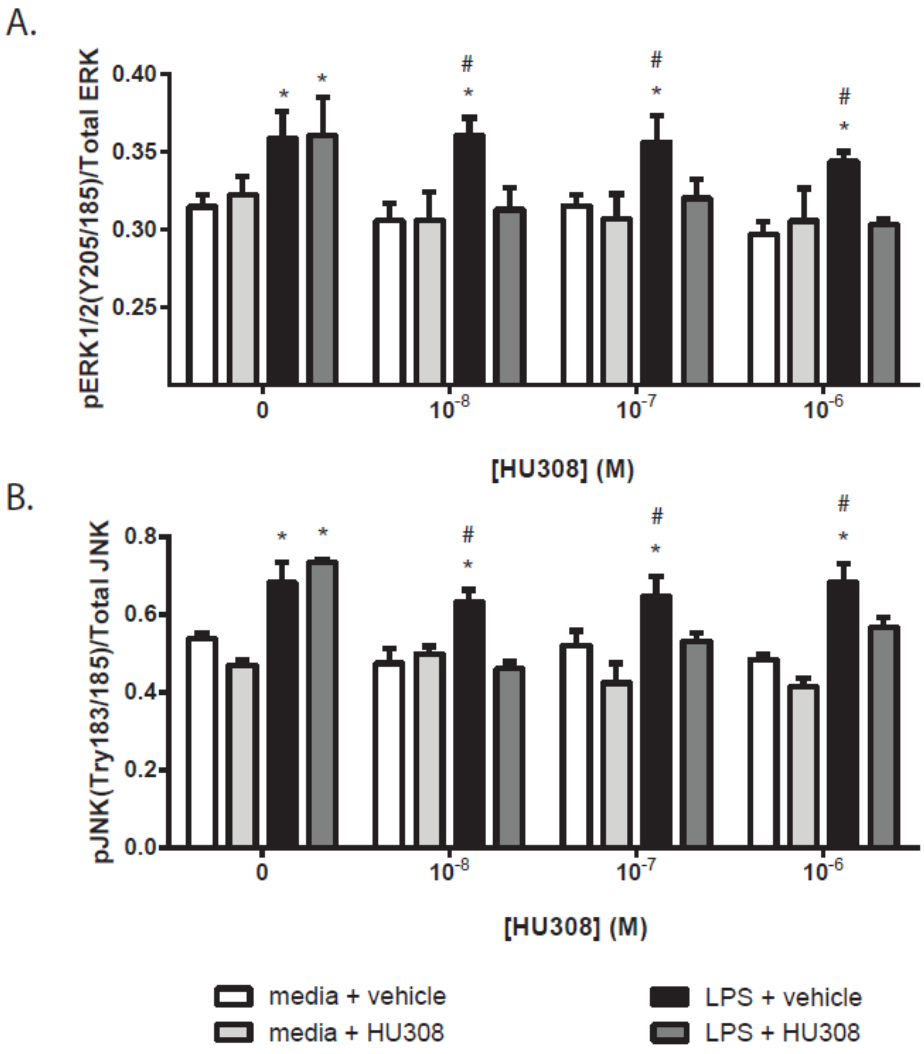
A.
pERK1/2(Y205/185)/Total ERK
0.40
0.35
0.30
0.25
0
10-8
10-7
10-6
[HU308] (M)
B.
pJNK(Try183/185)/Total JNK
0.8
0.6
0.4
0.2
0.0
0
10-8
10-7
10-6
[HU308] (M)
media + vehicle
media + HU308
LPS + vehicle
LPS + HU308

Figure 29. Inhibition of JNK phosphorylation by JNK inhibitor, SP600125, during EIU in BALB/c mice. **A)** Bar graph represents the mean number of adherent leukocytes at 6 h in the following groups: saline (n = 8); LPS (n = 13); LPS + vehicle (n = 4); LPS + SP600125 (n = 9). Values represent mean ± SEM. * $p < 0.05$ compared with the LPS group.

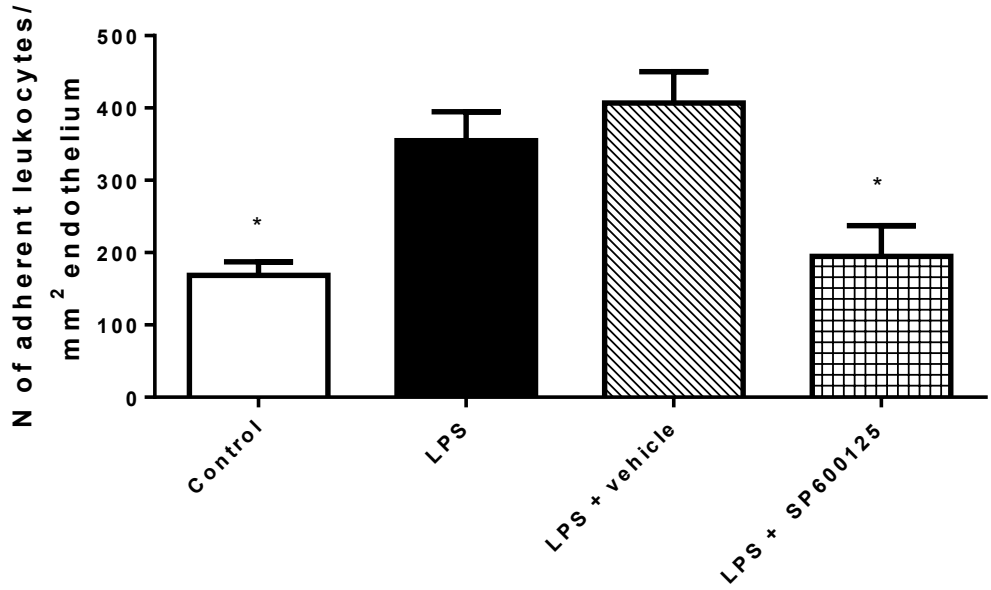
N of adherent leukocytes/ mm2 endothelium
500
400
300
200
100
0
*
*
Control
LPS
LPS + vehicle
LPS + SP600125

role in the development of EIU and this population of cells could be the cellular targets of HU308 to decrease the ocular inflammatory response *via* JNK and ERK of the MAP kinase pathways.

5.6.1 CB_2R Plays a Role in the Immune Modulation during EIU

Previously, our lab demonstrated that HU308 displays anti-inflammatory effects in a rat model of EIU (Toguri *et al*., 2014). However, a clear cellular target or signalling mechanism had yet to be demonstrated. The first objective of the current study was to confirm the anti-inflammatory properties of HU308 in an alternative animal species during EIU and confirm the role of CB_2R. EIU by intraocular injection of LPS was generated in BALB/c mice resulting in a significant increase in adherent leukocytes as described by Rosenbaum *et al*., (2011) as well as Kezic *et al*., (2011). The concentration of LPS necessary to induce inflammation was considerably higher in mice than rats (250 ng in 2 µL compared to 100 ng in 5 µL) (Rosenbaum *et al*., 1980, 2011; Toguri *et al*., 2014). As mice and rat CB_2R share 90% nucleic acid sequence similarity and 93% amino acid sequence similarity, we deemed it important to confirm the anti-inflammatory effects of HU308 in mice (Basu & Dittel, 2011; Liu *et al*., 2009). Additionally, mouse strain plays a role in the generation of a significant inflammatory response because CD-1 mice are relatively resistant to EIU compared to BALB/c mice (Li *et al*., 1995). Our results confirmed that HU308

was able to significantly reduce leukocyte-endothelial adhesion in the iridial microcirculation of BALB/c mice.

5.6.2 CB_2KO Genotype Influences Inflammation

To confirm the role of CB_2R during ocular inflammation we generated a CB_2KO mouse on a BALB/c background to allow for live imaging of iridial leukocyte-endothelial interactions during EIU. Buckely *et al*. (2000) first described the use of CB_2KO mice as a research tool for the study of CB_2R on the immune response. They noted that there were no differences in numbers of populations of different immune cells between WT and CB_2KO mice spleens and lymph nodes; however, their immunogenic profile was altered. THC significantly reduced T cell secretion of the cytokine IL-2 co-stimulated by macrophages, while T cells from CB_2KO animals were unaffected by the treatment (Buckley *et al*., 2000). Following this initial study, the CB_2R-mediated effects on the inflammatory response were more thoroughly studied with selective CB_2R agonists. Modulation of the immune response has been conducted in several different models including sepsis (Csoka *et al*., 2009; Tschöp *et al*., 2009) and LPS-induced inflammation (Ramirez *et al*., 2012; Rom *et al*., 2013; Zhang *et al*., 2009). Subsequently, Ramirez *et al*. (2012) demonstrated the CB_2R agonists JWH133 and O1966 decrease leukocyte-endothelial adhesion in blood brain barrier 4 and 24 h after the administration LPS. JWH133 or O1966 were

ineffective in CB_2KO animals. In agreement with our findings, others have demonstrated that lack of the CB_2R exacerbates the inflammatory response (Rom & Persidsky, 2013; Tschöp *et al*., 2009). Rom *et al*. (2013) conducted adaptive transfer of WT or CB_2KO leukocytes (donor) to WT or CB_2KO recipients in an LPS-induced encephalitis model. During experiments with either donor or recipient CB_2KO mice leukocyte adhesion to the blood brain barrier was increased compared to when WT mice were both recipient and donor. These results indicate that the CB_2R on leukocytes plays an important role not only in the resolution of but also in development of the inflammatory response.

Rom *et al*. (2013) primarily attributes the decrease in leukocyte adhesion to CB_2R agonists acting on monocytes during LPS-induced inflammation. As several reports on EIU describe mononuclear and polymorphonuclear cell migration to the iris, we investigated this subset of inflammatory cells (Baatz, Tonessen, *et al*., 2001; McMenamin & Crewe, 1995). During EIU in WT animals, we observed an influx of monocytes and neutrophils (Fig. 2) as previously described (Planck *et al*., 1998, 2008). This data is consistent with the results found by Murikinati *et al*. (2010), yet contrasts with Rom *et al*. (2013) who found that the cellular infiltrates are primarily mononuclear cells. Murikinati *et al*. (2010) indicated the CB_2R agonist JWH-13 decreased infarct volume during cerebral ischemia by decreasing neutrophil migration. The actions of JWH-133 were attributed to inhibiting migration to the chemokine CXCL2, indicating that

CB_2R mediated effects directly on neutrophils (Murikinati *et al*., 2010). These results corroborate with previous work conducted by our group indicating CB_2R activation decreases leukocyte migration. However, *in vivo* this effect could also be attributed to a CB_2R-facilitated decrease in inflammatory mediators (Toguri *et al*., 2014). This could explain the reduced leukocyte recruitment observed in the iridial microcirculation. Indeed, our group has previously demonstrated that treatment with a CB_2R agonist during EIU significantly reduced levels of several pro-inflammatory cytokines: TNF-α, IL-1β, IL-6, IL-10, IFN-γ and chemokines, CCL5 and CXCL2 (Toguri *et al*., 2014).

5.6.3 Endogenous Cannabimimetic Ligands and CB_2R Levels

Several *in vitro* and *in vivo* studies have shown changes in AEA and 2-AG levels in animal models. During LPS induced inflammation AEA and 2-AG production was increased in murine RAW 264.7 macrophage cell line and circulating rat macrophages (Di Marzo *et al*., 2000; Liu *et al*., 2003). *In vivo* during hepatic ischemia-reperfusion, levels of AEA and 2-AG increased alongside levels of inflammatory mediators including TNF-α, MIP-1α and MIP-2. Ischemia alone did not cause an increase in endocannabinoid levels (Bátkai *et al*., 2007). Levels of AEA and 2-AG are increased in human eyes from individuals with atypical chronic ocular inflammation in age-related macular degeneration and diabetic retinopathy (Matias *et al*., 2006). Interestingly, in our

experiments no significant changes were observed with saline control injections, LPS induced EIU or animals with EIU and HU308 treatment. The lack of any significant alterations in AEA or 2-AG of treatment groups could be attributed to the acute course we investigated compared to the alterations observed in chronic diseases seen in age-related macular degeneration and diabetic retinopathy (Di Marzo *et al*., 2000; Liu *et al*., 2003; Matias *et al*., 2006). The lack of acute changes in AEA and 2-AG by LPS could be due to compensatory mechanisms which are at play in the eye due to its immune privileged nature.

The current literature is lacking a thorough investigation of endocannabinoid levels during trauma. Some evidence demonstrates that, in the brain and spinal cord, traumatic injury causes an increase in 2-AG and AEA (Arevalo-Martin *et al*., 2012; Panikashvili *et al*., 2001). Levels of 2-AG are decreased in the ciliary body, and nowhere else in the ocular tissue of glaucomatous eyes (Matias *et al*., 2006). AEA levels are not changed in normal or glaucomatous eyes (Matias *et al*., 2006). Lower 2-AG levels are attributed to activation of PLA2, which releases AA from phospholipids and reduces the biosynthetic precursors needed to create 2-AG (Chen *et al*., 2005). It does not appear from our investigation that presence or absence of CB_2R influence either AEA or 2-AG levels in the eye, in naïve animals or those with acute EIU.

In our study, a lack of significant changes in endocannabinoid levels lead us to conclude that exacerbated acute ocular inflammation was not due to changes

in 2-AG or AEA in CB_2KO mice. The exacerbated inflammatory response observed in CB_2KO mice must, therefore, have been due to lack of CB_2R. This hypothesis is consistent with previous reports of CB_2R levels being increased during inflammation in tissue *in vivo* and on leukocytes primed with inflammatory mediators (Ashton & Glass, 2007; Carlisle *et al*., 2002; Merriam *et al*., 2008; Ramirez *et al*., 2012). Indeed, when we investigated levels of CB_2R expression in the eye, we found higher levels in LPS-treated animals, with our without HU308 treatment. In WT animals, levels of CB_2R increase during inflammation which could be stimulated by endocannabinoids and endogenously decrease the inflammatory response. Additional administration of CB_2R agonists such as HU308 could subsequently activate the now larger pool of CB_2R to ameliorate the inflammatory response, which is consistent with our IVM findings. The lack of CB_2R in CB_2KO animals exacerbates inflammation during EIU as 2-AG and AEA are unable to endogenously regulate the inflammatory tone.

5.6.4 The Role of Macrophages during EIU and Treatment by CB_2R Agonist, HU308

The LPS-induced inflammatory response occurs *via* TLR4 activation and subsequent increased levels of pro-inflammatory mediators. As TLR4 is located on immune and endothelial cells, we investigated the role of macrophages in the

inflammatory response. Pouvreau *et al*. (1998) showed macrophage depletion by clodronate injected 7 and 3 days prior to EIU significantly reduced clinical, histological, and TNF protein levels in the aqueous humor in a model of EIU derived by footpad injection in Lewis rat. The role of macrophages was also confirmed in an experimental melanin-protein induced uveitis (EMIU), a model of autoimmune anterior uveitis (Baatz, Puchta, *et al*., 2001). The data we obtained from the clodronate experiments identifies the importance of macrophages during EIU produced by local LPS in mice. This confirmation is important as the underlying pathology during EIU occurs similarly in mice than it does in rat despite needing different concentrations of LPS to generate an immune response (Rosenbaum *et al*., 1980, 2011; Toguri *et al*., 2014). Additionally our results demonstrate the importance of macrophages in EIU progression during an acute time-frame (< 6 h).

5.6.5 Investigation of the MAPK Pathway in Murine Monocyte/Macrophages Cell Line RAW 264.7 during LPS and CB_2R Activation

Due to the diminished inflammatory response after the elimination of macrophages, we hypothesized HU308 decreased production of pro-inflammatory mediators that arise from LPS-stimulated macrophages. It has previously been demonstrated that CB_2R agonism alters macrophage-dependent T cell proliferation and attenuates pro-inflammatory mediators such as TNF-α,

MIP-1, and MIP-2 (Sacerdote *et al*., 2000; Xu *et al*., 2007). Lower levels of cytokines and chemokines would result in reduced recruitment of leukocytes. LPS stimulation of the murine RAW 264.7 macrophage-like cell line has been shown to induce the MAPK pathways by phosphorylation of JNK, ERK and p38 (Dong *et al*., 2002) and transactivation of transcription factors NF-κB and AP-1 to induce inflammatory mediators (Hambleton, Weinsteint, *et al*., 1996; Wang *et al*., 2009). There have been several reports demonstrating stimulation of CB_2R can result in activation and inhibition of the MAPK pathways in both animal and cell models of inflammation. Both non-selective cannabinoid agonists cannabidiol and WIN 55212-2 inhibit phosphorylation of ERK in phorbol myristate acetate-stimulated splenocytes in a model of inflammation (Faubert Kaplan & Kaminski, 2003). WIN55,212-2 similarly inhibits ERK and JNK signalling in a chronic cerebral hypoperfusion model of CNS disease, which is important for neuronal survival (Su *et al*., 2015). The CB_2R agonist JWH133 also decreased pERK and pp38 in a model of cerebral haemorrhage, reducing microglia activation and accumulation (Tang *et al*., 2015). In our RAW cell model of acute inflammation by LPS stimulation, ERK and JNK phosphorylation were increased. HU308 reduced ERK and JNK phosphorylation. This modulation of the MAPK pathways could support our previous findings of decreased levels of mRNA expression of pro-inflammatory transcription factors NF-κB and AP-1, which were decreased after HU308 treatment during EIU and lead to the

reduction of pro-inflammatory cytokines: TNF-α, IL-1β, IFN-γ and chemokines: CCL5 and CXCL2 (Xu *et al*., 2007).

Inhibition of JNK *in vivo* by SP600125 confirmed the involvement of the JNK signaling pathway during EIU. In addition to *in vitro* data, this reiterates the potential role of CB_2R agonists potentiating their anti-inflammatory effects *via* inhibition of JNK. Our *in vitro* experiments did not show complete ablation of the pJNK following HU308 treatment. For this reason, we believe that pJNK plays a key role in the induction of inflammation by LPS, but inhibition of JNK is only one of several anti-inflammatory mechanisms for HU308.

In conclusion, this study has confirmed that the CB_2R plays a significant role during an acute ocular inflammation in a model of EIU. While this study elucidates potential inter- and intra-cellular signalling pathways by which the CB_2R agonist, HU308, acts during an acute model of EIU other cellular subsets and signal transduction pathways must be investigated. This study provides additional support for the targeting of CB_2R in the treatment of acute ocular inflammation.

Chapter VI: General discussion

The research presented in this dissertation investigated the endocannabinoid system and its modulation during ocular inflammation. The results of my studies have shown that both CB_1R and CB_2R activation can reduce ocular inflammation. In particular, systemic or topical CB_2R stimulation by HU308 reduced leukocyte-endothelial adhesion, release of inflammatory mediators and expression of pro-inflammatory transcription factors in EIU. Consistent with this, when CB_2R was blocked with the antagonist, AM630, or when EIU was induced in CB_2KO mice, inflammation was exacerbated. In the presence of CB_2R inhibition, CB_2R agonists failed to decrease leukocyte adhesion and release of pro-inflammatory mediators. Additionally, endocannabinoid and AA levels in CB_2KO mice and in WT mice following LPS administration were reported. Interestingly, no differences were observed in tissue concentrations of AEA or 2-AG between all treatments of animals on the same genetic background or the equivalent group on the alternative genetic background. AA levels were only decreased in CB_2KO animals with LPS compared to their WT counterparts. In this thesis, the CB_2R agonist, HU308, was also compared to current clinical treatments for uveitis, including NSAIDS and steroids and it was demonstrated that HU308 was more efficacious in reducing ocular inflammation than these clinical treatments. *In vitro* experiments, using

the monocyte/macrophage cell line RAW 264.7 cells, demonstrated that CB_2R activation inhibited phosphorylation of ERK and JNK, blocking increases in expression of the pro-inflammatory transcription factor AP-1.

Taken together, the results provide novel data on ECS signaling during ocular inflammation and indicate that CB_2R may represent a pharmacological target for the development of new therapeutics to treat ocular inflammation. These findings are discussed in more detail below with respect to current knowledge in the field.

6.1 Cannabinoid Receptor Modulation in Ocular Inflammation

It was initially demonstrated that the non-selective cannabinoid, WIN, was able to reduce leukocyte-endothelial adhesion within the iridial microcirculation during systemic LPS-induced inflammation, and that this effect was due to actions at both CB_1R and CB_2R. The effects of leukocyte adhesion was measured in two categories of vessel, those with a diameter greater or less than 25 μm.

Stimulation of CB_1R and CB_2R decreased leukocyte adhesion in all vessels within the iridial microvasculature. When CB_1R was activated by WIN in the presence of inhibition of CB_2R, leukocyte adhesion was attenuated in vessels that were less than 25 μm. In contrast to this, WIN in the presence of an inhibitor for CB_1R activated CB_2R which diminished leukocyte-endothelial adhesion in

vessels with diameters greater and less than 25 μm. Activation of either, or both, CB_1R or CB_2R diminished the decrease in local blood flow observed when LPS was given alone. These findings are in-line with similar observations documented in the literature. For example, WIN attenuated leukocyte-endothelial interactions in a model of EAE (Ni *et al*., 2004), an effect that was attributed to CB_1R activation (Rossi *et al*., 2011). CB_1R stimulation has also been reported to inhibit cytokine release during endotoxemia (Smith *et al*., 2000; 2001), and *in vitro* models of LPS-stimulated immune cells (Facchinetti *et al*., 2003). In both these latter studies, the cannabinoid agonist WIN was used together with a pharmacological block of CB_2R and, therefore, the effects of CB_2R were not specifically addressed. Furthermore, while leukocyte adhesion and cytokine release were investigated in these models following WIN treatment, other parameters such as blood flow and capillary density, as well as relative contributions of CB_1R and CB_2R to the anti-inflammatory actions of WIN were not considered.

In contrast to these earlier studies, my work showed that the anti-inflammatory effects of WIN in reducing leukocyte-endothelial adhesion were largely mediated via CB_2R, with more modest effects attributable to CB_1R (Toguri *et al*., 2015). Furthermore, the efficacy of CB_1R-mediated inhibition of leukocyte-endothelial interactions in EIU depend on the vessel size, with a significant decrease of leukocyte-adhesion only seen in vessels less than 25 μm.

This observation suggested that the anti-inflammatory actions of CB_1R activation may result from vascular changes, possibly via CB_1R-mediated increases in blood flow and shear forces, with a resultant decrease in adhesion of leukocytes (Bagher & Segal, 2011; Cunningham & Gotlieb, 2005). In addition to decreasing leukocyte-endothelial adhesion, WIN treatment prevented the decrease in iridial microcirculatory blood flow caused by inflammation, and this effect was independent of alterations in systemic blood pressure. Use of CB_1R and CB_2R antagonists after systemic LPS injection in these experiments (leukocyte adhesion, iridial blood flow measurements), demonstrated that activation of CB_2R alone was sufficient to mitigate ocular inflammation in EIU.

6.2 CB_2R Pharmacology in EIU

Given that CB_2R is highly localized to immune cells, is upregulated in inflammation, and was a more efficacious treatment in my initial experimental findings, my later studies primarily focussed on CB_2R as an anti-inflammatory target in the eye. Additionally, treatment by CB_2R agonists for the ocular inflammation would not be confounded by the behavioural actions associated with CB_1R activation, which might limit the potential clinical use (Ligresti *et al*., 2009). In support of therapeutic targeting of CB_2R in ocular inflammation, CB_2R agonists have been shown to decrease leukocyte-endothelial adhesion in the retina in an EAU model (Xu *et al*., 2007). However, it is important to note that

this is a chronic model of ocular inflammation primarily involving T cells, and thus different to the acute EIU model that I investigated, which involves primarily the innate immune system. However, CB_2R activation has also been reported to decrease leukocyte-endothelial interactions in other vascular beds, such as the intestinal microcirculation, in an acute LPS model of (Lehmann *et al*., 2012; Sardinha *et al*., 2014). In another model of sepsis, a cecal ligation and puncture model, a CB_2R agonist decreased mortality and neutrophil recruitment to lung as well as the peritoneal fluid (Tschöp *et al*., 2009).

In order to avoid the confounding effects of CB_2R activation in other tissues during systemic endotoxemia, I subsequently developed a model of local ocular inflammation using intraocular injection of LPS. Furthermore, in order to restrict off-target effects and provide a more relevant route of administration for the treatment of ocular inflammation, we utilized a topical delivery system for cannabinoids (Toguri *et al*., 2014, 2015). Using these approaches, I demonstrated that topical application of HU308, a CB_2R agonist, was able to significantly reduce leukocyte-endothelial adhesion in EIU and that this effect was blocked by prior administration of the CB_2R antagonist, AM630. Interestingly, when AM630 was administered alone during inflammation, leukocyte adhesion to the iridial microcirculation was exacerbated, suggesting inverse agonist action of this cannabinoid (Marini *et al*., 2013; Miller & Stella, 2008). Inverse agonism has been observed for several different ligands of both CB_1R and CB_2R, including

AM630. AM630 dose-dependently increases forskolin-stimulated cAMP in CB_2R transfected Chinese hamster ovary (CHO) cells. This effect persisted in the presence of CP 55,5940 (a non-selective cannabinoid agonist), which when administered on its own inhibits cAMP (Ross *et al*., 1999). These inverse agonist effects were defined by the alteration in constitutive cAMP. Similarly, during LPS induced inflammation, AM630 exacerbated leukocyte-endothelial adhesion compared to LPS alone-induced leukocyte adherence. These findings may be the result of AM630 antagonizing endocannabinoids from eliciting basal anti-inflammatory effects by CB_2R during inflammation; alternatively AM630 could be increasing leukocyte-endothelial adhesion through inverse agonist effects acting at second messengers such as cAMP. This would be consistent with observations of increases in adenylate cyclase activity following the stimulation of leukocytes with mitogens. Additionally, cannabinoids have been shown to inhibit cAMP signaling resulting in the inhibition of the immune response (Kaminski *et al*., 1998). Activation of CBR was shown to inhibit cAMP and cause c-fos, component of AP-1, to be retained in the cytoplasm (Faubert Kaplan and Kaminski, 2003). While others have used pre-treatment of CB_2R antagonists to abolish anti-inflammatory effects of CB_2R agonists (Ramirez *et al*., 2012; Sardinha *et al*., 2014), these studies did not report an exacerbated response of leukocyte adhesion during inflammation in the presence of the CB_2R antagonist block. Differences in experimental models used, vascular beds studied and

duration of inflammatory response may contribute to these different results. In the experiments I conducted is difficult to determine whether the effects seen by AM630 were caused by antagonism or inverse agonism of the CB_2R as I did not investigate modulation of second messengers. However, in support of my findings, I also demonstrated that CB_2R mRNA was upregulated in ocular tissue in EIU, as has been reported in other studies of inflammation (Maresz *et al*., 2005; Storr *et al*., 2009), and this finding may account for the apparent inverse agonist actions of CB_2R antagonists such as AM630 in ocular inflammation.

To examine possible signalling pathways implicated in the anti-inflammatory effects of CB2R activation in ocular tissue, I also investigated the levels of local inflammatory mediators including cytokines, chemokines and adhesion molecules before and after CB_2R modulation using cannabinoids. These experiments demonstrated that CB_2R activation by HU308 during EIU significantly decreased levels of the cytokines, TNF-α, IL-1β, IL-6, IL-10 and chemokines CCL5 and CXCL2, however HU308 did not alter tissue levels of adhesion factors, ICAM-1 or VCAM-1 during EIU. Others have documented similar findings in the decreases of cytokines and chemokines in the intestine (Lehmann *et al*., 2012), pial vasculature (Ramirez *et al*., 2012) and isolated macrophages and dendritic cells (Greineisen & Turner, 2010; Selvi *et al*., 2008). Interestingly, Rarmirez *et al*. (2012), showed a decrease in adhesion molecules PSGL-1 and LFA-1. This demonstrated that although I did not observe changes

in soluble adhesion molecule levels (ICAM-1 and VCAM-1) during in EIU it is possible that other adhesion molecules were modulated following CB_2R activation which contributed to the alteration in leukocyte adhesion. Alternatively, I may have observed the decrease in leukocyte-endothelial adhesion as cytokines and chemokines which regulate chemotaxis of leukocytes are modified by CB_2R activation, resulting in decreased leukocyte recruitment to the area of inflammation and thus a decreased probability of leukocyte adhesion.

Cannabinoids can modulate inflammatory signaling pathways and activation of both CB_2R and CB_1R has been reported to decrease TLR4 signaling and pro-inflammatory transcription factors (Facchinetti *et al*., 2003; Gui *et al*., 2013; Ramirez *et al*., 2012; Smith, Terminelli, *et al*., 2001); LPS-TLR4 interactions up-regulate inflammatory mediator release by increasing expression of transcription factors AP-1, NF-κB and IFR3 by two independent pathways, the MyD88-dependent and MyD88–independent paths (Fitzgerald *et al*., 2003; Lu *et al*., 2008). In an EIU model, I demonstrated that LPS administration produces increases in both AP-1 and NF-κB mRNA. CB_2R activation ablated this increase in AP-1 and NF-κB mRNA levels, while CB_2R inhibition significantly increased mRNA levels of both transcription factors in comparison to LPS alone.

The literature regarding CB_2R activation in the regulation of pro-inflammatory transcription factors including NF-κB (Do *et al*., 2004; Toguri *et al*., 2014), AP-1 (Jeong *et al*., 2013; Toguri *et al*., 2014) and nuclear factor of

activated T-cells (NFAT) (Ngaotepprutaram *et al*., 2013) is mixed, with some reports describing inhibition and others activation by cannabinoid agonists. It appears that the activation of transcription factors such as CREB, NF-κB, AP-1, NFAT is highly variable due to ligand signal transduction, inflammatory stimulus and cell type investigated (Bosier *et al*., 2010; Choi *et al*., 2013; Do *et al*., 2004; Faubert & Kaminski, 2000; Romero-Sandoval *et al*., 2009). In agreement with my data, Faubert and Kaminski (2000) also showed AP-1 was decreased by CB_2R activation during phorbol 12-myristate 13-acetate - induced inflammation. In a model of acute lung inflammation, CB_2R agonist, JWH133, inhibited NF-κB activation reducing several markers of inflammation (TNF-α, IL-1β levels and, histopathological damage) (Liu *et al*., 2014). Δ^9-THC reduced DNA-binding of two pro-inflammatory transcription factors NF-κB and NFAT in a model of T cell activation; however, in this study the authors attributed the decrease in DNA binding to be important in decreasing CD40L/CD154, a transmembrane protein which increases antigen presentation, cytokines and antibody production (Ngaotepprutaram *et al*., 2013). As NF-κB and AP-1 are downstream transcription factors in both the MyD88-dependent and -independent pathways, I investigated mRNA level of RIP-1, a signaling molecule found upstream of the transcription factors in only one of the TLR4 pathways, the MyD88 independent pathway (Akira & Takeda, 2004a; Kawai & Akira, 2010). My results demonstrated that LPS stimulation did not alter RIP-1 mRNA levels. This

indicated that LPS administration and thus CB_2R agonist inhibition of mRNA levels in EIU are primarily occurring through the MyD88 pathway. This result supports the study by Kezic *et al*. (2010) using MyD88 knockout mice. The authors reported that inflammation during EIU was dependent on the MyD88 pathway.

6.3 Validation of CB_2R as an Anti-inflammatory Target in Ocular Inflammation

Confirmation of the CB_2R as target for the anti-inflammatory actions of cannabinoids was established using CB_2KO mice. Consistent with my results using the CB_2R antagonist, AM630 (Toguri *et al*., 2014), leukocyte-endothelial adhesion was significantly exacerbated in CB_2R KO mice compared to WT (Toguri *et al*., 2015). Immunohistochemistry in CB_2R KO and WT mice after LPS injection demonstrated that the population of cells migrating to the eye during EIU was primarily neutrophils, although some monocytes were involved in the inflammatory response. These findings were similar to immune cell recruitment observed by others using similar models of EIU (McMenamin & Crewe, 1995; Planck *et al*., 1998, 2008).

As LPS can interact with TLR4 on many different cellular subsets, including other leukocytes and endothelial cells, it was important to examine the effects of LPS in animals in which specific populations of mononuclear cells were

depleted in order to further identify cell targets for the anti-inflammatory effects of CB_2R. Clodronate administration depletes mononuclear cells (Lehenkari *et al*., 2002; van Rooijen *et al*., 1996) and, in my experiments, inhibited the induction of EIU. Similar results were also reported by Pouvreau *et al*., (1998) who depleted macrophages prior to EIU in rats generated by LPS footpad injection. At 16 hr after LPS administration, Pouvreau *et al*., (1998) observed a significant decrease in ED2+ tissue resident macrophages in the iris and ciliary body after clodronate, however there were no significant effects on leukocytes, as measured by with OX42+ staining for PMN cells, microglia, tissue resident macrophages and DCs (Pouvreau *et al*., 1998). These results are contrary to those that I observed post-clodronate treatment, *i.e* few inflammatory cells were observed in clodronate-treated animals. One explanation for this is that Pouvreau *et al*., only administered clodronate on day 7 and 3 prior to LPS injection and therefore may not have depleted all mononuclear cells, whereas I used daily treatment which more successfully diminished the mononuclear cell population. These results are important in that they demonstrate that it is primarily mononuclear cells, which release the inflammatory mediators (cytokines, chemokines and adhesion molecules) which then stimulate chemotaxis of other immune cells. This also infers that TLR4s on endothelial cells play little role in the development of EIU.

Based on these findings, I hypothesized that the CB_2R activation on macrophages inhibits the release of inflammatory mediators following LPS

stimulation and consequently decreases the recruitment of neutrophils to injury site. To test this hypothesis, I used the murine macrophage cell line RAW 264.7 cells to investigate cannabinoid modulation of MAPK pathways (ERK, JNK and p38). These proteins are activated via phosphorylation during LPS stimulation of TLR4 and are associated with increases of the pro-inflammatory transcription factor AP-1 (Blasius & Beutler, 2010).

Using In-Cell Western®, I showed that pre-treatment of macrophages with the CB_2R agonist HU308 inhibited phosphorylation of ERK and JNK after stimulation with LPS. Unfortunately, due to rapid dephosphorylation of these proteins after LPS stimulation (Hambleton, Weinstein, *et al*., 1996; Xagorari *et al*., 2002), we were unable to demonstrate that post-LPS treatment with HU308 could also inhibit phosphorylation of ERK and JNK. I confirmed the importance of activation JNK in vivo using the JNK inhibitor. However, our results are consistent with other studies that have investigated CB_2R modulation of MAPK. For example, GW405833, a CB_2R agonist, significantly reduced phosphorylation of ERK in peritoneal macrophages stimulated with LPS. This study additionally demonstrated that GW405833 inhibited STAT3, and upstream regulator of NF-κB signalling, thus preventing the translocation of NF-κB to the nucleus (Gui *et al*., 2013). Interesting, in another study using primary mouse microglia and a microglia cell line N9 stimulated with LPS, the CB_2R agonist JWH-133 decreased pERK in the primary microglia cells, but in N9 cells initially it

produced a transient increase in pERK, followed by a decrease. The decrease in MAPKs was mediated by Gi/o activation as PTX inhibited changes in the MAPKs (Merighi *et al*., 2012).

Recently Liu *et al*. reported that CB_2R activation inhibited phosphorylation of JNK in zebra fish during acute inflammation following tail transection with a resultant decrease in leukocyte migration. This study also showed that JWH-015 inhibited JNK phosphorylation in THP-1 cells, a human acute monocytic leukemia (AML) cell line, although these cells were not challenged by an inflammatory agent (Liu *et al*., 2013). In addition, these authors reported a novel potential link between the CB_2R-mediated decrease in JNK phosphorylation and block of 5-lipoxygenase (Alox5); Alox5 synthesises leukotrienes, a group of inflammatory mediators (Liu *et al*., 2013).

Several studies have also examined CB_2R modulation of the MAPK, p38, in models of inflammation (Tang *et al*., 2015; Tschöp *et al*., 2009). For example, levels of pp38 were higher in peritoneal cells isolated from septic WT compared to CB_2KO mice, suggesting that endogenous activation of CB_2R during inflammation increases p38 phosphorylation (Tschöp *et al*., 2009). This same study also demonstrated that phosphorylation of p38 was increased in mice treated with CB_2R agonist compared to untreated animals. The authors of this study suggested that CB_2R signaling was contributing to neutrophil recruitment and priming, important in the clearance of pathogens (Tschöp *et al*., 2009).

In addition to MAPK signaling, others have also reported that CB_2R activation can increase phosphorylation of AMP-activated protein kinase (AMPK) and cAMP responsive element-binding protein (CREB) (Choi *et al*., 2013; Ofek *et al*., 2011). CREB plays a role in the induction of mitogen-activated protein kinase-phosphatase-1 (MKP-1), a MKP which dephosphorylates MAPKs (Casals-Casas *et al*., 2009). MKP-1 has recently been reported to be activated by CB_2R agonists, although the mechanism remains to be elucidated (Eljaschewitsch *et al*., 2006; Romero-Sandoval *et al*., 2009). Taking into consideration the studies discussed above it is possible that CB_2R activation induced the activation of CREB or increase in MKP, which could effect the decrease ERK and JNK phosphorylation I observed. This activation of CREB or MKPs could then decreased levels mRNA of the transcription factors AP-1 and NF-κB (Eljaschewitsch *et al*., 2006; Romero-Sandoval *et al*., 2009; Wen *et al*., 2010).

.

6.4 Hypothetical Model for CB_2R Anti-inflammatory Actions

Based on my results, and the current literature, I propose the following model for the anti-inflammatory actions of CB_2R signaling in ocular inflammation. This model proposes that agonists acting at CB_2R on tissue-resident mononuclear cells, specifically resident macrophages in the eye, activate Gβδ-coupled MAPK or CREB signaling, thereby increasing MKPs to inhibit ERK and JNK phosphorylation (Figure 30A) (Cabral & Griffin-Thomas, 2010;

Figure 30. Proposed CB_2R mechanisms to decrease ocular inflammation. A) Signaling pathways to decrease o decreasing inflammatory mediator release B) The effect of inhibiting inflammatory mediators decreases leukocyte recruitment.

A

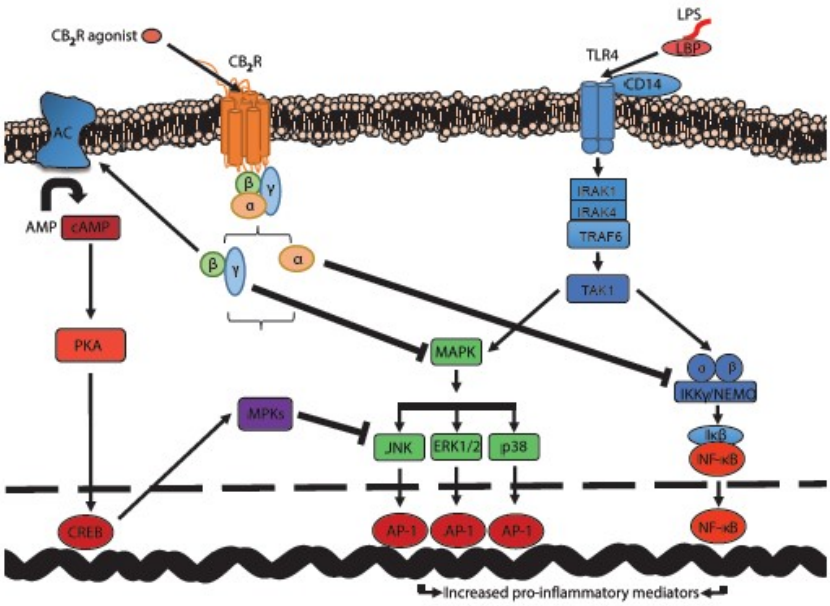
CB2R agonist
CB2R
LPS
LBP
TLR4
CD14
AC
β
γ
α
IRAK1
IRAK4
TRAF6
AMP
cAMP
TAK1
PKA
MAPK
α β
IKKγ/NEMO
MPKs
JNK
ERK1/2
p38
IκB
NF-κB
CREB
AP-1
AP-1
AP-1
NF-κB
Increased pro-inflammatory mediators

B

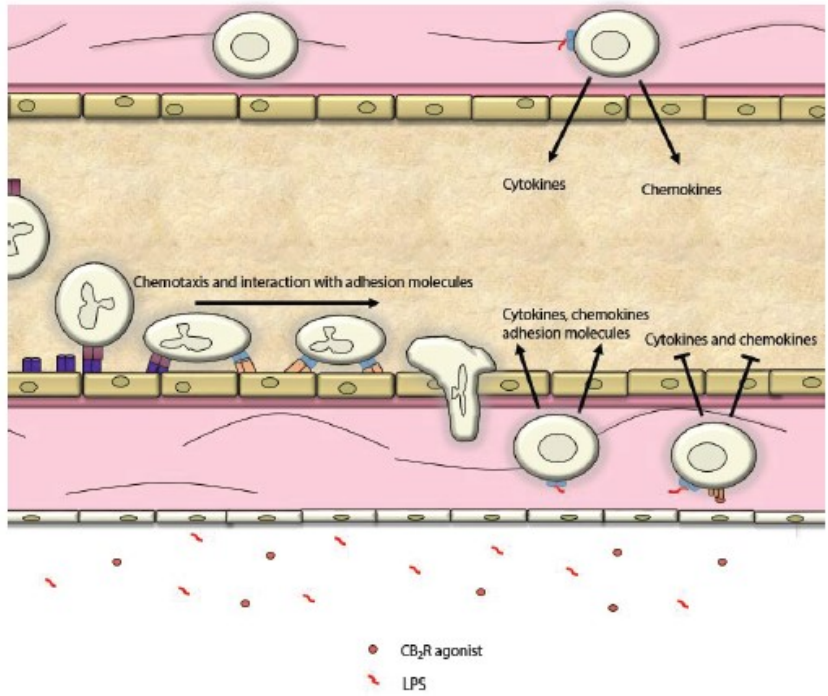
Cytokines
Chemokines
Chemotaxis and interaction with adhesion molecules
Cytokines, chemokines
adhesion molecules
Cytokines and chemokines
CB2R agonist
LPS

Casals-Casas *et al*., 2009; Eljaschewitsch *et al*., 2006; Krishnan & Chatterjee, 2012; Romero-Sandoval *et al*., 2009). As phosphorylation of ERK and JNK is downstream of LPS-TLR4 signaling and activates pro-inflammatory transcription factors AP-1 and NF-κB, CB_2R-mediated inhibition of ERK and JNK phosphorylation suppresses these actions. Although we did not investigate alternative mechanisms, Gui *et al*., (2013) have demonstrated CB_2R activation decreases the degradation of IκBα which could block NF-κB mRNA production through negative feedback. Attenuation of transcription factors AP-1 and NF-κB consequently decreases the concentration of inflammatory factors, namely the cytokines, TNF-α, IL-1β, IL-6, IL-10 and chemokines CCL5 and CXCL2 (see Figure 30B), decreasing the recruitment of neutrophils that migrate to and interact with the iridial endothelium, and limiting inflammation and tissue damage.

6.5 Therapeutic Potential of Cannabinoids in Ocular Inflammation

My research demonstrated that activation of CB_2R was anti-inflammatory during EIU; CB_2R activation decreased leukocyte-endothelial adhesion, reduced levels of pro-inflammatory mediators and diminished mRNA levels of pro-inflammatory transcription factors NF-κB and AP-1. All of these actions are promising outcomes for the development of a topical ocular CB_2R anti-inflammatory agent for uveitis. One of the most important findings of my work was demonstrating the potential clinical application of CB_2R agonism. I selected

three currently used clinical anti-inflammatory treatments: the steroids, dexamethasone and prednisolone, and the NSAID, nepafenac, to compare to CB_2R agonist, HU308. Measurable indicators of inflammation including leukocyte-endothelial adhesion and tissue levels of inflammatory mediators were examined in all four drug groups over a 6 hr period after LPS injection with a single drug dose. CB_2R activation decreased leukocyte adhesion by 6 hr and this effect was comparable if not superior to clinical doses of nepafenac and dexamethasone and prednisolone, respectively. However, as my studies at this time were limited to an acute endotoxemia model, further studies are now required to examine different dosing regiments and more chronic inflammatory time course to fully evaluate the efficacy of CB2R agonists versus current clinical drugs for the treatment of ocular inflammatory disease.

6.6 Future Directions

The work presented in this thesis describes the pharmacodynamics of CB_2R modulation during ocular inflammation. Although the data presented provide promising results for the use of CB_2R agonists for treatment of ocular inflammation, there are still several areas that must be addressed. Presently, I have only studied CB_2R activation in two models of ocular inflammation (systemic and local LPS administration), specifically the inflammatory response within the eye during endotoxemia, a model of acute local inflammation derived

from a bacterial toxin that primarily involves the innate immune response. Ultimately, CB_2R agonists, should be investigated in several alternative models of ocular inflammation including models generated with live pathogens, autoimmune disorders and chronic inflammatory models mediated by adaptive immunity (Xu *et al*., 2007). This will provide further evidence as to whether CB_2R anti-inflammatory properties are specific to cells involved in the innate immune response, as seen in the EIU model I used in my research, or whether, the actions of CB_2R signalling may also modify the adaptive immune response. Differentially actions of CBR signaling in terms of the innate or adaptive immune response may affect therapeutic use.

With this in mind, further clarification of the signalling pathways contributing to the anti-inflammatory actions of CB_2R activation in cells involved in both innate and adaptive immune is required. While my research has suggested that the anti-inflammatory effects of CB_2R stimulation during acute endotoxemia may result, in part, from inhibition of inflammatory mediator release from APCs it would be important to confirm this by direct stimulation of CB_2R on APCs *in vitro.* I also suggest to investigate how the time point when CB_2R agonist are given influences the ant-inflammatory outcome. I believe that if the CB_2R is not activated soon after an inflammatory stimuli it may not decrease inflammation with the same efficacy as I observed. I believe this as the MAPKs are an acutely regulated systems and if not inhibited immediately, pro-inflammatory

transcription factors will still be activated. If the MAPKs and thus pro-inflammatory are not inhibited then immune cell recruitment would not be altered as the pro-inflammatory transcription factors (NF-κB and AP-1) are activated and would increase the release of pro-inflammatory mediators (Eljaschewitsch *et al*., 2006; Larsen & Henson, 1983; Romero-Sandoval *et al*., 2009). Although I have shown that cannabinoid agonists decrease LPS-induced phosphorylation of MAPKs, I did not investigate the potential mechanism of actions of how decreased MAPK phosphorylation decreases NF-κB mRNA. It has been shown by others that CB_2R activation can inhibit degradation of the inhibitory factor IκBα protein, which allows for NF-κB to translocate to the nucleus. It is possible that the same mechanism is occurring by CB_2R activation in the model I investigated and contributes to the anti-inflammatory properties I observed. Due to this further investigation into the mechanism by which CB_2R stimulation elicits its anti-inflammatory effects ocular inflammation must occur.

Key to the development of ocular CB_2R drugs are the pharmacokinetics of CB_2R ligands. Although, my work demonstrated that cannabinoid ligands can be delivered topically via the cornea using an emulsion delivery system (Tocrisolve®), and are able to penetrate the cornea without major side effects, additional pharmacokinetic assays are now required to examine absorption, distribution and metabolism of these agents using different optimized topical

delivery systems. This would involve investigation of aqueous humor, tissue and plasma levels of cannabinoids, using gas chromatography and/or mass spectrometry. Examination of the metabolism of synthetic cannabinoids is also important as drug metabolites could influence drug-drug interactions and modulate the metabolic pathways of alternative drugs. These studies would also need to be complimented by ocular toxicology studies examining the safety of these compounds for both acute and chronic use.

6.7 Final Thoughts

Although much work must still be done on the use of CB_2R agonist as therapeutics for ocular inflammation in the clinic, the work I have conducted during my PhD established a strong foundation for future investigation in this field. My work has contributed to the growing literature attributing anti-inflammatory properties to the CB_2R activation. I have presented here that the use of a CB_2R agonist might be an appropriate therapeutic approach to target ocular inflammation, however these results may have further implications in the modulation of inflammation in other organ systems. In my studies CB_2R activation had no major side effects and proved more efficacious than current clinical treatments. Currently the modulation of the ECS for the treatment of inflammation has been trivialized and must be investigated further.

References

Adhikary, S., Kocieda, V. P., Yen, J.-H., Tuma, R. F., & Ganea, D. (2012). Signaling through cannabinoid receptor 2 suppresses murine dendritic cell migration by inhibiting matrix metalloproteinase 9 expression. *Blood*, *120*(18), 3741–3749.

Akerman, S., Kaube, H., & Goadsby, P. J. (2004). Anandamide acts as a vasodilator of dural blood vessels in vivo by activating TRPV1 receptors. *British Journal of Pharmacology*, *142*(8), 1354–1360.

Akira, S., & Takeda, K. (2004a). Toll-like receptor signalling. *Nature Reviews. Immunology*, *4*(7), 499–511.

Akira, S., & Takeda, K. (2004b). Toll-like receptor signaling. *Nature Reviews. Immunology*, *4*(7), 499–511.

Akpek, E. K., & Gottsch, J. D. (2003). Immune defense at the ocular surface. *Eye*, *17*(8), 949–956.

Al-Banna, N. A., Toguri, J. T., Kelly, M. E. M., & Lehmann, C. H. (2013). Leukocyte-endothelial interactions within the ocular microcirculation in inflammation and infection. *Clinical Hemorheology and Microcirculation*, *55*, 423–443.

Arevalo-Martin, A., Garcia-Ovejero, D., Sierra-Palomares, Y., Paniagua-Torija, B., Gonzalez-Gil, I., Ortega-Gutierrez, S., & Molina-Holgado, E. (2012). Early Endogenous Activation of CB1 and CB2 Receptors after Spinal Cord Injury Is a Protective Response Involved in Spontaneous Recovery. *PLoS ONE*, *7*(11), 1–12.

Ashton, J. C., & Glass, M. (2007). The cannabinoid CB2 receptor as a target for inflammation-dependent neurodegeneration. *Current Neuropharmacology*, *5*(2), 73–80.

Assadi, A., Desebbe, O., Rimmelé, T., Florence, A., Goudable, J., Chassard, D., & Allaouchiche, B. (2012). Small-volume hypertonic saline/pentastarch improves ileal mucosal microcirculation in experimental peritonitis. *Infectious Disease Reports*, *4*(22), 77–83.

Atwood, B. K., & MacKie, K. (2010). CB2: A cannabinoid receptor with an identity crisis. *British Journal of Pharmacology*, *160*(3), 467–479.

Baatz, H., Puchta, J., Reszka, R., & Pleyer, U. (2001). Macrophage depletion prevents leukocyte adhesion and disease induction in experimental melanin-protein induced uveitis. *Experimental Eye Research*, *73*(1), 101–109.

Baatz, H., Tonessen, B., Prada, J., & Pleyer, U. (2001). Thalidomide inhibits leukocyte-endothelium interaction in endotoxin-induced uveitis. *Ophthalmic Research*, *33*, 256–263.

Bagher, P., & Segal, S. S. (2011). Regulation of blood flow in the microcirculation: role of conducted vasodilation. *Acta Physiologica*, *202*, 271–284.

Barisani-Asenbauer, T., Maca, S. M., Mejdoubi, L., Emminger, W., Machold, K., & Auer, H. (2012). Uveitis- a rare disease often associated with systemic diseases and infections- a systematic review of 2619 patients. *Orphanet Journal of Rare Diseases*, *7*(1), 57–64.

Barreiro, O., Martín, P., González-Amaro, R., & Sánchez-Madrid, F. (2010). Molecular cues guiding inflammatory responses. *Cardiovascular Research*, *86*(2), 174–182.

Basu, S., & Dittel, B. N. (2011). Unraveling the complexities of cannabinoid receptor 2 (CB2) immune regulation in health and disease. *Immunologic Research*, *51*, 26–38.

Bátkai, S., Osei-Hyiaman, D., Pan, H., El-Assal, O., Rajesh, M., Mukhopadhyay, P., Hong, F., Harvey-White, J., Jafri, A., Haskó, G., Huffman, J. W., Gao, B., Kunos, G., & Pacher, P. (2007). Cannabinoid-2 receptor mediates protection against hepatic ischemia/reperfusion injury. *Federation of American Societies for Experimental Biology*, *21*(8), 1788–1800.

Begg, M., Baydoun, A., Parsons, M. E., & Molleman, A. (2001). Signal transduction of cannabinoid CB1 receptors in a smooth muscle cell line. *The Journal of Physiology*, *531*(1), 95–104.

Bennett, B. L., Sasaki, D. T., Murray, B. W., O'Leary, E. C., Sakata, S. T., Xu, W., Leisten, J. C., Motiwala, a, Pierce, S., Satoh, Y., Bhagwat, S. S., Manning, a M., & Anderson, D. W. (2001). SP600125, an anthrapyrazolone inhibitor of Jun N-terminal kinase. *Proceedings of the National Academy of Sciences of the United States of America*, *98*(24), 13681–13686.

Berdyshev, E. V. (2000). Cannabinoid receptors and the regulation of immune response. *Chemistry and Physics of Lipids*, *108*(1-2), 169–90.

Bharadwaj, A. S., Appukuttan, B., Wilmarth, P. a., Pan, Y., Stempel, A. J., Chipps, T. J., Benedetti, E. E., Zamora, D. O., Choi, D., David, L. L., & Smith, J. R. (2013). Role of the retinal vascular endothelial cell in ocular disease. *Progress in Retinal and Eye Research*, *32*(1), 102–180.

Bianchi, M. E. (2007). DAMPs, PAMPs and alarmins: all we need to know about danger. *Journal of Leukocyte Biology*, *81*(1), 1–5.

Blasius, A. L., & Beutler, B. (2010). Intracellular toll-like receptors. *Immunity*, *32*(3), 305–315.

Blázquez, C., Chiarlone, A., Sagredo, O., Aguado, T., Pazos, M. R., Resel, E., Palazuelos, J., Julien, B., Salazar, M., Börner, C., Benito, C., Carrasco, C., Diez-Zaera, M., Paoletti, P., Díaz-Hernández, M., Ruiz, C., Sendtner, M., Lucas, J. J., De Yébenes, J. G., Marsicano, G., Monory, K., Lutz, B., Romero, J., Alberch, J., Ginés, S., Kraus, J., Fernández-Ruiz, J., Galve-Roperh, I., & Guzmán, M. (2011). Loss of striatal type 1 cannabinoid receptors is a key pathogenic factor in Huntington's disease. *Brain*, *134*(1), 119–136.

Bodaghi, B., Cassoux, N., Wechsler, B., Hannouche, D., Fardeau, C., Papo, T., Huong, D. L., Piette, J. C., & LeHoang, P. (2001). Chronic severe uveitis: etiology and visual outcome in 927 patients from a single center. *Medicine*, *80*(4), 263–70.

Borish, L. C., & Steinke, J. W. (2003). Cytokines and chemokines. *The Journal of Allergy and Clinical Immunology*, *111*(2 Suppl), S460–S475.

Bosier, B., Muccioli, G. G., Hermans, E., & Lambert, D. M. (2010). Functionally selective cannabinoid receptor signalling: therapeutic implications and opportunities. *Biochemical Pharmacology*, *80*(1), 1–12.

Brito, B. E., Zamora, D. O., Bonnah, R. a., Pan, Y., Planck, S. R., & Rosenbaum, J. T. (2004). Toll-like receptor 4 and CD14 expression in human ciliary body and TLR-4 in human iris endothelial cells. *Experimental Eye Research*, *79*, 203–208.

Brown, A. J. (2007). Novel cannabinoid receptors. *British Journal of Pharmacology*, *152*(5), 567–75.

Buckley, N. E., McCoy, K. L., Mezey, E., Bonner, T., Zimmer, A., Felder, C. C., & Glass, M. (2000). Immunomodulation by cannabinoids is absent in mice deficient for the cannabinoid CB(2) receptor. *European Journal of Pharmacology*, *396*(2-3), 141–9.

Burston, J. J., & Woodhams, S. G. (2014). Endocannabinoid system and pain: an introduction. *The Proceedings of the Nutrition Society*, *73*, 106–117.

Buys, Y. M., & Rafuse, P. E. (2010). Canadian Ophthalmological Society policy statement on the medical use of marijuana for glaucoma. *Canadian Journal of Ophthalmology*, *45*(4), 324–326.

Cabral, G. A., & Griffin-Thomas, L. (2010). Emerging role of the CB2 cannabinoid receptor in immune regulation and therapeutic prospects. *Expert Reviews in Molecular Medicine*, *11*, 1–31.

Caldwell, C. C., Kasten, K. R., Tschöp, J., & Tschöp, M. H. (2010). The cannabinoid 2 receptor as a potential therapeutic target for sepsis. *Endocrine, Metabolic & Immune Disorders Drug Targets*, *10*, 224–234.

Carlisle, S. J., Marciano-Cabral, F., Staab, A., Ludwick, C., & Cabral, G. A. (2002). Differential expression of the CB2 cannabinoid receptor by rodent macrophages and macrophage-like cells in relation to cell activation. *International Immunopharmacology*, *2*, 69–82.

Casals-Casas, C., Álvarez, E., Serra, M., de la Torre, C., Farrera, C., Sánchez-Tilló, E., Caelles, C., Lloberas, J., & Celada, A. (2009). CREB and AP-1 activation regulates MKP-1 induction by LPS or M-CSF and their kinetics correlate with macrophage activation versus proliferation. *European Journal of Immunology*, *39*(7), 1902–1913.

Caspi, R. R. (2006). Animal models of autoimmune and immune-mediated uveitis. *Drug Discovery Today: Disease Models*, *3*(1), 3–9.

Caspi, R. R. (2010). A look at autoimmunity and inflammation in the eye. *Journal of Clinical Investigation*, *120*(9), 3073 – 3083.

Chamot, S. R., Movaffaghy, A. M., Petrig, B. L., & Riva, C. E. (1999). Blood flow in the human iris measured by laser Doppler flowmetry. *Microvascular Research*, *57*, 153–161.

Chang, J. H., McCluskey, P. J., & Wakefield, D. (2005). Acute anterior uveitis and HLA-B27. *Survey of Ophthalmology*, *50*(4), 364–388.

Chang, J. H., Mccluskey, P. J., & Wakefield, D. (2006). Toll-like receptors in ocular immunity and the immunopathogenesis of inflammatory eye disease. *British Journal of Ophthalmology*, *90*, 103–108.

Chang, J., & Wakefield, D. (2002). Uveitis: a global perspective. *Ocular Immunology and Inflammation*, *10*(4), 263–279.

Chen, J., Matias, I., Dinh, T., Lu, T., Venezia, S., Nieves, A., Woodward, D. F., & Di Marzo, V. (2005). Finding of endocannabinoids in human eye tissues: implications for glaucoma. *Biochemical and Biophysical Research Communications*, *330*(4), 1062–7.

Chen, P., Li, J., Barnes, J., Kokkonen, G. C., Lee, J. C., & Liu, Y. (2002). Restraint of proinflammatory cytokine biosynthesis by mitogen-activated protein kinase phosphatase-1 in lipopolysaccharide-stimulated macrophages. *Journal of Immunology*, *169*(11), 6408–6416.

Chen, W., Hu, X., Zhao, L., Li, S., & Lu, H. (2009). Expression of toll-like receptor 4 in uvea-resident tissue macrophages during endotoxin-induced uveitis. *Molecular Vision*, *15*, 619–628.

Chestnov, O. Universal eye health: a global action plan 2014-2019 (2013). Geneva, Switzerland.

Chiou, L. C., Hu, S. S. J., & Ho, Y. C. (2013). Targeting the cannabinoid system for pain relief? *Acta Anaesthesiologica Taiwanica*, *51*(4), 161–170.

Choi, I.-Y., Ju, C., Anthony Jalin, A. M. a, Lee, D. I., Prather, P. L., & Kim, W.-K. (2013). Activation of cannabinoid CB2 receptor-mediated AMPK/CREB pathway reduces cerebral ischemic injury. *The American Journal of Pathology*, *182*(3), 928–39.

Chopra, I., & Roberts, M. (2001). Tetracycline antibiotics: mode of action, applications, molecular biology, and epidemiology of bacterial resistance. *Microbiology and Molecular Biology Reviews*, *65*(2), 232–260.

Chu, D. S., Johnson, S. J., Mallya, U. G., Davis, M. R., Sorg, R. a, & Duh, M. S. (2013). Healthcare costs and utilization for privately insured patients treated for non-infectious uveitis in the USA. *Journal of Ophthalmic Inflammation and Infection*, *3*(1), 64.

Cravatt, B. F., Giang, D. K., Mayfield, S. P., Boger, D. L., Lerner, R. a, & Gilula, N. B. (1996). Molecular characterization of an enzyme that degrades neuromodulatory fatty-acid amides. *Nature*, *384*, 83–87.

Csoka, B., Nemeth, Z. H., Mukhopadhyay, P., Spolarics, Z., Rajesh, M., Federici, S., Deitch, E. A., Batkai, S., Pacher, P., & Hasko, G. (2009). CB2 cannabinoid receptors contribute to bacterial invasion and mortality in polymicrobial sepsis. *PLoS ONE*, *4*(7), e6409.

Cunningham, K. S., & Gotlieb, A. I. (2005). The role of shear stress in the pathogenesis of atherosclerosis. *Laboratory Investigation*, *85*, 9–23.

Dannert, M. T., Alsasua, A., Herradon, E., Martín, M. I., & López-Miranda, V. (2007). Vasorelaxant effect of Win 55,212-2 in rat aorta: new mechanisms involved. *Vascular Pharmacology*, *46*(1), 16–23.

De Backer, D., Donadello, K., Sakr, Y., Ospina-Tascon, G., Salgado, D., Scolletta, S., & Vincent, J.-L. (2013). Microcirculatory Alterations in Patients With Severe Sepsis. *Critical Care Medicine*, *41*(3), 791–799.

De Filippo, K., Dudeck, A., Hasenberg, M., Nye, E., van Rooijen, N., Hartmann, K., Gunzer, M., Roers, A., & Hogg, N. (2013). Mast cell and macrophage chemokines CXCL1/CXCL2 control the early stage of neutrophil recruitment during tissue inflammation. *Blood*, *121*(24), 1–38.

Dellinger, R. P., Levy, M. M., Rhodes, A., Annane, D., Gerlach, H., Opal, S. M., Sevransky, J. E., Sprung, C. L., Douglas, I. S., Jaeschke, R., Osborn, T. M., Nunnally, M. E., Townsend, S. R., Reinhart, K., Kleinpell, R. M., Angus, D. C., Deutschman, C. S., Machado, F. R., Rubenfeld, G. D., Webb, S., Beale, R. J., Vincent, J.-L., & Moreno, R. (2013). Surviving Sepsis Campaign: international guidelines for management of severe sepsis and septic shock, 2012. *Intensive Care Medicine*, *39*(2), 165–228.

Devane, W. a, Hanus, L., Breuer, A., Pertwee, R. G., Stevenson, L. a, Griffin, G., Gibson, D., Mandelbaum, A., Etinger, A., & Mechoulam, R. (1992). Isolation and structure of a brain constituent that binds to the cannabinoid receptor. *Science*, *258*(5090), 1946–1949.

Devane, W. A., Dysarz 3rd, F. A., Johnson, M. R., Melvin, L. S., & Howlett, A. C. (1988). Determination and characterization of a cannabinoid receptor in rat brain. *Molecular Pharmacology*, *34*(5), 605–613.

Di Marzo, V., Melck, D., De Petrocellis, L., & Bisogno, T. (2000). Cannabimimetic fatty acid derivatives in cancer and inflammation. *Prostaglandins & Other Lipid Mediators*, *61*(1-2), 43–61.

Diana, M. A., Levenes, C., Mackie, K., & Marty, A. (2002). Short-term retrograde inhibition of GABAergic synaptic currents in rat Purkinje cells is mediated by endogenous cannabinoids. *The Journal of Neuroscience*, *22*(1), 200–208.

Dick, A. D. (2000). Immune mechanisms of uveitis: insights into disease pathogenesis and treatment. *International Ophthalmology Clinics*, *40*(2), 1–18.

Díez-Dacal, B., & Pérez-Sala, D. (2010). Anti-inflammatory prostanoids: focus on the interactions between electrophile signaling and resolution of inflammation. *The Scientific World Journal*, *10*, 655–675.

Do, Y., McKallip, R. J., Nagarkatti, M., & Nagarkatti, P. S. (2004). Activation through cannabinoid receptors 1 and 2 on dendritic cells triggers NF-kappaB-dependent apoptosis: novel role for endogenous and exogenous cannabinoids in immunoregulation. *Journal of Immunology*, *173*(4), 2373–2382.

Dong, C., Davis, R. J., & Flavell, R. A. (2002). MAP kinases in the immune response. *Annual Review of Immunology*, *20*, 55–72.

Drancourt, M., Berger, P., Terrada, C., Bodaghi, B., Conrath, J., Raoult, D., & LeHoang, P. (2008). High prevalence of fastidious bacteria in 1520 cases of uveitis of unknown etiology. *Medicine*, *87*(3), 167–76.

Dyson, A., & Singer, M. (2009). Animal models of sepsis: why does preclinical efficacy fail to translate to the clinical setting? *Critical Care Medicine*, *37*(1 Suppl), S30–37.

Eljaschewitsch, E., Witting, A., Mawrin, C., Lee, T., Schmidt, P. M., Wolf, S., Hoertnagl, H., Raine, C. S., Schneider-Stock, R., Nitsch, R., & Ullrich, O. (2006). The endocannabinoid anandamide protects neurons during CNS inflammation by induction of MKP-1 in microglial cells. *Neuron*, *49*(1), 67–79.

El-Remessy, A. B., Behzadian, M. A., Abou-Mohamed, G., Franklin, T., Caldwell, R. W., & Caldwell, R. B. (2003). Experimental diabetes causes breakdown of the blood-retina barrier by a mechanism involving tyrosine nitration and increases in expression of vascular endothelial growth factor and urokinase plasminogen activator receptor. *The American Journal of Pathology*, *162*(6), 1995–2004.

El-Remessy, A. B., Rajesh, M., Mukhopadhyay, P., Horváth, B., Patel, V., Al-Gayyar, M. M. H., Pillai, B. A., & Pacher, P. (2011). Cannabinoid 1 receptor activation contributes to vascular inflammation and cell death in a mouse model of diabetic retinopathy and a human retinal cell line. *Diabetologia*, *54*(6), 1567–1578.

Enigk, F., Wagner, A., Samapati, R., Rittner, H., Brack, A., Mousa, S. A., Schäfer, M., Habazettl, H., & Schäper, J. (2014). Thoracic epidural anesthesia decreases endotoxin-induced endothelial injury. *BMC Anesthesiology*, *14*, 23.

Eter, N., Engel, D. R., Meyer, L., Helb, H. M., Roth, F., Maurer, J., Holz, F. G., & Kurts, C. (2008). In vivo visualization of dendritic cells, macrophages, and microglial cells responding to laser-induced damage in the fundus of the eye. *Investigative Ophthalmology and Visual Science*, *49*(8), 3649–3658.

Facchinetti, F., Del Giudice, E., Furegato, S., Passarotto, M., & Leon, A. (2003). Cannabinoids ablate release of TNFalpha in rat microglial cells stimulated with lypopolysaccharide. *Glia*, *41*(2), 161–168.

Fan, J., Kapus, A., Marsden, P. A., Li, Y. H., Oreopoulos, G., Marshall, J. C., Frantz, S., Kelly, R. a, Medzhitov, R., & Rotstein, O. D. (2002). Regulation of Toll-like receptor 4 expression in the lung following

hemorrhagic shock and lipopolysaccharide. *Journal of Immunology*, *168*(10), 5252–5259.

Faubert, B. L., & Kaminski, N. E. (2000). AP-1 activity is negatively regulated by cannabinol through inhibition of its protein components , c-fos and c-jun. *Journal of Leukocyte Biology*, *67*, 259–266.

Faubert Kaplan, B. L., & Kaminski, N. E. (2003). Cannabinoids inhibit the activation of ERK MAPK in PMA/Io-stimulated mouse splenocytes. *International Immunopharmacology*, *3*(10-11), 1503–1510.

Fernández-López, D., Faustino, J., Derugin, N., Wendland, M., Lizasoain, I., Moro, M. A., & Vexler, Z. S. (2012). Reduced infarc size and accumulation of microglia in rats treated with WIN 55,212-2 after neonatal stroke. *Neuroscience*, *207*, 307–315.

Fiorelli, V. M. B., Bhat, P., & Foster, C. S. (2010). Nonsteroidal anti-inflammatory therapy and recurrent acute anterior uveitis. *Ocular Immunology and Inflammation*, *18*(2), 116–120.

Fitzgerald, K. A., Rowe, D. C., Barnes, B. J., Caffrey, D. R., Visintin, A., Latz, E., Monks, B., Pitha, P. M., & Golenbock, D. T. (2003). LPS-TLR4 signaling to IRF-3/7 and NF-kappaB involves the toll adapters TRAM and TRIF. *The Journal of Experimental Medicine*, *198*(7), 1043–1055.

Fowler, C. J. (2013). Transport of endocannabinoids across the plasma membrane and within the cell. *Federation of European Biochemical Societies Journal*, *280*(9), 1895–1904.

Frith, J. C., Monkkonen, J., Auriola, S., Monkkonen, H., & Rogers, M. J. (2001). The Molecular Mechanism of Action of the Antiresorptive and Antiinflammatory Drug Clodronate: Evidence for the Formation In Vivo of a Metabolite That Inhibits Bone. *Arthritis and Rheumatism*, *44*(9), 2201–2210.

Fritz, G. (2011). RAGE: A single receptor fits multiple ligands. *Trends in Biochemical Sciences*, *36*(12), 625–632.

Fujita, T. (2002). Evolution of the lectin-complement pathway and its role in innate immunity. *Nature Reviews. Immunology*, *2*(5), 346–353.

Galiègue, S., Mary, S., Marchand, J., Dussossoy, D., Carrière, D., Carayon, P., Bouaboula, M., Shire, D., Le Fur, G., & Casellas, P. (1995a). Expression of central and peripheral cannabinoid receptors in human immune tissues and leukocyte subpopulations. *European Journal of Biochemistry*, *232*(1), 54–61.

Galiègue, S., Mary, S., Marchand, J., Dussossoy, D., Carrière, D., Carayon, P., Bouaboula, M., Shire, D., Le Fur, G., & Casellas, P. (1995b). Expression of central and peripheral cannabinoid receptors in human immune tissues and leukocyte subpopulations. *European Journal of Biochemistry*, *232*(1), 54–61.

Gaoni, Y., & Mechoulam, R. (1964). Isolation, structure, and partial synthesis of an active constituent of hashish. *Journal of the American Chemical Society*, *86*, 1646–1647.

Ghannoum, M. A., & Rice, L. B. (1999). Antifungal agents: mode of action, mechanisms of resistance, and correlation of these mechanisms with bacterial resistance. *Clinical Microbiology Reviews*, *12*(4), 501–517.

Gill, E. A., Imaizumi, T., Carveth, H., Topham, M. K., Tarbet, E. B., McIntyre, T. M., Prescott, S. M., & Zimmerman, G. a. (1998). Bacterial lipopolysaccharide induces endothelial cells to synthesize a degranulating factor for neutrophils. *The FASEB Journal*, *12*(9), 673–684.

Ginhoux, F., & Jung, S. (2014). Monocytes and macrophages: developmental pathways and tissue homeostasis. *Nature Reviews. Immunology*, *14*(6), 392–404.

Gómez-Gálvez, Y., Palomo-Garo, C., Fernández-Ruiz, J., & García, C. (2015). Potential of the cannabinoid CB2 receptor as a pharmacological target against inflammation in Parkinson's disease. *Progress in Neuro-Psychopharmacology and Biological Psychiatry*, 1–9.

Gonsiorek, W., Lunn, C., Fan, X., Narula, S., Lundell, D., & Hipkin, R. W. (2000). Endocannabinoid 2-arachidonyl glycerol is a full agonist through human type 2 cannabinoid receptor: antagonism by anandamide. *Molecular Pharmacology*, *57*(5), 1045–1050.

González-navajas, J. M., Fine, S., Law, J., Datta, S. K., Nguyen, K. P., Yu, M., Corr, M., Katakura, K., Eckman, L., Lee, J., & Raz, E. (2010). TLR4

signaling in effector CD4 + T cells regulates TCR activation and experimental colitis in mice. *The Journal of Clinical Investigation*, *120*(2), 570–581.

Greineisen, W. E., & Turner, H. (2010). Greineisen and Turner. *International Immunopharmacology*, *10*(5), 547–55. Retrieved from http://www.ncbi.nlm.nih.gov/pubmed/20219697

Griffith, J. W., Sokol, C. L., & Luster, A. D. (2014). Chemokines and chemokine receptors: positioning cells for host defense and immunity. *Annual Review of Immunology*, *32*, 659–702.

Grötzinger, J. (2002). Molecular mechanisms of cytokine receptor activation. *Biochimica et Biophysica Acta*, *1592*(3), 215–223.

Gui, H., Sun, Y., Luo, Z., Su, D., Dai, S., & Liu, X. (2013). Cannabinoid Receptor 2 Protects against Acute Experimental Sepsis in Mice. *Mediators of Inflammation*, 1–10.

Guzik, T. J., & Korbut, R. (2003). Nitric oxide and superoxide in inflammation and immune regulation. *Journal of Physiology and Pharmacology*, *54*(4), 469–487.

Hajishengallis, G., & Chavakis, T. (2013). Endogenous modulators of inflammatory cell recruitment. *Trends in Immunology*, *34*(1), 1–6.

Hambleton, J., Weinstein, S. L., Lem, L., & DeFranco, A. L. (1996). Activation of c-Jun N-terminal kinase in bacterial lipopolysaccharide-stimulated macrophages. *Proceedings of the National Academy of Sciences of the United States of America*, *93*, 2774–2778.

Hambleton, J., Weinsteint, S. L., Lemt, L., Defrancots, A. L., & Bishop, J. M. (1996). lipopolysaccharide-stimulated Activation of c-Jun N-terminal kinase in bacterial lipopolysaccharide-stimulated macrophages. *Proceedings of the National Academy of Sciences of the United States of America*, *93*, 2774–2778.

Hamrah, P., Huq, S. O., Liu, Y., Zhang, Q., & Dana, M. R. (2003). Corneal immunity is mediated by heterogeneous population of antigen-presenting cells. *Journal of Leukocyte Biology*, *74*(2), 172–178.

Hanus, L., Breuer, A., Tchilibon, S., Shiloah, S., Goldenberg, D., Horowitz, M., Pertwee, R. G., Ross, R. a, Mechoulam, R., & Fride, E. (1999). HU-308: a specific agonist for CB(2), a peripheral cannabinoid receptor. *Proceedings of the National Academy of Sciences of the United States of America*, *96*(25), 14228–14233.

Hart, D. N. (1997). Dendritic cells: unique leukocyte populations which control the primary immune response. *Blood*, *90*(9), 3245–87.

Henstridge, C. M., Balenga, N. A. B., Ford, L. A., Ross, R. A., Waldhoer, M., & Irving, A. J. (2009). The GPR55 ligand L-alpha-lysophosphatidylinositol promotes RhoA-dependent Ca2+ signaling and NFAT activation. *Federation of American Societies for Experimental Biology*, *23*(1), 183–193.

Heo, J., Sepah, Y. J., Yohannan, J., Renner, M., Akhtar, A., Gregory, A., Shulman, M., & Do, D. V. (2012). The role of biologic agents in the management of non-infectious uveitis. *Expert Opinion on Biological Therapy*, *12*(8), 995–1008.

Hétu, S., Pouliot, M., Cordahi, G., Couture, R., & Vaucher, E. (2013). Assessment of retinal and choroidal blood flow changes using laser Doppler flowmetry in rats. *Current Eye Researc*, *38*(1), 158–167.

Hill, T., Galatowicz, G., Akerele, T., Lau, C. H., Calder, V., & Lightman, S. (2005). Intracellular T lymphocyte cytokine profiles in the aqueous humour of patients with uveitis and correlation with clinical phenotype. *Clinical and Experimental Immunology*, *139*(1), 132–137.

Hillard, C. J. (2000). Biochemistry and pharmacology of the endocannabinoids arachidonylethanolamide and 2-arachidonylglycerol. *Prostaglandins and Other Lipid Mediators*, *61*(1-2), 3–18.

Hiltebrand, L. B., Krejci, V., Banic, A., Erni, D., Wheatley, A. M., & Sigurdsson, G. H. (2000). Dynamic study of the distribution of microcirculatory blood flow in multiple splanchnic organs in septic shock. *Critical Care Medicine*, *28*(9), 3233–3241.

Holling, T. M., Schooten, E., & Van Den Elsen, P. J. (2004). Function and regulation of MHC class II molecules in T-lymphocytes: Of mice and men. *Human Immunology*, *65*(4), 282–290.

Hou, B., Reizis, B., & DeFranco, A. L. (2008). Toll-like receptor-mediated dendritic cell-dependent and - independent Stimulation of Innate and Adaptive Immunity. *Immunity*, *29*(2), 272–282.

Howlett, A. C., & Mukhopadhyay, S. (2000). Cellular signal transduction by anandamide and 2-arachidonoylglycerol. *Chemistry and Physics of Lipids*, *108*(1-2), 53–70.

Hu, Y.-W., Yang, J.-Y., Ma, X., Chen, Z.-P., Hu, Y.-R., Zhao, J.-Y., Li, S.-F., Qiu, Y.-R., Lu, J.-B., Wang, Y.-C., Gao, J.-J., Sha, Y.-H., Zheng, L., & Wang, Q. (2014). A lincRNA-DYNLRB2-2/GPR119/GLP-1R/ABCA1-dependent signal transduction pathway is essential for the regulation of cholesterol homeostasis. *Journal of Lipid Research*, *55*(4), 681–697.

Iba, T., Miki, T., Hashiguchi, N., Yamada, A., & Nagaoka, I. (2014). Combination of antithrombin and recombinant thrombomodulin attenuates leukocyte-endothelial interaction and suppresses the increase of intrinsic damage-associated molecular patterns in endotoxemic rats. *Journal of Surgical Research*, *187*(2), 581–586.

Ince, C. (2005). The microcirculation is the motor of sepsis. *Critical Care*, *9 Suppl 4*, S13–19.

Iwamura, H., Suzuki, H., Ueda, Y., Kaya, T., & Inaba, T. (2001). In vitro and in vivo pharmacological characterization of JTE-907, a novel selective ligand for cannabinoid CB2 receptor. *Journal of Pharmacology and Experimental Therapeutics*, *296*(2), 420–425.

Jeong, D., Lee, J., Yi, Y. S., Yang, Y., Kim, K. W., & Cho, J. Y. (2013). P38/AP-1 pathway in lipopolysaccharide-induced inflammatory responses is negatively modulated by electrical stimulation. *Mediators of Inflammation*, *2013*, 1–11.

Johns, D. G., Behm, D. J., Walker, D. J., Ao, Z., Shapland, E. M., Daniels, D. A., Riddick, M., Dowell, S., Staton, P. C., Green, P., Shabon, U., Bao, W., Aiyar, N., Yue, T.-L., Brown, A. J., Morrison, A. D., & Douglas, S. A. (2007). The novel endocannabinoid receptor GPR55 is activated by atypical cannabinoids but does not mediate their vasodilator effects. *British Journal of Pharmacology*, *152*(5), 825–831.

Kadoi, Y., Hinohara, H., Kunimoto, F., Kuwano, H., Saito, S., & Goto, F. (2005). Effects of AM281, a cannabinoid antagonist, on systemic haemodynamics, internal carotid artery blood flow and mortality in septic shock in rats. *British Journal of Anaesthesia*, *94*(5), 563–568.

Kaminski, N. E. (1998). Inhibition of the cAMP signaling cascade via cannabinoid receptors: a putative mechanism of immune modulation by cannabinoid compounds. *Toxicology Letters*, *102-103*, 59–63.

Kanai, K., Ito, Y., Nagai, N., Itoh, N., Hori, Y., Chikazawa, S., Hoshi, F., & Higuchi, S. (2012). Effects of instillation of eyedrops containing disulfiram and hydroxypropyl-β-cyclodextrin inclusion complex on endotoxin-induced uveitis in rats. *Current Eye Research*, *37*(2), 124–131.

Karin, M. (1995). The regulation of AP-1 activity by Mitogen-activated Protein Kinases. *The American Society for Biochemistry and Molecular Biology*, *270*(28), 16483–16486.

Karin, M. (1999). How NF-kB is activated : the role of the IkB kinase (IKK) complex. *Oncogene*, *18*, 6867–6874.

Karin, M., Liu, Z. G., & Zandi, E. (1997). AP-1 function and regulation. *Current Opinion in Cell Biology*, *9*, 240–246.

Kasuga, K., Suga, T., & Mano, N. (2015). Bioanalytical insights into mediator lipidomics. *Journal of Pharmaceutical and Biomedical Analysis*, 1–12.

Kawai, T., & Akira, S. (2010). The role of pattern-recognition receptors in innate immunity: update on Toll-like receptors. *Nature Immunology*, *11*(5), 373–384.

Kezic, J., & McMenamin, P. G. (2008). Differential turnover rates of monocyte-derived cells in varied ocular tissue microenvironments. *Journal of Leukocyte Biology*, *84*(3), 721–729.

Kezic, J., Taylor, S., Gupta, S., Planck, S. R., Rosenzweig, H. L., & Rosenbaum, J. T. (2011). Endotoxin-induced uveitis is primarily dependent on radiation-resistant cells and on MyD88 but not TRIF. *Journal of Leukocyte Biology*, *90*, 305–311.

Kianian, M., Kelly, M. E. M., Zhou, J., Hung, O., Cerny, V., Rowden, G., & Lehmann, C. (2013). Cannabinoid receptor 1 inhibition improves the intestinal microcirculation. *Clinical Hemorheology and Microcirculation*, *58*(2), 33–342.

Klijn, E., Den Uil, C. A., Bakker, J., & Ince, C. (2008). The heterogeneity of the microcirculation in critical illness. *Clinics in Chest Medicine*, *29*(4), 643–654.

König, S., Nitzki, F., Uhmann, A., Dittmann, K., Theiss-Suennemann, J., Herrmann, M., Reichardt, H. M., Schwendener, R., Pukrop, T., Schulz-Schaeffer, W., & Hahn, H. (2014). Depletion of cutaneous macrophages and dendritic cells promotes growth of basal cell carcinoma in mice. *PLoS ONE*, *9*(4), 1–8.

Krakauer, T. (2002). Stimulant-Dependent Modulation of Cytokines and Chemokines by Airway Epithelial Cells : Cross Talk between Pulmonary Epithelial and Peripheral Blood Mononuclear Cells. *Clinical and Diagnostic Laboratory Immunology*, *9*(1), 126–131.

Krishnan, G., & Chatterjee, N. (2012). Endocannabinoids Alleviate Proinflammatory Conditions by Modulating Innate Immune Response in Muller Glia During Inflammation. *Glia*, (60), 1629–1645.

Krustev, E., Reid, A., & McDougall, J. J. (2014). Tapping into the endocannabinoid system to ameliorate acute inflammatory flares and associated pain in mouse knee joints. *Arthritis Research & Therapy*, *16*(437), 1–12.

Kumamaru, H., Saiwai, H., Kobayakawa, K., Kubota, K., van Rooijen, N., Inoue, K., Iwamoto, Y., & Okada, S. (2012). Liposomal clodronate selectively eliminates microglia from primary astrocyte cultures. *Journal of Neuroinflammation*, *9*(116), 1–16.

Kumar, V., & Sharma, A. (2010). Neutrophils: Cinderella of innate immune system. *International Immunopharmacology*, *10*(11), 1325–1334.

Kyriakis, J. M., & Avruch, J. (2001). Mammalian mitogen-activated protein kinase signal transduction pathways activated by stress and inflammation. *Physiological Reviews*, *81*(2), 807–869.

Laaris, N., Good, C. H., & Lupica, C. R. (2010). Neuropharmacology D 9 - tetrahydrocannabinol is a full agonist at CB1 receptors on GABA neuron axon terminals in the hippocampus. *Neuropharmacology*, *59*(1-2), 121–127.

Lambert, D. M., & Fowler, C. J. (2005). The endocannabinoid system: drug targets, lead compounds, and potential therapeutic applications. *American Chemical Society*, *48*(16), 5059–5087.

Laprairie, R. B., Kelly, M. E. M., & Denovan-Wright, E. M. (2013). Cannabinoids increase type 1 cannabinoid receptor expression in a cell culture model of striatal neurons: Implications for Huntington's disease. *Neuropharmacology*, *72*, 47–57.

Laprairie, R. B., Warford, J. R., Hutchings, S., Robertson, G. S., Kelly, M. E. M., & Denovan-Wright, E. M. (2014). The cytokine and endocannabinoid systems are co-regulated by NF-κB p65/RelA in cell culture and transgenic mouse models of Huntington's disease and in striatal tissue from Huntington's disease patients. *Journal of Neuroimmunology*, *267*(1-2), 61–72.

Larsen, G. L., & Henson, P. M. (1983). Mediators of inflammation. *Annual Review of Immunology*, *1*(85), 335–359.

Larson, T., Nussenblatt, R. B., & Sen, H. N. (2011). Emerging drugs for uveitis. *Expert Opinion on Emerging Drugs*, *16*(2), 309–322.

Lawrence, T., Willoughby, D. a, & Gilroy, D. W. (2002). Anti-inflammatory lipid mediators and insights into the resolution of inflammation. *Nature Reviews. Immunology*, *2*(10), 787–795.

Lehenkari, P. P., Kellinsalmi, M., Napankangas, J. P., Ylitalo, K. V, Mönkkönen, J., Rogers, M. J., Azhayev, A., Vaananen, H. K., & Hassinen, I. E. (2002). Further Insight into Mechanism of Action of Clodronate : Inhibition of Mitochondrial ADP / ATP Translocase by a Nonhydrolyzable, Adenine-Containing Metabolite. *Molecular Pharmacology*, *62*(5), 1255–1262.

Lehmann, C., Kianian, M., Zhou, J., Kuster, I., Kuschnereit, R., Whynot, S., Hung, O., Shukla, R., Johnston, B., Cerny, V., Pavlovic, D., Spassov, A., & Kelly, M. E. M. (2012). Cannabinoid receptor 2 activation reduces

intestinal leukocyte recruitment and systemic inflammatory mediator release in acute experimental sepsis. *Critical Care*, *16*(2), R47.

Lehmann, C., Sharawi, N., Al-Banna, N., Corbett, N., Kuethe, J. W., & Caldwell, C. C. (2014). Novel approaches to the development of anti-sepsis drugs. *Expert Opinion on Drug Discovery*, *9*(5), 1–9.

Lehoang, P. (2012). The Gold Standard of Noninfectious Uveitis: Corticosteroids. *Developments in Ophthalmology*, *51*, 7–28.

LeHoang, P. (2012). The Gold Standard of Noninfectious Uveitis: Corticosteroids. *Developments in Ophthalmology*, *51*, 7–28.

Levy, M. M., Fink, M. P., Marshall, J. C., Abraham, E., Angus, D., Cook, D., Cohen, J., Opal, S. M., Vincent, J.-L., & Ramsay, G. (2003). 2001 SCCM/ESICM/ACCP/ATS/SIS International Sepsis Definitions Conference. *Critical Care Medicine*, *31*(4), 1250–1256.

Li, N., Hu, H., Lindqvist, M., Wikström-Jonsson, E., Goodall, a H., & Hjemdahl, P. (2000). Platelet-leukocyte cross talk in whole blood. *Arteriosclerosis, Thrombosis, and Vascular Biology*, *20*, 2702–2708.

Li, Q., Peng, B., Whitcup, S. M., Jang, S. U., & Chan, C. C. (1995). Endotoxin induced uveitis in the mouse: susceptibility and genetic control. *Experimental Eye Research*, *61*(5), 629–632.

Li, S., Li, B., Jiang, H., Wang, Y., Qu, M., Duan, H., Zhou, Q., & Shi, W. (2013). Macrophage depletion impairs corneal wound healing after autologous transplantation in mice. *PloS one*, *8*(4), e61799.

Li, S., Lu, H., Hu, X., Chen, W., Xu, Y., & Wang, J. (2010). Expression of TLR4-MyD88 and NF-κB in the iris during endotoxin-induced uveitis. *Mediators of Inflammation*, *2010*, 1–7.

Li, X., Tupper, J. C., Bannerman, D. D., Winn, R. K., Rhodes, C. J., & Harlan, J. M. (2003). Phosphoinositide 3 kinase mediates Toll-like receptor 4-induced activation of NF-κB in endothelial cells. *Infection and Immunity*, *71*(8), 4414–4420.

Li, Y.-Y., Li, Y.-N., Ni, J.-B., Chen, C.-J., Lv, S., Chai, S.-Y., Wu, R.-H., Yüce, B., & Storr, M. (2010). Involvement of cannabinoid-1 and cannabinoid-2

receptors in septic ileus. *Neurogastroenterology and Motility*, *22*(3), 350–358.

Ligresti, A., Petrosino, S., & Marzo, V. Di. (2009). From endocannabinoid profiling to endocannabinoid therapeutics. *Current Opinion in Chemical Biology*, *13*, 321–331.

Liu, J., Bátkai, S., Pacher, P., Harvey-White, J., Wagner, J. A., Cravatt, B. F., Gao, B., & Kunos, G. (2003). Lipopolysaccharide Induces Anandamide Synthesis in Macrophages via CD14/MAPK/Phosphoinositide 3-Kinase/NF-κB Independently of Platelet-activating Factor. *Journal of Biological Chemistry*, *278*(45), 45034–45039.

Liu, J., Gao, B., Mirshahi, F., Sanyal, A. J., Khanolkar, A. D., Makriyannis, A., & Kunos, G. (2000). Functional CB1 cannabinoid receptors in human vascular endothelial cells. *The Biochemical Journal*, *346*, 835–840.

Liu, N., Liu, J.-T., Ji, Y.-Y., & Lu, P.-P. (2010). C-reactive protein triggers inflammatory responses partly via TLR4/IRF3/NF-κB signaling pathway in rat vascular smooth muscle cells. *Life Sciences*, *87*, 367–374.

Liu, Q.-R., Pan, C.-H., Hishimoto, A., Li, C.-Y., Xi, Z.-X., Llorente-Berzal, A., Viveros, M.-P., Ishiguro, H., Arinami, T., Onaivi, E. S., & Uhl, G. R. (2009). Species differences in cannabinoid receptor 2 (CNR2 gene): identification of novel human and rodent CB2 isoforms, differential tissue expression and regulation by cannabinoid receptor ligands. *Genes, Brain, and Behavior*, *8*(5), 519–530.

Liu, Y. J., Fan, H. B., Jin, Y., Ren, C. G., Jia, X. E., Wang, L., Chen, Y., Dong, M., Zhu, K. Y., Dong, Z. W., Ye, B. X., Zhong, Z., Deng, M., Liu, T. X., & Ren, R. (2013). Cannabinoid receptor 2 suppresses leukocyte inflammatory migration by modulating the JNK/c-Jun/Alox5 pathway. *Journal of Biological Chemistry*, *288*(19), 13551–13562.

Liu, Z., Wang, Y., Zhao, H., Zheng, Q., Xiao, L., & Zhao, M. (2014). CB2 receptor activation ameliorates the proinflammatory activity in acute lung injury induced by paraquat. *BioMed Research International*, *2014*(36).

London, A., Benhar, I., & Schwartz, M. (2013). The retina as a window to the brain-from eye research to CNS disorders. *Nature Reviews. Neurology*, *9*(1), 44–53.

Lu, Y.-C., Yeh, W.-C., & Ohashi, P. S. (2008). LPS/TLR4 signal transduction pathway. *Cytokine*, *42*(2), 145–151.

Maccarrone, M., Bari, M., Battista, N., & Finazzi-Agrò, A. (2002). Endocannabinoid degradation, endotoxic shock and inflammation. *Current Drug Targets. Inflammation and Allergy*, *1*(1), 53–63.

Macintyre, J., Dong, A., Straiker, A., Zhu, J., Howlett, S. E., Bagher, A., Denovan-Wright, E., Yu, D. Y., & Kelly, M. E. M. (2014). Cannabinoid and lipid-mediated vasorelaxation in retinal microvasculature. *European Journal of Pharmacology*, *735*(1), 105–114.

Malhotra, A., Minja, F. J., Crum, A., & Burrowes, D. (2011). Ocular Anatomy and Cross-Sectional Imaging of the Eye. *Seminars in Ultrasound, CT and MRI*, *32*(1), 2–13.

Mangmool, S., & Kurose, H. (2011). Gi/o protein-dependent and -independent actions of pertussis toxin (ptx). *Toxins*, *3*(7), 884–899.

Maresz, K., Carrier, E. J., Ponomarev, E. D., Hillard, C. J., & Dittel, B. N. (2005). Modulation of the cannabinoid CB2 receptor in microglial cells in response to inflammatory stimuli. *Journal of Neurochemistry*, *95*(2), 437–445.

Marini, P., Cascio, M. G., King, A., Pertwee, R. G., & Ross, R. A. (2013). Characterization of cannabinoid receptor ligands in tissues natively expressing cannabinoid CB2 receptors. *British Journal of Pharmacology*, *169*(4), 887–899.

Markomichelakis, N. N., Halkiadakis, I., Pantelia, E., Peponis, V., Patelis, A., Theodossiadis, P., & Theodossiadis, G. (2004). Patterns of macular edema in patients with uveitis: Qualitative and quantitative assessment using optical coherence tomography. *Ophthalmology*, *111*(5), 946–953.

Matias, I., Pochard, P., Orlando, P., Salzet, M., Pestel, J., & Di Marzo, V. (2002). Presence and regulation of the endocannabinoid system in human dendritic cells. *European Journal of Biochemistry*, *269*(15), 3771–3778.

Matias, I., Wang, J. W., Moriello, A. S., Nieves, A., Woodward, D. F., & Di Marzo, V. (2006). Changes in endocannabinoid and palmitoylethanolamide levels in eye tissues of patients with diabetic

retinopathy and age-related macular degeneration. *Prostaglandins Leukotrienes and Essential Fatty Acids*, *75*(6), 413–418.

Matsuda, L. A., Lolait, S. J., Brownstein, M. J., Young, A. C., & Bonner, T. I. (1990). Structure of a cannabinoid receptor and functional expression of the cloned cDNA. *Nature*, *346*(6284), 561–564.

McDougall, J. J., Yu, V., & Thomson, J. (2008). In vivo effects of CB2 receptor-selective cannabinoids on the vasculature of normal and arthritic rat knee joints. *British Journal of Pharmacology*, *153*(2), 358–66.

McHugh, D., Hu, S. S. J., Rimmerman, N., Juknat, A., Vogel, Z., Walker, J. M., & Bradshaw, H. B. (2010a). N-arachidonoyl glycine, an abundant endogenous lipid, potently drives directed cellular migration through GPR18, the putative abnormal cannabidiol receptor. *BMC Neuroscience*, *11*, 44.

McHugh, D., Hu, S. S. J., Rimmerman, N., Juknat, A., Vogel, Z., Walker, J. M., & Bradshaw, H. B. (2010b). N-arachidonoyl glycine, an abundant endogenous lipid, potently drives directed cellular migration through GPR18, the putative abnormal cannabidiol receptor. *BMC Neuroscience*, *11*, 44.

McHugh, D., & Ross, R. A. (2009). Endogenous cannabinoids and neutrophil chemotaxis. *Vitamins and Hormones*, *81*, 337–365.

McHugh, D., Tanner, C., Mechoulam, R., Pertwee, R. G., & Ross, R. A. (2008). Inhibition of Human Neutrophil Chemotaxis by Endogenous Cannabinoids and Phytocannabinoids : Evidence for a Site Distinct from CB 1 and CB 2. *Molecular Pharmacology*, *73*(2), 441–450.

McIntosh, B. T., Hudson, B., Yegorova, S., Jollimore, C. A. B., & Kelly, M. E. M. (2007). Agonist-dependent cannabinoid receptor signalling in human trabecular meshwork cells. *British Journal of Pharmacology*, *152*(7), 1111–1120.

McMenamin, P. G. (1997). The distribution of immune cells in the uveal tract of the normal eye. *Eye*, *11*, 183–193.

McMenamin, P. G., & Crewe, J. (1995). Endotoxin-induced uveitis. Kinetics and phenotype of the inflammatory cell infiltrate and the response of the

resident tissue macrophages and dendritic cells in the iris and ciliary body. *Investigative Ophthalmology & Visual Science*, *36*(10), 1949–1959.

McMenamin, P. G., Crewe, J., Morrison, S., & Holt, P. G. (1994). Immunomorphologic studies of macrophages and MHC class II-positive dendritic cells in the iris and ciliary body of the rat, mouse, and human eye. *Investigative Ophthalmology & Visual Science*, *35*(8), 3234–3250.

Mechoulam, R., Ben-Shabat, S., Hanus, L., Gopher, A., Almog, S., Martin, B. R., Compton, D. R., Pertwee, R. G., Griffin, G., Bayewitch, M., Barg, J., & Vogel, Z. V. I. (1995). Identification of an endogenous 2-monoglyceride, present in canine gut, that binds to cannabinoid receptors. *Biochemical Pharmacology*, *50*(1), 83–90.

Medeiros, R., Bu, G., Figueiredo, P., Grumman, A., Menezes-de-lima, O., & Passos, G. F. (2008). Molecular Mechanisms of Topical Anti-Inflammatory Effects of Lipoxin A 4 in Endotoxin-Induced Uveitis. *Molecular Pharmacology*, *74*, 154–161.

Merighi, S., Gessi, S., Varani, K., Simioni, C., Fazzi, D., Mirandola, P., & Borea, P. A. (2012). Cannabinoid CB(2) receptors modulate ERK-1/2 kinase signalling and NO release in microglial cells stimulated with bacterial lipopolysaccharide. *British Journal of Pharmacology*, *165*(6), 1773–1788.

Merriam, F. V., Wang, Z., Guerios, S. D., & Bjorling, D. E. (2008). Cannabinoid receptor 2 is increased in acutely and chronically inflamed bladder of rats. *Neuroscience Letters*, *445*(1), 130–134.

Michelson, G., Groh, M., & Grundler, A. (1994). Regulation of ocular blood flow during increases of arterial blood pressure. *The British Journal of Ophthalmology*, *78*(6), 461–465.

Miller, A. M., & Stella, N. (2008). CB2 receptor-mediated migration of immune cells: it can go either way. *British Journal of Pharmacology*, *153*(2), 299–308.

Minutoli, L., Altavilla, D., Marini, H., Passaniti, M., Bitto, A., Seminara, P., Venuti, F. S., Famulari, C., Macrì, A., Versaci, A., & Squadrito, F. (2004). Protective effects of SP600125 a new inhibitor of c-jun N-terminal kinase

(JNK) and extracellular-regulated kinase (ERK1/2) in an experimental model of cerulein-induced pancreatitis. *Life Sciences*, *75*, 2853–2866.

Mochizuki, M., Sugita, S., & Kamoi, K. (2013). Immunological homeostasis of the eye. *Progress in Retinal and Eye Research*, *33*(1), 10–27.

Moore, A. R., & Willoughby, D. a. (1995). The role of cAMP regulation in controlling inflammation. *Clinical and Experimental Immunology*, *101*(3), 387–389.

Mukhopadhyay, S., Das, S., Williams, E. a., Moore, D., Jones, J. D., Zahm, D. S., Ndengele, M. M., Lechner, A. J., & Howlett, A. C. (2006). Lipopolysaccharide and cyclic AMP regulation of CB2 cannabinoid receptor levels in rat brain and mouse RAW 264.7 macrophages. *Journal of Neuroimmunology*, *181*, 82–92.

Munro, S., Thomas, K. L., & Abu-Shaar, M. (1993). Molecular characterization of a peripheral receptor for cannabinoids. *Nature*, *365*(6441), 61–65.

Murikinati, S., Jüttler, E., Keinert, T., Ridder, D. A., Muhammad, S., Waibler, Z., Ledent, C., Zimmer, A., Kalinke, U., & Schwaninger, M. (2010). Activation of cannabinoid 2 receptors protects against cerebral ischemia by inhibiting neutrophil recruitment. *Federation of American Societies for Experimental Biology*, *24*(3), 788–98.

Murumalla, R., Bencharif, K., Gence, L., Bhattacharya, A., Tallet, F., Gonthier, M.-P., Petrosino, S., di Marzo, V., Cesari, M., Hoareau, L., & Roche, R. (2011). Effect of the Cannabinoid Receptor-1 antagonist SR141716A on human adipocyte inflammatory profile and differentiation. *Journal of Inflammation*, *8*, 33.

Ngaotepprutaram, T., Kaplan, B. L. F., & Kaminski, N. E. (2013). Impaired NFAT and NF-kB activation are involved in suppression of CD40 ligand expression by delta 9-tetrahydrocannabinol in human CD4+ T cells. *Toxicology and Applied Pharmacology*, *273*(1), 209–218.

Ni, X., Geller, E. B., Eppihimer, M. J., Eisenstein, T. K., Adler, M. W., & Tuma, R. F. (2004). Win 55212-2, a cannabinoid receptor agonist, attenuates leukocyte/endothelial interactions in an experimental autoimmune encephalomyelitis model. *Multiple Sclerosis*, *10*(2), 158–164.

Nicolussi, S., & Gertsch, J. (2015). Endocannabinoid Transport Revisited. *Vitamins and Hormones*, *98*, 441–485.

Nomura, F., Akashi, S., Sakao, Y., Sato, S., Kawai, T., Matsumoto, M., Nakanishi, K., Kimoto, M., Miyake, K., Takeda, K., & Akira, S. (2000). Cutting edge: endotoxin tolerance in mouse peritoneal macrophages correlates with down-regulation of surface toll-like receptor 4 expression. *Journal of Immunology*, *164*(7), 3476–3479.

Nussenblatt, R. B. (1990). The natural history of uveitis. *International Ophthalmology*, *14*(5-6), 303–308.

O'Sullivan, S. E., Kendall, D. A., & Sullivan, S. E. O. (2010). Cannabinoid activation of peroxisome proliferator-activated receptors: potential for modulation of inflammatory disease. *Immunobiology*, *215*(8), 611–616.

Ofek, O., Attar-Namdar, M., Kram, V., Dvir-Ginzberg, M., Mechoulam, R., Zimmer, A., Frenkel, B., Shohami, E., & Bab, I. (2011). CB2 cannabinoid receptor targets mitogenic Gi protein-cyclin D1 axis in osteoblasts. *Journal of Bone and Mineral Research*, *26*(2), 308–316.

Oyster, C. W. (1999). *The Human Eye Structure and Function*. Sinauer Associates, Inc.

Pacher, P., Batkai, S., & Kunos, G. (2006). The endocannabinoid system as an emerging target of pharmacotherapy. *Pharmacological Reviews*, *58*(3), 389–462.

Pacher, P., Bátkai, S., & Kunos, G. (2004). Haemodynamic profile and responsiveness to anandamide of TRPV1 receptor knock-out mice. *The Journal of Physiology*, *558*(2), 647–657.

Pacher, P., Bátkai, S., & Kunos, G. (2005). Cardiovascular pharmacology of cannabinoids. *Handbook of Experimental Pharmacology*, (168), 599–625.

Page, A. V, & Liles, W. C. (2013). Biomarkers of endothelial activation/dysfunction in infectious diseases. *Virulence*, *4*(6), 507–516.

Panikashvili, D., Simeonidou, C., Ben-Shabat, S., Hanus, L., Breuer, a, Mechoulam, R., & Shohami, E. (2001). An endogenous cannabinoid (2-AG) is neuroprotective after brain injury. *Nature*, *413*(6855), 527–531.

Parker, L., Whyte, M., Downer, S., & Sabroe, I. (2005). The expression and roles of Toll-like receptors in the biology of the human neutrophil. *Journal of Leukocyte Biology*, *77*, 886–892.

Parver, D. L., Dreher, R. J., Kohanim, P., Garrett, G., Devisetty, L., & Pasquale, L. R. (2012). Ocular Injury After Laser Hair Reduction Treatment to the Eyebrow. *Archives of Ophthalmology*, *130*(10), 1330–1334.

Pertwee, R. G. (2006). Cannabinoid pharmacology: the first 66 years. *British Journal of Pharmacology*, *147*, S163–171.

Petrosino, S., Ligresti, A., & Di Marzo, V. (2009). Endocannabinoid chemical biology: a tool for the development of novel therapies. *Current Opinion in Chemical Biology*, *13*(3), 309–320.

Pinar-Sueiro, S., Rodríguez-Puertas, R., & Vecino, E. (2011). Cannabinoid applications in glaucoma. *Archivos de la Sociedad Espanola de Oftalmologia*, *86*(1), 16–23.

Planck, S. R., Becker, M. D., Crespo, S., Choi, D., Galster, K., Garman, K. L., Nobiling, R., & Rosenbaum, J. T. (2008). Characterizing extravascular neutrophil migration in vivo in the iris. *Inflammation*, *31*(2), 105–111.

Planck, S. R., Han, Y. B., Park, J. M., O'Rourke, L., Gutierrez-Ramos, J. C., & Rosenbaum, J. T. (1998). The effect of genetic deficiency of adhesion molecules on the course of endotoxin-induced uveitis. *Current Eye Research*, *17*(9), 941–946.

Płóciennikowska, A., Hromada-Judycka, A., Borzęcka, K., & Kwiatkowska, K. (2014). Co-operation of TLR4 and raft proteins in LPS-induced pro-inflammatory signaling. *Cellular and Molecular Life Sciences*, *72*(3), 557–581.

Poltorak, A. (1998). Defective LPS Signaling in C3H/HeJ and C57BL/10ScCr Mice: Mutations in Tlr4 Gene. *Science*, *282*(5396), 2085–2088.

Popel, A. S., & Johnson, P. C. (2005). Microcirculation and Hemorheology. *Annual Review of Fluid Mechanics*, *37*, 43–69.

Pouvreau, I., Zech, J. C., Thillaye-Goldenberg, B., Naud, M. C., Van Rooijen, N., & de Kozak, Y. (1998). Effect of macrophage depletion by liposomes

containing dichloromethylene-diphosphonate on endotoxin-induced uveitis. *Journal of Neuroimmunology*, *86*(2), 171–181.

Pranskunas, A., Pilvinis, V., Dambrauskas, Z., Rasimaviciute, R., Planciuniene, R., Dobozinskas, P., Veikutis, V., Vaitkaitis, D., & Boerma, E. C. (2012). Early course of microcirculatory perfusion in eye and digestive tract during hypodynamic sepsis. *Critical Care*, *16*(3), R83.

Purves, D., Augustine, G., Fitzpatrick, D., Katz, L., LaMantia, A.-S., McNamara, J., & Williams, M. (2001). *Neuroscience. 2nd edition*. *Sunderland (MA): Sinauer Associates; 2001.*

Rajesh, M., Mukhopadhyay, P., Bátkai, S., Haskó, G., Liaudet, L., Huffman, J. W., Csiszar, A., Ungvari, Z., Mackie, K., Chatterjee, S., & Pacher, P. (2007). CB2-receptor stimulation attenuates TNF-alpha-induced human endothelial cell activation, transendothelial migration of monocytes, and monocyte-endothelial adhesion. *American Journal of Physiology. Heart and Circulatory Physiology*, *293*(4), H2210–2218.

Rajesh, M., Mukhopadhyay, P., Haskó, G., Liaudet, L., Mackie, K., & Pacher, P. (2010). Cannabinoid-1 receptor activation induces reactive oxygen species-dependent and -independent mitogen-activated protein kinase activation and cell death in human coronary artery endothelial cells. *British Journal of Pharmacology*, *160*(3), 688–700.

Ramirez, S. H., Haskó, J., Skuba, A., Fan, S., Dykstra, H., McCormick, R., Reichenbach, N., Krizbai, I., Mahadevan, A., Zhang, M., Tuma, R., Son, Y.-J., & Persidsky, Y. (2012). Activation of cannabinoid receptor 2 attenuates leukocyte-endothelial cell interactions and blood-brain barrier dysfunction under inflammatory conditions. *The Journal of Neuroscience*, *32*(12), 4004–4016.

Read, R. W. (2006). Uveitis: advances in understanding of pathogenesis and treatment. *Current Rheumatology Reports*, *8*(4), 260–266.

Reimer, T., Brcic, M., Schweizer, M., & Jungi, T. W. (2008). poly(I:C) and LPS induce distinct IRF3 and NF-kappaB signaling during type-I IFN and TNF responses in human macrophages. *Journal of Leukocyte Biology*, *83*(5), 1249–1257.

Resnikoff, S., Pascolini, D., Etya'ale, D., Kocur, I., Pararajasegaram, R., Pokharel, G. P., & Mariotti, S. P. (2004). Global data on visual impairment in the year 2002. *Bulletin of the World Health Organization*, *82*(11), 844–851.

Ricciotti, E., & Fitzgerald, G. A. (2011). Prostaglandins and inflammation. *Arteriosclerosis, Thrombosis, and Vascular Biology*, *31*(5), 986–1000.

Richardson, J. D., Kilo, S., & Hargreaves, K. M. (1998). Cannabinoids reduce hyperalgesia and inflammation via interaction with peripheral CB1 receptors. *Pain*, *75*, 111–119.

Rom, S., & Persidsky, Y. (2013). Cannabinoid Receptor 2: Potential Role in Immunomodulation and Neuroinflammation. *Journal of Neuroimmune Pharmacology*, *8*(3), 608–620.

Rom, S., Zuluaga-Ramirez, V., Dykstra, H., Reichenbach, N. L., Pacher, P., & Persidsky, Y. (2013). Selective activation of cannabinoid receptor 2 in leukocytes suppresses their engagement of the brain endothelium and protects the blood-brain barrier. *The American Journal of Pathology*, *183*(5), 1548–1558.

Romano, M., Cianci, E., Simiele, F., & Recchiuti, A. (2015). Lipoxins and aspirin-triggered lipoxins in resolution of inflammation. *European Journal of Pharmacology*, *760*, 49–63.

Romero-Sandoval, E. A., Horvath, R., Landry, R. P., & DeLeo, J. a. (2009). Cannabinoid receptor type 2 activation induces a microglial anti-inflammatory phenotype and reduces migration via MKP induction and ERK dephosphorylation. *Molecular Pain*, *5*, 25.

Rosenbaum, J. T., McDevitt, H. O., Guss, R. B., & Egbert, P. R. (1980). Endotoxin-induced uveitis in rats as a model for human disease. *Nature*, *286*(5773), 611–613.

Rosenbaum, J. T., Woods, A., Kezic, J., Planck, S. R., & Rosenzweig, H. L. (2011). Contrasting ocular effects of local versus systemic endotoxin. *Investigative Ophthalmology & Visual Science*, *52*(9), 6472–6477.

Ross, R. A., Brockie, H. C., Stevenson, L. A., Murphy, V. L., Templeton, F., Makriyannis, A., & Pertwee, R. G. (1999). Agonist-inverse agonist

characterization at CB1 and CB2 cannabinoid receptors of L759633, L759656, and AM630. *British Journal of Pharmacology*, *126*(3), 665–672.

Rossi, S., Furlan, R., De Chiara, V., Muzio, L., Musella, A., Motta, C., Studer, V., Cavasinni, F., Bernardi, G., Martino, G., Cravatt, B. F., Lutz, B., Maccarrone, M., & Centonze, D. (2011a). Cannabinoid CB1 receptors regulate neuronal TNF-α effects in experimental autoimmune encephalomyelitis. *Brain, Behavior, and Immunity*, *25*(6), 1242–8.

Rossi, S., Furlan, R., De Chiara, V., Muzio, L., Musella, A., Motta, C., Studer, V., Cavasinni, F., Bernardi, G., Martino, G., Cravatt, B. F., Lutz, B., Maccarrone, M., & Centonze, D. (2011b). Cannabinoid CB1 receptors regulate neuronal TNF-α effects in experimental autoimmune encephalomyelitis. *Brain, Behavior, and Immunity*, *25*(6), 1242–1248.

Ryan, G. B., & Majno, G. (1977). Acute inflammation. *American Journal of Pathology*, *86*, 185–276.

Sacerdote, P., Massi, P., Panerai, A. E., & Parolaro, D. (2000). In vivo and in vitro treatment with the synthetic cannabinoid CP55, 940 decreases the in vitro migration of macrophages in the rat: involvement of both CB1 and CB2 receptors. *Journal of Neuroimmunology*, *109*(2), 155–163.

Sagar, D. R., Gaw, a G., Okine, B. N., Woodhams, S. G., Wong, A., Kendall, D. a, & Chapman, V. (2009). Dynamic regulation of the endocannabinoid system: implications for analgesia. *Molecular Pain*, *5*, 59.

Sarantos, M. R., Raychaudhuri, S., Lum, A. F. H., Staunton, D. E., & Simon, S. I. (2005). Leukocyte function-associated antigen 1-mediated adhesion stability is dynamically regulated through affinity and valency during bond formation with intercellular adhesion molecule-1. *Journal of Biological Chemistry*, *280*(31), 28290–28298.

Sardinha, J., Kelly, M. E. M., Zhou, J., & Lehmann, C. (2014a). Experimental cannabinoid 2 receptor-mediated immune modulation in sepsis. *Mediators of Inflammation*, *2014*, 1–7.

Sardinha, J., Kelly, M. E. M., Zhou, J., & Lehmann, C. (2014b). Experimental Cannabinoid 2 Receptor-Mediated Immune Modulation in Sepsis. *Mediators of Inflammation*, *2014*, Article ID 978678.

Savinainen, J. R., Saario, S. M., & Laitinen, J. T. (2012). The serine hydrolases MAGL, ABHD6 and ABHD12 as guardians of 2-arachidonoylglycerol signalling through cannabinoid receptors. *Acta Physiologica*, *204*(2), 267–276.

Schenten, D., & Medzhitov, R. (2011). The Control of Adaptive Immune Responses by the Innate Immune System. *Advances in Immunology*, *109*, 87–124.

Selvi, E., Lorenzini, S., Garcia-Gonzalez, E., Maggio, R., Lazzerini, P. E., Capecchi, P. L., Balistreri, E., Spreafico, A., Niccolini, S., Pompella, G., Natale, M. R., Guideri, F., Laghi Pasini, F., Galeazzi, M., & Marcolongo, R. (2008). Inhibitory effect of synthetic cannabinoids on cytokine production in rheumatoid fibroblast-like synoviocytes. *Clinical and Experimental Rheumatology*, *26*(4), 574–81.

Silverman, M. D., Zamora, D. O., Pan, Y., Texeira, P. V, Planck, S. R., & Rosenbaum, J. T. (2001). cell adhesion molecule expression in cultured human iris endothelial cells. *Investigative Ophthalmology and Visual Science*, *42*(12), 2861–2866.

Smith, J. R., Hart, P. H., & Williams, K. A. (1998). Basic pathogenic mechanisms operating in experimental models of acute anterior uveitis. *Immunology and Cell Biology*, *76*(6), 497–512.

Smith, S. R., Denhardt, G., & Terminelli, C. (2001). The anti-inflammatory activities of cannabinoid receptor ligands in mouse peritonitis models. *European Journal of Pharmacology*, *432*(1), 107–19.

Smith, S. R., Terminelli, C., & Denhardt, G. (2001). Modulation of cytokine responses in Corynebacterium parvum-primed endotoxemic mice by centrally administered cannabinoid ligands. *European Journal of Pharmacology*, *425*(1), 73–83.

Sophocleous, A., Landao-Bassonga, E., Van't Hof, R. J., Idris, A. I., & Ralston, S. H. (2011). The type 2 cannabinoid receptor regulates bone mass and ovariectomy-induced bone loss by affecting osteoblast differentiation and bone formation. *Endocrinology*, *152*(6), 2141–2149.

Speth, C., Rambach, G., Würzner, R., Lass-Flörl, C., Kozarcanin, H., Hamad, O. a., Nilsson, B., & Ekdahl, K. N. (2015). Complement and platelets:

Mutual interference in the immune network. *Molecular Immunology*, *67*(1), 108–118.

Storr, M. a., Keenan, C. M., Zhang, H., Patel, K. D., Makriyannis, A., & Sharkey, K. a. (2009). Activation of the cannabinoid 2 receptor (CB2) protects against experimental colitis. *Inflammatory Bowel Diseases*, *15*(11), 1678–1685.

Straiker, A. J., Maguire, G., Mackie, K., & Lindsey, J. (1999). Localization of Cannabinoid CB1 Receptors in the Human Anterior Eye and Retina. *Investigative Ophthalmology & Visual Science*, *40*(10), 2442–2448.

Streilein, J. W. (2003). Ocular immune privilege : the eye takes a dim but practical view of immunity and inflammation. *Journal of Leukocyte Biology*, *74*, 179–185.

Streilein, J. W., Ohta, K., Mo, J. S., & Taylor, A. W. (2002). Ocular immune privilege and the impact of intraocular inflammation. *DNA and Cell Biology*, *21*(5-6), 453–459.

Stuart, J. M., Paris, J. J., Frye, C., & Bradshaw, H. B. (2013). Brain levels of prostaglandins, endocannabinoids, and related lipids are affected by mating strategies. *International Journal of Endocrinology*, *2013*, 1–14.

Su, S.-H., Wu, Y.-F., Lin, Q., Yu, F., & Hai, J. (2015). Cannabinoid receptor agonist WIN55,212-2 and fatty acid amide hydrolase inhibitor URB597 suppress chronic cerebral hypoperfusion-induced neuronal apoptosis by inhibiting c-Jun N-terminal kinase signaling. *Neuroscience*, *301*, 563–575.

Sugiura, T., Kondo, S., Sukagawa, A., Nakane, S., Shinoda, A., Itoh, K., Yamashita, A., & Waku, K. (1995). 2-Arachidonoylgylcerol: A Possible Endogenous Cannabinoid Receptor Ligand in Brain. *Biochemical and Biophysical Research Communications*, *215*, 89–97.

Sunderkötter, C., Nikolic, T., Dillon, M. J., Rooijen, V., Stehling, M., Drevets, D. A., Leenen, J. M., Sunderko, C., Nikolic, T., Dillon, M. J., & Rooijen, N. Van. (2004). Subpopulations of Mouse Blood Monocytes Differ in Maturation Stage and Inflammatory Response. *Journal of Immunology*, *172*, 4410–4417.

Suttorp-Schulten, M. S., & Rothova, A. (1996). The possible impact of uveitis in blindness: a literature survey. *The British Journal of Ophthalmology*, *80*(9), 844–848.

Szczesniak, A.-M., Maor, Y., Robertson, H., Hung, O., & Kelly, M. E. M. (2011). Nonpsychotropic cannabinoids, abnormal cannabidiol and canabigerol-dimethyl heptyl, act at novel cannabinoid receptors to reduce intraocular pressure. *Journal of Ocular Pharmacology and Therapeutics*, *27*(5), 427–435.

Takaoka, A., Yanai, H., Kondo, S., & Duncan, G. (2005). Integral role of IRF-5 in the gene induction programme activated by Toll-like receptors. *Nature*, *434*(10), 243–249.

Takeda, K., Kaisho, T., & Akira, S. (2003). Toll-like receptors. *Annual Review of Immunology*, *21*(1), 335–376.

Tanasescu, R., & Constantinescu, C. S. (2010). Cannabinoids and the immune system: an overview. *Immunobiology*, *215*(8), 588–597.

Tang, J., Tao, Y., Tan, L., Yang, L., Niu, Y., Chen, Q., Yang, Y., Feng, H., Chen, Z., & Zhu, G. (2015). Cannabinoid receptor 2 attenuates microglial accumulation and brain injury following germinal matrix hemorrhage via ERK dephosphorylation in vivo and in vitro. *Neuropharmacology*, *95*, 424–433.

Taylor, A. W. (2003). A review of the influence of aqueous humor on immunity. *Ocular Immunology and Inflammation*, *2*(4), 231–241.

Taylor, A. W., & Kaplan, H. J. (2010). Ocular immune privilege in the year 2010: ocular immune privilege and uveitis. *Ocular Immunology and Inflammation*, *18*(6), 488–92.

Toguri, J. T., Lehmann, C., Laprairie, R. B., Szczesniak, A. M., Zhou, J., Denovan-Wright, E. M., & Kelly, M. E. M. (2014). Anti-inflammatory effects of cannabinoid CB2 receptor activation in endotoxin-induced uveitis. *British Journal of Pharmacology*, *171*(6), 1448–1461.

Toguri, J. T., Moxsom, R., Szczesniak, A. M., Zhou, J., Kelly, M. E. M., & Lehmann, C. (2015). Cannabinoid 2 receptor activation reduces leukocyte adhesion and improves capillary perfusion in the iridial

microvasculature during systemic inflammation. *Clinical Hemorheology and Microcirculation*.

Tomar, S., Zumbrun, E. E., Nagarkatti, M., & Nagarkatti, P. S. (2015). Protective Role of Cannabinoid Receptor 2 Activation in Galactosamine / Lipopolysaccharide-Induced Acute Liver Failure through Regulation of Macrophage Polarization and MicroRNAs. *The Journal of Pharmacological and Experimental Therapeutics*, *353*, 369–379.

Tosi, M. F. (2005). Innate immune responses to infection. *Journal of Allergy and Clinical Immunology*, *116*(2), 241–249.

Tschop, J., Kasten, K. R., Nogueiras, R., Goetzman, H. S., Cave, C. M., England, L. G., Dattilo, J., Lentsch, A. B., Tschop, M. H., & Caldwell, C. C. (2009). The cannabinoid receptor 2 is critical for the host response to sepsis. *The Journal of Immunology*, *183*(1), 499–505.

Tschöp, J., Kasten, K. R., Nogueiras, R., Goetzman, H. S., Cave, C. M., England, L. G., Dattilo, J., Lentsch, A. B., Tschöp, M. H., & Caldwell, C. C. (2009a). The cannabinoid receptor 2 is critical for the host response to sepsis. *Journal of Immunology*, *183*(1), 499–505.

Tschöp, J., Kasten, K. R., Nogueiras, R., Goetzman, H. S., Cave, C. M., England, L. G., Dattilo, J., Lentsch, A. B., Tschöp, M. H., & Caldwell, C. C. (2009b). The cannabinoid receptor 2 is critical for the host response to sepsis. *The Journal of Immunology*, *183*(1), 499–505.

Uchiyama, E., Papaliodis, G. N., Lobo, A.-M., & Sobrin, L. (2014). Side-Effects of Anti-Inflammatory Therapy in Uveitis. *Seminars in Ophthalmology*, *29*(5-6), 456–467.

Ullrich, O., Merker, K., Timm, J., & Tauber, S. (2007). Immune control by endocannabinoids - new mechanisms of neuroprotection? *Journal of Neuroimmunology*, *184*(1-2), 127–135.

Van Rooijen, N., Sanders, A., & van den Berg, T. K. (1996). Apoptosis of macrophages induced by liposome-mediated intracellular delivery of clodronate and propamidine. *Journal of Immunological Methods*, *193*(1), 93–99.

Van Sickle, M. D., Duncan, M., Kingsley, P. J., Mouihate, A., Urbani, P., Mackie, K., Stella, N., Makriyannis, A., Piomelli, D., Davison, J. S., Marnett, L. J., Di Marzo, V., Pittman, Q. J., Patel, K. D., & Sharkey, K. A. (2005). Identification and functional characterization of brainstem cannabinoid CB2 receptors. *Science*, *310*(5746), 329–332.

Vanegas, H., Vazquez, E., & Tortorici, V. (2010). NSAIDs, Opioids, Cannabinoids and the Control of Pain by the Central Nervous System. *Pharmaceuticals*, *3*(5), 1335–1347.

Varga, R., Wagner, J. A., Bridgen, D. T., & Kunos, G. (1998). Platlet - and macrophage-derived endogenous cannabinoids are involved in endotoxin-induced hypotension. *Federation of Amerian Societies for Experimental Biology*, *12*, 1035–1044.

Vartanian, K. B., Stevens, S. L., Marsh, B. J., Williams-Karnesky, R., Lessov, N. S., & Stenzel-Poore, M. P. (2011). LPS preconditioning redirects TLR signaling following stroke: TRIF-IRF3 plays a seminal role in mediating tolerance to ischemic injury. *Journal of Neuroinflammation*, *8*, 140.

Vemuri, V. K., Janero, D. R., & Makriyannis, A. (2008). Pharmacotherapeutic targeting of the endocannabinoid signaling system: drugs for obesity and the metabolic syndrome. *Physiology & Behavior*, *93*(4-5), 671–686.

Verme, J. Lo, Fu, J., Astarita, G., Rana, G. La, Russo, R., Calignano, A., Piomelli, D., & Verme, L. (2005). The Nuclear Receptor Peroxisome Proliferator-Activated Receptor- alpha Mediates the Anti-Inflammatory Actions of Palmitoylethanolamide. *Molecular Pharmacology*, *67*(1), 15–19.

Villela, N., dos Santos, A., de Miranda, M., & Bouskela, E. (2014). Fluid resuscitation therapy in endotoxemic hamsters improves survival and attenuates capillary perfusion deficits and inflammatory responses by a mechanism related to nitric oxide. *Journal of Translational Medicine*, *12*, 232.

Wagner, J. A., Járai, Z., Bátkai, S., & Kunos, G. (2001). Hemodynamic effects of cannabinoids: coronary and cerebral vasodilation mediated by cannabinoid CB(1) receptors. *European journal of pharmacology*, *423*(2-3), 203–210.

Wakefield, D., Chang, J. H., Amjadi, S., Maconochie, Z., Abu El-Asrar, A., & McCluskey, P. (2011). What is new HLA-B27 acute anterior uveitis? *Ocular Immunology and Inflammation*, *19*(2), 139–144.

Wang, J.-X., Hou, L.-F., Yang, Y., Tang, W., Li, Y., & Zuo, J.-P. (2009). SM905, an artemisinin derivative, inhibited NO and pro-inflammatory cytokine production by suppressing MAPK and NF-kappaB pathways in RAW 264.7 macrophages. *Acta Pharmacologica Sinica*, *30*(10), 1428–1435.

Wen, A. Y., Sakamoto, K. M., & Miller, L. S. (2010). The role of the transcription factor CREB in immune function. *Journal of Immunology*, *185*, 6413–6419.

Witkowska, A. M., & Borawska, M. H. (2004). Soluble intercellular adhesion molecule-1 (sICAM-1): An overview. *European Cytokine Network*, *15*(2), 91–98.

Xagorari, A., Roussos, C., & Papapetropoulos, A. (2002). Inhibition of LPS-stimulated pathways in macrophages by the flavonoid luteolin. *British Journal of Pharmacology*, *136*(7), 1058–1064.

Xie, J., Li, R., Kotovuori, P., Vermot-Desroches, C., Wijdenes, J., Arnaout, M. a, Nortamo, P., & Gahmberg, C. G. (1995). Intercellular adhesion molecule-2 (CD102) binds to the leukocyte integrin CD11b/CD18 through the A domain. *Journal of Immunology*, *155*(7), 3619–3628.

Xu, H., Cheng, C. L., Chen, M., Manivannan, A., Cabay, L., Pertwee, R. G., Coutts, A., & Forrester, J. V. (2007). Anti-inflammatory property of the cannabinoid receptor-2-selective agonist JWH-133 in a rodent model of autoimmune uveoretinitis. *Journal of Leukocyte Biology*, *82*(3), 532–541.

Xu, H., Dawson, R., Crane, I. J., & Liversidge, J. (2005). Leukocyte diapedesis in vivo induces transient loss of tight junction protein at the blood-retina barrier. *Investigative Ophthalmology and Visual Science*, *46*(7), 2487–2494.

Yanaba, K., Bouaziz, J.-D., Matsushita, T., Tsubata, T., & Tedder, T. F. (2009). The development and function of regulatory B cells expressing IL-10 (B10 cells) requires antigen receptor diversity and TLR signals. *Journal of Immunology*, *182*(12), 7459–7472.

Yuan, Q., Wang, J., Fang, Q.-H., Liu, Y.-Y., Fan, J.-Y., Zhang, S.-W., & Ma, Y.-M. (2011). Attenuating effect of pretreatment with Yiqifumai on lipopolysaccharide-induced intestine injury and survival rate in rat. *Journal of Inflammation*, *8*, 10.

Zarruk, J. G., Fernández-López, D., García-Yébenes, I., García-Gutiérrez, M. S., Vivancos, J., Nombela, F., Torres, M., Burguete, M. C., Manzanares, J., Lizasoain, I., & Moro, M. A. (2012). Cannabinoid type 2 receptor activation downregulates stroke-induced classic and alternative brain macrophage/microglial activation concomitant to neuroprotection. *Stroke*, *43*(1), 211–219.

Zelasko, S., Arnold, W. R., & Das, A. (2014). Endocannabinoid metabolism by cytochrome P450 monooxygenases. *Prostaglandins & Other Lipid Mediators*, *116-117*, 112–123.

Zhang, M., Adler, M. W., Abood, M. E., Ganea, D., Jallo, J., & Tuma, R. F. (2009). CB2 receptor activation attenuates microcirculatory dysfunction during cerebral ischemic/reperfusion injury. *Microvascular Research*, *78*(1), 86–94.

Zhao, Q., Ren, H., & Han, Z. (2015). Mesenchymal Stem Cells: immunomodulatory capability and clinical potential in immune diseases. *Journal of Cellular Immunotherapy*.

Appendix I: Copyright Permission

This Agreement between James T Toguri ("You") and John Wiley and Sons ("John Wiley and Sons") consists of your license details and the terms and conditions provided by John Wiley and Sons and Copyright Clearance Center.

License Number	3652050276041
License date	Jun 18, 2015
Licensed Content Publisher	John Wiley and Sons
Licensed Content Publication	British Journal of Pharmacology
Licensed Content Title	Anti-inflammatory effects of cannabinoid CB2 receptor activation in endotoxin-induced uveitis
Licensed Content Author	J T Toguri,C Lehmann,R B Laprairie,A M Szczesniak,J Zhou,E M Denovan-Wright,M E M Kelly
Licensed Content Date	Mar 4, 2014
Pages	14
Type of use	Dissertation/Thesis
Requestor type	Author of this Wiley article
Format	Print and electronic
Portion	Full article
Will you be translating?	No
Title of your thesis / dissertation	Endocannabinoid system modulation of the ocular immune response
Expected completion date	Jul 2015
Expected size (number of pages)	200
Requestor Location	James T Toguri 5850 College Street Tupper Medical Building

	Halifax, NS B3H4R2 Canada Attn: James T Toguri
Billing Type	Invoice
Billing Address	James T Toguri 5850 College Street Tupper Medical Building Halifax, NS B3H4R2 Canada Attn: James T Toguri
Total	0.00 CAD

Terms and Conditions

TERMS AND CONDITIONS

This copyrighted material is owned by or exclusively licensed to John Wiley & Sons, Inc. or one of its group companies (each a"Wiley Company") or handled on behalf of a society with which a Wiley Company has exclusive publishing rights in relation to a particular work (collectively "WILEY"). By clicking ﷺacceptﷺ in connection with completing this licensing transaction, you agree that the following terms and conditions apply to this transaction (along with the billing and payment terms and conditions established by the Copyright Clearance Center Inc., ("CCC's Billing and Payment terms and conditions"), at the time that you opened your Rightslink account (these are available at any time athttp://myaccount.copyright.com).